Tu-Pos 1-30

Tu-Pos- 1-30

Student Education Program

No abstracts submitted.

INTRACELLULAR COMMUNICATION-IP₃ AND RYANODINE

Tu-Pos31

HOW SMALL IS THE "QUANTUM" OF INOSITOL 1,4,5-TRISPHOSPHATE INDUCED CA RELEASE? ((Ilya Bezprozvanny and Barbara E. Ehrlich)) Depts. of Medicine and Physiology, Univ. of Connecticut, Farmington, CT 06030.

To estimate the amount of Ca released from the intracellular Ca pool with each opening of an inositol 1,4,5-trisphosphate $(InsP_3)$-gated Ca channel, we measured permeation properties of this channel after it was incorporated into planar bilayers. Channel currents were recorded after addition of 2 μM $InsP_3$ and 0.5 mM ATP to the cytoplasmic (cis) side and with Ba or Ca on the lumenal (trans) side as the current carrier. The following results were obtained: (1) With a transmembrane voltage of 0 mV, the unitary current was 1.6 times smaller with Ca than with Ba as the current carrier. With 55 mM divalent cation trans/110 mM Tris cis, the single channel current was 2.25 $\pm$ 0.07 pA (n=8) with Ba and 1.4 $\pm$ 0.04 pA (n=6) with Ca. (2) When $InsP_3$-gated channels were measured at different trans Ba and Ca concentrations, the half-maximal unitary current was obtained at 10 mM for each of these cations. (3) When 110 mM potassium was used in the cis chamber instead of Tris, the unitary current with Ba as the current carrier was 1.75 times larger; the current was 3.95 $\pm$ 0.12 pA (n=5). From these results the size of the unitary current under physiological conditions (1 mM free Ca in the lumen of the reticulum/110 mM K in the cytosol) was estimated to be 0.26 pA. With this current and the mean open time of the channel observed in our experiments of 5 ms, approximately 4000 Ca ions will be released into the cytosol each time a channel opens. The estimated amount of Ca released at each opening of the ryanodine receptor is 10-100 times larger. Thus, the existence of two types of intracellular Ca channels may account for the wide range in the observed rates of change of cytosolic Ca.

Tu-Pos32

CAFFEINE INDUCED INHIBITION OF INOSITOL 1,4,5-TRISPHOSPHATE-GATED CA CHANNELS ((Svetlana Bezprozvannaya, Ilya Bezprozvanny, and Barbara E. Ehrlich)) Depts. of Medicine and Physiology, Univ. of Connecticut, Farmington, CT 06030.

The effects of the xanthine drug caffeine on inositol 1,4,5-trisphosphate $(InsP_3)$-gated Ca channels were studied after canine cerebellar microsomes were incorporated into planar bilayers. Channel currents were recorded after addition of 2 μM $InsP_3$ and 0.5 mM ATP to the cytoplasmic (cis) side and with Ba on the lumenal (trans) side as the current carrier. Caffeine, used widely as an agonist of ryanodine receptors, inhibited the activity of $InsP_3$-gated Ca channels in a non-cooperative fashion with half-maximal inhibition at 1.64 mM caffeine. In the presence of 5 mM caffeine the observed mean closed time of the channels increased 3.3 $\pm$ 0.8 fold (n=4); there was only a small effect on mean open time of the channels (6.3 $\pm$ 1.2 ms (n=4) in the absence and 4.8 $\pm$ 0.8 ms (n=4) in the presence of 5 mM caffeine) and the single channel conductance was unchanged. Thus, caffeine acted mainly by decreasing the frequency of channel openings. An increase in the $InsP_3$ concentration (to 20 μM) partially reversed the inhibitory action of caffeine, but caffeine was not a competitive inhibitor of $InsP_3$ receptors because caffeine did not reduce specific [³H]$InsP_3$ binding to the receptor. A model that accounts for these results will be discussed. The inhibitory action of caffeine on $InsP_3$ receptors suggests that the action of caffeine on the intracellular Ca pool must be interpreted with caution when both ryanodine receptors and $InsP_3$ receptors are present in the cell.
Supported by NIH grants HL33026 GM 39029 and a Grant-in-Aid from the American Heart Association, Connecticut Affiliate.

Tu-Pos33

IP₃ INDUCES A TRANSIENT ELEVATION OF INTRA-SARCOPLASMIC RETICULUM FREE Ca²⁺ IN CULTURED ARTERIAL SMOOTH MUSCLE CELLS ((T. Sugiyama and W.F. Goldman)) Dept. Physiology, Univ. Maryland Med. Sch. and the Geriatric Research Education and Clinical Ctr., Baltimore V.A.M.C., Baltimore, MD 21201.

The apparent concentrations of intra sarcoplasmic reticulum (SR) free Ca²⁺ were estimated in fura-2AM-loaded, saponin-skinned cultured aortic smooth muscle cells (A7r5). Images of intracellular fura-2 fluorescence elicited by illumination at 360 nm (isosbestic point) revealed that after cell skinning cytosolic fura-2 was washed from continuously superfused preparations and only fura-2 that was trapped, primarily, in SR remained. Under these conditions, SR Ca²⁺ was estimated to range from 1200-1600 nM and remained stable during superfusion with ATP-containing intracellular solution ([Ca²⁺]=100-200nM) for up to 20 min. When cells were exposed to 1μM IP₃, a biphasic response was observed. There was an initial transient rise in apparent SR Ca²⁺ which was followed by rapid decline during which 80-90% of SR Ca²⁺ was released. Intra-SR Ca²⁺ transients ranged from 200-600 nM in amplitude and had durations of ~1min. In contrast, gradual decreases or increases in SR Ca²⁺ were observed in skinned cells superfused with intracellular solutions containing either [Ca²⁺]=0 or 2000 nM, respectively. When cells were exposed to 5μM Br-A23187, there was a rapid monotonic decline in SR Ca²⁺ until SR depletion was complete. Elevation of SR Ca²⁺ were not observed in the presence of Br-A23187. These results suggest that, in contrast to Br-A23187, IP₃ may elicit a rise in intra-SR free Ca²⁺, perhaps as a consequence of decreased buffering by SR Ca²⁺ binding proteins. In this way, agonist evoked SR Ca²⁺ release which is mediated by IP₃ should be facilitated.

Tu-Pos34

PURIFICATION OF AN IP₃ RECEPTOR FROM LIVER PLASMA MEMBRANE. ((Rainer Schäfer, Kai Hell, and Sidney Fleischer)) Vanderbilt University, Nashville, TN 37235

A high affinity inositol 1,4,5-trisphosphate receptor from rat liver plasma membranes (PM-IP₃ Rec) was solubilized with the nonionic detergent Nonidet P-40. The solubilized IP₃ receptor was purified ~300-fold by sucrose-gradient centrifugation, affinity chromatography on heparin-agarose and ion-exchange chromatography to 70% homogeneity, as judged by scanning densitometry of Coomassie Blue stained SDS gels. The purified PM-IP₃ receptor bound 0.53 nmol InsP/mg of protein with a K_d of 3.4 nM; Ins(1,4,5)P₃ binding was markedly affected by the NaCl concentration (IC₅₀ ~140 mM). Binding was specific for InsP₃. Other inositol polyphosphates, i.e., Ins(1,3,4,5)P₄, Ins(1,3,4,5,6)P₅, InsP₆ and Ins(3,5,6)P₃ competed for Ins(1,4,5)P₃ binding but only at much higher concentrations; IC₅₀ values were 0.5, 2.0, 3.0, and 10 μM, respectively. The purified PM-IP₃ receptor protein migrates as a doublet at 240 kDa in SDS PAGE gels, and by sucrose density gradient centrifugation as a high molecular weight oligomer similar in size to the InsP₃ receptors from smooth muscle and brain. Our studies suggest that the PM-IP₃ Rec is a homotetramer. The PM-IP₃ receptor was found to be an IP₃ activated calcium channel (cf. Mayrleitner, M., Schäfer, R., and Fleischer, S., Biophys. J. 65, abstract [1994]). Supported in part by NIH HL 32711 (SF) and DK 20593-15 (RS).

Tu-Pos35

PURIFIED IP3 RECEPTOR FROM LIVER PLASMA MEMBRANE DISPLAYS IP3 ACTIVATED AND IP4 INHIBITED CALCIUM CHANNEL ACTIVITY. ((Martin Mayrleitner, Rainer Schäfer and Sidney Fleischer)) Dept. Molecular Biology, Vanderbilt Univ., Nashville, TN 37235

We have recently purified an inositol-1,4,5-trisphosphate (IP3) receptor from rat liver plasma membrane (PM-IP3 Rec.) (Schäfer, R., Hell, K., and Fleischer, S. Biophys.J. 65, abstract [1994]). The purified PM-IP3 receptor incorporated into vesicle derived planar bilayers forms an IP3 (1μM) activated ion channel which is inhibited by Inositol-1,3,4,5-tetrakisphosphate (IP4) (5μM) as well as by heparin (40μg/ml). In symmetrical 100mM KCl buffer, the channel displays a unitary conductance of 9pS, and 13pS in symmetrical 500mM KCl. Cs+ ions pass through the ion pore, similar to other intracellular Ca^{2+} release channels, i.e. the brain IP3 receptor and ryanodine receptor from skeletal muscle or heart. In symmetrical 250mM cesium methanesulfonate, a slope conductance of 11pS is obtained. The IP3 activated ion channel is most permeable to Ca^{2+} ($Ca^{2+} > K^+ >> Cl^-$; and $Cs^+ \geq K^+$). Channel activity is not voltage dependent (within $\pm$ 100mV applied voltage). The open probability of the IP3 induced channel activity shows a bell shaped calcium dependency ($P_o = f([Ca^{2+}]_{free}$) at the cis-side of our system, where IP3 also is added). Thus, the observed functional properties indicate that the PM-IP3 receptor purified from liver plasma membrane is a Ca^{2+} release channel. Our studies suggest that in liver IP3 may regulate Ca^{2+} influx through the plasma membrane. Supported in part by the Austrian Science Foundation (MM) and NIH HL 32711 (SF).

Tu-Pos36

SOLUBILISATION OF THE TYPE 3 RYANODINE RECEPTOR FROM RABBIT BRAIN ((John J. Mackrill and F. Anthony Lai)) MRC National Institute for Medical Research, Mill Hill, London NW7 1AA, UK

Distinct ryanodine-sensitive calcium channels have been previously isolated and characterised in skeletal and cardiac muscle (type 1 and 2 ryanodine receptor, respectively). Recently, an additional ryanodine receptor (RyR) gene regulated by growth factors and expressed in brain has been identified by cDNA cloning approaches (type 3 RyR). Using a synthetic peptide derived from the type 3 RyR sequence, an isoform specific antiserum was prepared to enable characterisation of the type 3 RyR protein. Immunoblot analysis of rabbit brain microsomes indicated the presence of two high molecular weight immunoreactive bands with mobilities greater than that of type 1 RyR and were similar to the type 2 RyR. Solubilisation in zwitterionic detergents and centrifugation on linear sucrose gradients revealed the type 3 RyR sediments disparately from the type 1 and 2 RyRs which were previously shown to migrate as large oligomeric 30S particles. Analysis of various brain regions with type 2- and type 3-specific antisera indicated a differential distribution of RyR immunoreactivity, with the cerebellum expressing highest levels of type 3 RyR. These studies show that the type 3 RyR displays a distinct pattern of expression, and the solubilised protein from brain microsomes does not possess identical oligomeric properties to that observed for both type 1 and 2 RyRs.

Tu-Pos37

CHARACTERIZATION OF SINGLE RYANODINE-SENSITIVE Ca^{2+} CHANNELS FROM ENDOPLASMIC RETICULUM OF CHICKEN CEREBELLUM. ((Jimena Sierralta*, B. Suarez-Isla*, and M. Fill)) Dept. Physiology & Biophysics, Univ. Texas Medical Branch, Galveston, TX 77555-0641 and the *Dept de Fisiologia y Biofisica, Univ. Chile, Fac. Med., Casilla 70005, Santiago 7, CHILE.

Ca^{2+} signalling in neurons involves intracellular Ca^{2+} release. Two types of Ca^{2+} release channels, IP3-sensitive and ryanodine-sensitive, have been shown to coexist with other important proteins (e.g. calsequestrin & Ca^{2+}-pump) in certain intracellular organelles in chicken cerebellum (Volpe et al. EMBO J. 10:3183, 1991). Starting from a microsomal preparation of chicken cerebellum, a microsomal fraction rich in ryanodine binding (B_{max} 630 fmoles/mg protein) was isolated on a discontinuous sucrose gradient. These microsomes were fused into planar lipid bilayers containing a 5:3:2 mix of PE, PS, and PC (in decane). Standard channel recording solutions contained (in mM): 400 $CsCH_3SO_3$, 20 Tris-HEPES (pH 7.4), 0.02 $CaCl_2$. In the presence of IP3, heparin-sensitive channels were observed. In the absence of IP3, a high conductance (300-350 pS) ryanodine-sensitive channel was consistently observed. This channel was Ca^{2+}-dependent, activated by ATP (1 mM) and caffeine (1 mM). It was blocked by Mg^{2+} (1 mM) and ryanodine (2 μM). These results show that the absence of IP3 is sufficient to isolate ryanodine-sensitive channels in preparations which contain both channel types. Supported by NIH R01NS29640 and FONDECYT 293-0003 & 91-1294.

Tu-Pos38

COULD "ACTIVATION" OF $InsP_3$-INDUCED Ca^{2+} RELEASE BY CYTOSOLIC Ca^{2+} BE THE ARTEFACTUAL INDIRECT CONSEQUENCE OF AN INHIBITORY EFFECT OF MOST Ca^{2+} CHELATORS ? *Philippe Champeil and +Laurent Combettes, *URA CNRS 1290 & SBPM/DBCM/CEA, C.E de Saclay, 91191 Gif-sur-Yvette, and +INSERM U274, Université Paris-Sud, 91405 Orsay (France).

One of the pathways for regulation of cytosolic free Ca^{2+} levels involves inositol 1,4,5-triphosphate ($InsP_3$)-induced Ca^{2+} release from intracellular stores. The dependence of this release on the preexisting level of free Ca^{2+} in the cytoplasm was recently suggested to comprise both Ca^{2+}-induced activation of the $InsP_3$-gated channel, at low, physiological concentrations of Ca^{2+}, and Ca^{2+}-induced inhibition of this channel, at much higher concentrations. Positive and negative feedbacks exerted by the cytoplasmic Ca^{2+} level on Ca^{2+} release obviously play an important role for the understanding of the spatiotemporal aspects of Ca^{2+} signalling, as well as for the steepness of the $InsP_3$ dose-response relationships. The particular Ca^{2+} dependence mentioned above has indeed been incorporated in various models describing hormone-induced oscillations in cellular Ca^{2+} and propagation of Ca^{2+} waves. In this work, we aimed at measuring in a simple way with filtration methods the Ca^{2+} dependence of $InsP_3$-induced $^{45}Ca^{2+}$ efflux from microsomes derived from cerebellum, a tissue known to be enriched in $InsP_3$ receptors. Unexpectedly, we found that most if not all of the apparent activating effect of Ca^{2+} we observed, arose from an inhibitory effect of the Ca^{2+} chelators used to adjust the free Ca^{2+} concentration. Under ionic conditions different from ours, various Ca^{2+} chelators were also recently found to competitively antagonize $InsP_3$ binding to purified $InsP_3$ receptors. In view of the importance of the issue, careful reexamination of the Ca^{2+} dependence of $InsP_3$-gated Ca^{2+} fluxes is therefore desirable in other experimental systems.

INTRACELLULAR COMMUNICATION-THAPSIGARGIN

Tu-Pos39

MODULATION OF THAPSIGARGIN-MEDIATED Ca^{2+} UPTAKE IN RAT THYMIC LYMPHOCYTES. ((M.J. Mason and I. Marriott)) Dept. of Physiology, Tulane University School of Medicine, New Orleans, LA 70112

The purpose of the present experiments was to investigate the modulatory influence of transmembrane potential (E_m) and phorbol ester on electrogenic thapsigargin-mediated Ca^{2+} uptake in rat thymic lymphocytes. To distinguish between effects of alterations in E_m on the influx pathway from possible simultaneous effects on extrusion mechanisms, we have monitored unidirectional Ca^{2+} uptake isotopically at different values of E_m following thapsigargin stimulation. E_m was altered by varying extracellular [K+] and emperically determined in parallel measurements of E_m using Bis-oxonol. Unidirectional Ca^{2+} uptake, was monitored in Bapta-loaded cells pre-treated with 100 nM thapsigargin and equilibrated in Ca^{2+}-free medium containing 3 to 140 mM K+. Uptake was initiated by the re-introduction of 4 mM Ca^{2+}. When plotted as a function of the driving force for Ca^{2+}, the unidirectional Ca^{2+} uptake rate followed a curvilinear function with uptake in 140 mM K+ (-4 mV) being ~30% of that measured in 3 mM K+ (resting potential -53 mV). This Ca^{2+} uptake rate was significantly lower than the ~70% predicted on the basis of the effect of E_m on driving force alone. Additionally, at normal E_m, the unidirectional uptake rate measured 15 minutes after re-introduction of cold Ca^{2+} was reduced to ~23% of that measured immediately after Ca^{2+} addition. However, both baseline unidirectional Ca^{2+} uptake and thapsigargin-mediated uptake were unaffected by the phorbol ester PMA. On the basis of these data we conclude that the permeability of the thapsigargin-mediated uptake pathway; 1) is modulated by E_m, 2) inactivates in a time dependent fashion and 3) is most likely not modulated by protein kinase C.

Tu-Pos40

AMILORIDE ANALOGS INHIBIT THAPSIGARGIN-INDUCED CALCIUM INFLUX IN CHINESE HAMSTER OVARY CELLS. ((J. H. Cho, J. P. Gardner, A. Aviv and J. P. Reeves)) Hypertension Research Center and Physiology Department, UMD-NJ Medical School, Newark, NJ 07103.

Thapsigargin (Tg) induces capacitative Ca entry in many cell types due to its effects in depleting intracellular Ca stores. In CHO cells, Tg-induced ^{45}Ca influx was blocked by methylisobutylamiloride (MIA; IC_{50} = 4 μM) and ethylisopropylamiloride (EIPA; IC_{50} = 10 μM). Benzamil also inhibited Tg-induced ^{45}Ca influx, although it was less potent than either MIA or EIPA. This suggests that the effects of the amiloride derivatives are not due to blockade of Na/H exchange, since benzamil does not inhibit the latter process. We tested this further by examining the effects of Tg in CHO cells that are deficient in Na/H exchange activity (AP-1 cells). Tg stimulated ^{45}Ca influx in AP-1 cells as effectively as in normal CHO cells, and this effect was blocked by both MIA and EIPA (IC_{50} = 20 μM and 45 μM respectively). To determine whether the amiloride analogs blocked the Ca entry pathway, we examined their effects in transfected CHO cells expressing the cardiac Na/Ca exchanger (CK1.4 cells; cf. Reeves et al., these Proceedings). EIPA blocked Tg-stimulated ^{45}Ca influx in CK1.4 cells under conditions where Na/Ca exchange is the principal Ca entry pathway; EIPA had little or no inhibitory effect on Na/Ca exchange in these cells. The results indicate that amiloride analogs modulate intracellular Ca handling in CHO cells; these effects do not appear to be exerted by blockade of Na/H exchange.

Tu-Pos41

PROTO-ONCOGENE bcl-2 MAINTAINS THAPSIGARGIN-SENSITIVE Ca^{2+} POOL IN JURKAT CELLS AND INHIBITS APOPTOSIS.
((I. Kudryashova*, R.W. Tuckert, J.C. Reed** and R.G. Hansford*))
NIA,NIH, Baltimore, MD 21224*; Depart. Oncology, Johns Hopkins Univ., Baltimore, MD 21205†: La Jolla Cancer Res. Found., La Jolla, CA 92037**.

The Jurkat human T-cell line undergoes apoptosis when deprived of serum, in a process which is sensitive to Ca^{2+} and can be delayed by overexpression of the proto-oncogene bcl-2. We studied the effects of serum-starvation (S-S) upon intracellular free Ca^{2+} ($[Ca^{2+}]_c$) and the size of organelle Ca^{2+} pools in Jurkat cells which had been transfected with the bcl-2 gene (bcl_2) and in control cells (neo). $[Ca^{2+}]_c$ was monitored in cell suspensions loaded with indo 1/AM, and the endoplasmic reticulum pool (ER) was indexed by the rise in $[Ca^{2+}]_c$ due to thapsigargin (thaps; 0.5 µM), an inhibitor of the ER Ca^{2+}-ATPase. S-S for 4 days produced 71% and 26% mortality in neo and bcl_2 cells, respectively. ER Ca^{2+} was maintained to a much greater extent during S-S in bcl_2 cells than neo cells. Thus, resting $[Ca^{2+}]_c$ was 77±5 (n=10) and 73±5 (n=10) nM in 4 day-starved neo and bcl-2 cells, respectively; on thaps addition, these values rose to 136±15 (n=4) and 334±48 (n=5) nM, respectively. In non-starved cells, the rise in $[Ca^{2+}]_c$ due to thaps was not affected by the bcl-2 gene. Digital image analysis of single cells revealed relative homogeneity of basal and stimulated $[Ca^{2+}]_c$, so that damaged cells did not contribute to the measurements of $[Ca^{2+}]_c$ in suspended cells. These results suggest that ER Ca^{2+} content is important in preventing apoptotic death.

Tu-Pos42

THAPSIGARGIN STIMULATES TRANSLOCATION OF THE CAFFEINE-SENSITIVE Ca^{2+} STORE IN SMOOTH MUSCLE FROM BOVINE CORONARY ARTERY. ((G.M. Dick and M. Sturek)) Vascular Cell Biophysics Laboratory, Dalton Cardiovascular Research Center and Department of Physiology , University of Missouri, Columbia, MO 65211.

Using fura-2 microfluorometry, it was found that thapsigargin (TG; 10^{-8} M) depletes the caffeine-sensitive Ca^{2+} store without an elevation of myoplasmic free Ca^{2+} (Ca_m). It was hypothesized that during an eight minute exposure to TG Ca^{2+} was released from the sarcoplasmic reticulum (SR) and extruded from the cell. Accordingly, we predicted that inhibition of sarcolemmal Na^+-Ca^{2+} exchange during TG exposure would increase Ca_m. However, reduction of extracellular Na^+ to 68 mM (with equimolar Li^+ replacement) during TG exposure did not elevate Ca_m. Ionomycin (10^{-6} M) was used to assay the content of the SR Ca^{2+} store. The ionomycin-releasable Ca^{2+} store was not different after TG treatment. These data indicate that TG does not release the caffeine-sensitive SR Ca^{2+} store; instead, TG causes translocation of Ca^{2+} to a caffeine-insensitive store. This translocation may occur by direct coupling of Ca^{2+} stores or indirectly via localized Ca^{2+} gradients that are probably not subsarcolemmal.
(Supported by NIH HL02872 and AHA 93011900 to M.S., T-32 H07094, and a Predoctoral Fellowship from the AHA-Missouri Affiliate to GMD)

Tu-Pos43

THAPSIGARGIN (TG) INHIBITS CALCIUM RECYCLING IN CHO CELLS TRANSFECTED WITH THE BOVINE CARDIAC SODIUM-CALCIUM EXCHANGER.((J. P. Reeves, G. Chernaya, J. F. Aceto, J. P. Gardner and M. Condrescu)) Department of Physiology & Hypertension Research Center, UMD-NJ Medical School, Newark, NJ 07103 and Roche Institute of Molecular Biology, Roche Research Center, Nutley, NJ 07110.

The effects of 50 nM Tg on ^{45}Ca influx were compared in transfected cells permanently expressing the bovine cardiac Na/Ca exchanger (CK1.4 cells) and in nontransfected, or vector-transfected, control cells. Tg markedly stimulated ^{45}Ca uptake in the nontransfected cells but not in the CK1.4 cells unless the latter had been pretreated with ouabain or assayed in a Na-free medium. When ouabain-treated CK1.4 cells were assayed for ^{45}Ca uptake in a low-Na (40 mM) medium, Tg enhanced uptake 2.4-fold. Tg had little or no effect on the initial rate of ^{45}Ca influx under these conditions, but markedly inhibited ^{45}Ca efflux. Inhibition of Ca efflux by Tg was dependent upon the presence of physiological levels of $|Ca|_o$. The mitochondrial inibitors oligomycin (2.5 µg/ml) and rotenone (2 µM) blocked the stimulatory effect of Tg on ^{45}Ca uptake but were without effect in the absence of Tg. Thus, Tg enhances Ca uptake by Na/Ca exchange in CK1.4 cells but does not affect turnover of the exchanger itself. The results suggest that Tg alters the distribution of incoming ^{45}Ca so that it is accumulated by the mitochondria and removed from the vicinity of calcium efflux processes in the plasma membrane. The results are consistent with the participation of the endoplasmic reticulum (or other Tg-sensitive compartments) in the recycling of cytosolic Ca to the exterior, as proposed in the "buffer barrier" hypothesis (van Breemen & Saida, *Ann. Rev. Physiol.* 51: 315, 1989).

Tu-Pos44

INCREASED CALCIUM INFLUX FOLLOWING THAPSIGARGIN TREATMENT IN APLYSIA BAG CELL NEURONS. ((S. Levy and A. Levin)) Dept. of Physiology, Boston Univ. Sch. Med., Boston, MA 02118.

In *Aplysia* bag cell neurons, initiation of the afterdischarge is associated with a transient elevation of intracellular calcium (Ca_i), which may result from Ca^{2+} release induced by Ca^{2+} influx. In isolated bag cell neurons, evoked action potentials in barium-seawater induce a prolonged depolarization and a robust Ca_i increase (Biophys. J. 59:588a). Following depletion of intracellular stores by thapsigargin, evoked action potentials lead to a shorter depolarization and no Ca_i increase (Biophys. J. 64:317a). To further characterize calcium fluxes following depletion, we have measured extracellular calcium (Ca_o) at the plasma membrane using calcium-sensitive electrodes. The tip of the calcium-sensitive electrode was beveled and the flat portion gently positioned against the plasma membrane. A separate microelectrode was used to measure membrane potential and stimulate the cell. To reduce the background calcium concentration, Ca_o in the seawater was lowered to 1 mM. In 1 mM Ca-SW, evoked action potentials induced a transient Ca_o increase. Following bath application of thapsigargin (1 µM), Ca_o increased after a delay of about 3 minutes, suggesting calcium efflux following depletion of intracellular stores. In such thapsigargin-treated cells, evoked action potentials led to no change in Ca_o. In some calcium-depleted cells however, evoked action potentials led to a rapid and transient Ca_o decrease, suggesting an increased calcium influx. These results indicate that following depletion of intracellular stores by thapsigargin, calcium is not merely redistributed but leaves the cell through the plasma membrane. The transient Ca_o decrease following evoked action potentials is consistent with an increased calcium influx induced by depletion of intracellular stores.

INTRACELLULAR COMMUNICATION-SIGNALLING

Tu-Pos45

ACTIVATION OF PROTEIN KINASE C IN VITRO BY PHOTOLABILE CAGED DIACYLGLYCEROLS ((Xu Pei Huang and Jeffery W. Walker)) Department of Physiology, University of Wisconsin, Madison, WI 53706

The properties of caged diacylglycerols were determined in vitro using a mixed micelle assay system containing 0.3% Triton X-100, phosphatidylserine, rat brain protein kinase C and histone III. Two compounds were evaluated: O-1'(2'-nitro)phenylethyl 1,2 sn-dioctanoylglycerol (α-methyl caged diC_8; $\epsilon_{260nm} = 3.2 \times 10^4$ M^{-1} cm^{-1} in $CHCl_3$) and O-α-carboxyl 2,4-dinitrobenzyl 1,2 sn-dioctanoylglycerol (α-carboxyl caged diC_8; $\epsilon_{260nm} = 2.4 \times 10^4$ M^{-1} cm^{-1} in $CHCl_3$). The stereochemistry of photo-released diC_8 was confirmed by E. coli diacylglycerol kinase which phosphorylates 1,2 sn-diC_8 but not 1,3 sn- or 2,3 sn-diC_8. Neither α-methyl nor α-carboxyl caged diC_8 influenced protein kinase C activation before photolysis. Near-UV photolysis in the presence of caged diC_8 increased protein kinase C activity from 0.7 ± 0.7 pmol/min to 34 ± 5.8 pmol/min. Photolysis effected by a continuous 100 watt xenon arc lamp (UG-11 filtered) was half-maximal after 2 min and complete in 5 min. The conversion efficiency using a xenon arc flash lamp was 20% per flash. Protein kinase C activation varied with the initial concentration of caged diC_8 and was augmented by 20-100 µM arachidonic acid. α-Carboxyl caged $[^{14}C]$-diC_8 was partially soluble in aqueous buffers at neutral pH and was efficiently incorporated into isolated rat ventricular myocytes. In preliminary experiments, photolysis of myocytes containing α-carboxyl caged diC_8 reduced contractility in a reversible manner.

Tu-Pos46

EFFECTS OF ANGIOTENSIN II ON INTRACELLULAR pH IN NEONATAL RAT VENTRICULAR MYOCYTES. ((Trudy A. Kohout and Terry B. Rogers)) Dept. of Biol. Chem., Univ. of Maryland School of Medicine, Baltimore MD 21201

Angiotensin II (AngII) has been shown to have direct effects on neonatal myocytes as manifested by positive chronotropic and a negative inotropic effects. The underlying mechanisms of these effects have not yet been fully elucidated; however, evidence suggests that activation of voltage gated ion channels and stimulation of several second messenger systems, including phosphoinositide/protein kinase C pathway and arachidonic acid release, play a role in AngII-evoked responses. Further, these effects are mediated through two AngII receptor types present in heart, the AT_1 subtype, responsible for the activation of the phosphoinositide pathway, and AT_2, involved in arachidonic acid release (Lokuta *et al., J.Biol.Chem.* 269, in press).

Results from this lab and several others suggest that PKC activates the Na^+/H^+ exchanger causing an alkalinization of the cell. Hence, the goal of this study was to determine whether an effect on intracellular pH, pH_i, was also a mechanism of action of AngII. Changes in pH_i were measured in spontaneously beating neonatal rat ventricular myocytes using single cells loaded with the fluorescent pH indicator SNARF-1/AM acetate. Superfusion of the myocytes with AngII (100 nM) resulted in a sustained alkalinization of the cells by 0.09±0.02 pH units which was blocked by the general AngII antagonist [Sar^1,Leu^8]AngII. Furthermore, it was also blocked by the AT_1-specific antagonist, CGP42112A. These data suggest manipulation of the intracellular pH is an important mechanism for AngII-mediated effects.

Tu-Pos47

POLYCLONAL ANTIBODIES TO SH3 DOMAINS. ((Anita S. Zot and Henry G. Zot)) Dept. of Physiology, UT Southwestern Medical Center, Dallas, TX 75235.

The SH3 sequence motif is common to a number of protein involved in signal transduction and membrane-cytoskeletal interactions, including several myosin-I's from *Acanthamoeba*. To provide tools for the study of the roles of SH3-containing proteins, we raised polyclonal antibodies which would react with this region of myosin-I, as well as with SH3 regions of other cellular proteins. We designed three overlapping peptides that together span the SH3 domain and are composed partially of sequence identical to myosin-I and partially of sequence based on an SH3 consensus sequence. Peptides were coupled to BSA for injection into rabbits. ELISA's of the antisera revealed high titers in the final bleeds and competitive ELISA's confirmed that the antibodies recognize the uncoupled peptides. Antisera to two different peptides display cross-reactivity, suggesting that the epitope for these antibodies is the four-residue sequence identical between these two peptides. All antisera recognize a bacterially-expressed, SH3-containing segment of the *Acanthamoeba* myosin-I tail on a Western blot. Western blots of *Acanthamoeba* lysates probed with the antisera exhibit a number of reactive bands, one of which is the size of myosin-I. Further characterization of the antisera and the proteins with which they react will contribute to an understanding of the roles of myosin-I and other SH3-containing proteins in the cell. Supported by AHA 92-1571 and NSF MCB-9205344.

Tu-Pos48

CELL SWELLING AND SUBSEQUENT INDUCTION OF INTRACELLULAR VESICLE ALKALINIZATION: A PUTATIVE SIGNALLING MECHANISM FOR INSULIN. ((G.L. Busch[1], H. Völkl[2], D. Häussinger[3] & F. Lang[1])) Dept. Physiol. Universities of [1]Tübingen, D-72076 Tübingen and [2]Innsbruck, A-6020 Innsbruck; [3]Clinic of Internal Medicine, University of Freiburg, D-79104 Freiburg. (Spon. by J. Maylie)

Hepatic proteolysis, which occurs largely within acidic lysosomes, is known to be achieved by pH-sensitive lysosomal proteinases. The anti-proteolytic effect of insulin has been shown to be mediated by cell swelling, although the mechanism linking cell volume to proteolysis was unclear. In order to investigate a possible link, rat hepatocytes loaded with one of two different pH-sensitive fluorescent dyes were treated with 40 nM insulin and/or hypoosmotic solution (220 mOsm, 150 mOsm). Fluorescence was measured using microspectrofluorometric techniques. Both treatments resulted in an increase in acridine orange (AO) fluorescence (450-490 nm), a result of its release from intracellular compartments. According to the chemico-physical properties of AO, this corresponds to an alkalinization of these compartments. Cell swelling induced by hypoosmotic solution stimulated an increase in the fluorescence ratio (490/440 nm) of fluorescein isothiocyanate dextran (FID)-loaded hepatocytes. This again reflected an alkalinization of acidic intracellur compartments, based on calibration of the FID fluorescence ratio with pH. These results suggest that inhibition of proteolysis by insulin is mediated by cell swelling and subsequent lysosomal alkalinization.

Tu-Pos49

THE EFFECTS OF PACAP ON CALCIUM AND POTASSSIUM CHANNEL CURRENTS IN RAT PINEALOCYTES. ((Qin-Yue Liu, Bing Li, Constance L. Chik, Anthony K. Ho and Edward Karpinski)) Univ. of Alberta, Edmonton, Alberta T6G 2H7

Pituitary adenylate cyclase activating polypeptide (PACAP) is a new member of the vasoactive intestinal peptide family. The demonstration of high concentrations of PACAP and high affinity PACAP receptors in many brain regions suggests that PACAP may have a physiological role as a neuro-modulator. Recently, we have found that PACAP regulates pineal function. In this study, the effects of PACAP on ionic currents were investigated using the whole cell version of the patch clamp technique. PACAP (10^{-9}-10^{-6} M) decreased the dihydropyridine-sensitive (L-channel) current by as much as 33.5%. The inhibitory action of PACAP on the L-channel current was concentration-dependent and reversible. Experiments were conducted to identify the intracellular mediator(s) of the PACAP effect on the L-type channels. Prior treatment of the pinealocytes with Rp-cAMPs abolished the effect of PACAP. Furthermore, 8-bromo-cAMP decreased the L-channel current, indicating that the effect of PACAP on the L-channel is in part mediated by cAMP. The effect of PACAP on K^+ channel current was also characterized. PACAP (10^{-7} M) increased the delayed rectifier and transient outward K^+ channel currents in these cells. Taken together, the results from these experiments suggest that PACAP may function as a neuromodulator in the rat pineal gland.

Tu-Pos50

REGULATION OF CD2 LATERAL MOBILITY BY CALMODULIN AND CALCINEURIN IN JURKAT T CELL MEMBRANES. ((Si-qiong J. Liu and David E. Golan)) Dept. of Biol. Chem. & Mol. Pharm., Harvard Medical School, Boston, MA 02115.

T cell activation is associated with increased intracellular Ca^{2+}, which causes a decrease in the lateral mobility of the cell surface adhesion molecule CD2. We examined the role of calmodulin in Ca^{2+} mediated CD2 immobilization. Fluorescence photobleaching recovery was used to measure the lateral mobility of CD2 labelled with FITC conjugated TS2/18 in human Jurkat T leukemia cell membranes. Jurkat cells were incubated with the calmodulin inhibitor trifluoperazine (TFP), and then activated either by cross-linking the TCR/CD3 complex with OKT3 + goat anti-mouse IgG2a (OG) or via CD2 by treatment with the activating pair of anti-CD2 mAbs, 9-1 + TS2/18 (9T). OG-induced CD2 immobilization was progressively prevented by increasing [TFP]; complete prevention occurred at 100 nM TFP. Treatment with 500 nM TFP partially prevented 9T-induced CD2 immobilization. Calmodulin activation therefore appears to be necessary for CD2 immobilization induced by increased intracellular Ca^{2+}. OG-induced CD2 immobilization spontaneously reversed at 2 hr after OG treatment. Since Ca^{2+}/calmodulin regulates both protein phosphorylation and calcineurin phosphatase activity, we tested the role of calcineurin in the reversal of Ca^{2+}-dependent CD2 immobilization. Treatment with cyclosporin A (CsA) had no effect on OG-induced CD2 immobilization, but CsA prevented the recovery of CD2 mobility for at least 3.5 hr. Calcineurin phosphatase activity therefore appears to be necessary for the reversal of Ca^{2+}-dependent CD2 immobilization. These data suggest that Ca^{2+}/calmodulin modulates CD2 lateral mobility by regulating phosphorylation and dephosphorylation of CD2 or a closely associated protein.

Tu-Pos51

MOBILIZATION OF INTRACELLULAR FREE Ca^{2+} UPON T CELL ACTIVATION VIA TCR/CD3 IS REQUIRED TO INDUCE A DECREASE IN CD2 LATERAL MOBILITY IN JURKAT T CELL MEMBRANES. ((Si-qiong J. Liu and David E. Golan)) Dept. of Biol. Chem. & Mol. Pharm., Harvard Medical School, Boston, MA 02115.

T cell activation via the TCR/CD3 complex regulates the avidity of the adhesion molecule CD2 for its ligand CD58, possibly through activation-induced lateral redistribution of CD2 and CD58. We have previously demonstrated that T cell activation by pairs of anti-CD2 mAbs results in CD2 immobilization, and that CD2 immobilization is at least partially mediated by intracellular Ca^{2+} mobilization. In the present work we examined the effect of T cell activation via TCR/CD3 on CD2 lateral mobility. Human Jurkat T leukemia cells were activated by OKT3 (IgG2a), an anti-CD3 mAb, and goat anti-mouse IgG2a (GaM), which cross-linked OKT3. Fluorescence photobleaching recovery was used to measure the lateral mobility of cell surface CD2 labelled with FITC conjugated anti-CD2 mAb TS2/18 (IgG1). Treatment with OKT3 reduced the fractional mobility of CD2 from the control value of 68±1% (mean±SEM) to 63±3%. Addition of GaM caused the f value to decrease to 54±2%. Two hr after cell activation the f value returned to the control level. TCR/CD3 cross-linking has been found to increase the intracellular free [Ca²+] ([Ca²+]ᵢ) in Jurkat cells. Cells treated to measure the intracellular free [Ca²+] ([Ca²+]ᵢ) in Jurkat cells. Cells treated with EGTA+ionomycin manifested reduced [Ca²+]ᵢ in the unperturbed state and were unable to increase [Ca²+]ᵢ upon OKT3+GaM treatment. TCR/CD3 cross-linking did not alter CD2 fractional mobility on EGTA+ionomycin treated cells. Further, under all treatment conditions the fraction of cells with significantly elevated [Ca²+]ᵢ was highly correlated ($R^2 = 0.955$) with the fraction of cells manifesting significantly reduced CD2 mobility. We conclude that [Ca²+]ᵢ mobilization is required for CD2 immobilization in cells stimulated with OKT3+GaM.

Tu-Pos52

JUNCTIONAL UNCOUPLING BY ATP OR ARACHIDONIC ACID IS Ca$_i$-MEDIATED. ((A. Lazrak, A. Peres*, S. Giovannardi* and C. Peracchia)) Department of Physiology, University of Rochester, Rochester, NY, and *Dipartimento di Fisiologia e Biochimica Generali, Università di Milano, Milano, Italy.

Evidence for gating sensitivity to nanomolar [Ca²+]ᵢ (Lazrak and Peracchia, Biophys. J., 65, Nov. 1993) suggests that coupling may change following receptor activation. To test it, we have studied the effects of ATP-induced activation of purinergic receptor in Novikoff hepatoma cells, while monitoring either [Ca²+]ᵢ (with Fura-2) or both membrane and junctional currents. ATP (100 µM) increased [Ca²+]ᵢ to ~400 nM. [Ca²+]ᵢ internal. [Ca²+]ᵢ rapidly, peaked briefly and recovered following a single exponential decay with a time constant of ~1.5 min. This was observed both with and without Ca²+ₒ, suggesting an internal Ca²+ release. The same cells were studied by either double whole-cell clamp (DWCC) or perforated patches (PP, nystatin). With PP, junctional conductance (G$_j$) decreased with ATP by ~30%, following the same time course of the increase in [Ca²+]ᵢ. Simultaneously, an outward current (at normal [K⁺]ₒ; Vₕ = -20 mV), with a reversal potential of -80 mV, developed; the current became inward at 140 mM [K⁺]ₒ (Vₕ = -60 mV), with a reversal potential of 0 mV. This indicates that it is a Ca²+-activated K⁺-current. Current peaks coincided with G$_j$ minima, indicating that both phenomena are caused by an increase in [Ca²+]ᵢ. This is also supported by the observation that both G$_j$ decrease and membrane current are only seen with PP or DWCC with weak Ca²+ buffering (0.5 mM EGTA), but not with 1 mM BAPTA. Arachidonic acid (AA, 20 µM) had similar effects on [Ca²+]ᵢ and G$_j$; also in this case, buffering of Ca²+ᵢ with BAPTA prevented G$_j$ changes. Consistent with our previous data, BAPTA also prevented uncoupling by acidification (CO₂), but not that by heptanol. The data indicate that both ATP and AA decrease G$_j$ via Ca²+ᵢ, probably by InsP₃-induced Ca²+-release. This suggests a junctional participation in functions modulated by second messengers. Supported by NIH (GM20113) and the Italian CNR (CT92.00730.CT04.115.11537).

Tu-Pos53

RECONSTITUTION OF CARDIAC NUCLEAR IONIC CHANNELS (NIC) INTO PLANAR LIPID BILAYERS.

((Rousseau E., A. Alioua, S. Proteau and A. Decrouy)) Dept. of Physiology and Biophysics, University of Sherbrooke, Sherbrooke (Quebec) Canada.

Recent evidences suggest that the nuclei possess specific ion transport mechanisms to regulate the electrolyte concentrations of the nucleoplasm and perinuclear space.
Rabbit and sheep cardiac nuclei were purified according to Kaufmann et al. (1983, J.B.C. 258). Vesicles derived from the nuclear membranes (NM) were isolated after DNA and RNA digestion, sonication and centrifugation. Both preparations were observed in electron microscopy and their protein profiles compared to the sarcolemma and SR membrane fractions on SDS-PAGE. Then, we investigated the activity of channel proteins upon fusion of NM-vesicles into lipid bilayers using various buffer conditions. In KCl (50 mM trans/250 mM cis, pH 7.2) large conducting channels (typically 85, 169 and 625 pS) were recorded. The values of the reversal potential argue in favor of a chloride selectivity. NIC display high open probabilities (Po) which were poorly voltage dependent. We assume that the 85 and 169 pS NIC are derived from the outer NM since similar conductances were reported in rat liver nuclei by Tabares et al. (1991, J.Memb.Biol. 123).
Furthermore, our approach allows the study of channel proteins from the inner membrane of the nuclear envelope
Supported by an HSFC grant. ER is a FRSQ Scholar.

INTRACELLULAR COMMUNICATION-Ca SIGNALLING

Tu-Pos54

SARCOPLASMIC RETICULUM AND MYOPLASMIC Ca²⁺ VISUALIZED IN LIVING VASCULAR SMOOTH MUSCLE CELLS WITH CONFOCAL MICROSCOPY

((M. Sturek)) Vascular Cell Biophysics Laboratory, Dalton Cardiovascular Research Center and Department of Physiology, Univ. of Missouri, Columbia, MO 65211. (Spon.: J.O. Bullock)

The association of sarcoplasmic reticulum (SR) morphologically with myoplasmic free Ca²⁺ (Ca$_m$) gradients was studied. Coronary artery cells were loaded by incubation with 2.5×10^{-7} M of the SR marker 3,3'-dihexyloxacarbocyanine iodide (DiOC$_6$) for 5 min and 10^{-5} M of the Ca$_m$ indicator Fura Red for 20 min. Both dyes were excited at 488 nm and emission was measured for DiOC$_6$ at 522 nm and Fura Red at >585 nm. No crossover of emission signals into either photomultiplier from the other channels was detected, thus pure DiOC$_6$ and Fura Red signals were measured. DiOC$_6$ had a reticular, continuous morphology in 91% of the cells (20 of 22 cells); 80% of these cells (16 of 20) showed a "web-like" morphology in the nuclear region. Minimal DiOC$_6$ was detected in confocal sections near the sarcolemma, consistent with minimal superficial SR. The ionomycin (10^{-5} M)-induced increase in Ca$_m$ was detected as a spatially homogeneous change by Fura Red, but there were no obvious spatial gradients of Ca$_m$ during slow Ca²⁺ release from the SR ("SR Ca²⁺ unloading"). These data are consistent with a highly localized subsarcolemmal Ca²⁺ (Ca$_s$) gradient during SR Ca²⁺ unloading that is best resolved with Ca²⁺-activated K⁺ currents (J. Physiol. 451:49, 1992). (Supported by NIH HL41033, RCDA HL02872 and AHA 93011900)

Tu-Pos55

REGULATION OF SPONTANEOUS TRANSIENT OUTWARD CURRENTS BY Ca RELEASE AND Ca INFLUX IN VASCULAR SMOOTH MUSCLE CELLS.

((Y.Liu, A.W.Jones and M.Sturek)) Dalton Cardiovascular Research Center and Dept. of Physiology, Univ. of Missouri, Columbia, MO 65211. (Spon. by V.Huxley)

Whole-cell K currents and fura-2 ratios were measured simultaneously in smooth muscle cells from rat aorta and saphenous arteries. Spontaneous transient outward currents (STOCs) were observed predominantly in saphenous cells (SC, ~60% vs. <10% of aortic cells). STOCs represent a localized increase of subsarcolemmal Ca concentration and activation of Ca-activated K channels, since they were not accompanied by a fura-2 ratio increase and were eliminated by replacing K with Cs or clamping Ca to zero in the pipette, or by bath application of tetraethylammonium (10 mM). While La (200 µM) did not affect STOCs, caffeine (5 mM) caused a transient increase in STOCs and later disappearance of STOCs. At physiological external Ca concentration (2 mM), about 60% of SC also displayed a low threshold (-50 mV) Ca current which was not observed in aortic cells. The current was maximal at -30 mV and could be blocked by Ni (360 µM). Furthermore, Bay K 8644 (10^{-7}M) also caused an increase in number of STOCs in SC. These data suggest that 1) STOCs are mainly related to the sarcoplasmic reticulum (SR) Ca release; and 2) pronounced increase of Ca influx may generate STOCs by either directly increasing subsarcolemmal Ca concentration or stimulating SR Ca release via Ca-induced Ca release. (Supported by HL41033, RCDA HL02872, and HL15852 and AHA 93011900)

Tu-Pos56

CALMODULIN GATES INTRACELLULAR CALCIUM WAVES IN A STOCHASTIC MODEL OF CALCIUM SIGNALING

((A. B. Stundzia, C. J. Lumsden and C. Whiteside)), University of Toronto, Toronto, Ontario, Canada M5S 1A8. (Spon. by C. Whiteside)

Intracellular calcium is a key second messenger within a dynamic signaling pathway that regulates many cellular processes. The intracellular free cytosolic calcium ([Ca⁺⁺]$_i$) signals have been observed to propagate as concentration waves in certain cell types such as Xenopus oocyte. While the [Ca⁺⁺]$_i$ signal can exhibit a heterogeneous spatio-temporal organization, the possible biological significance that the frequency and amplitude of these propagating wave patterns may have in intracellular signaling has yet to be elucidated. We have used a Monte Carlo simulation, based on the reaction-diffusion probability density function, to model the interaction of a propagating [Ca⁺⁺]$_i$ wave with calmodulin (CaM). CaM was chosen due to its central role in the regulation of cellular activity and its ubiquitous presence in eukaryotic cells. With our simulation we find that the localized intracellular CaM concentration gates [Ca⁺⁺]$_i$ wave propagation and the amplitude of the [Ca⁺⁺]$_i$ wave regulates the localized, post [Ca⁺⁺]$_i$ - CaM interaction, concentration of biologically active CaM - Ca protein-ligand complexes.

Tu-Pos57

IMAGING DEPLETION AND FILLING OF INTRACELLULAR CALCIUM STORES IN VASCULAR MYOCYTES

((L. A. Blatter)) Department of Physiology, Loyola University Chicago, Maywood, IL 60153

In vascular smooth muscle binding of vasoactive substances to surface membrane receptors leads to a rise of intracellular cytoplasmic calcium and to contraction. [Ca²⁺]$_i$ increases through release of Ca²⁺ from intracellular stores and Ca²⁺ entry through surface membrane ion channels. Membrane-permeant and membrane-impermeant forms of fura-2 were used to distinguish changes in intracellularly stored Ca²⁺ ([Ca²⁺]$_s$) from changes in cytoplasmic free Ca²⁺ ([Ca²⁺]$_i$). Digital imaging fluorescence microscopy was used to observe the spatio-temporal patterns of the movement of Ca²⁺ between these two cellular compartments in cultured vascular smooth muscle cells (A7r5 cell line). [Ca²⁺]$_s$ was measured after quenching the fura-2 fluorescence in the cytoplasmic compartment with manganese. The following results were obtained: 1) Stimulation with vasopressin (AVP) led to a transient increase of [Ca²⁺]$_i$ and to a concomitant decrease of [Ca²⁺]$_s$ (Fig. 1). The rise of [Ca²⁺]$_i$ could be blocked completely by intracellular heparin and could be terminated prematurely by NCDC, a blocker of receptor operated surface membrane calcium channels. In the absence of external Na⁺, the [Ca²⁺]$_i$-transients were larger and declined more slowly. 2) After stimulation with vasopressin, [Ca²⁺]$_i$ returned rapidly to normal resting levels, whereas the recovery of [Ca²⁺]$_s$ was much slower (Fig. 1). 3) When intracellular stores were depleted, vasopressin could still transiently increase [Ca²⁺]$_i$ (if external calcium was present), but the increase could be blocked by NCDC. 4) The refilling pathway of depleted stores involved Ca²⁺ entry into the bulk cytoplasmic compartment through receptor operated calcium channels. 5) Contrary to previous results cytoplasmic and nuclear [Ca²⁺]$_s$did not differ in resting and in stimulated cells.
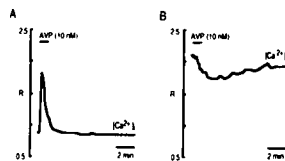
Fig. 1. Differential changes of [Ca²⁺]$_i$ and [Ca²⁺]$_s$ upon stimulation with AVP. R=F$_{360}$/F$_{380}$. A. Time course of the [Ca²⁺]$_i$-transient triggered by 10 nM AVP. The transient declined rapidly to resting levels after removal of the agonist (fura-2/salt loaded cell). B, Changes of [Ca²⁺]$_s$ during and after exposure to AVP (10 nM) recorded from a fura-2/AM loaded cell after Mn²⁺ quenching.

Tu-Pos58

CA2+ WAVE FREQUENCY MODULATION BY CA2+ - ATPASE ISOFORMS IN *XENOPUS* OOCYTES. ((P. Camacho and J.D. Lechleiter)) Dept of Neuroscience, Univ of Virginia Med Sch, Charlottesville, VA 22908.

Activated inositol 1,4, 5 trisphosphate receptors (IP_3Rs) release Ca^{2+} from intracellular stores in excitatory propagating waves (Science **252**, 123-126). The annihilation of colliding Ca^{2+} waves reveals an underlying refractory period during which further Ca^{2+} release is inhibited. We proposed and demonstrated that over-expression of a sarco-endoplasmic reticulum Ca^{2+} ATPase (SERCA1) would increase the frequency of Ca^{2+} wave activity by reducing the period of inhibition for Ca^{2+} release (Science **260**, 226-229). Here we examine Ca^{2+} ATPase isoforms SERCA2a and SERCA2b, which encode two alternatively spliced products of the same gene (J Biol Chem. **263**, 15032). The cDNAs encoding each isoform were inserted between the 5' and the 3' untranslated regions of *Xenopus* β-globin (Neuron, **9**, 861). Synthetic mRNAs were injected into stage VI oocytes. IP_3-induced Ca^{2+} release was imaged confocally, 2-9 days after mRNA injections in oocytes preloaded with Ca^{2+} Green dextran (Molecular Probes). These constructs yield higher expression levels than previously obtained with SERCA1 and result in higher IP_3-induced Ca^{2+} wave frequencies. Our experiments reveal a strong dependence of the propagation velocity (v) on wavelength (λ) as prediced by the dispersion relation (Physica D **30**, 177). We find that for $\lambda > 40$ μm, $v = 21 \pm 4$ μm/s (n=17), but when $\lambda = 20$ to 30 μm, v is reduced to 9 ± 2 μm/s (n=9) and below 20 μm, individual waves break up and fail to propagate. We are currently comparing the effects of different Ca^{2+} ATPases isoforms on Ca^{2+} wave activity. This work is supported by NIH grant # GM48451.

Tu-Pos59

ORIGIN OF NUCLEAR CALCIUM SIGNALS ((N. L. Allbritton, E. Oancea, M. A. Kuhn, and T. Meyer)) Department of Neurobiology, Stanford University, Stanford, CA 94305 (N.L.A.), Departments of Cell Biology and Pharmacology, Duke University, Durham, NC 27710 (E.O. and T.M.), and Molecular Probes, Box 22010, Eugene, OR 97402 (M.A.K.)

Transient increases in the nuclear Ca^{2+} concentration regulate gene transcription, DNA synthesis, and other nuclear processes. We determined the mechanism of nuclear calcium signaling with a novel fluorescent Ca^{2+} indicator that was targeted to the nucleus by coupling a nuclear localization peptide to Calcium Green dextran. Cytosolic Ca^{2+} signals were also measured by coinjection of nuclear and cytosolic (unmodified Calcium Green dextran) indicators. Stimulation of rat basophilic leukemia (RBL) cells by antigen or by uncaging of IP3 induced nuclear and perinuclear cytosolic Ca^{2+} transients that were separated by less than 200 ms. To determine whether nuclear Ca^{2+} ions originate from the inner membrane of the nuclear envelope or from perinuclear Ca^{2+} stores, we designed a competitive cytosolic inhibitor of the IP3 receptor by coupling heparin to a dextran matrix. This heparin-dextran was too large to passively enter the nucleus. Microinjection of heparin-dextran into RBL cells suppressed Ca^{2+} transients in both the cytosol and the nucleus. Consequently, nuclear Ca^{2+} ions originate from Ca^{2+} channels outside the nucleus and enter the nucleus through nuclear pores in less than 200 ms. These results suggest that the amplitude of nuclear Ca^{2+} signals is controlled by the density and type of Ca^{2+} channels in the perinuclear region.

Tu-Pos60

SEPARATE PATTERNS OF CALCIUM SIGNALING TRIGGERED THROUGH TWO COMPONENTS OF THE B LYMPHOCYTE ANTIGEN RECEPTOR ((D. Choquet*, G. Ku#, S. Cassard$, B. Malissen#, H. Korn*, W. H. Fridman$ and C. Bonnerot$)) *INSERM U 261, Institut Pasteur, 75724, #Marseille-Luminy, 13288, $ U 255, Institut Curie, 75005, FRANCE.

B cell antigen receptor (BcR) engagement is the first step of antigenic stimulation of B lymphocytes and is followed by multiple patterns of calcium mobilization. The BcR complex is composed of membrane immunoglobulins, as antigen recognition subunits, and of associated-chains (Ig-α and Ig-β) which couple the receptor to cytoplasmic effectors. To investigate the relative signalling capacity of Ig-α and Ig-β in isolation, chimeric proteins containing the cytoplasmic domains of either Ig-α or Ig-β were expressed on a B cell line and their ability to elicit calcium signals was tested. We found that Ig-α and Ig-β activate two distinct intracellular signalling pathways. The engagement of Ig-α chimeras provokes a complete release of calcium from intracellular stores lasting ~50 sec, followed by transmembrane calcium influx and late cell activation signals, detected by lymphokine secretion. In contrast, Ig-β chimeras do not induce lymphokine secretion or calcium influx but provoke short oscillatory release of calcium (~10 sec in duration every ~100 sec). These oscillations were dependent on the activity of the calcium ATPase pump of the endoplasmic reticulum since they were blocked by thapsigargin and DBHQ. In contrast, calcium release triggered through Ig-α chimeras was insensitive to these drugs. These results provide a structural basis for the diversity of B calcium responses and suggest that they may arise from the differential activity of calcium pumps.

Tu-Pos61

MONITORING NEAR-MEMBRANE CHANGES IN [Ca^{2+}] IN SMOOTH MUSCLE CELLS ((E.F. Etter, *M. Poenie, *A. Minta, F.S. Fay)) Biomedical Imaging Group, UMMC, Worcester, MA 01605, * Zoology Department, University of Texas, Austin, TX 78712

In stomach smooth muscle cells, as membrane depolarization triggers an influx of Ca^{2+} across the plasma membrane (PM) and a release of Ca^{2+} from the adjacent SR, the [Ca^{2+}] just beneath the membrane would be expected to rise higher and change more rapidly than the [Ca^{2+}] in the bulk cytoplasm. In images obtained using soluble Ca^{2+} indicators such localized changes in [Ca^{2+}] are obscured by fluorescence from the surrounding cytosol. Recently, Ca^{2+} indicators with lipophilic tails have been developed to selectively monitor near-membrane [Ca^{2+}]. FFP18 is the newest and has a lower Ca^{2+} affinity (Kd = 400 nM). In voltage clamped smooth muscle cells with nearly equal peak inward Ca^{2+} currents, the initial rates of rise of the FFP18-reported Ca^{2+} transients were 2-3 times faster than the rates of rise of Ca^{2+} transients reported by fura-2. This result suggests that the majority of the FFP18 signal represents the fast [Ca^{2+}] changes occurring just beneath the membrane near points of Ca^{2+} entry. As 3D images of the intracellular distribution of FFP18 indicated that 60% of the dye is bound near the PM, we calculated out a near-membrane Ca^{2+} signal from the whole-cell FFP18 fluorescence that rose almost instantaneously to >1μM upon depolarization and then decayed back to cytosolic levels. This predicted Ca^{2+} signal is being directly tested for in high resolution images of the FFP18 Ca^{2+} signal in cells, acquired every 10 msec.

Tu-Pos62

HOW WELL CAN LOCAL Ca^{2+} SIGNALS BE MEASURED IN SMOOTH MUSCLE CELLS? ((Gary J. Kargacin)) Depts. of Physiology, Univ. of Calgary, Calgary, Alberta, T2N 4N1 and Univ. of Massachusetts Med. Sch., Worcester, MA 01655.

In previous work with mathematical models of Ca^{2+} diffusion and regulation (Kargacin. Biophys. J. **64**:363a, 1992), it was concluded that high Ca^{2+} concentrations are likely to develop in smooth muscle cells near the plasma membrane during transient Ca^{2+} signals. This was especially true when the models included a barrier to free diffusion located near the membrane. In the work reported here, the models were modified to determine how well such local Ca^{2+} signals might be resolved by fluorometric Ca^{2+} indicators. In the presence of a diffusion barrier, the models predicted that a [Ca^{2+}]$_{free}$ of approxiamtely 6 μM could be reached near the plasma membrane of a cell during a transient Ca^{2+} signal that increased the central cytoplasmic [Ca^{2+}]$_{free}$ in the cell from 150 nM to approximately 500 nM. The change in [Ca^{2+}] near the membrane was resolved only poorly (maximum [Ca^{2+}]$_{free}$ = 700 nM) by an indicator that reported the average [Ca^{2+}] in the model cell. An imaging system (operating at video frame rates) with high spatial resolution reported a peak [Ca^{2+}] of 4 μM near the plasma membrane for the same simulation. Local membrane signals were also better resolved when it was assumed that the indicator was distributed preferentially to the region near the plasma membrane in the model cell. (supported by NIH AR39678 and the Heart and Stroke Foundation of Alberta)

Tu-Pos63

INHIBITION OF PROTEIN TYR PHOSPHORYLATION IS LINKED TO INHIBITION OF RECEPTOR ACTIVATED INCREASES IN INTRA-CELLULAR CALCIUM. ((L.A. Semenchuk and J. Di Salvo)) Department of Medical and Molecular Physiology, Duluth, MN 55812.

Phosphorylation of proteins on tyrosine residues participates in diverse signaling pathways. Although vascular smooth muscle exhibits high levels of tyrosine-kinase activity, surprisingly little is known of the function(s) of protein tyr-phosphorylation in this tissue. Recently we suggested that phosphorylation of proteins on tyrosine residues was linked to regulation of smooth muscle contraction (Biochem.Biophys.Res.Comm., 1993). Our data also suggest that tyr-phosphorylation may be important in regulating cytosolic calcium (Archives, 1993). Accordingly, we studied the temporal relationship between agonist induced increases in intracellular calcium ([Ca]i) and phosphorylation of proteins on tyr residues in cultured canine femoral arterial cells. Stimulation with serotonin (10μM) induced a rapid transient 4-5 fold increase in [Ca]i. Western blot analysis of parallel cultures treated with the same agonist exhibited marked transient increases in phosphorylation of a number of substrates (Mr 42-205 Daltons). Tyrphostin (80μM), a synthetic tyrosine kinase inhibitor, markedly inhibited both the increase in protein tyrosine phosphorylation and the increase in [Ca]i. Similarly, a structurally different tyrosine kinase inhibitor, genistein (30μg), also inhibited the increases in phosphorylation and [Ca]i. In contrast, pre-incubation with diadzein, a structural analog of genistein which purportedly does not inhibit tyrosine kinase activity, did not inhibit either the increase in protein tyr phosphorylation or the increase in [Ca]i. These data suggest the exciting possibility that protein-tyr phosphorylation functions in signaling mechanisms which regulate intracellular calcium. Supported by the Edwin Eddy Foundation.

Tu-Pos64

REGULATION OF INTRACELLULAR CALCIUM SIGNALLING IN INTACT CARDIOVASCULAR ENDOTHELIUM
((L. Li., R.E.Laskey., C.Van Breemen)) University of British Columbia, Vancouver, B.C V6T 1Z3 CANADA

A new method was designed for imaging $[Ca^{2+}]_i$ in endothelial cells of intact pulmonary and aortic valves of rabbit. Control experiments involving removal of the endothelium or focusing on the other elements of the valves confirmed that the fura-2 signal derived from the intact endothelial cells. In contrast to merely cultured preparation, acetylcholine induced a marked biphasic increase in $[Ca^{2+}]_i$. The activity of the Na^+/Ca^{2+} exchanger was investigated by substituting external Na^+ with NMDG or treatment with ouabain. Na^+ substitution caused a large but transient $[Ca^{2+}]_i$ signal at rest, which also increased the $[Ca^{2+}]_i$ plateau induced by carbachol; while inhibition of Na^+/K^+-pump by ouabain resulted in a slowly developing steady state increase in $[Ca^{2+}]_i$. It was concluded that the Na^+/Ca^{2+} exchanger mediates both inward and outward Ca^{2+} fluxes, and contributes to Ca^{2+} homeostasis when $[Ca^{2+}]_i$ is elevated in intact endothelial cells.

Tu-Pos65

SUPERFICIAL BUFFER BARRIER IN VENOUS SMOOTH MUSCLE
((Q. Chen and C. van Breemen*)) Dept. of Mol. Cell. Pharmacol., U. of Miami, Sch. Med., Miami, FL 33101. * Dept. of Pharmacol. & Therap., Faculty of Med., U. of British Columbia, B.C., V6T 1Z3, Canada.

It has been observed by several laboratories that discharge of calcium (Ca^{2+}) from the endoplasmic reticulum (ER) or sarcoplasmic reticulum (SR) cause an increase in the steady state intracellular Ca^{2+} concentration ($[Ca^{2+}]_i$). This observation can be explained either by an increase in Ca^{2+} influx or a decrease in Ca^{2+} efflux. In certain types of cells depletion of ER Ca^{2+} leads to an increase in the plasmalemmal permeability to Ca^{2+}. Previous work in our laboratory did not support this mechanism for venous smooth muscle based on the observation that SR depletion by itself did not increase the rate of decay in fura-2 fluorescence believed to be caused by Mn^{2+} entry in venous smooth muscle of the rabbit inferior vena cava.

Our present work offers an alternate explanation to the increase in the steady state $[Ca^{2+}]_i$ caused by SR depletion. By loading the endothelium-removed rabbit inferior vena cava with fura-2/AM, we are able to monitor the changes in $[Ca^{2+}]_i$ in the venous smooth muscle cells. After first raising $[Ca^{2+}]_i$ with a high K^+, high Ca^{2+} solution, subsequent replacement of Ca^{2+}-free external solution will result in a decline in $[Ca^{2+}]_i$. By comparing the $[Ca^{2+}]_i$ declining traces and their converted "rate-concentration" curves under different conditions, we were able to show prior SR depletion by caffeine or thapsigargin actually slows the rate of decline of $[Ca^{2+}]_i$ which reflects the process of Ca^{2+} extrusion from the cells. Inhibition of the plasmalemmal Na^+/Ca^{2+} exchanger by application of Na^+-free external solution also slows the rate of decline in $[Ca^{2+}]_i$ and there were no significant additive effects between the inhibition of Na^+/Ca^{2+} exchanger and SR depletion. We therefore conclude that SR depletion has an inhibitory effect on Ca^{2+} extrusion which results in an increase in the steady state $[Ca^{2+}]_i$. The above results support the component of the "Superficial Buffer Barrier" hypothesis which proposes that ER Ca^{2+} is discharged to the extracellular space via vectorial Ca^{2+} release into junctional cytoplasmic regions followed by extrusion via the Na^+/Ca^{2+} exchanger.

Tu-Pos66

RELEASE OF Ca^{2+} FROM INTRACELLULAR STORES ACTIVATES ELECTROGENIC Ca^{2+} UPTAKE IN CULTURED B-LYMPHOCYTES
((I. Marriott, and M.J. Mason)) Dept. of Physiology, Tulane University School of Medicine, New Orleans, LA 70112. (Sponsored by S. Grinstein)

An electrogenic Ca^{2+} influx pathway has been shown to operate in B-lymphocytes following receptor stimulation and subsequent IP_3 formation. However, the mechanism responsible for this sustained Ca^{2+} influx has not been elucidated. We have investigated the role of intracellular Ca^{2+} stores in the regulation of the Ca^{2+} permeability of cultured B-lymphocytes (CH12.LX.C4.5F5). We have used indo-1 to monitor $[Ca^{2+}]_i$ and report that depletion of an internal Ca^{2+} store by addition of thapsigargin or ionomycin results in membrane potential-sensitive changes in $[Ca^{2+}]_i$ consistent with uptake from the extracellular medium (store-regulated calcium uptake; SRCU). In order to further establish the electrogenic nature of this uptake pathway we have measured the membrane potential changes accompanying Ca^{2+} influx stimulated by release of Ca^{2+} from intracellular stores using Bis-oxonol. Addition of 5 mM Ca^{2+} to Bapta-loaded cells pretreated with doses of thapsigargin or ionomycin shown to activate SRCU induced a 21 mV (n=11) depolarization which was; 1) dependent upon Bapta loading, 2) dependent upon extracellular Ca^{2+}, 3) abolished by 5 mM Ni^{2+}, and 4) independent of extracellular Na^+. This depolarization was followed by a charybdotoxin-sensitive repolarization consistent with secondary activation of K^+ channels. These membrane potential changes temporally correlated with Ca^{2+} uptake from the extracellular medium as measured fluorimetrically with indo-1. On the basis of these experiments we conclude that an electrogenic Ca^{2+} permeable pathway exists in these cells which is regulated in large part by the degree of filling of an internal Ca^{2+} store.

Tu-Pos67

POSSIBLE INVOLVEMENT OF RYANODINE RECEPTORS IN SPHINGOSYL PHOSPHORYLCHOLINE-INDUCED CALCIUM RELEASE FROM BRAIN MICROSOMES. ((C. Dettbarn, R. Betto, P. Palade, G. Salviati and R. Sabbadini)) Dept. Physiology & Biophysics, Univ. Texas Medical Branch, Galveston, TX 77555-0641; Dipartimento di Scienze Sperimentali, University of Padova, Italy; and Dept. Biology, San Diego State Univ, San Diego, CA 92182-0057

At concentrations of 50 μM and higher, sphingosyl phosphorylcholine (SPC) produces Ca release from canine brain microsomes loaded with calcium in the presence of phosphate, ATP, an ATP regenerating system and antipyrylazo III. The release is not blocked by heparin, a competitive antagonist of inositol 1,4,5-trisphosphate (IP_3) binding to its receptor, nor inhibited as strongly as IP_3-induced Ca release is by certain blockers (100 μM W7, 200 μM tetrapentylammonium and 500 μM TMB-8) which act elsewhere on the IP_3 receptor/channel. In contrast to IP_3-induced Ca release, release induced by SPC is equally large from cerebrum microsomes as it is from cerebellar microsomes. The density of ryanodine receptors is known to be similar in both parts of the brain. Rate of SPC-induced Ca release is relatively insensitive to ruthenium red but is inhibited by the following other ryanodine receptor blockers: 87% by 100 μM added barium, 63% by 500 μM tetracaine, and 90% by 100 μM 9-aminoacridine. We conclude that SPC is more likely to open ryanodine receptors in the brain than IP_3 receptors. Such an effect of SPC would be analogous to its reported action with skeletal and cardiac ryanodine receptors.

Tu-Pos68

A SINGLE BRIEF Ca^{2+} TRANSIENT CAUSES DOWNREGULATION OF THE ACETYLCHOLINE RECEPTOR α SUBUNIT GENE IN MUSCLE ((C-F. Huang, J. Schmidt, S.S. Stroud and B.E. Flucher)) Dept. of Biochemistry and Cell Biology, SUNY, Stony Brook, NY 11794, and Lab. of Neurobiology, NINDS, NIH, Bethesda, MD 20892.

Passive depolarization of cultured myotubes with 50 mM KCl, which activates L-type Ca channels and release of Ca from the SR, is accompanied by the downregulation of extrajunctional acetylcholine receptors (AChRs). Nuclear run-on assays in C2 myotubes transfected with a reporter gene linked to the promoter of the AChR α subunit show a significant decrease of AChR gene activity 5 min after addition of 50 mM KCl and continuing decline for 1 h. Activation of L-channels with Bay-K8644 or Ca influx through the ionophore A23187 has a similar effect, while removal of extracellular Ca or buffering of cytoplasmic Ca with the membrane-permeable Ca chelator BAPTA-AM inhibit downregulation of the AChR gene. Clamping cytoplasmic free Ca concentration to 2 μM for 30 min causes half-maximal inactivation. The L-channel antagonists D600 and nifedipine also block the inhibitory effect of passive depolarization on gene regulation. Thus, the increase of cytoplasmic free Ca mediated by the dihydropyridine-sensitive Ca channel acts as second messenger in the transcriptional control of the AChR gene. The effect of Ca on gene regulation can be blocked with staurosporine, an inhibitor of protein kinase C, suggesting that Ca acts upstream of PKC. Analysis of the depolarization-induced changes in cytoplasmic free Ca using fluorescent calcium indicators shows that immediately after addition of 50 mM KCl Ca rises to levels comparable to those during tetanic stimulation and declines to resting levels within 20 s of continued depolarization with high KCl. Therefore a single calcium transient of less than 20 s in duration is sufficient to trigger inactivation of the AChR α subunit gene.

Tu-Pos69

ISOPROTERENOL DEPLETES SR Ca^{2+} IN ARTERIAL SMOOTH MUSCLE CELLS; DIFFERENTIAL EFFECT OF AGING. ((Yoshiyuki Miyashita, Steven J. Sollott, James L. Kinsella, Edward G. Lakatta and Jeffrey P. Froehlich)) NIA, NIH, Baltimore, MD 21224.

Freshly-isolated rat arterial smooth muscle cells (SMC) loaded with fura-2 and digital ratiometric fluorescence imaging were used to investigate the mechanism of isoproterenol (ISO)-induced relaxation. Pre-incubation of SMC with 1 μM ISO produced a biphasic time-dependent decrease in the sarcoplasmic reticulum (SR) Ca^{2+} pool evaluated by brief exposure to 1 μM phenylephrine (PE) or 10mM caffeine. The amount of Ca^{2+} remaining in the SR pool was greater in old (30 mo.) F344XBN rats (37.6 ± 2.36% of the pre-ISO level) than in young (6 mo.) rats (30.74 ± 7.76%; p < .05). ISO did not affect basal cytoplasmic Ca^{2+} levels. Addition of 1 μM FCCP with 1 μM PE or removal of extracellular Na^+ and Ca^{2+} (isosmotic replacement of Na^+ with choline) blocked the effect of ISO suggesting that Ca^{2+} re-distribution depends on the presence of mitochondrial and sarcolemmal membrane potentials and Na^+/Ca^{2+} exchange. Old rats showed a significant elevation in mean systolic blood pressure (155.3 ± 1.64 mm) compared to young rats (131.3 ± 5.96 mm: p < .001). We propose that the larger amounts of Ca^{2+} remaining in SR from old animals after exposure to ISO leads to more Ca^{2+} release and greater contractile activity following stimulation with smooth muscle agonists and that this may contribute to the hypertension associated with aging.

Tu-Pos70

CALCIUM CHANNELS ACTIVATED BY DEPLETION OF INTERNAL CALCIUM STORES IN A431 CELLS
((A. Lückhoff and D.E. Clapham)) Dept. Pharmacology, Mayo Foundation, Rochester, MN 55905

Depletion of internal calcium stores is one mechanism by which transmembrane Ca^{2+} influx may be induced. We studied Ca^{2+} and Ba^{2+}-permeable ion channels in A431 cells after store depletion by dialysis of the cytosol with 10 mM BAPTA solution. Cell-attached patches of cells held at low (0.5 μM) external Ca^{2+} exhibited transient channel activity, lasting for 1-2 min. Activity was prolonged when cation entry through the patch was attenuated by positive transmembrane potentials. The channel had a slope conductance of 2 pS with 200 mM $CaCl_2$ and 16 pS with 160 mM $BaCl_2$ in the pipette. Channel activity quickly ran down in patches pulled back into the inside-out configuration and was not restored by $InsP_3$ and $InsP_4$. Thapsigargin induced activation when the cells were kept in 1 mM external Ca^{2+} after BAPTA dialysis. Thapsigargin also induced transient whole-cell Ba^{2+} currents which were inhibited by Ca^{2+}. Whole-cell Ca^{2+} currents could not be resolved. The channels described here represent one Ca^{2+} entry pathway activated by depletion of internal calcium stores and are distinct from previously identified receptor-operated entry pathways in A431 cells and from calcium repletion currents in other cell types.
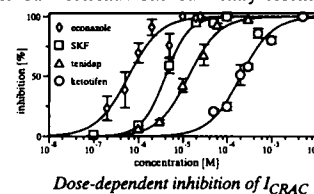
Tu-Pos71

DEPLETION OF INTRACELLULAR Ca^{2+} STORES ACTIVATES AN INWARD CURRENT IN CORONARY VENULAR ENDOTHELIAL CELLS. ((J.B. Song, C.L. Windstein, and M.J. Davis)) Dept. of Medical Physiology, Texas A&M University Health Science Center, College Station, TX 77843.

In many non-excitable cells, a Ca^{2+}-influx pathway is coupled to agonist-induced intracellular Ca^{2+} release. Although the exact mechanism which links these events remains controversial, it may involve one or more diffusible second messengers. Several lines of evidence indicate that the degree of emptiness of the Ca^{2+} store determines the activation of this influx pathway. To test this hypothesis, we applied BHQ (50 μM), an inhibitor of the intracellular Ca^{2+}-ATPase, to coronary venular endothelial cells (CVECs) while recording whole-cell current and intracellular Ca^{2+} ($[Ca^{2+}]_i$) changes. At V_h=-70 mV, BHQ activated an inward current (18/38 cells) and elevated $[Ca^{2+}]_i$ (38/38 cells). The reversal potential (E_{rev}) of the BHQ-induced current in Tyrode's bath (150 mM K^+ in pipette) averaged -12.2 ± 2.9 mV, suggesting that the pathway is not highly selective for Ca^{2+}. However, switching the bath from 1 to 20 mM Ca^{2+} in the presence of BHQ, increased $[Ca^{2+}]_i$ and inward current (n=5). Buffering intracellular Ca^{2+} abolished the $[Ca^{2+}]_i$ increase (n=4) but did not inhibit the current, suggesting that Ca^{2+} is not the signal for activation of the influx pathway. There appeared to be a threshold such that a certain amount of the Ca^{2+} store needed to be depleted before the influx pathway was triggered. When similar protocols were performed with the endothelial-dependent vasodilator, bradykinin (BK), E_{rev} for BK-induced current averaged -10 ± 1 mV (not significantly different from that for BHQ). However, the BK current was much larger in magnitude and activated much more quickly than the BHQ current. These results suggest that depletion of intracellular Ca^{2+} stores by BK activates a Ca^{2+}-influx pathway in CVECs. The differences in the magnitude and time course of the BK current may simply reflect more complete and rapid depletion of the Ca^{2+} stores by BK or indicate that additional currents are activated by BK. Supp. by NIH HL-46502.

Tu-Pos72

A CALCIUM CURRENT ACTIVATED BY STORE DEPLETION IN HUMAN LYMPHOCYTES IS ABSENT IN A PRIMARY IMMUNO-DEFICIENCY. ((M. Partiseti, F. Le Deist*, C. Hivroz*, A. Fischer*, H. Korn and D. Choquet)) INSERM U261 Institut Pasteur, 75724, *U132, Hopital Necker 75743, FRANCE

Sustained increase of intracellular free Ca^{2+} plays a crucial role in lymphocyte activation and it requires the influx of extracellular Ca^{2+} through a poorly characterized pathway. Using whole-cell and perforated patch-clamp configurations, we found that an inward Ca^{2+} current of small amplitude (ranging from -8.4 to -0.5 pA at -60 mV, 10 mM extracellular Ca^{2+}, n=72) is triggered via depletion of intracellular Ca^{2+} stores. A similar depletion was obtained by i) intracellular perfusion of IP3 ii) extracellular perfusion of ionomycin, iii) thapsigargin, a blocker of the CaATPase pump of the endoplasmic reticulum. This current displayed strong inward rectification below zero mV. It was blocked by Zn^{2+}, Cd^{2+}, Mn^{2+} and La^{3+}. It was insensitive to removal of extracellular Na^+ and its amplitude was proportional to external Ca^{2+} concentration. The physiological relevance of this current was suggested by the analysis of abnormal Ca^{2+} signaling in lymphocytes from a patient with a primary immunodeficiency. Using fura-2 video imaging, a sustained Ca^{2+} influx was detected upon antigenic stimulation, or addition of thapsigargin and ionomycin in normal lymphocytes, but not in patient's cells. In contrast, the release of Ca^{2+} from internal stores was similar in both populations. Ca^{2+} current triggered by emptying internal stores was absent in pathological cells. Our data strongly suggest that this current is responsible for sustained Ca^{2+} influx during antigenic stimulation.

Tu-Pos73

PHARMACOLOGICAL PROFILE OF CALCIUM ENTRY IN MAST CELLS ((Dorothee Franzius, Markus Hoth & Reinhold Penner)) Max-Planck-Institut für biophysikalische Chemie, Am Fassberg, 37077 Göttingen, Germany (Spon. by L. Y. M. Huang)

Ca^{2+} entry following depletion of internal Ca^{2+} stores by stimulation of plasma membrane receptors plays an important role in signal transduction (i.e., exocytosis, replenishing depleted Ca^{2+} stores). Several pharmacological agents have been used in order to discriminate between different influx mechanisms. In mast cells, the pharmacological profile of the highly selective Ca^{2+} current I_{CRAC} (Calcium Release-Activated Calcium current) was compared with the pharmacological profile of two other ion channels that play a significant role in calcium influx: a non-specific cation channel of 50-pS unitary conductance and a cAMP-activated Cl^--channel, which hyperpolarizes the membrane and therefore increases the driving force for Ca^{2+}-currents. The Ca^{2+}-entry blockers econazole, SKF and tenidap as well as the antiallergic drugs cromolyn and ketotifen blocked the different channel types with similar potencies (IC_{50}-values in the micromolar range). Therefore, one should be cautious to use these drugs as tools to separate different Ca^{2+} influx mechanisms.

Dose-dependent inhibition of I_{CRAC}

Tu-Pos74

SUBSTANCE P-INDUCED Ca^{+2} INFLUX IN ENDOTHELIAL CELLS OCCURS SECONDARY TO DEPLETION OF STORES. ((N.R. Sharma and M.J. Davis)) Dept. Med. Physiol., Texas A&M Univ. Health Science Center, College Station, TX 77843.

Substance P (SP), a potent endothelium-dependent vasodilator, induces membrane hyperpolarization in porcine coronary artery endothelial cells (PCAECs) and a biphasic elevation in cytosolic Ca^{+2} ($[Ca^{+2}]_i$) via Ca^{+2} influx and release from intracellular stores. Ca^{+2} influx occurs, at least in part, via leak mechanisms in response to an increased inward driving force for Ca^{+2} during hyperpolarization. We used the perforated patch technique and fura-2 microfluorimetry to test the hypothesis that SP activates an additional Ca^{+2} influx pathway. Changes in $[Ca^{+2}]_i$ in response to voltage steps between 0 and -100 mV were recorded in PCAECs maintained in primary culture. In the absence of SP, $[Ca^{+2}]_i$ increased by 2 nM per 1 mV decrease in membrane potential as compared to 5 nM/mV in presence of SP (n=3), implying an increase in Ca^{+2} conductance. D-tubocurarine (DTC), a blocker of Ca^{+2}-activated K^+ channels, was used to block the large outward currents activated by SP and unmask possible inward currents. In physiological saline with 1 mM DTC, an initial hyperpolarization was followed by depolarization during the $[Ca^{+2}]_i$ plateau phase, suggesting that cation influx occured at this time. Voltage-clamp recordings at a holding potential (V_h) close to the K^+ equilibrium potential showed SP-induced inward current that peaked to 45±15 pA at 60-90 secs (n=5) after SP application. Increasing bath Ca^{+2} from 1 mM to 20 mM potentiated the current, while eliminating extracellular Na^+ reduced the current. Inward current was also blocked by extracellular La^{+3} (50 μM). When cells were dialysed with 120 mM Cs^+, SP-induced inward current reversed at 3±1 mV (n=5), which was not significantly different from the reversal potential (1.2±2 mV, n=5) for inward current recorded in response to store depletion by 1,4-benzohydroquinone (BHQ). These results suggest that the SP-induced increase in Ca^{+2} conductance can be completely explained by activation of a Ca^{+2} influx pathway secondary to depletion of stores. (Supported by NIH HL#45602)

Tu-Pos75

TWO MECHANISMS OF CA^{2+}-DEPENDENT INACTIVATION OF DEPLETION-ACTIVATED CA^{2+} CHANNELS. ((Adam Zweifach and Richard S. Lewis)) Dept. Mol. Cell. Physiol., Stanford U. Sch. Med., Stanford, CA 94305. (SPON: P. Drain).

Depletion of intracellular Ca^{2+} stores in many non-excitable cells activates a Ca^{2+} current, I_{CRAC} (Calcium Release Activated Ca^{2+} Current). I_{CRAC} was activated in Jurkat leukemic T cells by intracellular dialysis with 1.2-12 mM EGTA ($[Ca^{2+}]_i$=10 nM) through the whole-cell recording pipette. Two types of inactivation, fast and slow, were observed. Fast inactivation reduced I_{CRAC} ~50% during 200 ms steps from -25 to -100 mV. Fast inactivation appears to be Ca^{2+}-dependent, since (1) substitution of 12 mM $BAPTA_i$ for 12 mM $EGTA_i$ reduced the rate and extent of inactivation for a given potential, and (2) depletion-activated current carried by Ba^{2+} did not inactivate. In addition, fast inactivation was enhanced by conditions that increase the Ca^{2+} flux through open channels (hyperpolarization or elevated $[Ca^{2+}]_o$), but was unaffected by a blocker (SKF 96365) that reduced the whole-cell current. These results suggest that fast inactivation is confined to a local microdomain of elevated $[Ca^{2+}]_i$ generated by each channel. Slow inactivation developed over 10's to 100's of sec after elevation of $[Ca^{2+}]_o$ from 0 to 22 mM. Slow inactivation is also Ca^{2+}-dependent, since with 1.2 mM $EGTA_i$, I_{CRAC} decayed to ~0 within 80-100 s, whereas with 12 mM $EGTA_i$, inactivation was only ~50% complete after 600 s. Recovery from slow inactivation occurs during perfusion with a Ca^{2+}-free external solution. 0.2-1 μM thapsigargin (TG) prevented ~40% of the slow inactivation observed with 1.2 mM $[EGTA]_i$, suggesting that refilling of TG-sensitive Ca^{2+} stores contributes to this process.

Tu-Pos76

STRUCTURAL STUDIES OF BULGED ADENINES THAT ARE HIGHLY CONSERVED IN THE 16S RRNA
((Renée R. Johnson, Darryl A. LeBlanc & Kathleen M. Morden)) Dept. of Biochemistry, Louisiana State University, Baton Rouge, LA 70803

Nucleic acid structures in which only one strand of the helix contains an unpaired base (or bases) are known as bulges. Single and multiple base bulges are ubiquitous features of folded RNA molecules and clearly play important functional roles in RNA-protein and RNA-RNA interactions. Bulged purines, adenine in particular, are thought to be important for the structure and function of 16S rRNA in which they are extremely common and in some cases highly conserved.

We are using multidimensional heteronuclear magnetic resonance (NMR) spectroscopy to probe the structures of two RNA hairpins which contain highly conserved adenine bulges derived from 16S rRNA. For an A-bulge between two G•C bp, NOESY data that the bulge is stacked within the helix.

```
5'  GGAGUG-GUUC   G  C      5'  GGAGCU-CGUC   G  C
3'  CUUCACACAAG   A  A      3'  CUUCGAAGCAG   A  A
```

Estimation of coupling constants and supporting NOESY data reveal that the riboses of the bulge and C 3' to the bulge adopt a C2'-endo conformation. Studies of the A-bulge with a neighboring A•U base pair, which allows either of the two As to be bulged, are in progress and will be discussed.

Tu-Pos77

NUCLEIC ACID MODELING TOOL(NAMOT):AN INTERACTIVE GRAPHIC TOOL FOR MODELING NUCLEIC ACID STRUCTURES.((Chang-Shung Tung and Eugene S. Carter)) Theoretical Biology and Biophysics(T-10), Theoretical Division, Los Alamos National Laboratory, Los Alamos, NM 87545

The helical nature of most nucleic acids makes the modeling of these structures a unique task. The integrity of the structure of nucleic acids depends strongly on the base pairing geometry. Alterations in the tertiary structure(i.e, bending,streching, compressing, etc.), in general should not alter the base pairing. A molecular modeling tool accounting for this unique property of the molecule has been developed. The modeling is carried out on a set of reduced coordinates developed in our laboratory, as opposed to the set of Cartesian coordinates. The set of reduced coordinates allows for structural alterations without disturbance of the base pairing. The package has a Graphical User Interface for user freindliness as well as graphic routines to display the image of the molecule while the work is being executed. The program was written using X11R5 Xlib routines and the XView toolkit to ensure portability to different unix platforms. Currently, NAMOT is supported under Solaris 1.x, Solaris 2.x, and Linux.

Tu-Pos78

AB INITIO VIBRATIONAL ANALYSIS OF DIMETHYL PHOSPHATE: A MOLECULAR FORCE FIELD FOR THE PHOSPHATE GROUP OF DNA. ((Yifu Guan and George J. Thomas, Jr.)) Division of Cell Biology and Biophysics, School of Biological Sciences, University of Missouri, Kansas City, MO 64110.

In order to develop a satisfactory molecular force field for the DNA phosphate group and to gain an improved understanding of the conformational dependence of its vibrational spectrum, we have carried out *ab initio* calculations (3-21+G*) on the dimethyl phosphate (DMP) anion. The DMP anion serves as the simplest model compound for the nucleic acid phosphodiester moiety. *Ab initio* calculations were performed on the geometry-optimized *gauche-gauche* conformation of three DMP isotopomers, $(CH_3O)_2PO_2^-$, $(CD_3O)_2PO_2^-$ and $(^{13}CH_3O)_2PO_2^-$, for which vibrational spectra are available. The *ab initio* results are in good agreement with both the experimental data and with the results of normal coordinate calculations obtained with a generalized valence force field for DMP. The experimental and calculated results have been combined to develop a consistent molecular force field for all normal modes of the C-O-P-O-C network and its alkyl substituents. The present force field resolves previous problematic assignments for the conformationally-sensitive symmetric and antisymmetric skeletal stretching modes and demonstrates substantial anharmonicity in hydrogen-stretching vibrations. This force field is being adapted to *gauche-trans* and *trans-trans* conformers of DMP and to more complex models of the DNA phosphodiester backbone.
[Supported by NIH Grant AI18758.]

Tu-Pos79

FRET STUDIES OF OLIGO-DNA INTERACTIONS. ((K. M. Parkhurst and L. J. Parkhurst)) Dept. of Chemistry, Univ. of Nebraska, 68588-0304

Fluorescence resonance energy transfer (FRET) was used to follow the binding of the double labeled deoxy-oligo 5'R-GTAAAACGACGGCCAG-3'F (O16) to complementary oligos and to M13mp18(+). R is x-rhodamine and F is fluorescein. Changes in the 3'-5' distance distribution P(R) were explored using steady-state and lifetime methods (SLM 4850 MHF FT Spectrofluorometer) to analyze the fluorescence of F. The steady-state methods employed additions of I⁻ at constant ionic strength. They proved unreliable since the quenching constant showed a strong dependence on (I⁻). Excellent fits to the lifetime data were obtained using shifted Gaussian distributions for P(R). For O16 alone, the average end-to-end distance, <R>, in 0.18M NaCl was 54.1Å; in 1M KCl, the distance was 45.3Å, whereas the corresponding values for σ(R) were 6.5 and 15.3Å. In the 16-mer duplex structure <R> was 68.5Å, and σ(R) was 6.4Å. These values were obtained assuming $\kappa^2 = 2/3$. Part of the apparent distance distribution must also reflect $P(\kappa^2)$. From data fitting we conclude that the assumption that the joint distribution is separable is untenable if $P(\kappa^2)$ is that for completely random orientations of the two transition dipoles. The kinetics of hybridization of O16 to M13mp18(+) are consistent with rapid secondary structural fluctuations around the target site and not with multiple initiation sites. (Grant Support NIH DK 36288, Univ. of Nebraska Center for Biotechnology.)

Tu-Pos80

INTERACTION OF ACTINOMYCIN D WITH NON-GpC SITES OF DNA. ((S. A. Bailey, D. E. Graves)) Department of Chemistry, University of Mississippi, University, MS 38677.

Strong binding of the antitumor antibiotic ACT D to the sequence 5'-TGGGT-3' in double stranded DNA has recently been established with equilibrium binding studies (Bailey, *et al.*, 1993). ACT D binding to this -TGGGT- containing sequence was shown to be comparable to that of an -XGCY-containing oligonucleotide ($K_{int} \sim 10^6$ M⁻¹). Investigation of -TGGGT- as a high affinity binding site for ACT D follows from the 1989 sequencing study by Riill, *et al.* in which the photoaffinity analog of ACT D (7-azidoactinomycin D) was used to determine DNA base sequence specificities and neighboring base effects. The studies presented here examine the guanine requirements for ACT D binding to such nonclassical dGpC sites by varying the number of central guanine residues in a series of selected duplex oligonucleotides. The central -T(G)ₙT- motif varies from n = 1 to 4. ACT D binding to each of these elevenmers is characterized and correlated with binding to oligonucleotides of identical length and similar sequences that contain classical dGpC binding sites. Binding affinities of ACT D to this series of oligonucleotides can be summarized as -TGGGT- > -TGGT- > -TGGGGT- > -TGT-. The kinetics of SDS-induced dissociation of ACT D from these oligonucleotides revealed single exponential decays of varying duration. With the exception of the -TGGGT-containing oligomer, dissociation times for the T(G)ₙT duplexes were drastically different and much shorter than the times obtained for the dissociation of ACT D from oligonucleotides having classical GpC sites. Dissociation constants ranged from 1155 sec for -TGGGT- to 83 sec for -TGGGGT-. The binding energetics for these drug-DNA interactions are quantitated and are presented as a function of the number of central guanines. We observed an unusual (positive) binding enthalpy for ACT D with the -TGGT- sequence, whereas binding to all of the other sequences exhibited negative enthalpies. Thus, addition or deletion of one G to or from the original -TGGGT-site we examined causes significant changes in both binding affinity and energetics, with the number of binding sites per duplex remaining constant. These changes and how they correlate with changes in the base sequence are presented as a full thermodynamic profile.

Tu-Pos81

ANOMALOUS PROTONIC EQUILIBRIA IN THE MINOR GROOVE OF DNA. ((Sue Hanlon & George Pack)) University of Illinois Col. of Medicine at Chicago (Chicago, IL 60612) & Rockford (Rockford, IL 61107).

To test the prediction of Lamm & Pack ((1990) **Proc. Natl. Acad. Sci., U.S. 87,** 9033-9036) that the grooves of the DNA duplex have an excess of protons, 1 to 2 orders of magnitude higher than that of bulk solvent, we have linked a pH sensitive probe to DNA. Specifically, glycine, β-alanine and γ-amino butyric acid have been coupled through their amino groups to random sequence DNA utilizing a reaction extensively investigated by Hanlon & coworkers (Maibenco, et al (1989) **Biopolymers 28,** 549-571). Using formaldehyde, a primary amine can be coupled to the amino group of G residues in a manner which does not interfere with the B structure of DNA. The positive charge introduced in the minor groove induces overwinding of the duplex, which can be monitored by CD spectroscopy. The adducts created with the amino acids exhibit lower rotational strengths of the positive CD band above 260 nm, compared to the controls, when the pH of the solvent (5 to 7) is 2 to 3 units above the pKa's of the COOH groups. This effect is reversed by rapid titration to higher solvent pH's, without significant loss of the adduct. These results reveal that the adducts bear a net positive charge at solvent pH's between 5 and 7, implying that the carboxyls are substantially protonated under these conditions, in accord with Lamm & Pack's model. We cannot entirely rule out, however, contributing factors such as conformational effects and/or hydrogen bonding of the COOH groups to the backbone. Nevertheless, we can unequivocally conclude that the protonic equilibria in the local environment of the minor groove are significantly different from that in bulk solvent. (CRBF92-124).

Tu-Pos82

STRUCTURE OF THE ALTROMYCIN B (N7-GUANINE)-DNA ADDUCT.
((Mark Hansen, and Laurence Hurley)) DDI, College of Pharmacy, The University of Texas at Austin, Austin, Texas 78712-1074

Altromycin B belongs to the pluramycin family of antitumor antibiotics, which also includes kidamycin, hedamycin, pluramycin, neopluramycin, DC92-B, and rubiflavin A. In the present investigation, we have used nuclear magnetic resonance to determine the structure of the altromycin B–DNA adduct and propose a mechanism for covalent modification of DNA. The altromycin B–guanine adduct was isolated from calf thymus DNA after thermal depurination of the alkylated DNA. Mass spectrometry confirmed that altromycin alkylated DNA through guanine, and ^{1}H-, ^{15}N- and ^{13}C-NMR were used to confirm the covalent linkage sites between altromycin B and guanine. The structure of the bis-altromycin B-d(GAAGTACTTC)₂ adduct, as determined through high field NMR, demonstrates that the drug intercalates into DNA interacting with both grooves of the DNA. Based upon these results, we propose that altromycin B first intercalates into DNA via a threading mechanism, reminiscent of nogalamycin, inserting the disaccharide into the minor groove and positions the epoxide in the major groove in proximity to N7 of guanine. Nucleophilic attack from N7 of guanine leads to an acid catalyzed opening of the epoxide, resulting in the altromycin B–DNA adduct. Based upon these results, a general mechanism for the interaction of the pluramycin family of antibiotics with DNA is proposed.

Altromycin B

Tu-Pos83

A NEW METHOD FOR DNA FOOTPRINTING BY PHOTOLYSIS OF METHYL-AND ADENOSYLCOBALAMIN BOUND TO DNA.

((B. Sclavi, J. Newman, M.R. Chance, M.D. Brenowitz)) Departments of Physiology and Biophysics and of Biochemistry, Albert Einstein College of Medicine, Bronx, NY, 10461

We have developed a new "footprinting" method based on the photolysis of methyl- and adenosylcobalamin. The anaerobic photolysis of methyl- and adenosylcobalamin generates Co(II) and a methyl and a nucleoside free radical respectively. In the presence of O_2, aquocobalamin, formaldehyde and adenosine 5'-aldehyde are also produced from the methyl and the adenosyl species. A decrease in the electrophoretic mobility upon agarose electrophoresis of plasmid DNA photolyzed in the presence of cobalamin suggests the the carbon radicals generated from this reaction can modify the DNA. Multiple intermediates were observed in this reaction. Upon treatment with piperidine of the ^{32}P labeled DNA modified by cobalamin photolysis, cleavage occurs at each base that is modified. Analysis of the products by denaturing gel electrophoresis shows that guanines are the only bases not modified. This photolysis technique can potentially be used for footprinting of DNA-protein complexes on millisecond time scales when coupled with stopped flow methods.
Supported by grants from the Hirshl-Weill Caulier Trust and the American Cancer Society.

Tu-Pos84

CONFORMATION AND STABILITY OF THREE-ARM DNA JUNCTIONS CONTAINING UNPAIRED BASES

((Min Zhong, Michael S. Rashes and Neville R. Kallenbach))
Department of Chemistry, New York University, New York, NY 10003

Three arm DNA junctions, in which three double helices intersect at a branch, have unique structure and reactivity of bases at and near the branch. Their solution conformation is asymmetric in the presence of Mg²⁺, while bases at the branch are sensitive to single strand specific agents. Following the surprising report by Leontis' group that unpaired bases at the branch stabilize three arm junctions, we have investigated the geometry and thermodynamics of three arm junctions containing pendant T and A bases. The results are consistent with formation of additional structure in junctions containing up to four pendant bases at the branch: relative to the tight junction, the thermal stability of junctions with two T's or A's at the branch increases; bases near the branch become less reactive to single strand reactive probes; and the enthalpy of formation is more negative. The interaction of ethidium observed at the branch in three arm junctions is enhanced in junctions containing unpaired bases at the branch. The geometry of three arm junctions is perturbed only slightly by the presence of pendant bases, as seen by measuring the electrophoretic mobility of junctions to which long duplex arms are appended pairwise.

This research was supported by Grant CA24101 from the National Cancer Institute, NIH.

Tu-Pos85

REFINEMENT OF THE STRUCTURE OF A BRANCHED DNA THREE-WAY JUNCTION AND INTERACTIONS WITH CATIONIC PORPHYRINS. (((I.V.Ouporov and N.B.Leontis)) Chemistry Department, BGSU, Bowling Green, OH 43403

We have refined the structure of the DNA Three-Way Junction (TWJ) proposed in earlier work (Leontis et al, JBMSD, 1993). The refinement calculations were made in two steps: First we used simulated annealing with interproton constraints obtained from a short mixing time 2D NOESY experiment (60 ms mixing time). Then we used the back-calculation refinement procedure (XPLOR v. 3.1) with intensities from a 2D NOESY spectrum acquired with 200 ms mixing time. Both spectra were acquired at 600 MHz on the same day. The stability of the resulting structure in water solution was investigated by carrying out a 30 ps MD simulation using the CHARMM 22 force field. The conformations of the sugar-phosphate backbone and parameters of DNA helicies were investigated. Computer modeling technques were also applied to explore the intercalative binding of cationic porphyrins (meso-tetra(para-N-trimethylaniliniumyl) porphine, meso-tetra(4-N-methylpyridiniumyl) porphine) to the DNA junction. The refined NMR structure of the TWJ was used as a starting point. Two binding locations were identified for porphyrin inside the junction region. The porphyrins were docked by hand and the structures subjected to gentle minimization followed by MD simulation in water.

N.B. Leontis, M.T. Hills, M. Piotto, A. Malhotra, J. Nussbaum, and D.G. Gorenstein (1993), "A Model for the Solution Structure of a Branched, Three-strand DNA Complex." Journal of Biomolecular Structure and Dynamics, In Press.

Tu-Pos86

TRIPLEX FORMATION WITH MIXED PYRIMIDINE-PURINE SINGLE-STRANDED SEQUENCES INVOLVING C-NUCLEOSIDES IN THE SECOND STRAND. ((T. Trapane, M. Christopherson, D. Wang, C. Roby and P. Ts'o)) Dept. of Biochemistry, Johns Hopkins SHPH, Baltimore, MD 21205.

Recognition of single-stranded, nucleic acid targets without restriction of sequence (mixed pyrimidine-purine content) is studied by triplex formation involving (a) second strands containing pyrimidine C-nucleoside residues and (b) third strands containing homopyrimidine or homopurine sequence. Two deoxyoligonucleotide sequences (d-T₂AT₃AT₂ATAT and d-A₂TA₃TA₂TATA) which contain A and T residues in a nonsymmetrical arrangement, are used as target strands in this study. Second strands (d-AψAψA₂ψA₃ψA₂ and d-ψAψAψA₂A₃A₂) contain the crucial nucleoside residue, pseudouridine (ψ), which has Watson·Crick complementarity to adenosine. In our triplex model, the nitrogen function at N1 in ψ provides an extra H-bonding site for third strand binding to duplexes comprised of T·A and A·ψ base pairs. Homopyrimidine third strands contain T and C residues which may form T·A T and A·ψ C triads in a parallel second third strand (Hoogsteen) motif, or which may form T·A C and A·ψ T triads in an antiparallel motif. Homopurine third strands contain G and A which may form T·A G and A·ψ A triads in a parallel motif, or which may form T·A A and A·ψ G triads in an antiparallel (tRNA) motif. The second and third strand oligomers in our model system contain the nonionic methylphosphonate backbone. Incorporation of the deoxypseudouridine residue into the second strand is accomplished through a challenging synthetic procedure. [Supported by NCI, DOE and Genta]

Tu-Pos87

TRIPLEX FORMATION BY METHYLPHOSPHONATE THIRD STRANDS CONTAINING PSEUDOISOCYTIDINE vs CYTIDINE OR ISOADENOSINE vs ADENOSINE WITH A DNA DUPLEX TARGET. ((T. Trapane, Y. Zhao, D. Wang and P. Ts'o)) Biochemistry, Johns Hopkins SHPH, Baltimore, MD 21205.

Triplex formation involving natural duplex DNA containing homo-pyrimidine·homopurine strands has been studied under a variety of situations, usually involving thymidine and protonated cytosine for a pyrimidine (Hoogsteen) third strand binding motif or guanosine and adenosine for a purine (tRNA) motif. Our experimental study is designed to test whether third strands containing nonionic backbone (methylphosphonate) affords a highly favorable situation for triplex formation. Our previous investigation (Ono, et al., *J. Org. Chem.*, 57, 3225, 1992) indicated that substitution of cytosine (C) by pseudoisocytidine (ψiC) allows triplex formation at neutral pH in a homopyrimidine third strand Hoogsteen binding motif via a C·G ψiC base triad. In addition, our model study proposes a new purine third strand binding motif (based upon G-tetrad pur pur base pair geometry) which involves isoadenosine (iA, 2-aminopurine) instead of adenosine (A, 6-aminopurine) to give the isomorphic base triads C·G G and T·A iA. Third strand polarities in both the Hoogsteen and G-tetrad motifs are parallel to the homopurine strand of the target duplex. The target duplex used in these studies (d-TG₂TC₆T₄CT₄G₂T·d-AC₂A₄GA₄G₆AC₂A) is found in the HTLV-III virus and was studied earlier by our laboratory. Third strands with nonionic methylphosphonate backbone have these sequences: 1) d-T₄CT₄C₆T, 2) d-T₄(ψiC)T₄(ψiC)₆T, 3) d-A₄GA₄G₆A and 4) d-(iA)₄G(iA)₄G₆A. [Supported by NCI, DOE and Genta]

Tu-Pos88

MOLECULAR DYNAMICS STUDIES OF SUPERCOILED DNA: GENERATION OF THERMODYNAMIC ENSEMBLES. ((D. Sprous, R.K.Z. Tan and S.C. Harvey)) Dept. of Biochemistry and Molecular Genetics, Univ.of Alabama at Birmingham, Birmingham, AL 35294

Most modeling studies of supercoiled DNA are based on equilibrium structures. Since closed circular DNAs are very flexible, it is not known whether substantial errors are introduced by calculating properties from a single equilibrium structure, rather than from a complete thermodynamic ensemble. We have investigated this question using a low-resolution molecular dynamics model in which each basepair is represented by three points (a plane). This allows the inclusion of sequence-dependent variations of the roll, tilt, and twist. We examined the rate of convergence of various parameters, the most slowly converging of which is the *antipodes profile*. In a plasmid with N basepairs, the antipodes distance is the distance d_{ij} from basepair i to basepair j = i+N/2, and the antipodes profile at time t is a plot of $d_{ij}(t)$ over the range i = 1,N/2. In a homogenous plasmid, convergence requires that the antipodes profile averaged over time must be flat. Convergence is slowest for homogenous sequences, more rapid for random sequences, and most rapid for sequences containing sequence-directed curves. Doubling the size of a plasmid increases the CPU time required for convergence by a factor of about ten. The average properties of the ensembles were found to differ from those of static equilibrium structures. Further, average and dynamic properties are affected by both plasmid size and sequence.

Tu-Pos89

MOLECULAR DYNAMICS STUDIES OF SUPERCOILED DNA: EFFECTS OF SEQUENCE AND LINKING DIFFERENCE ON STRUCTURAL TRANSITIONS. ((R.K.-Z. Tan, D. Sprous and S.C. Harvey)) Department of Biochemistry and Molecular Genetics, University of Alabama at Birmingham, Birmingham, AL 35294 (Sponsored by A. Malhotra)

Motions within DNA were studied with a simplified model with three atoms per base pair, using molecular dynamics. Small plasmids were investigated, up to 600 bp. We find that slithering (in which the DNA slides along the circular helix axis without changing the overall conformation) is a primary means by which different regions within the plasmid are brought into close contact. Slithering is relatively free in sequences that have no intrinsic curvature. In a random sequence with small irregularly distributed curves, slithering is very much inhibited. Branching or looping provides an additional means by which distant parts of the DNA are brought together. For a straight sequence with a small insert containing curved DNA, the structure is immobilized with little slithering or looping.

Tu-Pos90

MONTE-CARLO SIMULATION OF CIRCULAR DNAS: FIRST TRANSITION IN WRITHE AND TWIST ENERGY PARAMETERS ((J.A. Gebe and J.M. Schurr)) Department of Chemistry, University of Washington, Seattle, WA ,98195

Circular DNAs were modeled as semi-flexible filaments whose potential energies are determined by the bending and torsional rigidities of the DNA and also by screened coulomb self interactions. Monte-Carlo simulations were used to (1) determine the feasibility of observing the first transition to writhe of small circles, and 2) to ascertain the relative supercoiling free energies of plectonemic (straight interwound) and trefoil (simply knotted) DNAs as a function of linking difference (ΔLk). Out algorithm simulates DNAs of fixed linking difference and samples Euler angle space in an unbiased manner. We find that the potential energy surface of 468 bp DNA at the transition point (ΔLk=1.60) exhibits two broad minima with the same energy at the writhe values w=0.1 and 0.8 separated by a barrier of about 1.6 k_BT, and their relative energies vary slowly with ΔLk, so the transition appears quite broad. Computed diffusion coefficients as a function of ΔLk also show a broad transition. The proportionality constant (E_T) between the supercoiling free energy and (ΔLk)^2 was determined for plectonemic and trefoil DNAs. For an 1800 bp DNA, we find E_T=1288 ± 29 for the plectonemic form, in agreement with experiment, and E_T=1614 ± 38 for the trefoil. Preliminary simulations on a 4.8 kbp DNA also indicates a larger E_T-value for the trefoil.

Tu-Pos91

EFFECT OF CIRCULARIZATION ON THE TORSION CONSTANT OF A SMALL DNA. ((P. J. Heath, S. A. Allison, and J.M. Schurr)) Department of Chemistry BG-10, University of Washington, Seattle, WA 98195.

Does circularization of a small DNA affect its secondary structure and torsion constant (α)? To answer this question, a sample containing a 4:1 mixture of 181 and 227 bp restriction fragments was characterized under various conditions by circular dichroism (CD) and time-resolved fluorescence polarization anisotropy (FPA). This sample was then circularized with very high efficiency by ligating in the presence of HU protein to obtain a 4:1 mixture of 181 and 227 bp circles. These circles were also investigated by CD and FPA. Our FPA data analysis code was extended to treat circular species and also adapted to treat a known concentration ratio of two species with different lengths (L) under the assumption that all other molecular parameters are the same. This code was tested on Brownian dynamics simulations of small (196 bp) linear and circular chains with input α-values and persistence lengths typical of real DNAs. These simulations contain the forces, as well as torques, that arise from the torsion potential and drive crankshaft motions. Such forces are omitted from the analytical theories in the data analysis code. For both linear and circular species, the best-fit α-value was 11 % lower than the input value, so a correction factor of 1.11 was applied to all α-values obtained from experimental data. The α-value of the linear species was anomalously low (3.4 x 10^{-12} erg) in the absence of Mg^{2+}, stiffened into the normal range in the presence of 10 mM Mg^{2+}, and returned to its low value upon removal of Mg^{2+}. Upon circularization the α-value increased 2.6-fold to 9.0 x 10^{-12} erg in the absence of Mg^{2+}! These changes in α were accompanied by significant changes in CD. Clearly, circularization substantially affects the secondary structure and torsion constant of this DNA.

Tu-Pos92

STIFF (DNA) AND FLEXIBLE (NaPSS) POLYELECTROLYTE CHAIN EXPANSION AT VERY LOW SALT CONCENTRATIONS. ((N.Borochov and H.Eisenberg))Structural Biology Department, The Weizmann Institute of Science, Rehovot 76100 Israel.

The expansion of sodium polystyrene sulfonate (NaPSS) polyelectrolyte coils has been studied by light scattering and velocity sedimentation at NaCl concentration 0.5 to 0.001M. Good agreement between the flexible NaPSS and the intrinsically stiff DNA is obtained in terms of the conformation-space renormalization-group approach. Present polyelectrolyte and excluded volume theories are not adequate to satisfactorily interpret the experimental results.

Tu-Pos93

END EFFECTS ON THE DETERMINATION OF THE DONNAN COEFFICIENT FOR SODIUM BINDING TO OLIGONUCLEOTIDES AS A FUNCTION OF SALT CONCENTRATION, BASE SEQUENCE AND LENGTH

((A. P. Williams)) Department of Chemistry, Swarthmore College, Swarthmore, PA 19081. (Sponsored by R. F. Pasternack)

We have used equilibrium dialysis experiments to determine the Donnan coefficient in solutions of double-stranded oligonucleotides as a function of salt concentration, oligonucleotide length and base sequence. The Donnan coefficient is a measure of electrostatic nonideality in ternary solutions and is used to ascertain the thermodynamic consequences of counterion association with nucleic acids (Strauss; 1967). We have designed a multi-cell equilibrium dialysis apparatus that restrains short oligomers (8-12 base pairs) but passes NaCl. The apparatus is immersed in an aqueous NaCl bath. The dialysis cells are equilibrated with the bath for at least 72 hours. Blank cells, containing no oligomer, are used to determine equilibration. The Na$^+$ concentration on the two sides of the dialysis membrane is determined using atomic absorption spectroscopy. The measured Donnan coefficient is compared with the results of the Counterion Condensation theory (Fenley; 1990) and Monte Carlo models of oligonucleotide solutions (Olmsted; 1989).

Strauss, U. P., Helfgott, C., Pink, H (1967) J. Phys. Chem. 71, 2550-2556
Fenley, M.O., Manning, G.S., Olson, W.K. (1990) Biopolymers 30, 1191-1203.
Olmsted, M., Anderson, C.F., Record, M.T. Jr. (1989) Proc. Natl. Acad. Sci. USA 86, 7766-7770.

Tu-Pos94

THEORY OF COMPETITIVE ELECTROSTATIC BINDING OF CHARGED LIGANDS TO CYLINDRICAL POLYELECTROLYTES. ((Ioulia Rouzina and V.A. Bloomfield)) Biochemistry, University of Minnesota, St.Paul MN 55108. (Spon. by M. Gulotta)

Binding constants of multivalent cations to DNA exhibit a strong dependence on salt concentration [M^+]. This is conventionally interpreted in terms of the displacement of N monovalent counterions by the N-valent ligand, leading to a slope $\partial logK_{obs}/\partial log[M^+]$ close to N. The dependence of K_{obs} on the degree of binding often has been analyzed by a McGhee-Von Hippel type of isotherm, with each ligand having the same intrinsic affinity for DNA, but with the binding process at later stages inhibited by steric exclusion of ligands bound at neighboring sites. This picture, though obviously irrelevant to the electrostatic problem, gives a reasonable account of the salt dependence of K_{obs} in the limit of zero binding, but misses the polyion influence on the value of K_{obs}. In the present work we use a more appropriate Poisson-Boltzman approach to calculate K_{obs}. For the simplest model of two point-charge counterion species, competitively screening a uniformly charged surface, we obtain an analytical expression which expresses the value of K_{obs}, and its dependence on salt concentration, in terms of polyion properties. This analysis shows the reason for the success of the conventional approach, as well as the limitations of its applicability. It puts the problem in the general context of the screening of a charged macroscopic body by electrolyte. DNA is shown to behave with increasing ionic strength first as a highly charged cylinder, then as a highly charged plane, and finally as a slightly charged plane.

Tu-Pos96

CO-CONDENSATION OF MONONUCLEOSOMAL AND PLASMID DNA BY HEXAAMMINE COBALT (III): EFFECT OF PERSISTENCE LENGTH DNA ON SIZE AND SHAPE OF CONDENSED PARTICLES. ((C.G. Baumann & V.A. Bloomfield)) Biochemistry, U. of Minnesota, St. Paul MN 55108 (Spon. by A. Rosenberg)

DNA condensation induced by hexaammine cobalt (III) cations yields compact states with either a toroidal shape, similar to that released from lysed bacteriophage heads, or a rod-like shape. DNA of >400 bp is known to form ordered particles, while shorter DNA (e.g., 160 bp mononucleosomal DNA) does not. The shorter DNA species are thought not to collapse due to their inability to form the required stable nucleus. We conjectured that the shorter DNA species would form ordered particles if a stable nucleus for condensation were provided by a larger DNA species. In the present study, mononucleosomal DNA was condensed in the presence of plasmid DNA under conditions in which plasmid DNA is known to condense. Electron microscopy showed that condensation did occur and was accompanied by pronounced changes in particle morphology as the weight fraction of plasmid DNA is increased at constant total DNA concentration. In the absence of plasmid DNA the shorter species did not form ordered particles. As the weight fraction of plasmid DNA increased, a gradually shift in morphology from rods to toroids was observed. The mean circumference (1100 Å) and width (150 Å) of the toroids formed at all weight fractions were nearly identical. Rod lengths fluctuated significantly from the mean (1300 Å) at low weight fractions of plasmid DNA (0.1-0.4) while rod widths (250 Å) fluctuated only slightly. Short DNA species cannot nucleate ordered particles, perhaps because they cannot bend and overlap sufficiently.

Tu-Pos98

CONFORMATIONAL CHANGES INDUCED IN DNA BY HEXA-AMMINE COBALT(III) AND ETHANOL. ((Jay Wenner & V.A. Bloomfield)) Biochemistry, U. of Minnesota. (Spon. by R. Lovrien)

We have used circular dichroism to study the conformational response of plasmid and 160 bp mononucleosomal calf thymus (CT) DNA to increasing ethanol concentration in the presence and absence of hexaammine cobalt (III) chloride (CoHx). Multivalent cations such as CoHx cause condensation, or orderly aggregation, of DNA longer than 400 base pairs. The morphology of the condensed particles changes with increasing ethanol concentration. The current work aims at correlating these morphological changes, which were detected by electron microscopy, with transitions in secondary structure of the DNA helix. Aggregation in this system makes data interpretation difficult. We have addressed this in two ways. The first is by using low DNA concentrations (5 μg/mL), to slow down if not eliminate aggregation. The second is by comparing plasmid DNA (which can condense) with CT DNA (which cannot condense under these conditions), to subtract the circularly polarized scattering effects due to condensation. Preliminary results suggest a B-form → A-form transition between 17 and 25 wt % ethanol (a change of dielectric constant from 70 to 65), which may correspond to a change in condensate morphology from toroid → rod. This ethanol concentration is well below that known to provoke a B → A transition, or DNA precipitation, in the absence of multivalent cations.

Tu-Pos95

ELECTROSTATIC AND SOLVENT EFFECTS IN THE CONDENSATION OF DNA BY MULTIVALENT CATIONS. ((P.G. Arscott, C. Ma and V.A. Bloomfield)) Biochemistry, U. of Minnesota, St. Paul MN 55108.

DNA condenses into compact structures - toroids or rods - when multivalent cations are added to aqueous solutions at low salt. Both electrostatic and solvation effects seem important. We used 2686 bp pUC18 plasmid DNA, mixtures of water with methanol, ethanol, and isopropanol to vary the dielectric constant ε from 80 to 50, and hexaammine cobalt(III) (CoHx) as the condensing cation. Electron microscopy shows that the proportion of rods increases strongly as ε decreases from 80 to 65. Below 65, DNA collapses into a network of multistranded fibers, each appearing to consist of several DNAs aligned side-by-side. The three alcohols produce similar, but not identical, results at the same ε: the initial rate and extent of condensation correlate with nonpolar character. These results indicate that, when little alcohol has been added, electrostatic factors governed by ε determine the critical concentration of CoHx required to cause condensation. When more alcohol is added, dehydration and other solvent-related effects dominate. We believe that the morphology of the particles depends strongly on the kinetics of condensation, and on the time available to adjust molecular positions within condensates. If condensation is relatively slow, DNA molecules have time to adjust to a highly ordered, compact, toroidal packing geometry. When condensation is fast and strongly driven (low ε, high alcohol), initial DNA contacts are relatively permanent, leading to a relatively disordered, open, fibrous network. Rods are intermediate between these extremes. The formation of fibrous networks of laterally associated DNAs may also be favored by stiffening of DNA under dehydrating, high alcohol conditions.

Tu-Pos97

A MODEL FOR DIVALENT METAL ION MEDIATED CROSSLINKING/AGGREGATION OF MELTED DNA. ((J.G. Duguid and V.A. Bloomfield)) Department of Biochemistry, University of Minnesota, St. Paul, Minnesota, 55108

We have used differential scanning calorimetry in combination with optical densitometry to characterize the aggregation and melting of 160 bp fragments of calf thymus DNA during heating in the presence of divalent metal cations. Our results show that DNA aggregation is mediated by these cations, which enhance crosslink formation as thermal denaturation is initiated. When the temperature is further increased, DNA aggregation/crosslinking becomes more extensive until the T_m is reached, above which the aggregates dissolve extensively. The order of effectiveness of the metals to induce aggregation is generally consistent with their ability to induce melting: Cd > Ni > Co > Mn ≈ Ca > Mg. Under our experimental conditions ([metal]/[DNA phosphate]=0.6), no measurable aggregates were observed for Ba- or SrDNA. We applied the Shibata-Schurr theory of aggregation in the thermal denaturation region and found that it provides a very convincing explanation of our experimental observations. Free energies of crosslinking, induced by the divalent cations, were estimated to be between 30 and 40% of the free energies of base stacking. A model was developed from both experiment and theory, which illustrates DNA aggregation as a result of base pair disruption, followed by metal-cation mediated crosslinking.

Tu-Pos99

APPARENT MOLAR VOLUMES AND APPARENT MOLAR ADIABATIC COMPRESSIBILITIES OF SYNTHETIC AND NATURAL DNA DUPLEXES AT 25°C.
((T.V. Chalikian, A. Sarvazyan*, G.E. Plum, and K.J. Breslauer)) Dept. of Chemistry, Rutgers Univ, New Brunswick, NJ 08903. *perm address: Inst of Theoretical and Exper Biophys, Russian Acad of Sciences, Pushchino, Russia.

Using high precision densimetric and ultrasonic measurements, we have determined at 25°C the apparent molar volumes and the apparent molar compressibilities of five natural and three synthetic B-form DNA duplexes. We interpret these data in terms of DNA hydration. Specifically, we find a linear relationship between the density and the coefficient of adiabatic compressibility of water in the hydration shell of the DNA duplexes studied. We also find that the hydration of these polymeric DNA duplexes studied depends primarily on the base composition, while only weakly being influenced by base sequence. In the aggregate, the data can be interpreted as suggesting that GC base pairs are solvated more strongly than AT base pairs, in contrast with the current conventional wisdom. Furthermore, we find that the homopolymeric duplex poly(dA)poly(dT) and the alternating copolymeric duplex poly(dAdT)poly(dAdT) at 25°C exhibit similar apparent molar volumes and apparent molar adiabatic compressibilities. These similarities may be interpreted as suggesting that these two all-AT polymeric duplexes exhibit similar degrees of hydration at 25°C; once again, a conclusion which contrasts with the conventional wisdom.

Tu-Pos100

OSMOTIC SENSITIVITY OF THE B-TO-Z TRANSITION IN DNA.
((Y. Choe, B.J. Short, Jr., H.H. Chen, R.S. Preisler, and D.C. Rau)) Dept. of Chemistry, Towson State Univ., Towson, MD 21204 and NIDDK, NIH, Bethesda, MD 20892.

Our previous observations of differential ion effects on the salt-induced B-to-Z transition suggested that water activity is an important variable in this system. In the present study we have measured a B-to-Z transition in solutions of sucrose and other hydroxylic compounds, providing more direct evidence for the thermodynamic role of water. An osmotic mechanism for the action of these solutes is verified by the linear dependence of cobalt hexammine binding at the transition midpoint of poly(d(G-C)) and poly(d(G-m⁵C)) on solution osmotic pressure. Sucrose and other polyols appear to be excluded from the DNA hydration layer. Dependence of the transition midpoint osmolality on polyol molecular weight suggests that excluded volume is proportional to molecular size of the osmolyte. The osmolality of sucrose required for the transition midpoint is independent of Na⁺ concentration below about 100 mM but decreases linearly with log [Na⁺] above 100 mM. One interpretation of these results is that 40 water molecules are released for each additional Na⁺ bound to DNA. Comparisons of different sodium salts in combination with sucrose show differential anion effects consistent with the role of solvent entropy in the transition. The present findings provide another example of the ubiquitous role of hydration in modulations of macromolecular structure.

Tu-Pos101

EFFECTS OF SUPERCOILING AND Z-FORMING SEQUENCES ON DNA CONDENSATION. ((Chenglie Ma & V.A. Bloomfield)) Biochemistry, U. of Minnesota, St. Paul MN 55108. (Spon. by E. Grim)

DNA molecules collapse into compact structures in the presence of multivalent cations. To probe the possible importance of supercoiling and conformational effects, pUC18 plasmids were modified by inserting 12 bp and 20 bp alternating CG sequences, which are capable of converting to the left-handed Z-conformation under appropriate conditions, into the polycloning region. Condensation was induced by rapid addition of hexaammine cobalt (III) (CoHx) and monitored by light scattering. Plasmids with longer (CG)$_n$ inserts condense more extensively at natural superhelical densities (σ=-0.05). Enzymatic analysis and chemical probing show that the (CG)$_n$ inserts in naturally supercoiled plasmids convert from B-form to Z-form in the presence of CoHx. To determine whether the enhanced condensation of (CG)$_n$-containing plasmids results from the change of supercoiling due to the B-Z transition, we treated wild type pUC18 molecules with topoisomerase I and increasing amounts of ethidium bromide to generate a range of superhelical densities. Light scattering indicates that the superhelical density did not affect the condensation process. We conclude that the Z conformation of (CG)$_n$ inserts enhance DNA condensation, perhaps through the greater exposure of bases to solvent in the Z-form.

Tu-Pos102

A STRUCTURAL AND THERMODYNAMIC ANALYSIS OF A-DNA.
((Beth Basham and P. Shing Ho)) Department of Biochemistry and Biophysics, Oregon State University, Corvallis, OR 97331, USA

A-DNA as a class has not been well defined either structurally or thermo-dynamically. Our analysis of torsion angles and other helical parameters has shown that A-DNA is a definite structure distinct from B-form DNA. Specifically, the backbone torsion angle δ and the glycosidic angle χ are direct indicators of A- or B-form DNA, as are twist and total displacement from the helix axis.

To date there has been no quantitative method to predict the thermodynamic stability of base pairs in an A-DNA versus a B-DNA conformation. Using A-DNA crystal structures from the Nucleic Acids Data Base, we were able to derive a set of energies to describe the thermodynamic preference of many base pairs for A-form DNA. We calculated the free energy of hydration of the solvent accessible surfaces (ΔG_H) for the A- and B-DNAs and each sequence modeled (using standard helical parameters) in both the A- and B-forms. The ΔG_H revealed that the crystal structure is the lowest energy form for both conformations of DNA. The models for B-DNA accurately predict the hydration energy of the crystal structures; however, the models for A-DNA do not predict an A-DNA conformation for sequences that have been shown to crystallize as A-DNA. Therefore, we used the difference in ΔG_H between the A-DNA crystal structures and the same structures modeled as B-DNA to calculate the difference in stability of sequences in the A-form versus the B-form. Finally, we calculated energies for each base pair in the environment of specific neighboring bases in the context of trinucleotides. This allows us to quantitate the contribution of a base pair to the stability of the A conformation.

Tu-Pos103

CALORIMETRIC INVESTIGATION OF THE DNA TRIPLE HELIX: d(CCT₅CT₅CC)/d(GGA₅GA₅GG)/d(CCT₅CT₅CC).

((Dionisios Rentzeperis, Huy Tran and Luis A. Marky))

Department of Chemistry, New York University, New York, NY 10003

We have used a combination of differential scanning calorimetry, temperature-dependent UV spectroscopy, and isothermal titration calorimetry to thermodynamically characterize the triplex-duplex-coil transitions of the DNA triplex: d(CCT₅CT₅CC)/d(GGA₅GA₅GG)/d(CCT₅CT₅CC). At 5°C and pH 6 to 7, continuous variation experiments at 260 nm demonstrate the formation of a triplex with a 2:1 stoichiometry (homopyrimidine/homopurine) in strands. Decreasing the pH from 7 to 6 or increasing the [NaCl] from 0.3 M to 2 M stabilizes the triplex by 12°C-14°C. The biphasic behavior of the triplex-duplex-coil transition takes place with T_m's of 37.8°C and 60.4°C, this corresponds to formation free energies of -6.4 kcal/mol (triplex) and -16.9 kcal/mol (duplex), as well as transition enthalpies of 65 kcal/mol (triplex) and 106 kcal/mol (duplex). Furthermore, the triplex-duplex transition is accompanied by a release of 0.18 mole of Na⁺ per P$_i$ and 0.15 mole of H⁺ per P$_i$, while the duplex-coil transition is accompanied by a release of 0.14 mole of Na⁺ per P$_i$ and no release of H⁺.

Supported by grant GM-42223 from the National Institutes of Health.

Tu-Pos104

SELF-ASSEMBLY OF DNA OLIGOMERS INTO HIGH MOLECULAR WEIGHT SPECIES POSSESSING BOTH DUPLEX AND TETRAPLEX DOMAINS. T.-Y. Dai, S. Marotta & R. D. Sheardy, Department of Chemistry, Seton Hall University, South Orange, NJ 07079

We have designed DNA oligomers with sequences amenable to self-association into higher order structures which possess both duplex and tetraplex domains separated by tethers of varying lengths in order to investigate the environmentally dependent conformational states of these molecules. Each oligomer possesses a duplex domain in the form of a hairpin with a stem of 4 G:C base pairs linked by a T₄ loop and, for some, T$_n$ or T$_m$G$_4$ tails, where n = 5-8 and m = 1-4, at the 3' end. The melting profiles of each oligomer in 50 to 200 mM NaCl indicate that the thermally induced denaturations are unimolecular and arise from a single predominant species present, a conclusion borne out by gel electrophoresis carried out under those same conditions. However, gel electrophoresis of these oligomers in 20 mM Mg⁺² with 100 mM K⁺ result in 2 distinct bands for those molecules possessing T tails and a ladder of bands of high molecular weight for those molecules possessing TG tails. For those oligomers with TG tails, a scaffolding of tetraplex/duplex hybrid is proposed to account for this electrophoresis data along with a mechanism for its formation. The results of studies aimed at proving this mechanism will be presented.

Tu-Pos105

CONFORMATIONAL HETEROGENEITY OF THE HOLLIDAY JUNCTION.
((M. Yang, P.S. Eis and D.P. Millar)) Department of Molecular Biology, The Scripps Research Institute, 10666 North Torrey Pines Road, La Jolla, CA 92037. (Spon. by Lee Walters)

Four-way Holliday junctions (HJs) are the key intermediates formed during genetic recombination between two duplex DNA molecules. The outcome of recombination at specific DNA sequences may depend on the three-dimensional structure at the junction site. A variety of studies have shown that HJs form stacked-X structures by pairwise stacking of duplex arms. Considerable heterogeneity may exist in HJ structure, since stacking can occur between different arms and the non-crossover strands can be aligned in either parallel or antiparallel orientations. In addition, HJs may form with a range of angles at the cross. We are using time-resolved fluorescence resonance energy transfer combined with distance distribution analysis to examine conformational heterogeneity in a series of related immobile and monomobile HJs. Donor (D) and acceptor (A) dyes were conjugated to the 5' termini of the duplex arms and the distribution of D-A distances present between each pair of arms was recovered from the fluorescence decay of the donor using a Gaussian distribution model. Measurements were made at different temperatures and solvent viscosity to probe the dynamic flexibility of the HJ. We are comparing distance distributions in related HJs with different sequences at the junction to determine whether specific sequences dictate preferred stacking arrangements and/or modulate the flexibility of the HJ. Distance distributions obtained for monomobile HJs reflect a mixture of migratory isomers.
Supported by NSF grant MCB9019250

Tu-Pos106

THE DEPENDENCE OF DNA LIQUID CRYSTALLINE PHASES ON THE CONTOUR LENGTH AND OTHER PHYSICAL PROPERTIES
((Kunal Merchant and Randolph L. Rill)) Dept. of Chemistry and Inst. of Molecular Biophysics. Florida State University, Tallahassee, Florida 32306

Comprehending DNA organization *in vivo* requires an understanding of how DNA self organizes to form liquid crystalline phases in highly concentrated solutions. Semi-rigid polymers such as DNA begin to form liquid crystalline phases above a critical concentration (C_i), and are fully liquid crystalline above another critical concentration (C_a). These critical concentrations decrease with increasing polymer length to a limit determined by the persistence length (P). Stiff chains (high P), form ordered phases more readily than flexible chains (low P). The critical concentrations for DNA solutions in buffered NaCl were determined using ^{31}P solid state NMR methods for DNA fractions of selected lengths, ranging from ≈50 to 2700 nm. Anisotropy was confirmed by polarized light microscopy. The observed decrease in critical concentration (C_i) with increasing DNA length was more pronounced than predicted by theory, using a consensus persistence length of 50 nm. The anisotropic phase for very long DNA exists beyond a concentration of ≈13 mg/ml, well within the physiological range. By contrast, the length dependencies of C_a are in reasonable accord with expectations based on a 50 nm persistence length. Since the dominant length scale for phase transitions of semi-flexible polymers is the persistence length and not the contour length, the unexpectedly broad biphasic region is consistent with recent indications of sequence-dependent variations in DNA flexibility. (Supported by NIH grant GM37098 and the FSU Center for Materials Research and Technology (MARTECH)).

Tu-Pos107

SOLUTION STRUCTURE OF A DUPLEX OLIGONUCLEOTIDE CONTAINING PROPANODEOXYGUANOSINE OPPOSITE A TWO-BASE DELETION.((J.P. Weisenseel, J.G. Moe, L.J. Marnett and M.P. Stone)) Center in Molecular Toxicology, Departments of Chemistry and Biochemistry, Vanderbilt University, Nashville, TN 37235

One type of mutation induced by the exocyclic adduct 1, N^2-propano-2'-deoxyguanosine (PdG) is a two-base deletion, when the adduct is inserted into an iterative $(CpG)_3$ repeat sequence contained in the *hisD3052* gene of *Salmonella typhimurium*. An oligonucleotide was synthesized with a two-base deletion opposite PdG to model the slipped intermediate speculated to cause two-base deletions at this site(shown below, where X = PdG).

```
5'-ATCGCXCGGCATG-3'
3'-TAGCG···CCGTAC-5'
```
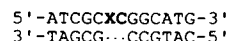
^1H NMR experiments demonstrated that the bulge consisted of the PdG adduct and its 3'-neighbor cytosine. Structural refinement was carried out using X-PLOR. Initial distances were derived from a NOESY spectrum, using the two spin approximation. These distances were incorporated into restrained molecular dynamics simulations starting from both canonical A- and B-form DNA structures. These structures were further refined via NOE back calculation using relaxation matrix analysis. The PdG adduct was intrahelical and 3'-neighbor cytosine was extrahelical. The two duplex portions of the molecule both exhibited a B-like conformation while the helix was bent at the site of bulge in order to accommodate PdG. Supported by the NIH: CA55678 (M.P.S.), CA47479 (L.J.M.), ES00267 (Toxicology Center), and GM08320 (pre-doctoral training, J.P.W.).

Tu-Pos108

NOVEL LIFETIME OBSERVED FOR ETHIDIUM BROMIDE BOUND TO IMMOBILE JUNCTIONS AND OTHER OPEN DNA STRUCTURES.
((Luis I. Hernández, Min Zhong, Scott H. Courtney, Neville R. Kallenbach)) Department of Chemistry, New York University, New York, NY 10003.

The structural and dynamic properties of unusual states of DNA are of interest in connection with the mechanisms of recombination, repair and mutagenesis. We have reported that the dye ethidium bromide (EB) interacts selectively with the branch site in immobile three and four arm DNA junctions as well as with duplexes containing an unstable single base pair mismatch. We have carried out fluorescence lifetime measurements on EB bound to a variety of three and four arm DNA junctions, and duplexes with mismatches. In all cases where an "open" state in DNA is implicated, such as three arm junctions and unstable mismatches, we detect an unusual 12-14 ns lifetime of the EB, in addition to the 20-25 ns lifetime characteristic of the complex with duplex DNA. This short lifetime is absent in DNA constructs lacking open structures, including an immobile 4 arm junction, and several mismatched duplex sequences with more stable base combinations, as well as duplex controls.
This short fluorescence lifetime provides support for previous observations by this laboratory of preferential binding by EB at the branch site of 3 & 4 arm junctions.
The relative populations of the short and long lifetimes are sequence [or construct] dependent but temperature independent. Therefore, dynamic changes in the shape of the junction due to large scale motions of the arms are likely irrelevant to the observed short lifetime, since such motions are temperature dependent. Supported by grants CA-24101 from NCI of the National Institutes of Health and 9011268 from the National Science Foundation.

Tu-Pos109

FLUORESCENCE AND PHOTOBLEACHING STUDIES OF METHYLENE BLUE BINDING TO DNA ((Bryant S. Fujimoto, James B. Clendenning, Jeffrey J. Delrow, Patrick J. Heath, and J. Michael Schurr)) Department of Chemistry, University of Washington, BG-10, Seattle, WA 98195

Time-resolved fluorescence, fluorescence polarization anisotropy, and transient photobleaching methods are used to investigate methylene blue/DNA complexes over a range of NaCl and $MgCl_2$ concentrations and a limited range of base composition. At least four, and probably five, different binding sites have been identified. Component 1 has the shortest fluorescence lifetime (26 ps) and represents the main intercalated component under low salt conditions. Component 2 has an intermediate fluorescence lifetime (130 ps). Component 3B has the longest fluorescence lifetime (620 ps), undergoes a modest amplitude (14°) of local rotation, and is significantly shielded from O_2 quenching of its triplet state. Its amplitude is enhanced by increasing %AT, and it appears to require AA, AT or TA steps. Component 3A has a long fluorescence lifetime (430 ps), undergoes a very large amplitude of local rotation, is evidently not intercalated, and exhibits two subcomponents that are differently shielded from O_2 quenching. With increasing ionic strength, the populations of components 1 and 3B shift into 3A. The relative amplitudes of components 1, 2 and 3B are unaffected by supercoiling, which implies that they all arise from intercalation sites with similar unwinding angles. By comparing the relative photobleach amplitudes with the relative fluorescence intensities, it can be inferred that components 3A and/or 3B dominate the triplet yield and photobleaching amplitude under practically all conditions. The suitability of methylene blue as the extrinsic probe in transient photodichroism experiments is discussed in light of these results.

Tu-Pos110

SYBR GREEN™-1: A NEW FLUORESCENT DYE OPTIMIZED FOR DETECTION OF PICOGRAM AMOUNTS OF DNA IN GELS. ((X. Jin, S. Yue, K.S. Wells, V.L. Singer)) Molecular Probes, Inc., Eugene, OR 97402.

A new ultrasensitive dye, SYBR Green™-1, has been developed by Molecular Probes for staining DNA in agarose or polyacrylamide gels. This dye is currently the most sensitive nucleic acid stain known for this application. SYBR Green-1 can be used to stain standard gels following electrophoresis and requires no destaining because it has essentially no measurable fluorescent background under normal staining conditions. The fluorescence enhancement of SYBR Green-1 upon DNA binding is several hundred fold — which is an order of magnitude greater than that of ethidium bromide. The sensitivity limit for double-stranded DNA stained with this dye and photographed using 254 nm epi-illumination and Polaroid 667 black and white print film, is less than 20 pg per band. This corresponds to at least 25 fold greater sensitivity than is seen with ethidium bromide. Using 300 nm transillumination, which is more commonly used for ethidium bromide, the detection limit of SYBR Green-1 is on the order of 60 pg per band. This is still nearly 10 fold more sensitive than ethidium bromide. SYBR Green-1 can also be used to detect RNA in gels, but with lower sensitivity. SYBR Green-1 forms complexes with DNA that are so stable that it can be used to prestain DNA prior to electrophoresis and remains bound during electrophoresis. The complexes are, however, readily accessible to restriction endonucleases under standard assay conditions. The fluorescence-detected formation of the dye/DNA complexes is salt-dependent, indicating that the binding mode of the dye is at least partially electrostatic.

Tu-Pos111

INFLUENCE OF NEAREST NEIGHBOR SEQUENCE ON SINGLE BASE BULGE STABILITIES IN LONG DNA: DETERMINATION BY TEMPERATURE-GRADIENT GEL ELECTROPHORESIS (TGGE) ((S-H. KE and R.M. Wartell)) School of Biology, Georgia Tech, Atlanta, GA 30332.

Temperature-Gradient Gel Electrophoresis was used to determine the thermal stabilities of 32 DNA fragments that differ by a single unpaired base or bulge. Homologous 373 bp and 372 bp DNA fragments differing by a single base pair substitution/deletion were employed. Heteroduplexes containing a single base bulge were formed by melting and reannealing pairs of 372 bp and 373 bp DNAs. Product DNAs were separated based on their thermal stability by parallel and perpendicular TGGE. The order of stability was determined for all single bulged bases in four different nearest neighbor environments; $d(GXT)\cdot d(AYC)$, $d(GXG)\cdot d(CYC)$, $d(CXA)\cdot d(TYG)$, and $d(TXT)\cdot d(AYA)$ with X = A, T, G or C, and Y = no base, or *visa versa*. DNA fragments containing a bulged base were destabilized by 1 °C to 4.5 °C with respect to homologous DNAs with complete Watson-Crick base pairing. Results indicate that both the identity of the bulged base and the sequence of the flanking base pairs influence the destabilization caused by the unpaired base. A bulged base with the same identity as the nearest neighbor base causes less destabilization than one with a different identity from its nearest neighbor base. The ability of a bulged base to H-bond to an adjacent base on the complementary strand seems to be a major factor in determining stability. We have also shown that two adjacent $G\cdot A$ mismatches, $d(GA)\cdot d(GA)$ in a long DNA creates a more stable molecule than a homoduplex DNA with $A\cdot T$ pairs at the same site. The TGGE approach provides a rapid way to evaluate how specific unpaired bases effect the stability of a long DNA fragment.

Tu-Pos112

THE AMES TEST AS A METHOD FOR DETECTING THE EFFECT OF ELECTROMAGNETIC FIELDS IN BIOLOGICAL SYSTEMS

(Paula Kosted, Bruce R. McLeod, Sam J. Rogers) Montana State University, Dept. of Chemistry and Biochemistry, Bozeman, MT 59717 (Sponsored by E. A. Dratz)

Endogenous electrical currents are inherent in any biological system and proper maintenance and balance of these currents is dependent upon ions and their movements across cell membranes. By using magnetic fields tuned to specific resonance frequencies of ions such as calcium, potassium, and magnesium, various effects on different biological systems have been observed.(McLeod, B. R., Liboff, A. R., and Smith, S. D.; J. Theor. Biol., 1992) The Salmonella typhimurium histidine reversion bioassay, referred to as the Ames mutagenicity assay, is being utilized for the purpose of detecting this effect on growth or reversion of genetically engineered bacteria. The Salmonella strains are sensitive to DNA damaging agents, and depending on the particular engineering of the bacteria, different types of DNA damage and repair mechanisms can be elucidated. The assay takes advantage of the histidine dependent bacteria which have been engineered to be unable to produce their own histidine. By adding a mutagen, a back mutation will allow for the production of more colonies called revertants to be formed above the background number. A mutagen is preincubated with the bacteria before it is placed in a top agar and plated onto a bottom agar. Plates are exposed to ion specific resonance magnetic fields during the 30 minute preincubation before plating and are then allowed to develop for 48 to 72 hours in the same fields. Results to date show this preincubation is essential for obtaining reproducibility. Both AC and DC fields have been examined as to their effect on the reversion of the Salmonella. The effects of the fields indicate either an increased or decreased amount of mutagenicity or a turning on or shutting down of the DNA repair mechanisms depending on the amount of mutagen being used and what fields are present.

Tu-Pos113

ANALYSIS OF HELIX BENDING IN CRYSTAL STRUCTURES AND MOLECULAR DYNAMICS SIMULATIONS OF DNA OLIGONUCLEO-TIDES.

((M.A.Young, R.Nirmala, J.Srinivasan, K. J.McConnell, G.Ravishanker H.M.Berman[1] and D.L.Beveridge)) Chemistry Department and Molecular Biophysics Program, Wesleyan University, Middletown, CT 06459. [1]Chemistry Department, Rutgers University, New Brunswick, NJ 08903.

Sequence dependent bending of the helical axis in 59 oligonucleotide duplex crystal structures resident in the Nucleic Acid Data Base (NDB) and in several new molecular dynamics simulations on the duplexes of sequence d(CGCGAATTCGCG) and d(CGCAAAAATGCG) have been analyzed and compared using "bending dials", a computer graphics tool. The patterns in bending preferences in the crystal structures are analyzed by base pair step, and emerging trends are noted. The results indicate that uniform trends within all pyrimidine-purine and purine-pyrimidine steps are not necessarily observed, but are recognizable in CG and GC steps. The MD simulations include solvent explicitly, and the trajectories were performed approaching the nanosecond time scale. The sequence dependent bending preferences are conserved across three MD simulations carried out on each sequence, regardless of the choice of starting structure. In some instances, bending effects in the MD model require hundreds of picoseconds to appear and to stabilize. Although the magnitudes of the deviations are greater in the solvated MD than those observed in the composite of crystal structures, many sequence dependent MD bending patterns are consistent with those observed in the NDB structures. The MD results support the idea that A tracts are relatively straight, and that large roll bends occur at the junctions of these A tracts with the flanking sequences.

FLUORESCENCE SPECTROSCOPY

Tu-Pos114

USE OF FLUORESCENCE RESONANCE ENERGY TRANSFER MEASUREMENTS TO ESTIMATE THE SITE DENSITY OF FUNCTIONAL GROUPS ON DERIVATIZED SILICA SURFACES.

((David Fujimoto, Arathi Sundaram, Cindy Nguyen, and Steven A. Sundberg)) Affymax Research Institute, Palo Alto, CA

As part of our effort to manipulate the surfaces of solid supports in order to optimize their performance for applications ranging from immobilization of antibodies to light-directed polymer synthesis, we have carried out fluorescence labeling studies to characterize the density of functional groups on surfaces of silane derivatized glass. Fluorescence imaging techniques were used to measure fluorescence signals on the labeled surfaces. The observation that signals rose and then decreased as the labeling reaction was driven to completion is qualitatively consistent with the predictions of fluorescence resonance energy transfer theory, and raises the possibility of using this technique to estimate the average spacing between functional groups on derivatized supports. Our efforts to model the experimental data within the theoretical framework of a two-dimensional lattice of immobilized fluorophores will be presented and discussed.

Tu-Pos115

FIBER OPTIC EVANESCENT WAVE IMMUNOPROBE: HIGH ACTIVITY OF IMMOBILIZED ANTIBODIES AND KINETICS OF ANTIGEN BINDING.

((S.F.Feldman and E.E.Uzgiris)) General Electric Research and Development Center, Schenectady, NY 12309.

A fiber optic evanescent wave immunoprobe is evaluated using all-optical and kinetics measurements to determine absolute sensitivity, activity of immobilized antibodies , and hydrodynamic dead layer thickness next to the fiber surface. We obtain $2.5 \times 10^{11}/cm^2$ active antibodies in the immobilization procedure ,which indicates that between 40 and 70% of bound molecules are capable of binding antigen. From kinetics data we deduce that a fraction of these antibodies are monovalent rather than divalent, suggesting some stearic hindrance in the active antibodies on the fiber surface. We see a striking transition from divalent binding at low antigen concentrations (below 1nM) to monovalent binding at higher concentrations. From optical determinations of bound antigen levels (in these experiments the antigen was FITC labeled rabbit $F(ab)_2$ and the immobilized antibody was goat antirabbit IgG) and the kinetics data we directly determine the hydrodynamic dead layer thickness to be 55 μm.The absolute sensitivity, i.e., the minimum number of labeled antigen molecules that we can detect is 10^9, allowing detection of 40 pM labeled antigen in about 10 minutes.

Tu-Pos116

COUPLED ROTATIONAL AND REVERSIBLE EXCITED-STATE KINETICS.

((R. E. Dale[1] and M. Ameloot[2])) [1]Paterson Institute for Cancer Research, Manchester M20 9BX, United Kingdom [2]Physiological Research Unit, Limburgs Universitair Centrum, B-3590 Diepenbeek, Belgium.

A simple and intuitively readily accessible derivation of the time-dependence of the anisotropy of systems in which a pair of fluorophores exhibiting different rotational behaviour are linked kinetically by a reversible two-state excited-state process not dependent on their relative orientation, is presented. The derivations are based directly on the well-known solutions for the binary set of homogeneous linear differential equations classically applied in examining the kinetics of the total fluorescence, independent of its polarization, of each species when only one is initially excited. Both isotropic and aniso-tropic rotations are considered. The results for limiting cases (i) in which the exchange between the excited species is so rapid that an excited-state equilibrium is essentially instan-taneously attained, (ii) when the reverse rate coefficient is negligibly small ("irreversible" excited-state process), and (iii) where the relationships between the set of rate co-efficients defining the kinetics lead to pathological behaviour of the usual functions, are also examined. The relationship of the solutions presented to those appearing previously in the literature is discussed, several representative graphical examples for both the simplest and more complex cases are presented for illustration, and their relevance to physically realistic situations examined.

Tu-Pos117

HOW TO IMPROVE THE ANALYSIS OF FLUORESCENCE DECAY DATA INVOLVING VERY SHORT LIFETIMES.

((Ž. Bajzer, A. Zelić, F.G. Prendergast)) Mayo Foundation, Rochester, MN 55905.

Considerable effort in instrumentation development has made possible detection of picosend lifetimes by time-correlated single photon counting. In particular, efforts have been made to markedly narrow the instrument response function (IRF). Much less attention has been paid to numerical procedures used for discretization of the convolution integral. Here we show that better discretization methods yield acceptable results for short lifetimes with an IRF several times wider than necessary when standard discretization procedures are employed (Wahl, Biophys. Chem. 10(1979)91). First, we present a general approach to discretization, which is also suitable for non-exponential models. This approach, in a simple way, allows any type of interpolation of the IRF. For the multi-exponential model, it yields formulae equivalent to those recently derived by Večer et al. (Rev. Sci. Instr., in press). We performed numerous simulations comparing the standard linear (LI) and the quadratic interpolations (QI). The latter proved much better in detection of short life-times; for example, using the maximum likelihood method, the lifetimes of 5 and 12ps (with equal amplitudes, channel width of 5ps and 50ps FWHM of IRF) can be detected with 13% of average relative error per parameter using QI while this error for LI amounts to an unacceptable 34%. Furthermore, the QI yields stable results for rather a wide range of IRF widths. We provide examples showing that the same accuracy can be obtained by QI for IRF FWHM=100ps as by LI with FWHM=50ps. In addition, we also consider the effects of zero-time shift and scattered light on detection of short lifetimes which have generally been neglected in the literature. Supported by GM34847.

Tu-Pos118

TIME-RESOLVED FLUORESCENCE STUDY OF PROTEINS IN USING A TUNABLE PICOSECOND TITANE-SAPPHIRE LASER AND THE QUANTIFIED MAXIMUM ENTROPY METHOD.

((J.C. Brochon and P. Tauc)) C.N.R.S. URA 1131, Groupe de Biofluorescence, Université Paris-Sud, Bât. 433, 91405 Orsay Cedex, France

The new picosecond titane-sapphire laser TSUNAMI was tested for time-resolved fluorescence measurement of proteins in the 280-310nm range by using a tripling frequency system. The tunability, intensity, stability and pulse width (using a standard MCP detector) of the source are presented. Fluorescence decays and fluorescence anisotropy decays of proteins containing a single tryptophane residue were measured by the time correlated single photon counting technique working in a parallel mode.

The Quantified Maximum Entropy Method (QMEM) allows the determination of accuracy on the position, the surface and the width of peaks in the recovered lifetime distribution from a given noisy data set. The fluorescence decay is analysed in term of lifetime distribution and the decays of polarised components of the fluorescence yield a two dimensional pattern of rotational correlation time distribution versus lifetime distribution. A new development of the maximum Entropy Method is also proposed. It intends to partially overcome some intrinsic difficulties with systematic errors in data obtained by the TCSPC technique. This development is based on a global analysis approach. Simulations and protein data analyses are presented.

Tu-Pos119

ANALOG PIPELINING TAC OUTPUTS FOR IMPROVED TIME-CORRELATED PHOTON COUNTING DETECTION CIRCUITS.

((G.T. Ying, D.W. Piston and J.M. Beechem)) Department of Molecular Physiology and Biophysics, Vanderbilt University, Nashville, TN 37232.

We have developed a four channel analog pipeline buffer that increases the overall throughput of a time-correlated photon counting detection system. One of the rate-limiting steps in this system is the relatively slow Wilkinson type pulse-height analysis analog-to-digital converter (ADC). An additional "analog memory" unit placed between the time-to-amplitude converter (TAC) and the ADC reduces this limitation. This unit uses a prioritizing scheme to direct the incoming pulse from the TAC into a free channel of a quad sample-and-hold (S/H) buffer. The outputs of the four buffers are polled serially with a 2 MHz clock. If a buffer is holding a valid TAC pulse when polled, its value is passed along to the ADC in the computer with a pulse shape that exactly mimics the TAC output. While the ADC is converting this signal, the ADC busy signal disables the serial polling. Valid TAC signals which arrive during this time are kept in the other S/H buffers, and are held until polled for output to the ADC. This buffer circuit allows collection of single photon events that would be lost in a non-buffered system. Since the ADC busy time is dependent on the magnitude of the signal, several short-time (small magnitude) events may occur during the ADC time for a single long-time (large magnitude) event. Capturing several events in the S/H buffers during the digitization of long-time events can increase counting rates by a factor of five.

Tu-Pos120

FREQUENCY DOMAIN FLUORESCENCE LIFETIME MICROSCOPE WITH GHz RESPONSE ((J.M. Xiao, A. Knüttel, B.S. Packard* and J.R. Knutson)) NHLBI, NIH, and *CBER, FDA: Bethesda, MD 20892.

Fluorescence microscopy is a valuable biophysical technique for probing cells, particularly when extended by lifetime capabilities. Using instrinsically modulated laser light, we developed a lifetime microscope with a frequency response up to 1 GHz. (modulation = 8% @ 1020 MHz).

The intensity modulated fluorescent signal was detected with a "heavy undercoat" photocathode (ca. 100 ohms, Hamamatsu V4323U), connected by low inductance tabs to the modulation source. Gated photoelectrons were amplified with a microchannel plate (MCP) intensifier. The photocathode gating down-converted high frequency information to 0.5 Hz for acquisition by a fiber coupled CCD camera. For improved accuracy, the phase and modulation of the fluorescent signal was referenced to a signal impinging on the camera in a reserved (masked) location. Phase and modulation images from reference materials and tissue will be presented.

Tu-Pos121

TIME RESOLVED FLUORESCENCE WITH SYNCHROTRON SOURCE EXCITATION: IMPROVED STABILITY OF PULSE WIDTH USING A POWERED FOURTH-HARMONIC CAVITY.

((K. Polewski, S.L. Kramer, and J.C. Sutherland)) Biology Dept. and NSLS, Brookhaven National Laboratory, Upton, NY 11973.

The continuous spectrum of synchrotron permits selection of any excitation wavelength and calibration of the detection system with the same wavelength used for excitation. Light from the UV ring at the National Synchrotron Light Source (NSLS) consists of pulses separated by times ranging from about 19 ns in 9 bunch mode to 170 ns in 1 bunch mode. Without modification by a 4th harmonic cavity, the width (FWHM) of the pulses is less than 1 ns, but the temporal profile changes as electrons are lost during the course of a "fill." The purpose of a 4th harmonic cavity is to lengthen the bunches of electrons, and hence reduce the rate of electron loss due to electron-electron collisions. Pulse-stretching is undesirable for timing experiments, as it results in longer pulses of light. Active powering of the 4th harmonic cavity maintains the spatial distribution of the bunches of circulating electrons as the current in the ring decays. This further reduces the rate of electron loss, but also stabilizes the temporal profile of the light pulses. Although the average width of the pulse is greater, the improved stability permits more accurate deconvolution of short lifetimes. We demonstrate accurate resolution of the ~90 ps temporal decay of the fluorescence from rose bengal in water, for excitation pulses with widths of about 1.5 ns.

Tu-Pos122

END-TO-END DIFFUSION COEFFICIENTS AND DISTANCE DISTRIBUTIONS FROM FLUORESCENCE ENERGY TRANSFER MEASUREMENTS: ENHANCED RESOLUTION BY USING MULTIPLE DONORS WITH DIFFERENT LIFETIMES ((Ignacy Gryczynski, Joseph R. Lakowicz and Józef Kuśba)) University of Maryland, School of Medicine, Center for Fluorescence Spectroscopy, Department of Biological Chemistry, 108 N. Greene Street, Baltimore, MD 21201. (Sponsored by J.R. Lakowicz)

We determined distance distributions and end-to-end diffusion coefficients of donor-acceptor pairs linked by a flexible methylene chain using frequency-domain fluorescence energy transfer measurements. The acceptor was a dansyl group and two donors with different lifetimes were used (indole, r_0 = 5.7 ns and naphthalene group, r_0 = 24.4 ns, in methanol).

r_0 = 5.7 ns   TU2D

r_0 = 24.4 ns

NU2D
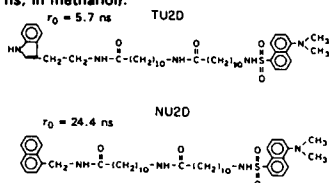
The uncertainties in the recovered parameters describing the end-to-end distance distribution and diffusion coefficient were rather large when each donor-acceptor pair was analyzed separately. Global analysis using two donors with different lifetimes dramatically improved the resolution. These experiments suggest the benefit of using global analysis with different lifetime donors to obtain reliable distance distribution parameters in the presence of diffusion.

Tu-Pos123

TWO-PHOTON FLUORESCENCE EXCITATION SPECTRA OF CALCIUM PROBE INDO-1. ((Chris Xu, Jeffrey Guild and Watt Webb)) School of Applied and Engineering Physics, Cornell University, Ithaca, NY 14853
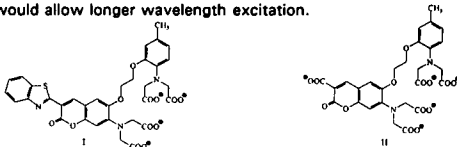
Due to the recent development of two-photon laser scanning microscopy for its application in 3-D real time imaging of living cells, there is an urgent need to understand the spectra of two-photon excitation of fluorescent dyes, such as indo-1, cascade blue, Hoechst DNA stains, rhodamine, etc. We report here the two-photon fluorescence excitation spectra and cross-sections of indo-1, both free and bound to calcium, for excitation wavelengths around 700 nm. A mode-locked titanium sapphire laser excites the spectral region of interest. Powdered KDP as a power square sensor measured the second order coherence of the laser. We have also measured the two-photon excitation spectra of Bis-MSB in the same wavelength region and the results are in good agreement with the existing literature. We found that the two-photon excitation spectra of the two indo-1 species generally follow the characteristic features of their one-photon spectra. However, the two-photon excitation cross-section of the free dye is nearly four times greater than that of the Ca^{2+} bound dye at 710 nm, while the one-photon excitation cross-section of the two species are about the same at 355 nm. Two-photon excited fluorescent emission spectra and quantum efficiency of indo-1 are being studied.

Tu-Pos124

COUMARIN-BASED RATIOMETRIC FLUORESCENT PROBES FOR Ca²⁺.((E.U. Akkaya and J.R. Lakowicz)) University of Maryland, School of Medicine, Center for Fluorescence Spectroscopy, Department of Biological Chemistry, 108 N. Greene Street, Baltimore, MD 21201. (Sponsored by E.U. Akkaya)

We have synthesized a number of coumarin-based fluorescent Ca²⁺ probes which contain the highly selective Ca²⁺ chelator BAPTA (1,2-bis-(2-amino-phenoxy)ethane-N,N,N',N',-tetraacetic acid) as an integral part of the fluorophore. Coumarin derivatives can be synthesized in a straightforward way from known intermediates and they have the advantage of good quantum yields in water. At present, we have synthesized Coumarin-6 and Coumarin-343 analogs, both of which are well-known laser dyes. We are at the early stages of the characterization of these probes, but preliminary results suggest that both compounds can be utilized as excitation wavelength-ratiometric probes. The absorption peak of Coumarin-6 derivative, on binding to Ca²⁺, shifts significantly (from 467 nm to 402 nm) to shorter wavelengths, wheras the emission (λ_{max} = 530 nm) is mostly unchanged. In the case
of Coumarin 343 analog, the emission peak at 484 nm is again unchanged on binding to Ca²⁺, but the absorption peak shifts hypsochromically from 408 nm to 358 nm. Conversion to cell permeable AM (acetoxymethyl) ester or silylated forms is feasible. We are in the process of synthesizing other Coumarin derivatives which would allow longer wavelength excitation.

Tu-Pos125

SIMULTANEOUS MEASUREMENT OF CALCIUM AND pH IN SINGLE INSULIN SECRETING CELLS BY FLUORESCENCE SPECTROSCOPY. (R. Martinez-Zagulian and R.M. Lynch) University of Arizona, Tucson AZ 85724

There are a variety of fluorescent dyes used to monitor Ca⁺⁺ within living cells. Unfortunately these dyes also exhibit a range of sensitivity to protons. We are interested in the role Ca⁺⁺ plays in regulating insulin secretion from beta cells of the pancreas. Since increased glucose metabolism stimulates secretion and alters both cell Ca⁺⁺ and pH, proton levels need to be precisely monitored. A spectral imaging system has been implimented to simultaneously monitor pH and Ca⁺⁺ using the combined spectral output of SNARF-1 and Fluo-3. Fluorescence is excited using a 480 nm band pass filter and a Hg lamp. Emitted light from a dye loaded cell is imaged onto the slit of a spectrograph and the spectral output is collected with a cooled CCD camera providing spatial information along the length of the slit. Measurements from multiple dyes at distinct positions in a cell are acquired simultaneously. A strong effect of H⁺ on the Kd of Fluo-3 for Ca⁺⁺ was observed from in situ dye calibration in insulinoma cells treated with ionophores. Using this measured parameter, the Ca⁺⁺ signal was corrected for shifts in pH. A heterogeneity in response of individual insulin secreting cells in terms of cell acidification and Ca⁺⁺ influx was observed. In many cases, apparent alterations in Ca⁺⁺ were due to glucose-induced changes in pH. Current work is designed to determine patterns of response of single cells that may underlie the range of glucose induced exocytotic activity observed in vivo.

Tu-Pos126

LONG WAVELENGTH Cl-SENSITIVE FLUORESCENT INDICATORS ((Joachim Biwersi, Barry Tulk and A.S. Verkman)) UCSF, CA 94143-0532. (Spon. by S. Bicknese)

The goal of this study was to develop long wavelength Cl indicators to minimize photodynamic cell injury and autofluorescence associated with SPQ and second generation Cl indicators. A series of quaternized tricyclic heterocycles was screened. We found that N,N'-dimethyl-9,9'-bisacridinium (DMBA) had very high halide sensitivity with Stern-Volmer constants for collisional quenching of 390 M⁻¹ (Cl), 585 M⁻¹ (Br), 590 M⁻¹ (I), 590 M⁻¹ (SCN), much higher than that for the reference compound SPQ [118 M⁻¹(Cl)]. DMBA fluorescence at 510 nm was excited with molar absorbances of 34000 M⁻¹cm⁻¹ (370 nm) and 7500 (455 nm). DMBA fluorescence was insensitive to phosphate, sulfate and nitrate. Because of its high halide sensitivity and membrane impermeability, DMBA was used as an internal indicator to measure chloride transport in proteoliposomes reconstituted with a Cl-channel. To examine structure-activity relationships, four 9-substituted N-methylacridinium compounds were synthesized (9-amino, 9-carbox-aldehyde, 9-carboxy and 9-carboxymethylester), of which N-methyl-acridinium-9-carboxymethylester (MACM) had the best optical properties. MACM had excitation and emission maxima at 420 and 520 nm and Stern-Volmer constants of 160 M⁻¹ (Cl), 250 M⁻¹ (Br), 265 M⁻¹ (I), 280 M⁻¹ (SCN). The quantum yields of the acridinium compounds were 0.6-0.7. These studies introduce acridinium compounds as long-wavelength Cl indicators for biological applications.

Tu-Pos127

SYNTHESIS OF SULFHYDRYL REACTIVE FLUORESCENT PROBES CONTAINING THE ANTHRANILOYL FUNCTIONALITY. ((Derek J. Pouchnik and Christine R. Cremo)) Dept. of Biochemistry and Biophysics, Washington State University, Pullman, Washington 99164-4460

We have synthesized a series of new fluorescent probes which react with sulfhydryls. Fluorescent anthraniloyl groups and derivatives thereof were attached to a sulfhydryl reactive haloacetyl group using linkers of various lengths. These new probes have been characterized by nuclear magnetic resonance spectroscopy, mass spectroscopy, u.v.-visible spectroscopy and fluorescence spectroscopy. Supported by N.I.H.

Tu-Pos128

SYNTHESIS AND SPECTRAL CHARACTERIZATION OF POTENTIAL SOLVATOCHROMIC FLUOROPHORES ((Jennifer Rutherford, Gretchen M. Rehberg, and Brian Wesley Williams)) Chem. Dept. Bucknell Univ., Lewisberg, PA 17837

With the goal of discovering useful or improved fluorescence probes, we have initiated the synthesis and spectral characterization of some potentially solvatochromic fluorophores (see figure). Structurally, these compounds are related to the dyes Nile Red and 1-PDMPO [1], where in the present work we are attempting to determine effects due to different substituents in the central heterocyclic ring and due to amine- or nitro- substituents. Synthetic approaches and preliminary spectral data for some compounds of this type will be discussed. (Supported by Bucknell Univ. and NSF-REU)
[1] T. A. Brugel and B. W. Williams, J. Fluor. (1994) (in press)

R= H, O, alkyl

X= S, NH, NR', etc.

Tu-Pos129

FLEXIBILITIES OF THE DNA HELIX DETERMINED FROM TIME-RESOLVED FLUORESCENCE EMISSION ANISOTROPY. ((Qi Chen and Mary D. Barkley)) Department of Chemistry, Louisiana State University, Baton Rouge, LA 70803

Internal motions of the DNA helix have been investigated in ≤ 40 ns time range using time-resolved fluorescence emission anisotropy with tomaymycin as fluorescent probe. The decay data were fitted to the predicted non-exponential anisotropy decay model for twisting and bending motions of a semi-flexible rod. A new global data analysis program was developed, which provides options of linking, fixing, and lifetime-anisotropy association. Unlike in the published works, the torsional rigidity (C), the bending rigidity (EI), the radius of the helix, the initial anisotropy of the drug (r_0), and the orientation of the emission transition dipole of the drug toward the DNA helix axis (ϵ) were recovered simultaneously. The fit resulted in r_0 of ~0.34 and ϵ of ~33°, which agreed with the limiting anisotropy of tomaymycin ethyl ether measured at 77 K and the average value of ϵ predicted from molecular modeling studies of tomaymycin-oligonucleotide adducts. The recovered flexibilities of the DNA helix were comparable with published data obtained by other methods, indicating the success of the decay model. Poly(dAdG)·poly(dTdC) (1000 ± 50 bp), poly(dGdC)·poly(dGdC) (950 ± 100 bp), and natural calf thymus DNA were studied in this work. Supported by NIH grant GM35009.

Tu-Pos130

FLUORESCENCE STUDIES OF 2-AMINOPURINE RIBOSIDE ((L. P. McMahon, Q. Zeng, and M.D. Barkley)), Department of Chemistry, Louisiana State University, Baton Rouge, LA 70803. (Spon. by W. Liu)

2-Aminopurine (2-AP), unlike other purine bases (e.g. guanine and adenine-the natural purine bases in DNA), is highly fluorescent. 2-AP riboside has a quantum yield in H_2O of about 0.65 and a fluorescent lifetime of about 10 ns. The quantum yield decreases in non-polar solvents. The photophysical properties of 2-AP free base and riboside have been investigated by several groups. The principle nonradiative process was attributed to intersystem crossing. We are investigating nonradiative decay processes in 2-AP riboside before we begin using it as a fluorescent probe. The fluorescence quantum yield is very temperature dependent, decreasing from 0.65 at 25° C to 0.44 at 40° C. There is no solvent isotope effect (H_2O vs. D_2O) on the quantum yield in this temperature range. We have determined the Arrhenius parameters of this nonradiative process and have also looked at Stern-Volmer quenching using acrylamide, 9-aminoacridine, KI, CsCl, and different nucleosides.

Tu-Pos131

SELECTIVE LABELING OF ECORI ENDONUCLEASE WITH DANSYL CHLORIDE ((Wei Liu, Linda Jen-Jacobson*, Mary D. Barkley)) Chemistry Department, Louisiana State University, Baton Rouge, LA 70803; *Department of Biological Science, University of Pittsburgh, Pittsburgh, PA 15260

EcoRI is a restriction endonuclease which recognizes the palindromic sequence GAATTC of double stranded DNA and cleaves the phosphodiester bond after guanosine. The N-terminal 5-12 amino acids of EcoRI are essential for DNA cleavage, but are not resolved in the X-ray structure. Fluorescence spectroscopy will be used to study the structure and dynamics of the N-terminus. We studied the labeling selectivity of dansyl chloride on EcoRI. Reverse phase HPLC technique for peptide mapping and amino acid analysis are used to locate the labeling sites of dansyl chloride and to determine the labeling selectivity between the N-terminal serine residue and internal lysine residues. The effect of pH on labeling has been studied. Several lysine residues are more reactive with dansyl chloride and are labeled preferentially even at neutral pH. The dye/protein ratio is constant below pH 6.0. When a stock solution of dansyl chloride in dimethylformamide is used in the labeling reaction, maximum labeling selectivity is obtained at pH 5.5 with the N-terminal residue serine and lysine-14 being labeled. When dansyl chloride is preabsorbed onto Celite and the solid is suspended in EcoRI solution, the N-terminal serine can be specifically labeled without the labeling of internal lysine residues. The effect of oligomer DNA with twelve base pairs upon the labeling of EcoRI was also studied. The presence of DNA lowers the dye/protein ratio but does not increase the labeling selectivity.

Tu-Pos132

THE DEVELOPMENT OF A FLUORESCENCE ASSAY FOR THE BAMHI RESTRICTION ENDONUCLEASE UTILIZING MODIFIED OLIGONUCLEOTIDES.((S.P. Lee*, D.K. Porter*, J.G. Chirikjian*, J.R. Knutson* and M.K. Han*)) *Georgetown U. Medical Center, Dept. of Biochemistry, Washington, DC 20007 and *NHLBI, NIH, Bethesda, MD 20892.

Fluorescent labeled oligonucleotides and DNA fragments have promise in nucleic acid research including DNA hybridization, automated DNA sequencing, and fluorescence anisotropy or resonance energy transfer studies. One concern with fluorescent-labeled DNA is that the interactions between fluorophores and DNA may result in quenching of the probe fluorescence. This quenching phenomenon is most problematic in fluorescence energy transfer studies because donor quenching can occur as a result of both resonance transfer and these non-transfer effects. In the present studies, the nontransfer quenching of a 14-mer FITC-labeled oligonucleotide with the BamHI restriction site was characterized with both steady-state and time-resolved fluorescence techniques. The FITC-labeled single strand was best fit by triexponential decay with lifetimes of 0.5, 2.7, and 4.2 ns. The 4.2 ns component was found to contribute more than 80% of total steady-state intensity. Upon annealing with an unmodified complementary strand, the 4.2 ns component was significantly decreased, resulting in 2-fold quenching of total fluorescence. We examined the reversible quenching process and applied our findings to quantify DNA strand separation and cleavage processes. Utilizing this information, we developed a continuous fluorescence assay for the restriction endonucleases reaction for BamHI.

Tu-Pos133

FLUORESCENCE PROPERTIES OF DNA BINDING DOMAINS OF *DROSOPHILA* HEAT-SHOCK FACTOR. ((S.-J. Kim*, J.R. Knutson* and C. Wu*)) NCI* and NHLBI*, NIH, Bethesda, MD 20892.

The tryptophan and tyrosine fluorescence of the DNA binding domain (dHSF(33-163)) of *Drosophila* heat shock transcriptional factor was characterized. This polypeptide contains 2 tryptophans (W54 & W68) and 3 tyrosines (Y36, Y92, and Y107) all located in the highly conserved region (except Y36 at the N-terminal end). In the presence of ~3X excess DNA, the dominant tyrosine emission is quenched ~50% with a ~10 nm red-shift, while the emission of tryptophan is almost unaffected. Fluorescence quenching experiments showed that, in the presence of DNA, there is a marked protection of tyrosine (but not tryptophan) environments. In contrast to steady-state results showing ~50% decrease in tyrosine emission intensity, there is only ~ 5% decrease in average lifetime upon binding of dHSF(33-163) to DNA. This discrepancy between steady-state and time-resolved results suggest that tyrosine residues are in proximity to DNA, resulting in static quenching.
A comparison of steady-state parameters of dHSF(33-163) with dHSF(1-163) containing the N-terminal negative segment (NS) including ten acidic residues indicates a lesser role for Y36 in DNA binding. Binding characteristics of the polypeptides were also compared. Both polypeptides have hyperbolic binding isotherms, indicating an absence of cooperativity. The DNA binding affinity of these polypeptides are similar, suggesting that the NS has little direct effect on DNA recognition. We also characterized the affinity and minimum DNA length requirement for stable binding to dHSF(33-163) by fluorescence titration. The binding of double-stranded DNAs longer than 11 bp all showed similar affinity, while 9 bp DNA yielded >10 fold decrease in affinity suggesting that a minimum of 10-11 bp is required for a stable protein-DNA interaction.

Tu-Pos134

A SPECTROSCOPIC STUDY OF THE BINDING OF M⁷GTP TO THE SMALL SUBUNIT OF WHEAT GERM INITIATION FACTOR (ISO)4F ((Ma Sha*, Ann Van Heerdon⁹, Karen S. Browning⁹ , and Dixie J. Goss*)) *Chemistry Department, Hunter College of CUNY, New York, NY 10021; ⁹Dept. of Chem. & Biochem., Univ. of Texas at Austin, Austin, TX 78712-1104.

The purified small subunit of wheat germ protein synthesis initiation factor eIF(iso)-4F has been obtained from expression of the cloned DNA. The binding of the 5'-terminal cap analog m⁷GTP to eIF(iso)-4F's small subunit(p28, 28KDa) as a function of pH and ionic strength is described. The pH-dependent binding showed an sharp pH optimum at pH 7.05. The KCl dependence shows that electrostatic interactions are not dominant in the p28-CAP binding, a Z_AZ_B (from Debye-Huckel theory) of -0.47 was obtained. The Z_AZ_B for a single positive and negative charge interaction is -1. Iodide quenching shows that all 9 trp residues in p28 are exposed while only 6 out of 16 trp residues are exposed in the intact (iso)-4F. Conformational changes during the p28 binding to the large subunit(p82) of (iso)-4F causes at least 3 surface trp residues to be buried. Grant support: NSF:DMB-9105353(to KSB) and MCB-9303661(to DJG).

Tu-Pos135

A FLUORESCENCE SPECTROSCOPIC STUDY OF THE BINDING OF PHOSPHORYLATED AND NON-PHOSPHORYLATED PROTEIN SYNTHESIS INITIATION FACTOR 4E TO RNA AND TO m⁷GTP AND m⁷GpppG. ((M.L. Balasta*, W. Minich*, R. Rhoads* and D.J. Goss*)) *Chem. Dept., Hunter College of CUNY, NY, NY 10021; *Biochem. & Mol. Biol Dept., Louisiana State Univ. Med. Ctr., Shreveport, LA 71130.

Studies on the interactions of the phosphorylated and non-phosphorylated forms of eIF-4E with RNA and with cap analogs can help elucidate the role of phosphorylation in protein translation. eIF-4E (cap-binding protein), is a 24-kDa subunit of eIF-4F, an initiation factor associated with cap recognition and with the helicase activity. eIF-4E is believed to become activated upon phosphorylation (Ser 53), thereby stimulating mRNA binding to the ribosomal subunits. Fluorescence binding studies show differences in the binding of phosphorylated and non-phosphorylated 4E to cap analogs and to mRNA. The equilibrium binding constants show that the phosphorylated 4E has 3 - 4 times greater affinity for cap analogs and mRNA than the non-phosphorylated 4E. These differences may account for the greater activity of phosphorylated 4E.

Tu-Pos136

A KINETIC STUDY OF THE BINDING OF THE WHEAT GERM PROTEIN SYNTHESIS INITIATION FACTOR ISO-4F WITH m7GpppG.((Y. Wang, T. Xiang, C. Wei, D. J. Goss)) Hunter College of CUNY, NY, NY 10021

We have previously reported extensive equilibrium measurements of initiation factor interactions with mRNA and 5' terminal cap analogs. We are now examining by direct fluorescence measurements the binding to alfalfa mosaic virus mRNA (AlMV), which is naturally capped but does not require the cap for efficient translation. These studies will attempt to elucidate mechanisms of translation initiation. Here we report the first kinetic measurements of this process. Stopped-flow measurements were carried out using the fluorescence signal changes of iso-4F upon binding to m7GpppG, a cap analog. The results show that the binding kinetics fit the following mechanism: Protein + Cap⇔B→C, under the condition of [Cap]>>[P] and the steady-state assumption. Fitting the experimental data to this mechanism gives the second step rate constant $k_2=11.0$ s^{-1} at 20°C. The activation energy of the second step (B→C conformational change upon binding) is 5.7 kcal/mol. Grant support: NSF MCB-9303661.

Tu-Pos137

GLOBAL ANALYSIS OF COMBINED STOPPED FLOW FLUORESCENCE ANISOTROPY AND TOTAL INTENSITY DATA: APPLICATIONS TO PROTEIN FOLDING AND PROTEIN:DNA INTERACTIONS. ((M.R. Otto and J.M. Beechem)) Vanderbilt University, Nashville, TN, 37232

In many studies of biomolecular reactions, changes in fluorescence anisotropy or total intensity signals are used to obtain information concerning reaction rates and/or mechanisms. For two state reactions, due to quantum yield effects on the anisotropy, kinetic anisotropy data will never superimpose with total intensity data. In reactions where the relative fluorescence quantum yield increases, the anisotropy rate obtained will be more rapid(see figure), whereas in cases where the relative quantum yield decreases the anisotropy rate obtained will be slower than the total intensity rate. At least three states are required if an equal

anisotropy and total intensity rate are obtained. We have used global analysis methodology to do an integrated analysis of the two types of data taking into account quantum yield terms to obtain internally consistent rates and physical parameters of transiently populated intermediate states. Protein unfolding and refolding of a deletion mutant of *Staph. aureus* nuclease show that the differences seen between total intensity and anisotropy rates can be attributed solely to quantum yield effects, and an intermediate exists between the folded and unfolded state. Other case studies will include changes in fluorescence upon binding of extrinsically labelled DNA by RNA polymerase and upon excision of fluorescent nucleotides by a DNA polymerase.

Tu-Pos138

QUENCHING OF INDOLE FLUORESCENCE BY CARBOXYLATE GROUPS. ((H.-T. Yu, W. Stryjewski, M.D. Barkley)) Department of Chemistry, Louisiana State University, Baton Rouge, LA 70803-1804

Carboxylates in the side chain of tryptophan derivatives are intramolecular quenchers of the chromophore indole's fluorescence. However, due to the coexistence of other decay processes which are also sensitive to changes in the side chain groups, it is difficult to single out the degree as well as the nature of the carboxylate quenching. But there is no such problem if an external (bimolecular) quencher is used. For various forms of the carboxylate, both the ester and the acid show strong quenching of indole fluorescence. The anion and amide (as in a peptide) show very little, if any, quenching ability. Fluorescence decays with and without a quencher were measured at various temperatures and fitted to an expression with an Arrenius term. It was found that ethylacetate quenches both indole and 3-methylindole with a temperature independent bimolecular quenching rate constant $k_q \approx 2 \times 10^8$ s^{-1} M^{-1}, the same as those obtained from Stern-Volmer quenching experiments. The fact that this quenching process is not temperature dependent suggests that it is activationless. Also, results of quenching versus reduction potential of various quenchers will be reported. (Supported by NIH Grant GM 42101)
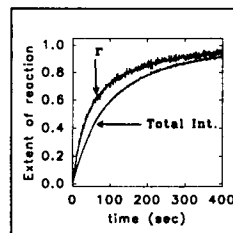
Tu-Pos139

γ-N- METHYLASPARAGINE: A POST-TRANSLATIONAL MODIFICATION THAT IMPROVES ENERGY TRANSFER EFFICIENCY IN PHYCOBILIPROTEINS. ((B.A. Thomas[a], L.P. McMahon[b] and A.V. Klotz[a])) Departments of Biochemistry[a] and Chemistry[b], Louisiana State University, Baton Rouge, LA 70803.

Phycobiliproteins are light-harvesting pigment-proten complexes found in cyanobacteria that transfer excitation energy to Photosystem II. A novel post-translationally modified asparagine, γ-N-methylasparagine (NMA), has been characterized at the β-72 site in many phycobiliproteins (Klotz, A.V. and Glazer, A.N. (1987) *J.Biol. Chem.* **262**: 17350-17355). The goal of this project is to substantiate the hypothesis that NMA uniquely interacts with the β-84 chromophore thereby optimizing energy transfer efficiency. Site-directed mutants of the cyanobacterium *Synechococcus* PCC 7002 that contain either an aspartate or glutamine at the β-72 site have been characterized in terms of their photosynthetic characteristics and by fluorescence spectroscopy. Introduction of aspartate leads to a 15% decrease in both the photosynthetic efficiency of whole cells and fluorescence quantum yield. Fluorescent lifetime data of the mutants show a decrease in one of the three lifetime components. Steady state anisotropy of purified mutant proteins indicate an average 33 and 21% increase over the wild-type for the aspartate and glutamine substitutions, respectively, which is attributed to decreased energy transfer efficiency. We are currently using time-resolved anisotropy to examine possible alterations in β-84 chromophore geometry and dynamics as a result of β-72 substitution.

Tu-Pos140

THE USE OF FLUORESCENCE METHODS TO MONITOR PROTEIN UNFOLDING REACTIONS. ((Maurice R. Eftink* and Cing-Yuen Wong**)) *Department of Chemistry, University of Mississippi, University, MS 38677 and **Department of Biology, The Johns Hopkins University, Baltimore, MD 21218. (Spon. by C. A. Ghiron)

Steady-state and time-resolved fluorescence methods are commonly used to monitor two-state protein unfolding. However, not all the observables (intensity, anisotropy, emission maximum, the average lifetime) track the population of the native or unfolded species in a linear manner. In this work, the assumptions and limitations of these methods will be highlighted through simulations of various two-state scenarios. The legitimacy of this concern will be further illustrated by comparison of the experimentally determined thermodynamic values recovered for the guanidine hydrochloride -induced unfolding of *Staph* nuclease, as tracked by the different fluorescence methods. Measurement of the fluorescence intensity as a function of denaturant concentration yields the thermodynamic values of the transition directly, whereas the signals from the other methods are weighted towards the more fluorescent native species, thereby skewing the transition towards higher denaturant concentrations. This research was supported by NSF grant DMB 91-06377.
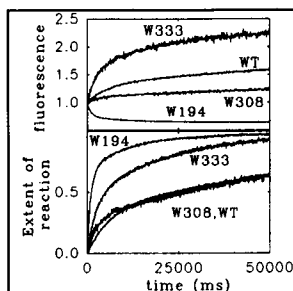
Tu-Pos141

COMPARISON OF THE FLUORESCENCE PROPERTIES OF WILD TYPE AND W15F MUTANT OF HORSE LIVER ALCOHOL DEHYROGENASE. ((Maurice R. Eftink*, Cing-Yuen Wong**, and Bryce V. Plapp***)) *Department of Chemistry, University of Mississippi, University, MS 38677, **Department of Biology, The Johns Hopkins University, Baltimore, MD 21218, and ***Department of Biochemistry, University of Iowa, Iowa City, IA 52242-1109

Horse liver alcohol dehydrogenase is a homodimeric protein; each subunit has two tryptophan residues that are located in distinctly different microenvironments. Trp-15 is located on the surface and Trp-314 is buried at the subunit interface. Steady-state and time-resolved fluorescence and phosphorescence studies have enabled the assignment of parameters, i.e. quantum yield, emission maximum decay times to the individual tryptophan residues in the protein. Recently, one of us (BVP) has prepared, by site-directed mutagenesis, the mutant W15F of this protein. We have characterized the fluorescence properties of this mutant and we show that the Trp-314 of the mutant experiences an apolar microenvironment, but that the fluorescence decay of the mutant is more complex than expected from the assignments for the wild type. This research was supported by NSF grant DMB 91-06377.

Tu-Pos142

STOPPED-FLOW STEADY-STATE FLUORESCENCE STUDY OF THE UNFOLDING TRANSITION KINETICS OF PGK USING WILD-TYPE AND THREE SINGLE-TRP PGK MUTANTS. ((N.E.Seethaler[1], M.R.Otto[1], M.T.Mas[2], J.M.Beechem[1])) [1]Vanderbilt University, Biophysics, Nashville TN; [2]Beckman Research Institute of the city of Hope, Duarte, CA.

Yeast Phosphoglycerate Kinase (PGK) is a well studied two domain hinge protein. Wild type PGK (WT) contains two Trp residues (W308, W333) both situated in the carboxy-terminal domain. Stopped-flow fluorescence total-intensity and anisotropy have been used to study the unfolding transition of the WT protein and three single-Trp mutants: W308, W333 and W194. W308 is situated on the surface, W333 is buried and W194 is located in the hinge region spanning the two domains. Examination of the un/refolding properties of these site-specific probes has the potential to provide

information concerning the temporal sequence of the folding event. The observed unfolding kinetics for these mutants are non-overlapping (upper fig. absolute intensities, lower figure normalized reactions). WT, W308 and W333 exhibit biphasic kinetics with fluorescence enhancement while W194 exhibits biphasic kinetics with fluorescence quenching. Steady-state stopped-flow refolding kinetics are now being examined.

Tu-Pos143

3-PHOSPHOGLYCERATE KINASE FOLDING-UNFOLDING DISTANCE CHANGES: A TIME-RESOLVED FLUORESCENCE AND STOPPED-FLOW ENERGY-TRANSFER STUDY. ((M.P. Lillo[1], B.K. Szpikowska[2], M.T. Mas[2] and J.M. Beechem[1])) [1]Vanderbilt University, Nashville, TN 37232; [2]Beckman Research Institute of the City of Hope, Duarte, CA 91010.

We are studying the conformational changes during the folding-unfolding transition in the two domain enzyme yeast PGK, using steady-state and time-resolved fluorescence energy-transfer experiments combined with stopped-flow fluorescence techniques. Different combinations of single and double cysteine PGK mutants were examined using site-specific mutagenesis of PGK and labeled with IAEDANS (donor) and IAF (acceptor) (G.Haran et al. (1992) PNAS 89, 11764). The distance distributions were determined from the global analysis of the donor

and donor-acceptor time-resolved fluorescence decays with the average distance between the probes (C135- C290) changing from 40Å (folded) to 70Å (unfolded). Kinetics of the energy transfer unfolding were monitored in T-format allowing quantitation of both intensity changes (donor increases and acceptor decreases, see fig). Two rate constants (0.3 s^{-1} and 0.04s[-1]) were obtained and the first phase appears to be accounting for 80% of the change in energy transfer efficiency. Double kinetics are being performed in order to obtain "millisecond motion-pictures" of these changes in intramolecular distances.

Tu-Pos144

TWO-WAY PACKING OF RIBONUCLEASE-T1 TRYPTOPHAN-59: FLUORESCENCE KINETICS, CRYSTALLOGRAPHIC, AND MINIMUM PERTURBATION MAPPING STUDIES ((Christopher Haydock, Salah S. Sedarous and Franklyn G. Prendergast)) Department of Biochemistry and Molecular Biology, Mayo Foundation, Rochester, Minnesota 55905.

Minimum perturbation mapping simulations of the ribonuclease-T1 tryptophan-59 side chain show that the χ^2 side chain dihedral angle may adopt either an antiperpendicular or a perpendicular conformation. The transition state theory estimate for the interconversion rate of these conformers is 10^{-4} s^{-1}, which is slower than experimental unfolding rates. The true rate of conformer interconversion is that for complete or partial protein unfolding and is somewhere in the milliseconds to hundreds of seconds range. The fluorescence intensity decay of ribonuclease T1 is biexponential and pH dependent. Assuming these decay components correspond to the two tryptophan conformers, the interconversion rate constant can be measured by a pH jump experiment. The rate constant is faster than the time resolution of our present measurements. Published crystallographic structures have tryptophan-59 in the *trans* antiperpendicular conformation. However, visual inspection of the electron density around tryptophan-59 suggests that both the *trans* antiperpendicular and perpendicular conformations are possible. Crystallographic refinement of the structure and occupancy of these conformations is in progress. This work is supported in part by the W. M. Keck Foundation and GM 34847.
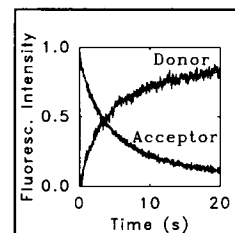
Tu-Pos145

Conformational Flexibility in a Staphylococcal Nuclease Mutant K45C from Time-Resolved Resonance Energy Transfer Measurements ((Pengguang Wu and Ludwig Brand)), Department of Biology, Johns Hopkins University, Baltimore, MD 21218

Thermal fluctuations exist in proteins and other macromolecules in solution. Fluctuations may play a role in ligand or receptor binding, control rates of enzymatic catalysis, or define a range of conformations a segment can adopt in solution. We apply the method of time-resolved resonance energy transfer to study the conformational flexibility of a staphylococcal nuclease mutant, K45C, where lysine 45 located at a flexible loop is replaced by a cysteine. We labeled the thiol group with DTNB (5,5'-dithiolbis-2-nitrobezoic acid) and used the TNB group covalently attached to the protein as an energy acceptor from the donor fluorescence of a single tryptophan at residue 140. Conformational flexibility occuring on the time scale of nanoseconds or longer is dispersed as an apparent distance distribution in time-resolved resonance energy transfer measurements. Below room temperature the apparent distance distribution was fitted with a symmetric Lorentzian model with a full width at half maximum height of about 6 Å, indicating substantial degrees of heterogeneity between residues 45 and 140. At room or higher temperature where the protein is in its native state, the apparent distance distribution is asymmetric, indicating the presence of static disorders. Segments in the protein that contribute to the static disorder can be converted to mobile ones with the addition of denaturing guanidinium chloride. Supported by NIH Grant GM-11632.

Tu-Pos146

BASIC FIBROBLAST GROWTH FACTOR: INTRINSIC FLUORESCENCE CHANGES UPON BINDING OF SURAMIN AND HEPARIN. ((M.R. Ranson*, A.L. Stone#, D.K. Porter+ and R.F. Chen+)) *Clinical Pharmacology Branch, NCI, NIH, #NIMH, NIH, and +Lab. of Cellular Biology, NHLBI, NIH, Bethesda, MD 20892.

The intrinsic fluorescence of basic fibroblast growth factor (bFGF) arises from the single Trp located in the receptor binding loop, and from multiple Tyr residues. Suramin, a potent inhibitor of bFGF-receptor interaction, binds to bFGF and completely quenches Trp fluorescence. Fluorescence resonance energy transfer (FRET) calculations based on the overlap of the Trp emission and Suramin absorption spectra, and a random orientation factor $\kappa^2 = 2/3$ show the Trp-Suramin distance must be only ≤9 Å. The use of $\kappa^2 = 2/3$ is rationalized by evidence for rotamer formation and segmental flexibility, both of which tend to randomize indole orientation. Heparin, which is required for strong binding of bFGF to receptor, strongly enhances Trp and quenches Tyr emission. CD spectra suggest that conformational changes which are effected by Suramin and heparin are different in nature, consistent with the opposing effects of these modulators. Both compounds seem to target the receptor binding region, as shown by the changes in the fluorescence of Trp, an intrinsic probe of this site.

Tu-Pos147

TIME-RESOLVED CIRCULARLY POLARIZED FLUORESCENCE STUDIES OF NADH BOUND TO LADH ((J.A. Schauerte, B.D. Schlyer, D.G. Steel & A. Gafni)) Institute of Gerontology University of Michigan, Ann Arbor, Michigan

We have used the Time-Correlated Single Photon Counting method based on high throughput Time-to-Digital Converters (TDC) and Histogramming Memory to perform the first demonstration of Time-Resolved Circularly Polarized Fluorescence (TR-CPF) on the subnanosecond time scale for fluorescence decays. Using this system we have measured the TR-CPF of Nicotinamide Adenine Dinucleotide (NADH) bound to Horse Liver Alcohol Dehydrogenase (LADH). The measurements have established the existence of a rapid excited state rearrangement of a group(s) near the nicotinamide chromophore while bound to LADH. This is reflected by a rapid reduction in the magnitude of NADH's excited state optical activity occurring with a decay time of less than 0.6nsec. This rearrangement occurs in binary mixtures of NADH/LADH, however it is inhibited in ternary complexes that include the substrate analogue isobutyramide (IBA). In addition, the short biexponential NADH fluorescence lifetime in solution (0.3 & 0.6 nsec) increases when the coenzyme is bound to LADH (0.5 & 2.0 nsec), with an additional increase in the lifetime with the formation of the ternary NADH/LADH/IBA complex (2.0 & 4.5 nsec). The shorter flourescence lifetime of the binary complex may reflect a continued exposure of the nicotinamide group to the solvent environment. During the excited state of NADH, a group in close proximity to nicotinamide may respond to the excited state dipole and adjust it's orientation, changing the excited state chiral environment.
Supported by NIA grant #AG09761 and by ONR N00014-91-J-1938

Tu-Pos148

FLUORESCENCE SPECTROSCOPY OF WILDTYPE AND A W314F MUTANT OF HUMAN ALCOHOL DEHYDROGENASE (T. EHRIG, S.S. SEDAROUS, B.B. MUHOBERAC, T.D. HURLEY, W.F. BOSRON AND F.G. PRENDERGAST) Mayo Foundation, Rochester, MN 55905, and Indiana University, Indianapolis, IN 46202. (Spon. by S.S. Sedarous)

The dimeric $\beta_1\beta_1$ human liver alcohol dehydrogenase has two tryptophans per subunit, Trp 15 and Trp 314. A W314F mutant was used to deconvolute the time-resolved fluorescence signals from the two tryptophans. Trp 314 in the dimeric protein shows an essentially monoexponential fluorescence intensity decay with a lifetime around 3 ns. Upon monomerization of the protein subunits, the decay becomes biexponential indicating a change in environment of Trp 314 which is located at the subunit interface. Trp 15 in the dimeric mutant protein has a quasi monoexponential fluorescence intensity decay with a lifetime around 7 ns, a high steady-state anisotropy of 0.23, and a quantum yield of 0.23. None of these parameters of Trp 15, nor its steady-state fluorescence emission spectrum, change substantially upon subunit monomerization in the mutant enzyme, indicating that the tertiary structure of the protein matrix surrounding Trp 15 is not substantially perturbed. This observation shows that monomerization does not lead to a gross rearrangement of the protein tertiary structure and is consistent with the previously demonstrated enzymatic activity of the monomeric form. (AA07117, GM 34847)

Tu-Pos150

THE TRYPTOPHAN ENVIRONMENTS OF THE INTERLEUKIN RECEPTOR ANTAGONIST PROTEIN AS REVEALED BY STEADY STATE AND DYNAMIC FLUORESCENCE MEASUREMENTS ((D.E. Epps, A.W. Yem, M.R. Deibel, and J.D. Petke')) Upjohn Laboratories, 7000 Portage, Kalamazoo, Mich. 49001

Interleukin receptor antagonist protein (IRAP) is a cytokine that binds to the same receptors as interleukin-1β (IL-1β) and acts as an antagonist. The two cytokines have been shown by NMR and X-ray crystallography to be structurally closely related in spite of the fact that their sequence is only 25% homologous. The differences in biological activities suggest that there are certain conformational determinants in IRAP which modulate its specific biological activities. IRAP and IL-1β both have a tryptophan at position 120, and IRAP has a additional Trp at position 17. We exploited the presence of these intrinsic fluorescent residues to characterize their microenvironments and used the results to define solution conformational differences in the two proteins. We employed wavelength-dependent quenching and lifetime-resolved emission methodologies, coupled with steady state quenching, chemical modification, and temperature-dependent tryptophan fluorescence measurements to compare thoroughly and to contrast the solution conformations of IRAP and IL-1β.

The data from the wavelength-dependent quenching and lifetime measurements were used to reconstruct the corrected emission spectra of the fluorescent species. We found that these emission spectra of the proteins, along with that of Trp in solution, could be analyzed as a function of wavenumber by fitting to Gaussian curves to obtain the emission maxima of individual species. These data, along with temperature-dependent steady state and dynamic fluorescence measurements and with hydrophobic probe binding allowed us to demonstrate solution conformation differences in the two proteins which may be related to their individual biological activities.

Tu-Pos152

FLUORESCENCE DEPOLARIZATION OF FLUORESCEIN-LABELED ERYTHROCYTE WATER CHANNEL CHIP28. ((Javier Farinas and A.S. Verkman)) Program in Biophysics, UCSF, CA 94143.

CHIP28 is an integral membrane protein that selectively transports water in a mercurial-inhibitable manner. To analyze nanosecond segmental dynamics of CHIP28, we developed procedures to label purified CHIP28 with a fluorescein chromophore. Purified CHIP28 in right-side-out vesicles was labeled with fluorescein isothiocyanate at a fluorescein-to-protein molar labeling ratio of <1. SDS-PAGE showed that fluorescein-labeled CHIP28 migrated identically to unlabeled CHIP28. To label CHIP28 at a -SH site, a sulfhydryl-specific fluorescein label, S-(chloromercuri)-N-(2' mercaptoethyl) fluoresceinamide (SNFA), was synthesized by reaction of fluorescein succinimidyl ester with cystamine, followed by reduction and stoichiometric addition of mercuric chloride. SNFA was bound specifically to cysteines on CHIP28 at a label-to-protein ratio of 0.23; binding was reversed by dithiothreitol. Functional studies showed that labeling of CHIP28 with FITC or SNFA did not affect water permeability or the inhibition of water permeability by mercurials. Steady-state anisotropy of FITC-labeled CHIP28 was ~0.1, much greater than that of unconjugated dye (0.01). Time-resolved anisotropy measurements as described by Thevenin, Periasamy, Shohet and Verkman (PNAS, in press) revealed ps and ns fluorescein rotations in a hindered environment. There was a small effect of mercuric chloride binding on anisotropy, consistent with a protein conformational change. The availability of fluorescently labeled CHIP28 will be useful for analysis of CHIP28 segmental dynamics and water transporting mechanisms.

Tu-Pos149

INTERACTION OF DIPYRIDAMOLE DERIVATIVES WITH BOVINE SERUM ALBUMIN. ((C.P.F. Borges, G. Sartor*, A. Spisni* and M. Tabak)) IFQSC-USP, C.P. 369, 13560-970, São Carlos, SP, Brasil. *Ist. Chim. Biol., Università di Parma, Parma, Itália.

Interaction of several derivatives of the vasodilator dipyridamole (DIP) with bovine serum albumin (BSA) has been studied through the analysis of emission spectra, fluorescence intensity and anisotropy in solution allowing the determination of binding parameters and stoichiometry. The derivatives were RA14, RA39, RA47 and RA25. The association constants obtained from emission intensities were in the range $1.0 - 10.0*10^3M^{-1}$ the values being greater at pH 7 as compared to pH 5 and the number of binding sites was in all cases close to one. In aqueous solution the anisotropy is essentially zero; binding to the protein leads to an increase of r_0 to $0.2 - 0.3$. Simple model allowed to obtain binding parameters from anisotropy in agreement with those from emission intensity. DIP and RA14 are tightly bound to the protein displaying the greater anisotropy while RA47 and RA25 show a weaker superficial binding. Fluorescence quenching using acrylamide, iodide and nitroxide radicals allowed the determination of the bimolecular constant which is very similar at pHs 7 and 5 for DIP and RA14 and acrylamide decreasing to 0.5 and 0.6 of its value in the presence of BSA. For RA25 this decrease is smaller $(0.8 - 0.9)$. For iodide a substantial decrease of k_q takes place at pH 5. So at pH 7 the drug is more protected in the interior of the protein becoming more exposed at pH 5.

Support: CNPq, FAPESP and FINEP brazilian agencies.

Tu-Pos151

DYNAMICS OF BOVINE Cu,Zn SUPEROXIDE DISMUTASE REVEALED BY TIME-RESOLVED FLUORESCENCE SPECTROSCOPY. ((S.T. Ferreira, L. Stella & E. Gratton)) Laboratory for Fluorescence Dynamics, Dept. of Physics, Univ. of Illinois at U-C, Urbana, IL 61801.

Bovine Cu, Zn superoxide dismutase (BSOD) is a dimeric enzyme containing a single solvent exposed tyrosine residue per subunit. We have studied the fluorescence emission of this residue as a probe of the conformational dynamics of BSOD. Our results indicate that the protein matrix fluctuates between multiple interconverting conformational substates, and that the fluorescence decay of the tyrosine residue is sensitive to these motions. Frequency-domain fluorescence lifetime measurements of BSOD revealed a heterogeneous fluorescence decay. We demonstrated that the fluorescence decay could be well described by a continuous Lorentzian distribution of lifetime values, corresponding to different environments sampled by the fluorescent probe during its excited state. The fluorescence intensity decay was measured at different temperatures and viscosities, and in the presence of different concentrations of the denaturant, guanidine hydrochloride. All these results can be rationalized in terms of our model of interconverting conformational substates. Fluorescence anisotropy decay measurements suggest that the heterogeneity in the intensity decay is not due to local mobility of the tyrosine residue, but rather to motions of the protein matrix surrounding this residue. Supported by National Institutes of Health grant RR03155. STF is a PEW Charitable Trusts Fellow in the Biomedical Sciences.

Tu-Pos153

INTERACTION OF PAF WITH HUMAN PLATELETS MEMBRANE REVEALED BY LAURDAN FLUORESCENCE. ((R. Fiorini and A. Kantar)) Departments of Biochemistry & Pediatrics, University of Ancona, 60100 Ancona, Italy.

Platelet activating factor (PAF) is a potent lipid mediator with a wide spectrum of biological activities in a variety of cells. The stimulation of human platelets by PAF is accompanied by a complex cascade of biochemical events that influence the plasma membrane (Mediators Inflammation 1992;1:127-131). Changes in membrane polarity of human platelets during the interaction with PAF were investigated by measuring the steady-state fluorescence emission spectra of 2-dimethylamino(6-lauroyl)naphthalene (Laurdan) which is known to be incorporated at the hydrophilic-hydrophobic interface of the membrane, displaying spectral sensitivity to the polarity of its surrondings. Laurdan shows a marked steady-state emission red-shift in polar solvents, with respect to non-polar solvents. Our results demonstrate that PAF (10^{-7} M) induces a red-shift of the fluorescence emission spectra of Laurdan. These changes were not observed in the presence of the PAF antagonist, L659,989. These data suggest that the interaction of PAF with platelets is accompanied by an increase in membrane polarity.

Tu-Pos154

ADAPTATION IN AN INSECT MECHANORECEPTOR NEURON INVOLVES BOTH OUTWARD AND INWARD CURRENTS ((P.H.Torkkeli and A.S. French)) Department of Physiology, University of Alberta, Edmonton, Alberta, Canada.

Rapid adaptation in the cockroach tactile spine neuron is produced during action potential encoding. Adaptation has several components with different time constants and it can be removed or reduced by extracellular application of the potassium channel blockers 4-aminopyridine (4-AP) and charybdotoxin (CTX) as well as by calcium channel blockers such as cadmium. The agents Chloramine-T and phentolamine, which remove slow sodium inactivation, also reduce adaptation. Voltage-clamp experiments have revealed at least three different currents underlying the adaptation process: 1. A 4-AP-sensitive, very rapidly inactivating transient outward potassium current (I_A), 2. A CTX- and cadmium-sensitive calcium-activated potassium current, and 3. A slowly inactivating component of inward sodium current. The delayed rectifier potassium current, which is also found in these neurons, does not seem to be involved in the adaptation.
Supported by the Medical Research Council of Canada and the Alberta Heritage Foundation for Medical Research.

Tu-Pos155

AMINOGLYCOSIDE BLOCKADE AND AMPHIPATH ACTIVATION OF STRETCH ACTIVATED ION CHANNELS FROM CHICK SKELETAL MUSCLE.
((M. Sokabe, N. Hasegawa, and K. Yamamori)) Dept. Physiol. Nagoya Univ. Sch. Med., 65 Tsurumai, Nagoya 466, Japan

Stretch activated (SA) ion channels are ubiquitously distributed in all organisms and supposed to have important roles in fundamental cell functions. However, because of the lack of useful blockers and activators the mechanism of activation or physiological role of the channels is unclear. We have found that aminoglycoside antibiotics such as neomycin and kanamycin strongly blocked the cation permeable SA channels of cultured chick skeletal muscle cells. Although these drugs block other ion channels like Ca or K channels, their dissociation constants (2-50 uM) for the SA channels is much lower than that for other channels. We also have found that several amphipaths could activate the SA channels without mechanical stimulations. For example, 10 uM chlorpromazine (CPZ) time dependently activated the SA channels, which might arise from the generation of stress caused by time dependent penetration of the drug into the lipid bilayer. The manner of the activation by these drugs was very similar to that by mechanical stimulations. As the activation of the SA channels in our preparation has been suggested to involve membraneous cytoskeletal structures, both cytoskeletons and lipids may contribute to SA channel activation.

Tu-Pos156

AMPLIFICATION OF Ca^{2+} SIGNALS DURING STRETCH-ACTIVATED CHANNEL ACTIVITY IN MEMBRANE PATCHES IN SINGLE SMOOTH MUSCLE CELLS. ((Agustin Guerrero, Michael T. Kirber, Richard A. Tuft, Fredric S. Fay, & Joshua J. Singer)), Dept. of Physiology, Biomedical Imaging Group, Univ. of Mass. Med. School, Worcester, MA 01605.

Stretch-induced contraction in smooth muscle presumably occurs because of a rise in intracellular $[Ca^{2+}]([Ca^{2+}]_i)$. We used simultaneous monitoring of $[Ca^{2+}]_i$ with Fura-2 loaded by its AM ester and unitary currents from stretch-activated channels to determine the mechanisms whereby membrane stretch causes a rise in $[Ca^{2+}]_i$. Activation of stretch-activated channels in cell-attached patches when suction was applied to the patch pipette caused an increase in $[Ca^{2+}]_i$. A portion of the rise in $[Ca^{2+}]_i$ appeared to result from Ca^{2+} entry through the membrane outside of the patch as this increase in $[Ca^{2+}]_i$ was reduced by the presence of 100 µM $GdCl_3$ or local application of BAPTA to the membrane outside of the patch electrode. The remainder of the $[Ca^{2+}]_i$ rise induced by membrane stretch was blocked by eliminating Ca^{2+} from or including $GdCl_3$ in the patch pipette. The Ca^{2+} that enters through stretch-activated channels appears to be amplified by Ca^{2+}-induced-Ca^{2+}-release from intracellular stores as ryanodine markedly inhibited the increase in $[Ca^{2+}]_i$ observed for a given level of current from membrane stretch. Images of $[Ca^{2+}]_i$ obtained with the ultrafast digital imaging microscope revealed that when Ca^{2+} was excluded from the bath, a $[Ca^{2+}]_i$ gradient was seen in the cell being highest near the tip of the patch pipette whereas when Ca^{2+} was included in the bath, changes in $[Ca^{2+}]_i$ in response to channel activity were more global in nature. These observations suggest that opening of stretch-activated channels can trigger elevations in $[Ca^{2+}]_i$ from both the channels themselves as well as other sources.

Tu-Pos157

Gd^{3+} SENSITIVE $[Ca^{2+}]_i$ INCREASE BY HYPOTONIC STIMULATION IN CULTURED HUMAN ENDOTHELIAL CELLS ((K. Naruse, M. Minami, and M. Sokabe)) Physiology, Nagoya Univ. Sch. Med. Nagoya 466 Japan.

Hypotonic treatment caused $[Ca^{2+}]_i$ changes, a transient increase followed by a sustained one, with 2 mM $[Ca^{2+}]_o$ in cultured human umbilical vein endothelial cells. Without extracellular Ca^{2+}, hypotonic treatment caused transient $[Ca^{2+}]_i$ increases without sustained level. In the presence of 10 µM Gd^{3+}, a blocker for stretch activated (SA) channels, the both responses were abolished. The first transient phase might be from internal Ca^{2+} stores and the sustained level from extracellular Ca^{2+} probably via stretch activated ion channels.
To test which internal Ca^{2+} stores are responsible for the transient response, psitectorigenin, which is an inhibitor of phospholypase C, and ryanodine, an inhibitor for Ca^{2+}-induced Ca^{2+}(CICR) release mechanism, were employed without extracellular Ca^{2+}. When pretreated with psitectorigenin to downregulate IP3 production, hypotonic treatment still raised $[Ca^{2+}]_i$ although ATP stimulated increase in $[Ca^{2+}]_i$ was abolished. Ryanodine also did not effect the $[Ca^{2+}]_i$ increase by hypotonic stimulation but Gd^{3+} did.
These results suggest that hypotonic stimulation caused $[Ca^{2+}]_i$ increase from another Ca^{2+} release mechanism other than CICR or IP3CR channels which is sensitive to extracellular Gd^{3+} and hypotonicity.

Tu-Pos158

CURRENTS EVOKED BY MECHANICAL DEFORMATION OF THE MEMBRANE IN *XENOPUS LAEVIS* OOCYTES. ((I. Medina[1], J. Stinnakre[2] and P. Bregestovski[3])) [1]Institute of Biochemistry, Lvov, 290005 Ukraine; [2]Laboratoire de Neurobiologie Cellulaire et Moléculaire, C.N.R.S., 91198-Gif/Yvette, France; [3]INSERM, U-29, 75014-Paris, France. (Spon. by R. Kado)

Single stretch-activated channels (SAC) have been studied in many preparations, but attempts to obtain whole-cell SAC currents were not always successful. Using double microelectrode voltage clamp we found that 2 different mechanical stimuli such as jets of saline and increase of external osmotic pressure modulate SAC current in *Xenopus laevis* oocyte membrane. Both, jet pressure pulses and osmolarity augmentation had opposite effects depending on cells. In 50% of cells, an inhibition of SAC current was observed, while in the other half the reverse effect was found. In both cases, mechanically modulated current had a similar E_{rev} (-18 mV) and did not depend on chloride ions. Gd^{3+} blocked all effects produced by the 2 types of stimulus.
The behavior of single SAC recorded from cell-attached patches confirmed the results obtained in whole-cell recording: rising the osmolarity of external solution increased strongly SAC activity in patches showing a low basal activity but decreased it when basal activity was high.
These results show that SAC activity in *X. laevis* oocytes could be recorded and that it is sensitive to osmotic pressure changes as well as mechanical deformation of the membrane. The possible physiological role of SAC in the processes of maturation, fertilization and early embryogenesis is discussed.

Tu-Pos159

MOLECULAR CHARACTERIZATION OF A SWELLING-INDUCED CHLORIDE CONDUCTANCE REGULATORY PROTEIN, pI_{Cln}. ((G.B. Krapivinsky, M.J. Ackerman, E.A. Gordon, L.D. Krapivinsky, and D.E. Clapham)) Department of Pharmacology, Mayo Foundation, Rochester, MN 55905.

Virtually all cells maintain strict control over their cell volume. Although the potassium and chloride conductance pathways which respond to perturbations in cell volume have been elucidated, the molecular identities of the channel/regulatory proteins responsible for volume regulation are essentially unknown. A novel protein (pI_{Cln}) from kidney epithelial cells was cloned using expression of a chloride current in *Xenopus laevis* oocytes (Paulmichl et al., 1992). We have cloned I_{Cln} homologs of Madin Darby Canine Kidney (MDCK) epithelia pI_{Cln} from rat heart and *Xenopus* oocytes and found a high degree of conservation between species and cell type. Endogenous pI_{Cln} was identified as an abundant and predominantly soluble cytosolic protein (~40 kD) in epithelial and cardiac cells, brain, and *Xenopus* oocytes and formed complexes with soluble actin as well as several other cytosolic proteins. Since I_{Cln}'s sequence is unlike that of any known ion channel and does not immunolocalize to the plasma membrane, it is possible that pI_{Cln} is a chloride conductance regulatory protein rather than an ion channel itself. Monoclonal antibodies specifically recognizing pI_{Cln} blocked activation of a native hypotonicity-induced chloride current ($I_{Cl,swell}$) in *Xenopus* oocytes, suggesting that pI_{Cln} may link actin-bound cytoskeletal elements to an unidentified volume-sensitive chloride channel protein. pI_{Cln}'s high degree of sequence identity and widespread expression suggest that pI_{Cln} is an important element in cellular volume regulation.

Tu-Pos160

HYPOTONICITY ACTIVATES A CHLORIDE CURRENT IN *XENOPUS* OOCYTES. ((M.J. Ackerman, K.D. Wickman, and D.E. Clapham)) Department of Pharmacology, Mayo Foundation, Rochester, MN 55905.

Xenopus oocytes are frequently utilized for *in vivo* expression of cellular proteins, especially ion channel proteins. A thorough understanding of the endogenous conductances and their regulation is paramount for proper characterization of expressed channel proteins. Here we detail a novel chloride current ($I_{Cl,swell}$) responsive to hypotonicity in *Xenopus* oocytes using the two-electrode voltage clamp technique. Reducing the extracellular osmolarity by 50% elicited a calcium-independent chloride current having an anion conductivity sequence identical with swelling-induced chloride currents observed in epithelial cells. The hypotonicity-activated current was blocked by chloride channel blockers, trivalent lanthanides, and nucleotides. G-protein, cAMP-PKA, and arachidonic acid signalling cascades were not involved in $I_{Cl,swell}$ activation. $I_{Cl,swell}$ is distinct from both stretch-activated nonselective cation channels and the calcium-activated chloride current in oocytes and may play a critical role in volume regulation in *Xenopus* oocytes.

Tu-Pos161

EFFECT OF GADOLINIUM ON THE INTRINSIC OSMOSENSITIVITY OF RAT SUPRAOPTIC NEURONS ((S. H. R. Oliet and C. W. Bourque)) Centre for Research in Neuroscience, Montreal General Hospital and McGill University, Montreal, P.Q., Canada.

The release of neurohypophyseal hormones from supraoptic neurons is modulated by extracellular fluid osmolality. We recently described the steady-state osmotic regulation of a non-selective cationic conductance in these neurons. This conductance was found to be regulated by changes in cell volume accompanying osmotic stimulation. Moreover, single-channel recordings have suggested the involvement of stretch-inactivated cationic channels in the transduction process of supraoptic neurons osmosensitivity (*Nature 364, 1993*). In order to confirm the role of mechanosensitive channels in this physiological response, we examined the effect of gadolinium (Gd^{3+}), a potent blocker of different types of stretch-sensitive cationic channels, on supraoptic neurons acutely isolated from adult rat. Whole-cell voltage-clamp recordings revealed that bath-application of Gd^{3+} induced a reversible inhibition of the osmotic responses elicited by hypertonic stimulations (IC50≈50μM, n=7). Preliminary results suggest that the block of the whole-cell osmotic responses by Gd^{3+} is due to a reduction of the mean open time of the mechanosensitive channel. These findings strenghten the link between microscopically-detected stretch-inactivated channels and macroscopic osmosensitivity in magnocellular neurosecretory cells of rat supraoptic nuclei.
Supported by the MRC and Heart & Stroke Foundation of Canada.

Tu-Pos162

CARDIAC CELL VOLUME RESPONSE TO OSMOTIC STRESS: TEMPERATURE-DEPENDENCE AND KINETICS. ((Mirik A. Suleymanian and Clive M. Baumgarten)) Dept. of Physiology, Medical College of Virginia, Richmond, VA 23298-0551 and Dept. of Biophysics, Armenian Academy of Sciences, Yerevan, Armenia

Cell volume changes induced by osmotic stress (± mannitol) were studied in rabbit ventricular myocytes at 37, 22, and 6°C. Volumes were measured by digital video microscopy. Each cell served as its own control, and volumes are expressed relative to the volume in isotonic (1T) media. Cell swelling on switching from 1T to 0.5T decreased in the cold from 1.58 ± 0.02 (n = 13) at 37° to 1.49 ± 0.02 (n = 15) at 22° to 1.44 ± 0.02 (n = 12) at 6°C. In contrast, shrinkage on switching from 1T to 2T was unaffected; 0.68 ± 0.01 (n = 29) at 37°, 0.70 ± 0.01 (n = 16) at 22°, 0.69 ± 0.01 (n = 7) at 6°C. The low temperature-dependence of swelling and shrinkage implies that osmolyte transport only modestly affects the volume change with osmotic stress. The kinetics of volume perturbations with 2-fold changes in osmolarity slowed on cooling with an apparent E_a of 7 and 10 kcal/mol from 37 to 22° and 22 to 6°C. Moreover, swelling was significantly slower than shrinkage.

	$T_{1/2}$, s (mean ± SE; (n))		
	37°C	22°C	6°C
1T→0.5T	37.0 ± 2.4 (13)	70.7 ± 4.0 (15)	185.0 ± 12.6 (12)
0.5T→1T	24.9 ± 1.1 (13)	50.6 ± 1.9 (15)	165.4 ± 14.9 (7)
1T→2T	15.1 ± 0.7 (29)	26.5 ± 1.3 (15)	66.4 ± 4.9 (7)
2T→1T	27.2 ± 1.2 (26)	39.7 ± 1.9 (13)	125.0 ± 11.5 (6)

Kinetic anisotropy is consistent with swelling-induced forces opposing osmotic water flux or an anisotropy of water permeability. The differences in the time-course of volume changes with temperature suggests that cardiac cells can withstand significant transmembrane pressure gradients without rupture.

Tu-Pos163

ARE SMALL CONDUCTANCE Cl CHANNELS SHAPE AND VOLUME SENSORS? ((L.C. Schlichter, P.A. Schumacher and G. Sakellaropoulos)) Playfair Neurosci. Unit, The Toronto Hosp. and Dep't of Physiology, U. of Toronto, Ontario, Canada M5T 2S8

Human peripheral T lymphocytes (T_L) undergo shape and volume changes when activated, during cell-cell interactions and when leaving the blood (extravasation). An experimental paradigm used to study volume regulation is the regulatory volume decrease (RVD), which involves a conductive pathway for Cl⁻ efflux. In the present study, a whole-cell Cl⁻ current in normal human T_L was characterized. The anion selectivity of this current resembles that of the Cl⁻ efflux pathway during RVD. The single-channel conductance is ~ 0.7 pS. The channel is acutely blocked by flufenamic acid, but poorly inhibited by DIDS or SITS. Channel regulation by second messengers and osmotic shock was investigated. Following break-in, the Cl⁻ current develops spontaneously with time then runs down with a mono-exponential time course over several minutes. The temperature dependence of the development of current is not consistent with diffusion washout of an inhibitory factor. Though hyperosmotic shock accelerates rundown, the current is only modestly regulated by cell shrinking and swelling, and then only after staurosporine preincubation. The presence or absence of intracellular ATP has no effect. The current is insensitive to intracellular pH and Ca^{2+}, whereas GTPγS, cAMP, and the kinase inhibitor, staurosporine, all stimulate the current. In contrast, the PKC activator, phorbol dibutyrate, and the phosphatase inhibitor, okadaic acid, are both inhibitory. We conclude that these small-conductance Cl⁻ channels are not just volume sensors.

Tu-Pos164

MULTIPLICITY OF MECHANOSENSITIVE ION CHANNELS OF THE NATIVE PLASMA MEMBRANE OF *E.COLI*.
((C. Berrier, M. Besnard, A. Coulombe and A. Ghazi)) URA CNRS 1116, URA CNRS 1121 Université Paris-Sud, F-91405 Orsay and Hôpital M. Lannelongue (URA CNRS 1159), F-92350 Le Plessis Robinson, FRANCE. (Spon. by R. Fischmeister)

Giant protoplasts (i.e. structure devoid of outer membrane) of *E.coli* were prepared from giant round cells by a combination of lysozyme-EDTA treatment and osmotic downshock. The protoplasts can be clearly distinguished from untreated cells by their optical aspect under light microscope. Patch-clamp experiments performed on these structures, revealed the existence of different conductances (100 to 2000 pS in 0.1 M KCl) activated by stretch. By comparison, in experiments performed with purified plasma membrane reconstituted into giant liposomes, each patch generally displayed multiple stretch-activated conductances of identical level, which varied from patch to patch (100 ,300, 500, 1000, 1400 and 2000 pS). In both preparations, the higher the conductance, the higher was the negative pressure needed for its activation. Taken as a whole these experiments are consistent with the notion that *E.coli* possesses a whole array of different mechanosensitive channels corresponding to different proteins. These channels can be collectively activated in the native membrane, but segregate into clusters of identical channels upon the dilution brought up by the reconstitution procedure. The localization of these channels in the plasma membrane is consistent with their putative role in osmoregulation

Tu-Pos165

CAN MEMBRANE PROTEINS DRIVE A CELL? ((K.H. Iwasa)) NIDCD, NIH, Bethesda, MD 20892

Unlike motilities in most cells, in which chemical energy is utilized by molecules associated with cytoskeletal proteins, the outer hair cell in the mammalian cochlea has a membrane potential-dependent motility in which the electrical energy at the plasma membrane appears to be directly utilized. This motility is examined by constructing a model, based on two kinds of experimental observations, elasticity and membrane capacitance of the cell. The elastic property of the cell is described by a membrane model with the cylindrical geometry and area- and shear moduli [J. Acoust. Soc. Am 92 (1992) 3169]. A charge of the motor element (or molecule), which is transferred across the membrane, is determined by the voltage-dependent capacitance of the cell. The membrane area change of this motile element is observed as stretch sensitivity of the membrane capacitance [Biophys. J. 65 (1993) 492]. It can be shown that the elastic element and the motor element are connected in series. Thus apparent strains of the cell are represented by a sum of true elastic strains applied to the elastic element and changes due to motor molecules. With this model it is possible to obtain isometric force and isotonic displacements of the cell. The model predicts the correct amplitude of the movement at load free condition. The predicted value for isometric force is also consistent with *in vivo* data.

Tu-Pos166

BINDING SITES FOR ANTIBODIES TO ANIMAL INTEGRIN, VITRONECTIN & FIBRONECTIN IN A PLANT MODEL FOR MECHANOSENSING.
((J.S. Gens, K.W. Doolittle, J.G. McNally & B.G. Pickard)) Biology Department, Washington University, St. Louis MO 63130.

Gravitropic stimuli as well as a wide range of other signals are putatively transduced by mechanosensory calcium-selective ion channels. These channels have been studied in onion epidermal cells from bulb scale and leaf sheath epidermis. Detecting and responding to mechanical signals as well as others has been postulated to involve force transmission from the extracellular matrix (cell wall) through clusters of wall-to-membrane linkers (WMLs) to clusters of transmembrane linkers (TMLs) which in turn convey force either through the membrane or through attached cytoskeletal elements to the channels (Ding & Pickard, Plant J. 3:83, 1993; Pont-Lezica, McNally & Pickard, Plant, Cell, & Environ. 16:11 1993; Pickard & Ding, Austr. J. Plant Physiol. 20, issue 4, in press). In animal cells, integrin often serves as a TML to which extracellular matrix proteins such as vitronectin and fibronectin are attached. Therefore, we have used antibodies to these proteins to investigate whether similar antigens might serve as WMLs and TMLs in bulb scale epidermis cells. Using computational optical sectioning fluorescence microscopy, we have created stereo-pair images of protoplasts exposed to paired primary antibodies labeled with different fluorescent secondary antibodies. Overlap of the labeled antibodies has been indicated by color-mapping. Antibodies to integrin and the two matrix proteins are seen bound in small patches scattered over the external surface of the cell membrane. There is extensive overlap of the binding areas for the three antibodies. We believe that these areas correspond to a population of loci where attachment of wall to membrane has been mechanically demonstrated. Additionally, anti-vitronectin and anti-fibronectin can bind to patches in isolated, partially depectinated cell walls. Thus, the possibility that force is transmitted between extracellular matrix and cell membrane by WML and TML proteins similar to those of animals deserves further study.

Tu-Pos167

CONTRIBUTION OF POTASSIUM CURRENTS OF THE TOADFISH HORIZONTAL SEMICIRCULAR CANAL HAIR CELLS TO AFFERENT FIBER PROPERTIES.((A. Steinacker *, S.M. Highstein # and R. Rabbitt +)) *Institute of Neurobiology, San Juan, P.R. 00901, #Washington Univ. Sch. Med., St. Louis, MO. 63110, +University of Utah, Salt Lake City, UT, 84112.

Sensory hair cells from acoustico-lateralis end-organs have different complements of ionic currents, presumably related to the end-organ function. Recent studies of the potassium currents using whole cell perforated patch recording methods and hair cells from the crista of the toadfish (Opsanus tau) horizontal semicircular canals (HSCC) have identified the presence of a calcium activated potassium current, an A current, a putative delayed rectifier and an inward rectifier. Previous work on toadfish HSCC afferent fibers showed that, in response to angular acceleration, fibers from the center of the crista are high gain acceleration sensitive fibers while those from the periphery show low gain responses (Boyle & Highstein, J. Neurophysiol. 10: 1990). In recent work (unpublished data from our laboratory), the central (and not peripheral) afferent fibers showed a response to pressure. To ascertain whether these afferent fiber properties may be influenced by the potassium currents of the hair cells, hair cell populations have been isolated from either the center or the periphery of the crista for recent experiments. Of the above potassium currents found in canal hair cells, the only current showing a regional distribution was the inward rectifier. While all hair cells from the center of the crista did not exhibit an inward rectifier, every cell that exhibited an inward rectifier came from the center of the crista. We are incorporating this data on inward rectifier properties into a single compartment computational model which incorporates the hair cell transduction current with the basolateral currents to explore the contribution of the inward rectifier to afferent fiber functional properties.

Tu-Pos168

ADAPTATION OF MECHANOSENSITIVE ION CHANNELS IN C6 GLIOMA CELLS. ((C.L. Bowman[1], and J. Lohr[2])). 1. Dept. Biophysics, SUNY at Buffalo, Buffalo, NY 14214. 2. VMAC, Buffalo, NY 14215.

The activity of mechanosensitive (MS) ion channels in Xenopus oocytes quickly peaks and then decreases following rapid change in pipette pressure - a process called adaptation (Hamill and McBride, Jr. PNAS 89: 7462, 1992). We find that MS ion channels in C6 glioma cells show similar adaptive behavior. Two conductance levels (40 pS and 58 pS) are frequently observed following a rapid change in pressure The activity of the 58 pS conductance level dominates in the early times (~1-3 seconds) following onset of the stimulus, but decreases substantially over a period of seconds. By contrast, the activity of the 40 pS conductance level is approximately constant for the duration of the stimulus (2 minutes). It appears that glioma cells can transduce the phasic and tonic characteristics of mechanical stimuli in different ways.

Tu-Pos169

WAVE DISPERSION IN COCHLEA MICROMECHANICS ((R. S. Chadwick and E. K. Dimitriadis)), Biomechanics Group, BEIP/NCRR, NIH, Bethesda, MD 20892. (Spon. by Murray Eden)

Outer hair cell (OHC) motility is activated by the response of their stereocilia to the acoustically-driven relative motions between the Reticular Lamina (RL) and the Tectorial Membrane (TM). The resulting fine tuning which precedes neural activation is believed to be critical to hearing quality. Here, we study the micromechanics of the coupled hydroelastic passive system with emphasis on the viscous flow in the RL-TM gap. The model includes the dynamic elastic properties of the TM and the basilar membrane (BM), both fluid loaded (by inertia and damping) via their coupling to the fluids filling the scalae. We study the response of this system to a pressure wave traveling toward the apical end of the cochlea. This wave has slowly varying wavenumbers reflecting variable geometry and physical properties along the cochlea axis. In the model, we attempt to include variations representative of the guinea-pig cochlea. The system is characterized by its complex dispersion diagram in frequency - wavenumber - axial location space. The feasible motion and pressure fields in the RL-TM gap, as deduced in relation to the dispersion diagram, show viscous damping to dominate the energy losses in the traveling wave. This damping, however, decreases sharply near the resonance location. We discuss implications for the fine tuning in the cochlea and plans for future integration of the OHC motility into the model.

Tu-Pos170

DELAYED ACTIVATION OF SINGLE MECHANOSENSITIVE CHANNELS IN LYMNAEA NEURONS. ((D.L. Small and C.E. Morris)) Loeb Institute, Ottawa Civic Hospital and Department of Biology, University of Ottawa, Ottawa, Ontario, Canada. K1Y 4E9
Stretch-activated (SA) cationic (Cat) channels challenged with suction jumps exhibit adaptation, a dynamic behavior that can be overlooked because of its mechanical fragility. In previous studies of neuronal SA K channels, we detected no adaptation, but the protocols used were not designed to detect dynamics. Here, we reproduce the adaptation seen in Xenopus SA Cat channels, but show with the same protocol, that no adaptation occurs with SA K channels; instead there is a delayed activation. Lymnaea SA K channels subjected to pressure jumps responded after a 1-2 s delay with a gradual, rather than abrupt, onset of activation. The delay was pressure-dependent and was longer for patches from older cultured neurons. Delayed responses were, like SA Cat channel adaptation, fragile. But, whereas SA Cat channel adpatation occurs only at hyperpolarized potentials, SA K channel delay was not voltage-dependent. Once SA Cat and SA K channels are "stripped" of their fragile (cytoskeleton-dependent?) dynamics, however, their gating behaviors show little fundamental difference: both are stretch-activatable and have a higher open probability at depolarized potentials.

Tu-Pos171

POTENTIAL-DRIVEN MOVEMENTS OF TYPE 1 VESTIBULAR HAIR CELLS ((K.J. Rennie[1], A.J. Ricci[1]and M.J. Correia[1,2])) Departments of Otolaryngology[1] and Physiology and Biophysics[2], University of Texas Medical Branch, Galveston Tx 77555-1063.

Type I cells in the vestibular neuroepithelium are flask-shaped and their basal and neck regions are enclosed by an afferent nerve calyx. We have recorded voltage-dependent movements of isolated type I hair cells dissociated from the semicircular canals of the Mongolian gerbil (n=17) and white king pigeon (n=8) in whole-cell ruptured or perforated patch experiments. Type II semicircular canal hair cells showed no voltage-driven movements under the same conditions (n=5). Type I cells were seen to elongate in response to membrane hyperpolarization and to shorten following membrane depolarization. These reversible longitudinal responses were due predominantly to changes in the length of the cell's neck (maximum length change = 61%), although the cuticular plate and cell body also swelled during elongation. In addition lateral movements of the neck were observed in response to voltage stimuli and increased with voltage depolarizations of increasing magnitude. Both types of motion were seen during injection of square wave pulses of 1 Hz frequency and during sinusoidal stimulation between 0.1-2 Hz, but not at 10 Hz. The cuticular plate and hair bundle appeared to passively follow the motion of the neck and the presence of a hair bundle was not necessary for neck motion. Voltage-driven movements still occured when the potassium currents were blocked by externally applied 4-aminopyridine (5 mM) and internally applied cesium ions. In one experiment a cell which remained laterally attached to others within a section of neuroepithelium underwent voltage-driven contractions, suggesting that type I hair cells may be capable of undergoing such movements in vivo.
Supported by NIH grant DC01273.

Tu-Pos172

MECHANOSENSITIVE MODULATION OF AGONIST-INDUCED MYOSIN LIGHT CHAIN PHOSPHORYLATION IN BOVINE CORONARY ARTERIES.

((B. Szeto and C.-M. Hai)) Division of Biology and Medicine, Brown University, Providence, RI 02912.

Myosin light chain phosphorylation is an important mechanism of crossbridge activation in smooth muscle. Changing muscle length (stretching or shortening) has been shown to affect agonist-induced myosin phosphorylation in several smooth muscle types. We compared myosin phosphorylation in activated coronary arteries during unloaded shortening and isometric contraction at optimal length (L_o). The initial transient in myosin phosphorylation was significantly lower during unloaded shortening in histamine- and endothelin-activated arteries, but not in K^+-depolarized arteries. Steady-state myosin phosphorylation at 30 min after unloaded shortening and isometric contraction in arteries activated by the three agonists were not significantly different. The amount of muscle shortening in histamine- and endothelin-activated arteries were determined by measuring active force as function of muscle length. Histamine- and endothelin-induced steady-state force were length-dependent, and decreased to zero at 0.2 and $0.4L_o$ respectively, but steady-state myosin phosphorylation at 0.2, 0.4, 0.6, 0.8, and 1.0 L_o were not significantly different. These results indicate that the initial transient and steady-state myosin phosphorylation exhibit different mechanosensitive modulation in large coronary arteries. (Supported by Am. Heart Assoc.)

Tu-Pos173

Molecular analysis of a gene that encodes a mechano-sensitive channel in E. coli

((Paul Blount[1], Sergei Sukharev[1], Boris Martinac[2], and Ching Kung[1,3])) Laboratory of Molecular Biology [1], and Dept of Genetics [3], Univ. of Wisconsin, Madison, WI 53706, USA, Dept. of Pharmacology [2], Univ. of Western Australia, Perth.

A large-conductance mechano-sensitive channel (MscL) activity in E. coli has been biochemically enriched, and amino acid sequence has been derived from a protein that correlated well with this activity (see S. Sukharev et al., and B. Martinac et al., this volume). Using standard molecular techniques, we have successfully cloned and sequenced the entire gene that encodes this putative MscL protein. The correlation between the mscL gene and channel activity has been strengthened using genetic techniques: insertional disruption of the E. coli mscL gene with a chloramphenicol resistance gene (Cm) abolishes MscL activity, over-expression of mscL (via an expression plasmid) in this knock-out background recovers MscL activity. Heterologous expression of mscL in vitro has confirmed that the mscL gene product is not only required, but is also sufficient for MscL channel activity. Analysis of the mscL gene sequence has predicted a novel protein, approximately 15kD, that contains a highly hydrophobic core spanning across two-thirds of the protein and a hydrophilic carboxyl tail. Using the E. coli mscL gene as a probe in low stringency Southern analysis, we have identified possible homologues of the mscL gene in several other microbial species. (PB was supported by NIH genetics training grant 5 T32 GMO 7131-15 and is currently a DOE-energy biosciences research fellow of the Life Sciences Research Foundation. SS is supported by DOE/NSF/USDA Collaborative Research in Plant Biology Program BIR 92-2003).

Tu-Pos174

MOLECULAR IDENTIFICATION OF LARGE-CONDUCTANCE MECHANOSENSITIVE CHANNEL PROTEIN FROM E. coli

((S.I. Sukharev[*], P. Blount[*], B. Martinac[#], and C. Kung[*@])) Lab. Molecular Biology[*] and Dept. of Genetics[@], Univ. of Wisconsin, Madison, WI 53706, USA, Dept. of Pharmacology[#], University of Western Australia, Perth, WA 6009, Australia.

Mechanosensitive channels (MSCs) are presumed to play a key role in fast osmoregulatory responses in bacteria. Previously we reported that two distinct types of MSCs from E. coli (the large MSC and the small MSC) are intact when reconstituted in liposomes following solubilization and chromatography [Sukharev et al., (1993) Biophys. J. 65:177]. The specific activity of each type of MS channel in the column eluate was assayed by reconstituting individual fractions into liposomes with subsequent statistical analysis of the channel occurrence in patches (patch-sampling). Using this functional approach we targeted the large MSC of 3 nS (MscL), as more stable and robust. Starting with 2% octylglucoside-solubilized E. coli (strain AW740, ompC- ompF-) membranes, two series of chromatographic separations were carried out. Seven to 20 patches were sampled from individual or pools of fractions. Series one included fractionation on hydroxylapatite, gel filtration, and chromatofocusing. Series two consisted of an ammonium-sulfate cut followed by hydrophobic interaction chromatography and gel filtration. The most MscL-active fractions resulting from each series of fractionations were relatively simple with only one observed common component, a protein of ~ 17,000 m.w. as judged by SDS-PAGE. The identified 17 kD protein was isolated, electroblotted and microsequenced. 37 N-terminal residues were revealed with little ambiguity. Using the obtained sequence we have been able to localize the corresponding gene, mscL, clone it, and correlate its expression with MscL activities (see P. Blount et al., and B. Martinac, et al., this volume). Besides identifying the first MSC protein and its gene, this work shows that certain channels, can be isolated like enzymes by fractionating extracts and following their activities in vitro.

Tu-Pos175

A MODEL OF LOCAL MECHANICAL OSCILLATIONS IN THE COCHLEA.

((V. S. Markin and A. J. Hudspeth)) Howard Hughes Medial Institute and Center for Basic Neuroscience Research, University of Texas Southwestern Medical Center, Dallas, Texas 75235-9117

The sharp tuning and high sensitivity of acoustic signal transduction in the cochlea suggest that an internal active process pumps additional energy into the oscillations of the cochlear partition. This force-producing function is generally attributed to outer hair cells. Existing theories of amplification encounter a fundamental difficulty, however: the phase difference between the movement of the basilar membrane and the force generated by the outer hair cells provides inhibition, rather than amplification, of oscillations. For this reason, modellers must artificially introduce either negative impedance or an appropriate phase shift, neither of which is justified by the physical analysis of the system.

We suggest here a physical model based upon the recent demonstration by Mammano and Ashmore that the reticular lamina and basilar membrane can move independently, though with elastic coupling by way of outer hair cells. The mechanical model consists of two oscillators (basilar membrane and reticular lamina) coupled through an intermediate spring. The spring's set point changes due to displacement of the reticular lamina, which causes deflection of the hair bundles and variation of outer-hair-cell length.

In good quantitative agreement with the experimental observations, the model describes relaxation in the cochlea after a step change in electrical potential that causes outer hair cells to change their length. Depending on the frequency of the acoustic signal, the reticular lamina and basilar membrane can oscillate either with the same phase or in counterphase. In the latter instance, the oscillation of force leads the oscillation of the basilar membrane, energy is pumped into basilar-membrane movement, and the external input can be strongly amplified. The model is also capable of producing spontaneous oscillations.

This research was supported by National Institutes of Health grant DC00317.

Tu-Pos176

LEOPARD FROG SACCULAR HAIR CELLS HAVE TWO TYPES OF INWARDLY RECTIFYING CURRENTS.

((Jeffrey R. Holt[1] and Ruth Anne Eatock[2])) [1]Dept. of Physiology, University of Rochester, Rochester, NY 14642. [2]Baylor College of Medicine, Dept. of Otolarynogology, Houston, TX 77030

The inwardly rectifying currents reported in hair cells resemble those classified as I-K1 in other cell types. Here we report that in addition to I-K1, frog saccular hair cells have an inwardly rectifying current similar to I-h of photoreceptors and cardiac cells. These two currents are easily distinguished by their kinetics, reversal potentials, sensitivity to divalent cations, and sensitivity to external K.

Using the whole-cell tight-seal technique, we found that I-h activated at potentials negative to −50 mV, was fully activated by −120 mV, and that the activation curve, which was fit with a Boltzmann, had a V_{half} of −85 mV. The maximal whole cell slope conductance was 7.2 ± 0.9 nS (mean±SEM, n=13). Activation of I-h was sigmoidal and was fit with a three-state model with one open state and two closed states. The time constants of activation were voltage-dependent increasing from ~50 ms at −150 mV to ~230 ms at V_{half}. I-h reversed around −40 mV, far from E_K (−78 mV), and its reversal potential shifted 15 mV with a ten-fold increase in external K suggesting that it was not K-selective. Increasing external K did increase the maximal slope conductance, but, unlike its effect on I-K1, did not alter the voltage range of activation. 2 mM external Cd^{2+} blocked I-h, but not I-K1, while 500 μM external Ba^{2+}, which blocks I-K1, had no effect on Ih.

A correlation between cell morphology and the type of inwardly rectifying currents present was observed. Cylindrical cells had both I-h and I-K1 and a mean resting potential of -67 ± 0.7 mV (n=75). The more spherical cells had I-h but not I-K1, and had significantly more positive resting potentials: -50 ± 0.7 mV (n=75).

Tu-Pos177

EFFECTS OF MECHANICAL STIMULATION ON EMBRYONIC CHICK HEART CELLS

((Hai Hu and Frederick Sachs)), Biophysical Sciences, Suny at Buffalo, Buffalo, NY 14214

Single channel studies have revealed that there are five types of stretch activated channels in embryonic chick heart cells (Ruknudin et al., Am. J. Physiol. 264:H960-H972). In corresponding whole cell studies, we have elicited mechano-sensitive currents with the perforated patch recording technique using a second micropipette for mechanical stimulation (Figure 1, horizontal bars from left to right stand for medium, small, and large stimuli respectively). The currents were reversible and increased with the magnitude of the stimulus. Twenty micromolar Gd^{3+} blocked 60-90% of the current. The I-V curve of the MS current was linear with a reversal potential of about -16 mV (Figure 2, dotted line for applied ramp voltage). The observed conductances ranged from 60 to 600 pS/pF. An estimation of the SACs density gave a value of 0.3 $/\mu m^2$, in accordance with the results from single channel studies.

About one third of the cells could be stimulated to contract by the procedure of making a seal, or simply by prodding with the pipette. In the presence of Gd^{3+}, no contractions were observed. With loose-seals (20-40 MΩ), applying suction to the recording pipette reversibly stimulated the cell to beat faster (Figure 3). Making the pipette positive had a similar effect due to the injection of the current into the cell. One pA was estimated as sufficient to increase the beating rate by 0.1Hz or by more than 10%. With tight-seals, we recorded both action currents and single channel activity. Suction increased both channel activity and beating rate. These findings provide evidence that SACs can play a physiological role. *Supported by ARO LS-22560 and NY Heart Association.*

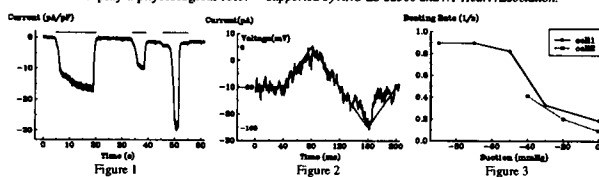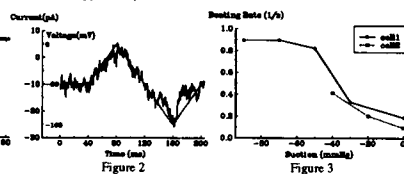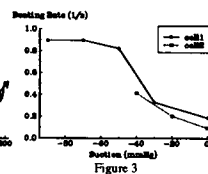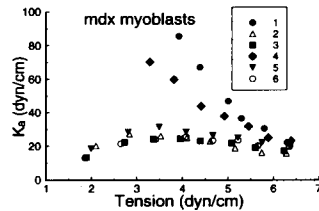Figure 1   Figure 2   Figure 3

Tu-Pos178

SARCOLEMMAL MECHANICAL PROPERTIES IN MOUSE MYOBLASTS AND MUSCLE FIBERS. ((Wade J. Sigurdson and Frederick Sachs)) Dept. Biophysical Sciences, SUNY at Buffalo, 14214. (Spon. by Michael Anbar).

In Duchenne muscular dystrophy, the absence of the membrane-associated protein dystrophin is linked with sarcolemmal fragility. Understanding dystrophin's mechanical contribution to the membrane cytoskeleton (if any) would lead to a better understanding of its physiological role. We have employed patch clamp recording and high resolution video microscopy to visualize the sarcolemma within a patch pipette under gigaseal conditions. Pressure steps induced changes in membrane area and radius of curvature. Video frames were fit to a geometric model of a hemispherical membrane within of the patch pipette. The radius of curvature was used to calculate membrane tension and when combined with membrane area, the area elasticity (K_a). With adult muscle fibers, control (C57/Bl6) membranes were stiffer (K_a = 145 dyn/cm) than mdx (dystrophin deficient) membranes (K_a=78 dyn/cm). However, with myoblasts we found no difference between mdx and control cells. In mdx myoblast patches K_a was dependent on the time between subsequent applications of suction. Small delays (~1-2s) between pressure steps series resulted in tension independent K_a 's (see Traces 2, 3, 5, and 6), but longer delays (~1-5 m) produced a pronounced increase in K_a (traces 1 and 4) which decreased with repeated pulses. Apparently the membrane/cytoplasmic plug was able to change its mechanical properties in a "use and time dependent" manner. This correlates with anatomical data on f-actin's response to stress. Supported by ARO DAAL039C0014.

Tu-Pos179

PHYSICAL MECHANISMS OF TENSION SENSITIVITY IN THE CHANNEL FORMING POLYPEPTIDE ALAMETHICIN. ((L.R. Opsahl* and W.W. Webb)) Appl. and Engin. Physics, Cornell University, Ithaca, NY 14853, *Current Address: General Electric Corporate Research and Development, Schenectady, NY 12301. (Spon. by J. Fetrow)

The mechanisms and physiology underlying the mechanical sensitivity in tension sensitive ion channels are difficult to assertain due to the elusiveness of the channel proteins and potential cytoskeletal interactions. We have shown that the ion channel alamethicin is mechanically sensitive and have used it as a model MS channel because it can be easily incorporated into phospholipid membranes, where it forms ion channels which switch between multiple conductance states. Single channel analysis has shown that membrane tension energizes mechanical work during conductance state changes by an amount equal to tension times the associated increase in membrane area. Using the magnitude of the area change together with kinetics data it has been possible to identify two simple physical mechanisms of cytoskeleton independent transduction involved in tension sensitivity of the alamethicin channel. Results show an ~ 40 Å^2 increase in pore area and transfer of an 80 Å^2 polypeptide into the membrane. Both mechanisms may be implicated in mechanical signal transduction by cells.

Tu-Pos180

THREE-DIMENSIONAL SHAPE CHANGES AND THE DETACHMENT OF EPITHELIAL CELLS ARISE FROM CHANGES IN THE KINETICS OF INTEGRIN BINDING AND CYTOSKELETAL ASSEMBLY. ((C. R. Cho, C. J. Lumsden, and C. I. Whiteside)) Membrane Biology Group, University of Toronto, Toronto, Ontario, Canada, M5S 1A8

The loss of detailed branching structure of the glomerular epithelial cells (GECs) and the detachment of GECs from the glomerular capillary wall are correlated with the massive leakage of protein across the wall that occurs in many renal diseases. We report a stochastic computer simulation of the temporal progression of GEC shape changes. The simulation is used to predict the GEC shape changes due to (1) altered integrin binding kinetics, (2) altered cytoskeletal polymerization and assembly kinetics, and (3) altered mechanical force balance at the cell surface. The dynamic changes in the fraction of receptors bound, the density of cytoskeleton, and the distribution of unbound receptors within both cell body and basolateral surface, are calculated using a Monte Carlo simulation of the chemical kinetics. GEC shape changes are modeled to arise from a redistribution of binding sites over the cell surface. For normal values of the rate constants and mechanical forces, cross-sections of the simulated GECs display the same branching structure seen in transmission electron micrographs from healthy rats. A 2-fold decrease in integrin binding rate causes a loss of GEC branching as seen in diseased cells. Changes in GEC morphology are found to be accompanied by an increase in the concentration of free receptors within the cell body.

CHEMOSENSORY TRANSDUCTION AND CHEMOTAXIS

Tu-Pos181

TWO DIFFERENT CALCIUM SIGNALLING PATHWAYS INDUCE DEFLAGELLATION IN CHLAMYDOMONAS REINHARDTII. ((L.M. Quarmby and H.C. Hartzell)) Department of Physiology, Emory University School of Medicine, Atlanta GA 30322.

We are using the powerful haploid genetics of the unicellular alga *Chlamydomonas reinhardtii* to dissect signalling pathways that regulate flagellar function. The intracellular machinery of deflagellation in *Chlamydomonas reinhardtii* is Ca²⁺ dependent (Sanders & Salisbury, 1989, *J. Cell Biol.* 108:1751-1760). We have previously demonstrated that deflagellation can be induced *in vivo* by intracellular acidification (Hartzell *et al.*, 1993, *Exp. Cell Res.* 208: 148-153) or by extracellular application of the wasp-venom peptide, mastoparan (Quarmby *et al.*, 1992, *J. Cell Biol.* 116: 737-744). We now report that mastoparan and the permeant organic acid, benzoate, trigger deflagellation by two different signalling pathways. We have characterized each pathway with respect to (1) the requirement for [Ca²⁺]ₒ, (2) sensitivity to Ca²⁺ channel blockers and (3) ⁴⁵Ca influx. We conclude that mastoparan induces deflagellation via mobilization of an internal pool of Ca²⁺ whereas acid induces deflagellation via an influx of extracellular Ca²⁺. The deflagellation mutant, adf-1, deflagellates in response to mastoparan, but not in response to acid (Quarmby, T. Saito & U.W. Goodenough). Adf-1 cells are defective in acid-activated Ca²⁺ influx. Experiments with other mutants suggest that the acid-activated channel is located on flagellar membranes. Efforts to clone the channel and its regulatory proteins are underway.

Tu-Pos182

LOCALIZATION OF COMPONENTS OF THE BACTERIAL FLAGELLAR ROTARY MOTOR BY DIFFERENCE IMAGE ANALYSIS (Dennis Thomas, Noreen R. Francis, Gina E. Sosinsky and David J. DeRosier.) Rosenstiel Basic Biomed. Res. Center, Brandeis University, Waltham,MA 02254.

The organelle of motility in *Salmonella typhimurium* is the bacterial flagellum. It is driven by a rotary motor at its base in the cell membrane. A proton gradient across the membrane provides the energy for rotation. Early attempts to isolate motors yielded structures having multiple copies of eight different proteins. A multimer of the protein, FliF, forms the M ring, which spans the cytoplasmic membrane. Neither FliF nor any of the other seven proteins, however, appeared to be involved in torque generation. Recently we developed gentler procedures to isolate motors. The motors, imaged by electron cryomicroscopy, contain additional mass associated with the M ring and an additional large ring (the C ring) located on the cytoplasmic face of the M ring. These additional structures contain three important proteins, FliG, FliM and FliN, which have been shown by genetics to be involved in torque generation and control of the direction of rotation. We have determined the structures of complete and partially stripped motors, which we prepared either from mutant strains or by varying preparative conditions. Using difference maps and immunomicroscopy, we find FliG associated with the M ring and have data suggesting that FliM and FliN are located in the C ring. There are also additional features not yet assigned to particular proteins.

Tu-Pos183

INDUCED INTEGRIN CELL SURFACE EXPRESSION AND CHEMOTACTIC RESPONSIVENESS BY ONCOIMMUNIN-M.
((Beverly Z. Packard)) DCB, CBER, FDA, Bethesda, MD. 20892

Oncoimmunin-M, a 36 kDa protein that was recently identified and purified to homogeneity, was shown to be able both to inhibit the proliferation of the human promyelocytic leukemic cell line HL-60 while maintaining viability in culture and to induce a bimodal distribution of CD11b, the α chain of the integrin MAC-1, on the cell surface (J. Biol. Chem. **268**: 6356-6363 (1993)). Further detailed study has revealed that treatment of HL-60 cells with this cytokine also brings about an increase in the mean level of surface expression of CD11c, the α chain of p150,95, which is another leukocyte integrin, but virtually unchanged (<10%) levels of CD11a, the α chain of the third leukocyte integrin LFA-1, and CD18, the putative β chain for all leukointegrins. Results from motility studies demonstrate that these altered integrin expression levels correlate with induced chemotactic responsiveness to a gradient of the chemoattractant human C5a. Specifically, separation of motile from nonmotile cell subpopulations after exposure to C5a reveals that on the surface of individual cells which respond to this chemoattractant the α/β integrin ratio is increased relative to unresponsive cells. These data suggest that biologic function may not be limited to existence of the integrin family of glycoproteins as α/β heterodimers.

Tu-Pos184

THE CYTOPLASMIC DOMAIN OF THE ASPARTATE RECEPTOR: NMR STUDIES INDICATE AN UNUSUALLY MOBILE STRUCTURE
((S.K. Seeley, R.M. Weis, and L.K. Thompson)) Department of Chemistry, University of Massachusetts, Amherst, MA 01003-4510.

The aspartate receptor, a transmembrane receptor involved in bacterial chemotaxis, is an excellent system for investigating the mechanism of transmembrane signaling. We are seeking a more detailed picture of proposed conformational change and oligomerization mechanisms by investigating the changes which occur in the cytoplasmic domain of the receptor during signaling. A number of point mutations in the cytoplasmic domain lead to either of the two behavioral extremes of constant tumbling or constant smooth-swimming, suggesting that these mutant proteins may be locked into the two extreme signaling states of the cytoplasmic domain. These behavioral changes are also observed when the mutations are expressed in a 31 kDa soluble fragment of the receptor corresponding to the cytoplasmic domain. Recent studies of the monomer-oligomer equilibria of these mutant cytoplasmic fragment proteins have demonstrated that the smooth mutant protein equilibrium is shifted toward the oligomeric state, and the tumble mutant protein equilibrium is shifted toward the monomeric state. Comparisons of the NMR properties of these mutant forms are being used to probe the structural differences between these signaling states of the protein. Studies have focused on both wildtype (predominantly monomeric) and a smooth mutant (Ser461→Leu, predominantly dimeric) cytoplasmic domain protein. Both proteins exhibit very little proton chemical shift dispersion and extremely rapid proton exchange (about 90% of the amide protons exchange within 11 minutes). Comparison of intensities with that of a single Trp resonance indicate at least 90% of the backbone is observable. Current studies aim to determine whether the unusually mobile structure indicated by these observations is relevant to signaling.

Tu-Pos185

IDENTIFICATION OF A DOMAIN THAT BINDS Ca²⁺-CALMODULIN IN OLFACTORY CYCLIC NUCLEOTIDE-ACTIVATED CHANNEL.
((M.-Y. Liu, J. Li and K.-W. Yau)) Howard Hughes Medical Institute and Department of Neuroscience, Johns Hopkins University School of Medicine, Baltimore, MD 21205.

In olfactory signal transduction, odorants bind to specific receptors, leading to the stimulation of adenylyl cyclase and elevation in cyclic AMP, which in turn activates the cyclic nucleotide-gated channel and results in the depolarization of olfactory neurons. The channel's affinity for cAMP has been shown to be dramatically reduced by Ca²⁺-calmodulin (Chen and Yau, Soc Neurosci Abstr 19: 13, 1993). We report here experiments to identify a domain of the channel protein that is involved in the interaction with calmodulin in the presence of Ca²⁺. Using a bacterial expression system (pGEX-2T), we produced two fusion proteins corresponding to the cytoplasmic N-terminal segment and the cytoplasmic C-terminal segment of the channel, respectively. In gel-overlay experiments with ¹²⁵I-labelled calmodulin, only the N-terminal fusion protein bound to calmodulin. Inspection of the amino acid sequence of this segment of the channel protein suggests the presence of a putative calmodulin-binding site. When this putative site was deleted, the mutant fusion protein lost its ability to bind calmodulin in the gel overlay assay. The identification of a calmodulin binding domain in the olfactory cyclic nucleotide-gated cation channel will help us understand the molecular mechanism of the channel's modulation by Ca²⁺-calmodulin.

Tu-Pos186

Ca²⁺ STORES AND Ca²⁺ SIGNAL POLARITY IN NEWT EOSINOPHILS.
S.H. Gilbert*, J.W Walkert†, R.A. Tuft*, D.S. Bowman* & F.S. Fay*.
*Biomedical Imaging Group, UMMC, Worcester MA, & †Dept. of Physiology, Univ. of Wisconsin, Madison WI.

On stimulation with chemoattractant large eosinophilic leukocytes from newts produce a Ca²⁺ spike, which is insensitive to external EGTA but is obliterated by heparin (injected to block InsP₃ receptors). Regardless of whether the stimulus is applied as a gradient with a puffer pipet or is introduced in the medium, [Ca²⁺]ᵢ is higher in the rear than in the front of the cell. Here we present evidence suggesting that InsP₃-sensitive Ca²⁺ stores are more dense in the rear than in the front. To explore the spatial distribution of Ca²⁺ stores, MagFura-2 was loaded as the permeant AM ester or injected as the K⁺ salt. In AM-loaded cells the 340/380 (λₑₓ) ratio was highest near the microtubule-organizing center and in a thin layer surrounding the lobes of the nucleus, while injected cells exhibited a spatially uniform ratio. Other cells were injected with caged InsP₃ [P⁴⁽⁵⁾-1-(2-nitrophenyl)ethyl ester] and 70 kD dextrans labelled with Calcium Green and Lucifer Yellow (as a volume marker). Fluorescence intensity (λₑₓ 490 and 420) measured at 5-6-sec intervals. On exposure of the entire cell to laser light (1-5 sec, λ 351 nm), the 490/420 ratio increased in ≤5 sec, with the highest increase in the perinuclear region. The results indicate that these cells contain InsP₃-sensitive Ca²⁺ stores that appear to be concentrated in the region exhibiting the highest [Ca²⁺]ᵢ, suggesting that the polarized distribution of Ca²⁺ stores may be an important determinant of the cytosolic Ca²⁺ gradient in active cells.

Tu-Pos187

CHARACTERISATION OF THE CALCIUM AND POTASSIUM CURRENTS IN GLOMUS CELLS OF THE CAROTID BODY.
((Maria Jeane Margort e Silva and Deborah Lewis)). Department of Pharmacology and Toxicology, Medical College of Georgia, Augusta, GA, 30912.

Glomus cells (chemoreceptors) of the carotid body participate in the detection of pO₂, pCO₂, pH, temperature and osmolarity in arterial blood. However, the chemotransduction and neuromodulatory mechanisms are not well understood. We have studied the voltage-activated calcium and potassium currents in cultured glomus cells by conventional whole-cell recording techniques. In the present experiments the cells were clamped to a holding potential of -80 mV (to record calcium current) or -50 mV (to record potassium current). The voltage-dependent calcium current peaked around -3 mV in 10 mM external Ca²⁺. Pharmacological manipulations showed that the glomus cell has several types of calcium channels: L-type (nimodipine blocks 32.8 ± 6.3% at -3 mV and +202-791 increases 106.1 ± 11.2% at -18mV); N-type (ω-conotoxin GVIA blocks 39.7 ± 4.7% at -3mV) and an unidentified type that was insensitive to nimodipine, ω-conotoxin GVIA and ω-agatoxin IVA. Several types of outward potassium currents were identified based on their pharmacology: a TEA-sensitive type and a calcium-dependent type. We found no modulation of the voltage-dependent Ca²⁺ channels by muscarine, NE, VIP, met-enkephalin, Sub P, 5-HT or adenosine. However, somatostatin blocked the calcium current by 19.8 ± 3.2% (n=5).

Tu-Pos188

RELATIONSHIP BETWEEN DOPAMINE RELEASE AND CYTOSOLIC CALCIUM IN DISPERSED GLOMUS CELLS.
((J. Ureña, R. Fernández-Chacón, G. Alvarez de Toledo and J. López-Barneo)). Departamento de Fisiología Médica y Biofísica. Universidad de Sevilla. 41009-Sevilla. SPAIN.

Glomus cells are the primary sensory receptors involved in oxygen chemoreception by the carotid body. These cells can be considered as presynaptic-like elements because they release dopamine, which acts on the afferent fibers of the sinus nerve conveying the information to the CNS. To study the stimulus-secretion coupling in enzymatically dispersed glomus cells, we have measured dopamine release by voltammetry in combination with patch-clamp and microflurometric techniques. In voltage clamped dyalized cells, membrane depolarization elicits small amperometric spikes, each one probably reflecting the fusion of a single secretory vesicle. The voltammogram of the secretory product shows that dopamine is in fact highly concentrated in the vesicles of glomus cells. The frequency and the size of these unitary events appear to be dependent on membrane potential. The secretory response is reversibly blocked by adding 200μM CdCl₂ to the bath solution suggesting that it is mediated by calcium influx through the plasma membrane. This finding is also supported by experiments done in FURA-2 loaded cells in which we estimated the average cytosolic calcium concentration. In these conditions, secretion is only detected when cytosolic calcium reaches a certain "threshold level", which suggests a complex relation between the two variables. This helps to understand the process of chemotransduction in the carotid body.

Tu-Pos189

TETRACAINE-INDUCED INTERDIGITATED LIPID PHASE IN ACETYLCHOLINESTERASE-CONTAINING MEMBRANES. ((Brandon M. Zuklie, Laurence G. Roth and Chang-Hwei Chen)) Wadsworth Center for Labs and Res., N.Y. State Dept. of Health, and Dept. of Biomedical Sciences, University at Albany, State University of New York, Albany, NY 12201-0509

Biphasic alterations of lipid phase and enzyme activity in biological membranes by tetracaine (TTC), an anesthetic, were demonstrated in acetylcholinesterase (AChE)-containing membranes from electric organ of Torpedo californica. AChE activity increased at a low [TTC] with an optimum at 0.33 mM, and then decreased as [TTC] increased. This biphasic behavior was also observed with membrane lipids in fluorescence polarization and differential scanning calorimetric measurements. Fluidity of lipid acyl chains (not polar groups) increased at [TTC] < 0.66 mM and decreased as [TTC] increased. The lipid phase transition peak occuring at 21°C was no longer evident upon the addition of 15 mM TTC, but reappeared with a greater magnitude at 40 mM TTC. These [TTC] were equivalent to 0.5 and 1.3 mM, respectively, if the same membrane concentration as in the fluorescence study was used. Such increases in membrane rigidity and enthalpy of lipid transition have been found to accompany the formation of an interdigitated lipid phase in model bilayer systems. Our findings suggested that tetracaine-induced interdigitated lipid phase may occur in AChE-containing membranes and consequently affect the activity of membrane-bound AChE.

Tu-Pos190

INTERDIGITATED BILAYERS WITH THREE OR FOUR CHAINS PER HEADGROUP: SURFACE HYDRATION PROPERTIES. ((J.T. Mason, M. Batenjany, T.J. O'Leary and I.W. Levin*)) Dept. of Cellular Pathology, A.F.I.P, Washington, D.C. 20306-6000, and *Section of Chemical Physics, NIH, Bethesda, MD 20892.

We have examined the surface properties of interdigitated bilayers whose phosphatidylcholine (PC) headgroups span 3 [1-octadecanoyl-2-decanoyl-PC (C18C10PC)] or 4 [1,2-dihexadecyl-rac-glycero-3-phosphocholine (DHPC)] hydrocarbon chains at the bilayer surface. The hydration properties of these two PCs have been characterized by Raman spectroscopy and calorimetry employing the D_2O substitution technique of Ohki [Ohki, K. (1991) B.B.R.C. 174, 102-106]. The effect of substituting D_2O for H_2O was to raise the transition temperature of all of the phase transitions of the PCs by 0.2-0.7°C except for the pretransiton of DHPC, which was lowered by 3.1°C. The increase in the transition temperature of C18C10PC contradicts the interfacial free energy model proposed by Ohki. Instead, it is suggested that the expansion of the surface to accommodate 3 chains per headgroup does not disrupt the continuous intermolecular hydration layer of the bilayer surface. The anomalous behavior of DHPC is interpreted to indicate that the expansion of the bilayer surface to accommodate 4 chains per headgroup disrupts the surface hydration layer such that the phosphate groups are intramolecularly hydrated and the terminal methyl groups of the interdigitating chains are hydrated by bulk water. The position of the terminal methyl deformation mode for DHPC in the interdigitated phase as measured by Raman spectroscopy supports this hydration model. These findings explain the unique properties of DHPC and suggest a mechanism whereby certain surface-active agents induce interdigitation in PC bilayers.

Tu-Pos191

PHASE BEHAVIOR OF DPPC BILAYERS CONTAINING BILE SALTS AND BILE SALT CONJUGATES: RAMAN SPECTROSCOPIC STUDIES. ((T. M. Herne and I. W. Levin)) Laboratory of Chemical Physics, NIDDK, NIH, Bethesda, MD 20892.

Bile salts play a critical role in the secretion of biliary lipids, such as cholesterol, yet the exact mechanism for this process is not yet known. One of the bile salts, the sodium salt of ursodeoxycholic acid (UDC), a highly hydrophilic bile salt, has been used as a drug for the dissolution of gallstones, and has been shown to reduce cholestasis and hepatocellular damage in cases of chronic liver disease. The mechanism for action is suggested to be its replacement of more hydrophobic bile acids in the hepatocellular membrane. Using Raman spectroscopy, we have investigated the effect of incorporating the bile salts of UDC, chenodeoxycholic acid, deoxycholic acid, cholic acid, lithocholic acid, as well as the the taurine and glycine conjugates of these salts, into model membranes comprised of 1, 2-dipalmitoyl-sn-glycero-3-phosphocholine (DPPC) bilayers. A direct correlation between the hydrophobicity of each bile salt and its ability to lower the gel to liquid crystalline phase transition T_m was found; the more hydrophobic bile salts decreased T_m by the largest amount. The T_m for pure DPPC bilayers is 41.3° C. For DPPC bilayers with incorporated glycoursodeoxycholic acid (ca. 18 mole %), the most hydrophilic of the compounds studied, the T_m was found to be 40.6° C; however, for DPPC bilayers containing the more hydrophobic bile salt glycocholic acid (ca. 18 mole %), T_m was determined to be 37.3° C. Interestingly, the most hydrophobic bile salts are also the most toxic. The effects of changing the UDC/DPPC mole fraction and of mixing hydrophilic and hydrophobic bile salts on bilayer order/disorder parameters will be presented.

Tu-Pos192

SLOW STRUCTURAL REORGANIZATION IN BINARY LIPID BILAYERS IN THE GEL-LIQUID CRYSTALLINE COEXISTENCE REGION ((A. Klinger, M. Braiman, K. Jorgensen and R. Biltonen)) Depts. of Biochemistry and Pharmacology, University of Virginia, Charlottesville, VA 22908

We have asked whether quenching of a binary lipid system from a homogeneous liquid crystalline state into its coexistence region could result in two distinguishable relaxation processes, the first being a relatively rapid condensation of regions containing a dominant amount of the higher melting lipid; and the second, a slower global reorganization into regions of appropriate composition as defined by the equilibrium phase diagram. When a bilayer system of a 1:1 mixture of $DC_{16}PC$ and $DC_{22}PC$ containing pyrenedecanoyl PC is subjected to a temperature change from about 80° C to 50° C the fluorescence intensity of the probe increases in concert with temperature change, then decreases slowly ($t_{\frac{1}{2}} \sim 100$min.) back to its equilibrium value. This result is consistent with the probe being trapped initially in a gel region and then slowly diffusing into the liquid domains which it thermodynamically prefers. Analogous experiments were performed without a probe using infrared spectroscopy. A series of FTIR spectra were measured at 2 cm⁻¹ resolution and at intervals of 2 min. from 20 min. before the temperature jump until 180 min. afterward. Kinetic analysis of the CH_2 and CH_3 stretching modes near 2850 cm⁻¹ suggests that the system rapidly supercools (the order becomes greater than its equilibrium value) and then slowly relaxes back to its equilibrium state. This result indicates that the slow relaxation process is a property of the lipid and not the probe, and suggests that complex lipid mixtures could exist in a non-equilibrium state for long times following a large isothermal perturbation such as a change in calcium, for example. (Supported by grants from the NIH)

Tu-Pos193

PEG-INDUCED AGGREGATION/FUSION OF PHOSPHOLIPID SUV: DEPENDENCE ON MW OF PEG AND PC/PE MOLAR RATIO OF THE VESICLE COMPONENTS. ((Y. Guo, Q. Yang, J.A. Alderfer, and S.W. Hui)) Biophysics Department, Roswell Park Cancer Institute, Buffalo, NY 14263.

The molecular weight (MW) dependence of poly(ethylene glycol) (PEG)-induced aggregation/fusion of egg phosphatidylcholine (EPC) small unilamellar vesicles (SUV) was monitored by quasi-elastic light scattering (QLS). Both aggregation and fusion show peak efficiencies at the PEG MW of 8K-10K, but efficiencies diminish at low (600) and high (20K) MW. Only PEG of 8K-10K MW range was shown to deplete from the vesicle surface, as measured by ³¹P NMR linewidth, which represents the tumbling rate of vesicles in a given surface viscosity environment. The observations are explained by the depletion/adsorption of PEG molecules on the vesicle surface. Adsorption counteracts depletion and the consequent osmotic pressure gradient which provides the driving force for aggregation.
PEG-induced aggregation/fusion of SUV composed of EPC and PE (phsphatidylethanolamine) at various PC/PE molar ratios were also monitored by QLS. High PE content samples were found to have high fusion susceptibility but low aggregation susceptibility. Vesicles containing highly unsaturated PE such as dilinoleoyl PE are much more susceptible to fusion than those containing egg PE and lyso PE, which is the least susceptible. Thus, the fusion susceptibility is related to the bending energy of PE packing in vesicles. The common aggregation behavior was explained by the different degree of adsorption of PEG to PC and PE.

Tu-Pos194

EFFECTS OF PEG ON LIPID MONO-AND BILAYERS

((M. Winterhalter, H. Bürner, K.H. Klotz, S. Marzinka, D.D. Lasic and R. Benz)), Biotechnologie, Am Hubland, D-97074 Würzburg, Germany.

We measured the surface potential of lipid monolayers in presence of polyethylene glycol (PEG) either in the aqueous subphase or covalently attached to the headgroup of some of the lipids. PEG interacts strongly with the lipid and the interaction varies with the surface pressure. Specifically, at low surface pressures, PEG dominates the surface potential, whereas at higher surface pressures, the surface potential is determined by the lipid dipole potential. Our results suggest that PEG is associated with the membrane for all surface pressures, even at the collapse pressure. We also extended a theoretical model to estimate the influence of microscopic observables (e.g. the dipole potential) on macroscopic properties of membranes (e.g. bending elasticity).

Tu-Pos195

EFFECTS OF DIACYLGLYCEROLS ON THE CONFORMATION OF PHOS-
PHATIDYLCHOLINE HEADGROUPS IN MIXED PHOSPHATIDYL-
CHOLINE/PHOSPHATIDYLSERINE BILAYERS. ((E.M. Goldberg*, D.S. Lester‡,
D.B. Borchardt§, and R. Zidovetzki*)) Departments of *Biology and §Chemistry,
University of California, Riverside, CA 92521, and ‡Neural Systems Section, National
Institutes of Health, Rockville, MD 20852.

The combined effects of five diacylglycerol (DAGs) , diolein, 1-stearoyl,2-arachidon-
oylglycerol, 1-oleoyl,2-acetylglycerol, dioctanoylglycerol, and dipalmitin (DP), and
Ca^{2+} on the structure of lipid membranes, composed of a mixture of phosphatidylcho-
line (PC) and phosphatidylserine (PS) were studied by ^{2}H-NMR. Dipalmitoylphospha-
tidylcholine, deuterated at the α and β positions of the choline moiety was used as a
^{2}H-NMR probe. Addition of each DAG, except for DP, induced monotonous decrease
in the β-deuteron quadrupole splittings with the concomitant increase in the α-deuteron
quadrupole splittings, indicating that this change is caused by DAG-induced
conformational changes of the PC headgroup, rather than by a change of the
headgroup mobility. At high ($\geq$20 mol%) DAG content the α-deuteron ^{2}H-NMR
peaks became doublets indicating that under these conditions the two α-deuterons were
not equivalent. The α-deuteron non-equivalence was enhanced by the presence of
Ca^{2+}, which otherwise had relatively minor effect on the PC headgroup conformation.
Unlike the effects of other DAGs, the spectral changes induced by DP were consistent
with the lateral phase separation of the bilayers on gel-like and fluid-like domains, with
the PC headgroups in the latter phase being virtually unaffected by the presence of DP.
The DAG-induced conformational change of the phospholipid headgroups may be
relevant to the mechanism of activation of protein kinase C.

Tu-Pos196

Measurement of Spontaneous Curvatures of Phospholipids by the
Size of Inverted Micelles. ((Arindam Sen and Sek-Wen Hui))
Biophysics, Roswell Park Cancer Institute,Buffalo, NY 14263

Spontaneous curvature of a phospholipid is by definition the
curvature that the given phospholipid would assume in the
absence of stress in both the polar and non-polar regions. We
used quasi-elastic light scattering to determine the size of
lipid inverted micelles in alkane. Micelles of dioleoyl-,
dilinoleoyl-, and dilinolenoyl-PE had radii of 3.2, 3.15 and
3.0 nm respectively. Whilst, mixed dilinoleoyl-PE and 1-
palmitoyl, 2-oleoyl-phosphatidylcholine (POPC) at (85/15) and
(70/30) had radii of 3.75 and 5.5 nm respectively. The radius
of inverted micelles of 3:1 dioleoyl-PE:dioleoyl-PC was 3.65
nm. We also made x-ray diffraction measurements using limited
hydration and addition of alkane, to determine the spontaneous
curvatures of the same series of phosphatidyl-ethanolamines
(PE) and mixed lipid systems containing PE and phosphatidyl-
choline (PC). The corresponding spontaneous radii of curvature
for the PE's were 3.2, 3.14 and 3.0 nm, and for the mixed
lipids they were 3.4 and 4.6 nm. Comparing the size of
inverted lipid micelles to their spontaneous curvatures
experimentally determined by x-ray diffraction, we found that
the size of lipid inverted micelles in alkane is the same (for
PE's) or within 10% (for mixed lipid systems) of their
spontaneous curvature. The inverted micelles method thus
provided a simple and rapid way to measure the spontaneous
curvatures of lipids.

Tu-Pos197

A STALK-MEDIATED MECHANISM FOR LAMELLAR/INVERTED CUBIC AND
LAMELLAR/INVERTED HEXAGONAL PHASE TRANSITIONS ((D. P. Siegel))
Procter & Gamble Co., P.O.Box 398707, Cincinnati, OH 45239-8707

Previously, I used a new model of lipid intermediate energies
to show [1] that a modified stalk mechanism is a more viable
fusion mechanism than one based on inverted micellar struc-
tures. Here, I use the same methods to study the mechanism of
L$_\alpha$/H$_{II}$ and L$_\alpha$/Q$_{II}$ phase transitions. The results suggest that
inter-bilayer stalks form first, and rapidly expand axially to
produce trans monolayer contacts (TMCs; [1]). TMCs have three
possible fates: elongation into line defects (LDs, growing
domains of H$_{II}$ phase [2]); radial expansion into small single-
bilayer diaphragms; and rupture to form bilayer connections
between lamellae (ILAs; [2]). The evolution of ILAs & Q$_{II}$ phase
vs. H$_{II}$ phase seems to be the result of a delicate balance of
forces on TMCs. Systems with strong van der Waals forces
between L$_\alpha$ lamellae and a steep dependence of spontaneous cur-
vature on temperature should form H$_{II}$ phases rapidly. Certain
types of defects (e.g., membrane folds) in the L$_\alpha$ lattice also
favor rapid H$_{II}$ formation. Compared to an IMI-mediated model,
the present model produces inherently faster L$_\alpha$/H$_{II}$ transitions
with faster epitaxial order development (matching results of
recent time-resolved studies, [3,4]); and ILAs & Q$_{II}$ phases are
thermodynamically stable in general for temperatures near T$_{H}$.
[1] Siegel, Biophys. J. (Nov. 1993). [2] Biophys. J. 49:1155.
[3] Siegel, (temperature-jump cryo-TEM), Biophys. J.(in press).
[4] Kreichbaum et al., Biophys. J. 64:A296 (1993).

Tu-Pos198

STRUCTURAL PARAMETERS AFFECTING THE LAMELLAR TO
REVERSED HEXAGONAL TRANSITION TEMPERATURES OF
PHOSPHATIDYLETHANOLAMINES AND GLYCOSYLGLYCERO-
LIPIDS. ((R.N.A.H.Lewis[1], D.A.Mannock[1], R.N.McElhaney[1], P.E.
Harper[2], D.C.Turner[2] & S.M.Gruner[2])), [1]Biochem. Dept., Univ. of Alta,
Edmonton, Canada; [2]Dept. of Physics, Princeton Univ, Princeton, NJ, USA.

The lamellar (L$_\alpha$) to reversed hexagonal (H$_{II}$) phase transition of a number of
phosphatidylethanolamines (PE) and monoglycosylglycerolipids (MGDG)
was examined by differential scanning calorimetry and X-ray diffraction. The
L$_\alpha$-H$_{II}$ transition temperatures (T$_H$) of the PEs are very sensitive to changes in
the length and chemical structure of the hydrocarbon chains. With the
PEs,T$_H$ decreases with increasing hydrocarbon chain length and, for the same
equivalent chain length, occurs at an approximately constant temperature
interval (ΔT$_{L/NL}$=25-35°C) above the main chain melting phase transition
temperature. Recent X-ray diffraction measurements suggest that this
transition to the H$_{II}$ phase may be determined, not by a critical bilayer
thickness but by the balance between the headgroup area frustration in the L$_\alpha$
phase and the chain length frustration in the H$_{II}$ phase. In contrast, the L$_\alpha$-H$_{II}$
transition temperatures of the MGDGs are less sensitive to the length and
chemical structure of the hydrocarbon chains, yet ΔT$_{L/NL}$ for the same
equivalent chain length shows greater scatter than in the PEs. The L$_\alpha$-H$_{II}$
transition temperatures of the MGDGs are also sensitive to the nature of the
anomeric linkage and the carbohydrate stereochemistry. Thus, although both
groups of lipids readily form non-bilayer structures and possibly fulfill similar
functional roles in biomembranes, their different sensitivities to the above
structural parameters are indicative of some fundamental differences in the
interactions underlying their "non-bilayer-forming tendencies".

Tu-Pos199

THE RELATIONSHIP BETWEEN PERMEANT SIZE AND PERMEABILITY IN LIPID
BILAYER MEMBRANES. ((T.-X. Xiang and B.D. Anderson)) Department of Pharmaceutics
and Pharmaceutical Chemistry, University of Utah, Salt Lake City, Utah 84112

Permeability coefficients (P$_m$) across planar egg lecithin bilayers and bulk hydrocarbon/water
partition coefficients (K$_{hc}$) have been measured for 24 solutes with wide ranges of molecular
volume and P$_m$ to explore the chemical nature of the bilayer barrier and the effects of
permeant size on permeability. A proper solvent was sought, which correctly mimics the
microenvironment of the barrier domain. Changes in P$_m$/K$_{hc}$ were then ascribed to solute size
effects and were first described by P$_m$/K$_{hc}$ = C/V^n. When n-decane was used as a reference
solvent, the correlation was poor with most of the lipophilic (hydrophilic) permeants lying
below (above) the regression line. Correlations improved significantly with more polarizable
solvents, 1-hexadecene and 1,9-decadiene. Values of n are 1.0±0.3, 1.3±0.2 and 1.5±0.1 for
decane, hexadecene, and decadiene, respectively. Decadiene was selected as the most
suitable solvent. The value for n in bilayer transport is higher than that for diffusion in
decane (n = 0.74±0.10). In parallel with this experimental study, a mean-field statistical
mechanical theory has been developed for molecular distributions in interphases. The
excluded volume interaction was modeled in terms of a reversible work which is required to
create a cavity of the solute size in an interphase against a pressure tensor exerted by the
surrounding molecules. The lateral pressure (p$_L$) versus depth in a model lipid bilayer (30.5
Å^2/chain molecule) has been calculated by molecular dynamics simulation. p$_L$ has a plateau
value of 309±48 bar in the highly-ordered region and decreases abruptly in the center of the
bilayer. Increased p$_L$ results in higher order and exclusion of solute from the interphase. The
log of the interphase partition coefficient decreases linearly with solute volume with a slope
of α = (2p$_L$ - p$_N$)/3k$_B$T, where p$_N$ is the normal pressure component. This theory, combined
with the empirical diffusion model, yielded P$_m$/K$_{hc}$ = C exp(-αV)/V^n. It gave an improved
fit of the data and a lateral pressure of 300±100 bar, in close agreement with our MD
simulation. It suggests that, contrary to the conventional view, the molecular size dependence
in bilayer permeability is the result of both partitioning and diffusivity changes with size.

Tu-Pos200

EFFECTS OF THE INTERBILAYER DISTANCE ON THE SURFACE
AND PERMEABILITY PROPERTIES OF LIPID MEMBRANES
((L.I. Viera, E.Lagomarsino and E.A.Disalvo)) Farma-
cia y Bioquimica, Universidad de Buenos Aires; INIFTA
Universidad de La Plata, Argentina.

The total repulsive interaction between electrically
neutral bilayers in the fluid state can be due to the
reorientation of water molecules, bilayer undulations
and head groups motions and protrusions. In addition,
the magnitude of the interbilayer forces is related
to the dipole potential which suggests that at least
part of them are due to the polarization of water and
lipid dipoles. In this work, we show that in the
presence of a surface potential sensitive probe in
the interlamellar space at a 1:200 ratio with respect
to lipids, the decrease of the distance between
egg phosphatidylcholine bilayers induced by osmotic
pressure promotes a steep decrease in the surface
potential at a distance between 8 and 20 Å. In the
low pressure region the bilayer remains impermeable
to anions. However, when the osmotic pressure corresp
onds to that in which the surface potential decreases
and the turbidity increases with the size of the
liposomes the bilayers become permeable to the anions
in relation to its ionic radius. It is concluded that
permeability determined by osmotic gradients can be
affected by the bilayer-bilayer interaction.

Tu-Pos201

EFFECTS OF INCREASED LIPID UNSATURATION ON ACYL CHAIN ROTATIONAL DYNAMICS: A COMPARISON OF SN-2 UNSATURATED AND DI-UNSATURATED CHAINS.
((Cojen Ho and Christopher D. Stubbs)) Thomas Jefferson University, Department of Pathology and Cell Biology, Philadelphia, PA 19107

Time-resolved fluorescence anisotropy (phase modulation method) of DPH attached to a PC sn-2 chain (DPH-PC) was used to compare the properties of bilayers of di-unsaturated PC and sn-2 unsaturated PC, varying the number of cis-double bonds from two to six per PC (using both hindered rotator and P2P4 models). It was found that fluorescence lifetimes of DPH-PC decreased with increasing unsaturation for both sn-2 and di-unsaturated systems, the di-unsaturated system (with same number of double bonds per PC) having significantly shorter lifetimes. Upon increasing unsaturation, lipid orientational order decreased and the rate of motion increased for both systems. Bilayers of sn-2 unsaturated lipids with four and six double bonds per PC gave nearly the same orientational order. By contrast, bilayers of di-unsaturated lipids with six double bonds per PC were significantly less ordered than with four double bonds per PC. Although the order in bilayers of di-unsaturated lipids was less than in bilayers of sn-2 unsaturated lipids (with same number of double bonds per PC), the rate of motion was reduced. This study indicates a potential problem with the common practice of using the physical properties of bilayers of di-unsaturated lipids to model the properties of unsaturation in natural membranes which are largely of the sn-2 unsaturation type. (Supported by US Public Health Grant AA08022).

Tu-Pos202

INFLUENCE OF sn-2 CHAIN UNSATURATION ON THE ^{2}H NMR ORDER PARAMETER PROFILE OF STEARIC ACID sn-1 CHAINS IN PHOSPHATIDYLCHOLINES.
((L.L. Holte, S.A. Peter, T. Sinnwell, and K. Gawrisch))
NIAAA, NIH, 12501 Washington Avenue, Rockville, MD 20852

Our goal is to understand why certain membranes found in brain synaptosomes and retinal rod outer segments require high levels of the poly-unsaturated docosahexaenoic acid, 22:6ω3, for proper functioning. ^{2}H NMR was used to study the order parameters of perdeuterated stearic acid in position sn-1 for a series of phosphatidylcholines with an 18:1, 18:2, 18:3, 20:4, 20:5, or 22:6 chain in position sn-2. Transitions between the gel and L_α phases were determined from the first moments of the spectra over the temperature range ±40°C. Order parameters of chain methylene segments were calculated from dePaked NMR powder patterns. At 37°C, increasing sn-2 chain unsaturation resulted in a small decrease in order of the sn-1 chain in the plateau region and a moderate decrease of order parameters towards the center of the bilayer (carbon atoms 10-18). Docosahexaenoic acid shortened the plateau region of the 18:0 chains. The effective length of the sn-1 chain in the L_α phase was calculated from average order parameters. The chain length of all lipids decreased with increasing temperature. Highly unsaturated PC's had shorter sn-1 chains but the chain length was somewhat less sensitive to temperature changes. Headgroup conformation and mobility as assessed by ^{31}P NMR were identical for all lipids in the L_α phase.

Tu-Pos203

WATER TRANSLATIONAL DIFFUSION CONSTANTS AT LIPID SURFACES. ((R. G. Bryant, D. S. Cafiso, J. Schreiber, C. Polnaszek, M. Whaley)) Department of Chemistry, University of Virginia, Charlottesville, VA 22901.

The magnetic field dependence of the water proton spin-lattice relaxation rate has been studied in several phospholipid preparations labeled with nitroxide at different positions on the lipid chain. The intermolecular proton-electron dipole-dipole coupling fluctuates because of the relative translational motion of the two magnetic moments. Analysis of the magnetic field dependence of the water proton relaxation using translational correlation function models yields the translational diffusion constant of the water near the nitroxide. The value of the diffusion constant is about $5 \times 10^{-6} cm^2 s^{-1}$ for several lipids and represents an average over the motions within approximately 10 Å of the nitroxide in the lipid and therefore characterizes the surface translational mobility of the water.

Tu-Pos204

A DIRECT MECHANICAL METHOD FOR THE MEASUREMENT OF TRANSBILAYER MOVEMENT OF PHOSPHOLIPID MOLECULES IN GIANT VESICLES. ((Robert M. Raphael and Richard E. Waugh)) Dept. of Biophysics, U. Rochester, Sch. Medicine and Dentistry. Rochester, NY 14642

The rate of spontaneous movement of phospholipid molecules across the bilayer ("flip-flop") has been studied using a variety of techniques in suspensions of vesicles at rest. Here we report evidence for the measurement of the flip-flop rate in a single vesicle subjected to elastic deformation. The technique involves applying an axial force to a phospholipid vesicle to produce a thin cylindrical tube of the bilayer, referred to as a tether. The high curvature tether results in a differential stretch between the two leaflets of the bilayer. In the absence of any movement of lipids between the constituent leaflets of the bilayer, this differential stretch is expected to result in a new equilibrium tether length after a change in membrane tension. Contrary to these expectations, we find that after an abrupt change in the membrane tension, the tether exhibits continuous slow growth beyond the expected equilibrium length at a rate of 0.5-5.0 µm/s. We postulate that this growth is due to the relaxation of the differential leaflet expansion by the net movement of phospholipids from the inner to the outer leaflet. Consistent with this hypothesis, we find a faster rate of tether growth (transbilayer movement) for larger step changes in the boundary tension. From calculations of the rate of transmembrane lipid movement as a function of the differential leaflet expansion we estimate a coefficient of interlayer permeation of 1250 cm/s/dyn. (Supported under NIH grant no. HL-31524.)

Tu-Pos205

^{2}H NMR STUDIES OF UNSATURATED PHOSPHOLIPID MEMBRANES: IMPORTANCE OF DOUBLE BOND LOCATION. ((Stephen R. Wassall[1], M. Alan McCabe[1], Cynthia W. Browning[1], Regina C. Yang McCabe[1], William D. Ehringer[2] and William Stillwell[2])) Departments of Physics[1] and Biology[2], Indiana University-Purdue University Indianapolis, Indianapolis, IN 46202.

The position of double bonds in unsaturated phospholipid membranes is the focus of our recent ^{2}H NMR studies which compare positional isomers. Moment analysis of spectra for monounsaturated [^{2}H$_{31}$]16:0-18:1PC (1-[^{2}H$_{31}$]palmitoyl-2-cis-octadecenoyl-phosphatidylcholine) membranes in which the double bond is at the Δ6, Δ9, Δ12 or Δ15 position reveals marked variation in phase behaviour and molecular ordering. The temperature of the gel to liquid crystalline transition exhibits a minimum when the unsaturation is at the Δ9 position. Average order in the liquid crystalline state is also a minimum for the Δ9 isomer when comparison is made at the same temperature, while at equal reduced temperature the dependence is inverted and there is a maximum for the Δ12 isomer. Position of unsaturation is similarly a critical determinant of phase behaviour and membrane order in polyunsaturated [^{2}H$_{31}$]16:0-α18:3 PC (1-[^{3}H$_{31}$]16:0-2-cis,cis,cis-octadeca-9,12,15-trienoyl-PC) and [^{2}H$_{31}$]16:0-γ18:3 PC (1-[^{2}H$_{31}$]16:0-2-cis,cis,cis-octadeca-6,9,12-trienoyl-PC). The gel to liquid crystalline transition possesses broad hysteresis and occurs at higher temperature for the α18:3 isomer, which is also less ordered in the liquid crystalline state. Thus, our results emphasize that double bond location is crucial in determining the properties of unsaturated membranes. Attempts to reconcile molecular models with our data and order parameter profiles derived from depaked spectra are currently in progress. (Supported by ACS, PRF and AHA, Ind. Affil.)

Tu-Pos206

THEORY OF NUCLEAR SPIN RELAXATION IN PHOSPHOLIPID MEMBRANES. ((Michael F. Brown, Theodore P. Trouard, and Todd M. Alam)) Dept. of Chemistry, University of Arizona, Tucson, Arizona 85721.

We have tested the hypothesis[1,2] that the dynamics of membranes include **collective fluctuations** of the assembly in addition to **molecular and segmental motions.** In the case of ^{2}H NMR the relaxation is governed by changes in the orientation of the electric field gradient tensor associated with the C-^{2}H bonds of the labeled molecules. These motions are related to the forces which influence the physical properties of phospholipids in the lamellar phase. ^{2}H NMR relaxation rates of phospholipid bilayers were evaluated using simple models for anisotropic rotational diffusion within an ordering potential having **odd or even parity** as a framework for describing (i) segmental reorientations of the chains, or alternatively (ii) molecular motions within the bilayer. In addition (iii) a simple quasi-hydrodynamic formulation involving collective fluctuations was considered. The **angular dependence** of the R_{1Z} relaxation rates can be explained in terms of a non-collective molecular model for the reorientational dynamics. Yet the **frequency dependence** of the R_{1Z} relaxation rates may be more amenable to interpretation in terms of a collective model.[3] The implications of the findings in relation to previous biophysical studies of membranes will discussed with innocent bystanders. [1]M.F. Brown (1982) J. Chem. Phys. 77, 1576-1599. [2]M.F. Brown et al. (1983) PNAS 80, 4325-4329. [3]M.F. Brown (1990) Mol. Phys. 69, 379-383. Supported by NIH Grants GM41413 and EY03754.

Tu-Pos207

^{2}H-NMR studies on the dynamics of nonfreezable water in fully hydrated phospholipid bilayers

((C-H Hsieh & W. Wu)) Institute of Life Sciences, National Tsing Hua University, Hsinchu, Taiwan

We have extended previous ^{2}H-NMR studies of the dynamics of nonfreezable water in sphingomyelin bilayers [Wu et al., (1991) J. Biol. Chem. 266, 13602-13606] to other phospholipid/D_2O systems of phosphatidylcholine (DMPC), phosphatidylethanolamine (DMPE), and phosphatidic acid (DMPA). Under fully hydrated condition and at subzero temperature, there are at least two types of water as reflected by the obtained NMR spectra of one isotropic peak superimposed by the Pake powder pattern. Dynamics of nonfreezable waters represented by sharp Lorentzian NMR resonances was then studied in three magnetic fields. T_1 and T_{2e} relaxation measurements on the nonfreezable water from -11C to -65C show that the water dynamics are similar between sphingomyelin/D_2O and DMPC/D_2O. Freezing of phosphocholine headgroup for DMPC/D_2O can also be detected by DSC and NMR to be at -35C , a temperature where T_{2e} value of D2O resonance shows a change in the slope of their temperature dependent profile. In contrast, nonfreezable water of DMPE/D_2O and DMPA/D_2O can only be detected from -11C to -35 C. There are no detectable DSC transition for the lipid dispersion within this temperature range, although ^{31}P NMR studies indicate that freezing of these phospholipid headgroups have already occured at -35C. Three types of motion, i.e, libration, anisotropic reorientation, and deuteron rearrangement are proposed to account for the the relaxation data obtained in this study. (supported by NSC, Taiwan)

Tu-Pos208

NMR STUDY OF PHOSPHATIDYL INOSITOL - ALPHA CYCLODEXTRIN ASSOCIATION, (F. FAUVELLE, J.C. DEBOUZY, Y.CHAPRON), CRSSA/BP - 38702 LA TRONCHE CEDEX - FRANCE

Hemolytic activity of Alpha-Cyclodextrin (ACD) was attributed to an aspecific phospholipid extraction followed by a moreless complete acyl chain inclusion. Our prévious works showed a quite different sheme of interaction. The mecanism does not involve any chain inclusion, at least in a first step. The phospholipid - ACD interaction was found very dependent from the nature of the polar head group of the phospholipid, in decreasing reactivity order : phosphatidyl - inositol) serine) ethanolamine)) choline. In the case of phosphatidyl inositol (PI), coupling constants and Overhauser measurements were used to built a molecular model of the PI - ACD association.

Tu-Pos209

CERAMIDE CHAIN-LENGTH AFFECTS STRATUM COR-NEUM MODEL MEMBRANE PHASE BEHAVIOR ((J. Thewalt, M. Bloom and N. Kitson*)) Dept. of Physics and *Div. of Dermatology, U.B.C., Vancouver, B.C., Canada, V6T 1Z1.

The impermeability of skin results from intercellular lipid membranes in the outer layer of the epidermis: the stratum corneum (SC). The composition of these membranes may be approximated by an equimolar mixture of ceramide (Cer), cholesterol (Chol) and fatty acid. The Cer's of SC are naturally very long-chained, predominantly greater than 20C. We have previously shown [Thewalt et al. (1992) BBRC 188: 1247-52] that a model SC membrane composed of bovine brain (BB) Cer, Chol and palmitic acid (PA) displays complex phase behaviour as determined by ^{2}H and ^{1}H NMR which closely parallels that found in actual SC. To determine the effect of varying the hydrocarbon chain length of the Cer on the phase behaviour of the model SC membrane we used synthetic Cer with a 16C chain. We present ^{2}H NMR data showing the temp. dependence of spectra of several mixtures: (1) BBCer:Chol:PA-d$_{31}$ 1:1:1 (2) Cer16:Chol:PA-d$_{31}$ 1:1:1 (3) Cer16:BBCer:Chol:PA-d$_{31}$ 1:1:2:2 (4) Cer16-d$_{31}$:BBCer:Chol:PA 1:1:2:2. These results show that the shorter hydrocarbon chain on the Cer has a marked influence on the phase behaviour of the system, reducing the proportion of solid phase at room temp. The unusually long-chained Cer's found in natural SC may thus be required for normal skin barrier function.

Tu-Pos210

FORMATION OF MICROSTRUCTURES WITH TORROIDAL TOPOLOGY FROM DIACETYLENIC SULPHOLIPID. ((A. Singh, M. A. Markowitz, and D. Puranik)) Center for Bio/Molecular Science and Engineering, Naval Research Laboratory, Washington, DC 20375 (Spons. By Dr. E. L. Chang)

Incorporation of diacetylenic group in acyl chains of a phospholipid not only provides the capability to stabilize the resulting self-organized structures by cross-linking acyl chains, but also adds to the capability of modulating bilayer morphologies. In an ongoing effort to build and study microstructures in various morphologies through molecular alterations in lipids, we took advantage of synergistic effect of diacetylenic acyl chains and headgroup geometry on molecular self-assembly process. To achieve this goal, we prepared two diacetylenic sulfo lipids in which tricosa-10,12-diynoyl is the acyl chain common to both lipids and the head group is -S-(CH$_2$)$_2$-NMe$_2$ (1) and -S(O)-(CH$_2$)$_2$-NMe$_2$ (2). Packing behavior of lipids was examined by Langmuir film balance at the air/water interface. Electron microscopy revealed that 1 formed large vesicles while 2 formed highly curved torroidal microstructures.

Tu-Pos211

FREELY SUSPENDED SOLVENT-FREE PHOSPHOLIPID BILAYERS FORMED BY LANGMUIR-BLODGETT TRANSFER TO MICROMACHINED APERTURES IN SILICON. ((T.D. Osborn and P. Yager)) Molecular Bioengineering Program, Center for Bioengineering, FL-20, University of Washington, Seattle, WA 98195, USA

Formation of planar phospholipid bilayers on solid and porous substrates by Langmuir-Blodgett transfer of monolayers from the air-water interface could be of much greater utility if the process were more reproducible. To that end the energetics of transferring two phospholipid monolayers to a hydrophilic surface have been examined. A mathematical relationship has been formulated that relates the surface pressure of the precursor monolayers to the tension within the bilayer created. The relationship correctly predicts the success of transfers to planar silicon substrates. Bilayer transfer can be carried out reproducibly even with refractory phospholipids such as phosphatidylcholine, but only over a narrow range of precursor monolayer surface pressures. This pressure range is related to the lysis tension of the bilayer. The morphologies of films formed within and below the acceptable range of surface pressures have been examined by fluorescence microscopy, and the observed features are discussed in terms of the mathematical relationship. The assembly method employed may be used to transfer a wide variety of lipid bilayers to hydrophilic supports. To test this a hydrophilic "bilayer support device" was micromachined from silicon with an array of 100 μm diameter apertures. The use of appropriate monolayer surface pressures permitted reproducible formation of long-lived solvent-free phosphatidylcholine bilayers across the apertures. Such mass producible devices for supporting lipid bilayers, along with this demonstrated method for using them, are of potential value for studies of ion channels, for receptor and drug assays, and for biosensors.

Tu-Pos212

EFFECT OF N-GLUTARYL-DPPE ON THE *IN VIVO* CIRCULATION LIFETIME OF DSPC LUVETS, MLV'S AND IFV'S. ((Patrick L. Ahl, Suresh K. Bhatia, Patricia Roberts and Andrew S. Janoff)) The Liposome Company, Princeton, NJ 08540

The *In Vivo* circulation lifetime of liposomes depends on both size and lipid composition. We have investigated how the plasma clearance of DSPC and DSPC /N-Glutaryl-DPPE (9:1 mole ratio) liposomes in Sprague Dawely rats is influenced by liposome size. DSPC MLVs, IFVs, and LUVETs were rapidly removed from the circulation. IFVs, i.e. Interdigitation-fusion Vesicles, are large unilamellar vesicles formed by interdigitation induced fusion of DSPC SUVs. The liposome plasma levels were less than 2 % of the total dose within 1/2 hr after intravenous injection of MLVs, while the average percent dose at 1/2 hr was less than 10 % for DSPC IFVs. The plasma clearance behavior of DSPC /N-glutaryl-DPPE MLVs and IFVs were indistinguishable from DSPC MLVs and IFVs. In contrast, for 150 nm DSPC /N-glutaryl-DPPE LUVETs the percent liposome dose remaining in the plasma 1/2 and 24 hr after injection were 79.2 ±9.8 % and 20.3 ±5.7 % (n=6) respectively. The circulation behavior for DSPC /N-glutaryl-DPPE LUVETs extruded through filter pore sizes ranging from 50 to 800 nm were also examined. The enhanced circulation time of DSPC /N-glutaryl-DPPE LUVETs resulted from liposome avoidance of the reticuloendothelial system, since the plasma clearance behavior did not show a strong dependence on liposome dose. Thus, the synthetic lipid N-glutaryl-DPPE significantly increased the circulation lifetime of DSPC LUVETs with an average diameter below 1 μ, but did not enhance the lifetime of DSPC MLVs or IFVs. (Supported by The Liposome Company)

Tu-Pos213

INCORPORATION OF POLYMER-LIPIDS INTO BILAYERS LEADS TO PHASE TRANSITION. ((K. Hristova and D.Needham)) Department of Mechanical Engineering and Materials Science, Duke University, Durham, NC 27708-0302

As X-ray diffraction studies on multilamellar vesicles suggest, polymer-lipids can be incorporated into a lipid bilayer only up to a certain maximum concentration. Above it the lipid mixture is expected to transform from lamellar into a micellar phase. To explain this phenomenon we develop a physical model, giving the energy of the polymer - lipid/lipid/water system as a function of the polymer concentration in the sample. Our results show that upon increase in this concentration the energy minimum of the system gradually moves from bilayer into a micellar phase. The characteristics of this transition depend crucially on the polymer molecular weight and on the packing of the hydrophobic lipid tails. The proposed theoretical model allows us to predict (1) polymer/lipid concentration in the bilayer (this is the concentration, relevant to the X-ray diffraction studies) and (2) polymer/lipid concentration in the micellar phase as a function of the polymer - lipid concentration in the sample. The distribution of material between the two phases depends on the elastic constants of the bilayer, the molecular weight of the polymer and the molecular characteristics of the lipids.

Tu-Pos214

QUANTIFICATION OF THE INTERACTIONS AMONG FATTY ACID, LYSOPHOSPHATIDYLCHOLINE, CALCIUM, DMPC VESICLES AND PHOSPHOLIPASE A_2. ((E.D. Bent and J.D. Bell)) Dept. of Zoology, Brigham Young University, Provo, Utah 84602.

The rate of hydrolysis of phosphatidylcholine bilayers by soluble phospholipase A_2 (PLA_2) is greatly enhanced by the presence in the bilayer of a threshold mole fraction of the reaction products: fatty acid (FA) and lysophosphatidylcholine (lyso). The threshold requirement of these products appears to vary as a function of vesicle and calcium concentration. To further identify the roles of FA, lyso and calcium in promoting optimal PLA_2 activity, we have quantified the various interactions among these components and dimyristoylphosphatidylcholine (DMPC) large unilamellar vesicles. The water/ bilayer partition coefficient for FA was obtained by competition of vesicles for the binding of FA to an acrylodan conjugate of an intestinal fatty acid binding protein as monitored by the acrylodan fluorescence emission spectrum. The partition coefficient for lyso was obtained by a similar procedure using the tryptophan emission spectrum of bovine serum albumin. The effect of calcium concentration on these interactions was also quantified. These results were incorporated into an empirical model to describe the threshold requirements for these products in the bilayer. This information is vital for elucidating the mechanism of activation of PLA_2 by the hydrolysis products.

FOLDING AND SELF-ASSEMBLY I: PROTEIN FOLDING AND UNFOLDING

Tu-Pos215

THERMODYNAMICS OF ACID-INDUCED CONFORMATIONAL CHANGES IN THE INFLUENZA VIRUS HEMAGGLUTININ.
((David P. Remeta, Mathias Krumbiegel, Robert Blumenthal and Ann Ginsburg)) NHLBI and NCI, National Institutes of Health, Bethesda, MD 20892

Hemagglutinin (HA) is a major surface membrane glycoprotein responsible for the binding of influenza virus to sialic-acid-containing receptors in target cells. Fusogenic activity is triggered by a pH-dependent conformational change of HA in the acidic milieu of the endosomes. HA is a trimeric protein (220,000 M_r) comprising an ectodomain of identical subunits, each of which contains two polypeptides (HA_1 and HA_2) linked by a disulfide bond. The conformational stability of HA purified from the influenza strain X31 has been investigated by differential scanning calorimetry (DSC) and circular dichroism (CD) spectroscopy to characterize the thermal unfolding/refolding pathway and elucidate pH-induced structural changes. A single endotherm with a transition temperature of 66.5 °C and an enthalpy change of ΔH_{cal} = 980 kcal/mol is observed in DSC profiles of HA rosettes (i.e., aggregates of trimers) in phosphate buffered saline (pH 7.4). Deconvolution of the HA endotherm reveals that the protein unfolds in a cooperative manner which may be adequately described by either an independent or sequential model involving three two-state transitions. The thermal stability of HA is reduced substantially (ΔT_m = 23.0 °C) over the pH range of 7.4 to 5.0 with a concomitant decrease in the unfolding enthalpy ($\Delta\Delta H_{cal}$ = 880 kcal/mol). Comparison of CD spectra acquired as a function of pH reveals that there are significant changes in the overall tertiary structure of HA, whereas the secondary structure remains essentially unperturbed. The loss in tertiary structure coupled with the significant reduction in unfolding enthalpy and relatively invariant secondary structure suggests that HA adopts a *molten globule* conformation under fusogenic conditions (i.e., pH 4.9, 37 °C).

Tu-Pos216

CONTRIBUTION OF HYDROGEN BONDING TO THE STABILITY OF PROTEIN. ((G.I. Makhatadze and P.L. Privalov)) Department of Biology, The Johns Hopkins University, Baltimore, MD 21218

The enthalpies and entropies of hydration of polar and non-polar groups upon protein unfolding have been estimated for fourteen globular proteins in the temperature range 5-125°C, using structural information on the groups in these proteins exposed to water in the native and unfolded states, and calorimetric information on the thermodynamics of transfer into water of various model compounds. Subtracting the total enthalpy of hydration of polar and non-polar groups from the calorimetrically determined enthalpy of protein unfolding, the total enthalpy of internal interactions maintaining the native protein structure has been obtained. Using thermodynamic information on the sublimation of organic crystals, the enthalpy of internal hydrogen bonding has been determined. If a hydrogen bond is formed in the presence of water, the positive Gibbs energy of dehydration of polar groups opposes the negative enthalpy of formation of the hydrogen bond. Therefore, only the difference of these two Gibbs energies contributes to protein stability. It has been shown, from the analysis of the thermodynamic information on fourteen proteins, that hydrogen bonding stabilizes the native protein structure.

Tu-Pos217

HYDROPHOBIC FREE ENERGY OF TRANSFER OF ALA AND LEU RESIDUES FROM SURFACE PRESSURE ISOTHERMS.
((P. Lavigne, P. Tancrède and F. Lamarche*)) Département de Chimie-Biologie, U.Q.T.R., B.P. 500, Trois-Rivières (Québec) Canada and *C.R.D.A, 3600 Boul. Casavant ouest, St-Hyacinthe (Québec) Canada.

The surface pressure (Π) - residual area (A) and surface potential (ΔV) - residual area (A) isotherms of poly-L-alanine in the α-helix conformation and poly-L-leucine in the anti-parallel β-sheet conformation have been studied at the air-water interface at 22°C. Phase transitions ascribed to monolayer-bilayer transitions are encountered on the Π-A isotherms. Strong hysteresis effects are also encountered when the films are submitted to compression-expansion cycles. Such compression-expansion cycles have been performed on both films in their respective monolayer to bilayer transitions. The surface area delimitated by the hysteresis increases linearly with the degree of advancement of the bilayer formation. From a thermodynamic point of view, the surface delimitated by the hysteresis is a measure of the variation of the Gibbs free energy (ΔG) of the films during the compression-expansion cycles. During the compression-expansion cycles a fraction of the residues in contact with the water surface are transferred to form a bilayer. It is then possible to extract a hydrophobic ΔG of transfer (ΔG_{tr}) on a per residue basis. The hydrophobic ΔG_{tr} so obtained is equal to 0.40 kcal·mol^{-1}·res.$^{-1}$ for Ala and 0.84 kcal·mol^{-1}·res.$^{-1}$ for Leu.

Tu-Pos218

MECHANISMS OF STABILIZATION OF PROTEINS BY ANIONS AT ACIDIC pH.((Bertrand García-Moreno E.)) Department of Biophysics, Johns Hopkins University, Baltimore, Maryland

Apomyoglobin, cytochrome c, and β lactamase are unfolded extensively at pH 2 under conditions of low salt concentration. The addition of anions at this pH (ie addition of acid or salt) can induce refolding of these proteins to a compact denatured state (Goto, Calciano and Fink (1990) Proc. Natl. Acad. Sci. 87, 573). We have used computational approaches to determine the molecular mechanisms through which simple salts (NaCl, KBr) in the range of concentrations between 10 mM and 300 mM stabilize folded structures of myoglobin at highly acidic pH. Our analysis entailed the computation of the electrostatic potentials (ψ) on crystallographic structures of myoglobin and on models of the compact denatured states. Screening of ψ proportional to the ionic strength was handled explicitly with Debye-Hückel type models. Binding of anions to the proteins was also considered explicitly. Specific sites of Cl⁻ binding on the surface of myoglobin were identified directly from examination of the electrostatic potential. The energetics of site-specific binding at the putative binding sites were quantitated as a function of salt concentration. Despite the dramatic ionic strength effects predicted for these highly charged forms of the protein, the computations indicate that under conditions of low pH the contributions to the stability of the folded forms of myoglobin by anion binding are more significant than the contributions due to screening of repulsive intramolecular interactions by ionic strength.

Tu-Pos219

ENERGETICAL DOMAINS IN GLOBULAR PROTEINS

A.A.Makarov, I.I.Protasevich, I.B.Grishina, R.W.Hartley*, N.G.Esipova, and G.I.Yakovlev, Engelhardt Institute of Molecular Biology, Acad. Sci. Russia, Moscow 117894; *NIDDK, NIH, Bethesda, MD 20892, USA.

The aim of the present study was to establish a correlation between electrostatic and solvent conditions and the types of cooperative thermodynamic transitions in bacterial RNases binase, barnase and their mutants, inorganic pyrophosphatase, pepsin and pepsinogen using microcalorimetric analysis of thermal denaturation at different pH, ionic content and in water-alcohol mixtures. Binase melts within pH4-7 as an integral cooperative system, whereas a second maximum appears on the heat absorption curve at pH below 4. We have shown that the binase globule separates into two "energetical" domains at acid pH. This process neither disturbs its secondary structure nor changes local surroundings of aromatic amino acids. For barnase, which is very similar to binase, we have found intermediates in the course of thermal unfolding only in 50% methanol. This could be due to different electrostatic characteristics of binase and barnase revealed in the patterns of dipole moment distribution for all possible fragments of these molecules. The pH and ethanol influence on the number of cooperative regions in pepsin were studied. While changing pH from 6.7 to 2.0 in 20% ethanol, the number of thermodynamic cooperative units decreases from four to two. The results indicate that the thermodynamic properties of these proteins are the first to change when the charges in the molecules are redistributed, while the molecular architecture remains practically unaltered. This can be a basis for discriminating between structural and energetical domains in proteins. This work was supported by Grant 93-04-21295 from the Russian Fund of Fundamental Research.

Tu-Pos220

WHAT THERMAL STABILITY OF LIPOXYGENASES REVEALS ABOUT CATALYTIC ACTIVITY.

((B.J. Gaffney, J.M. Sturtevant*, S.M. Yuan, D.M. Lang and E. Dagdigian)) Departments of Chemistry, Johns Hopkins University, Baltimore, MD 21218 and *Yale University, New Haven, CT 06511

It has long been known that the isozymes of soybean lipoxygenase differ in several aspects of catalysis, including pH optima, substrate specificity and specific activity. Recent solution of the crystal structure of the L-1 isozyme of soybean lipoxygenase showed that the N-terminal regions where the soybean isozymes differ most in sequence are located in a domain that is separate from the domain containing the catalytic site. Scanning calorimetry and thermal denaturation studies have been undertaken to examine unfolding of three soybean lipoxygenase isozymes and of rabbit reticulocyte lipoxygenase. The results are modeled as a two step process: a reversible unfolding followed by an irreversible kinetically limited denaturation. Under standard conditions of pH 7 and a DSC scan rate of 60°/ hour, isozymes L-1, L-2 and L-3 had calorimetric maxima at 73, 63 and 71 ± 1 °C respectively. That the thermal transition detected by DSC is associated with the major, catalytic domain of lipoxygenases is demonstrated by the similarity in thermal behavior of rabbit reticulocyte lipoxygenase to that of the plant enzymes. The reticulocyte protein lacks the N-terminal domain found in plant enzymes. The lipoxygenase structures are also destabilized by removal of the mononuclear iron center. There is strong pH dependence of unfolding, with lipoxygenases being less stable at high pH for the range pH 6 - 9. L-2 is thus relatively unstable at temperatures near 40°. Together, these results suggest that some of the differences in pH optima of lipoxygenases are due to different thermal stabilities in the high pH range.

Tu-Pos221

THERMOSTABILITY OF APO- AND Mg-CheY.

((G. T. DeKoster+, A. D. Robertson+, A. M. Stock*, J. B. Stock#)) +Dept. of Biochem., Univ. of Iowa, Iowa City, IA 52242, *Ctr. for Adv. Biotech. & Med., Piscataway, NJ 08854, #Dept. of Mol. Biol., Princeton Univ., Princeton NJ 08544.

We are investigating the thermodynamic stability of CheY, a 14 kD a protein of the chemotaxis system in *Salmolella typhimurium*. Using circular dichroism and calorimetry, we have measured the thermodynamic parameters describing CheY stability at pH 7. Thermal denaturation of CheY gives a T_m of 54°C and an enthalpy of unfolding, ΔH_m, of 65 kcal/mol. Using both calorimetry and the spectroscopic method of Pace and Laurents [(1989) Biochemistry 28, 2520-2525] thermal and chemical denaturation have been used to determine a ΔC_p, the heat capacity of protein unfolding, of approximately 2 kcal/(mol·K). We have also measured the thermostability of CheY in the presence of its biological co-factor, magnesium. These studies show that magnesium increases the global stability of CheY at pH 7. We have used hydrogen exchange to measure protection factors in both apo- and Mg-CheY. Comparisons of exchange patterns in apo- and Mg-CheY allow us to determine how CheY accomodates the binding of magnesium at the amino acid level.

Tu-Pos222

THERMODYNAMIC CHARACTERIZATION OF THE STRUCTURAL STABILITY OF A PREDOMINANTLY β-STRUCTURE PROTEIN: Rat Intestinal Fatty Acid Binding Protein (I-FABP).

Mari Mar Lopez#, James C. Sacchettini*, Ernesto Freire#
#Department of Biology and Biocalorimetry Center, The Johns Hopkins University, Baltimore, MD 21218, * Department of Biochemistry. Albert Einstein College of Medicine, Bronx, NY 10461

We have studied the thermal stability of the Intestinal Fatty Acid-Binding Protein (I-FABP) by high-sensitivity differential scanning calorimetry (DSC) and circular dichroism spectroscopy (CD) under equilibrium conditions. At pH 3.0 the transition temperature, Tm, is 53 °C and the unfolding is characterized by a ΔH of 79 Kcal/mol and a ΔCp of 1.9 Kcal/mol K. The Tm decreases upon lowering the pH. Circular dichroism spectroscopy (at pH 3.0 and pH 2.5) in the far UV-region, as a function of temperature, shows a well-defined isodichroic point at 209 nm. The CD data indicates that the thermally denatured protein is essentially unfolded with no measurable residual structure. The crystal structure of I-FABP was used to perform structural thermodynamic calculations getting a value of ΔH (at 53 °C) of 80 Kcal/mol and ΔCp of 2.1 Kcal/ mol K, which are close to the experimental ones. These results suggest that the structural parametrization of the enthalpy and heat capacity changes derived previously in this laboratory, also applies to predominantly β-sheet proteins. Experiments were also performed in the presence of saturating conditions of different fatty acids ligands: Oleate (C18), Palmitate (C 16) and Myristate (C14).

Tu-Pos223

THERMODYNAMIC AND STRUCTURAL CONDITIONS FOR THE STABILIZATION OF COMPACT DENATURED STATES

Dong Xie and Ernesto Freire, Department of Biology and Biophysics and the Biocalorimetry Center, The Johns Hopkins University, Baltimore, MD 21218

The heat denatured state of proteins has been usually assumed to be a fully hydrated random coil. It is now evident that under certain solvent conditions or after chemical or genetic modifications, the protein molecule may exhibit a hydrophobic core and residual secondary structure after thermal denaturation. This state of the protein has been called the "compact denatured" or "molten globule" state. Recently we have shown that α-lactalbumin at pH < 5 denatures into a compact denatured state upon increasing the temperature (Griko, et. al., 1993). This state has a lower heat capacity and a higher enthalpy at low temperatures than the unfolded state. In this work, we have examined a large ensemble of partly folded states of α-lactalbumin and identified those states that satisfy the experimental energetic criteria of the compact denatured state. Using the structural parametrization of the protein folding/unfolding energetics in combination with the CORE algorithm, we have identified a folding/unfolding pathway that satisfies the experimental criteria. At temperatures below 45 °C the state with the highest enthalpy is state 77 (corresponding to the binary code 0011011), and not the unfolded state. In this state, residues 34-82 corresponding mainly to the β-sheet and type I and III turns; and the residues from 105 to the carboxyl terminal are in an unfolded configuration. Helices B and C are folded in state 77. It is interesting that state 77 has a heat capacity very close to that observed for the acid pH compact denatured state of α-lactalbumin (980 cal·(mol·K)$^{-1}$). In addition, the folded regions of this state include those residues found to be highly protected by NMR hydrogen exchange experiments. Since at low temperatures, the compact denatured state is enthalpically unfavorable relative to the unfolded state, the necessary condition for its stabilization is that its entropy reaches a critical level. (Supported by NIH grants RR-04328, GM-37911, and NS-24520)

Tu-Pos224

SUBUNIT INTERACTIONS STABILIZING THE PHOSPHOLAMBAN (PLB) PENTAMER.

((H.K.B. Simmerman*, Y.M. Kobayashi, B. Strifler, and L.R. Jones)) *Repligen Corporation, Cambridge, MA 02139 and Indiana University School of Medicine, Indianapolis, IN 46202

Phospholamban (PLB) is a 30 kDa integral membrane protein of cardiac sarcoplasmic reticulum consisting of five identical noncovalently-associated polypeptide chains of 52 amino acids. Previous results have shown that PLB forms Ca^{2+}-selective channels in lipid bilayers. The channel-forming domain has been localized to amino acid residues 26-52, which form a stable pentameric, helical structure. We have identified the specific residues responsible for stabilizing the pentameric membrane domain of PLB by mutational analysis. Residues 27-52 were individually changed to Ala, and the ability of the resulting mutant to form a pentamer was assessed by SDS-PAGE. Replacement of L37, I40, L44, or I47 by Ala completely abolished pentamer formation, indicating their essential involvement in oligomeric assembly. Replacement of other residues by Ala did not eliminate PLB oligomeric structure. The heptad repeat of leucines at positions 37, 44, and 51 conforms to the structural motif of a leucine zipper, and the further heptad repeat of isoleucines at positions 40 and 47 renders an overall 3-4 residue repeat spacing of hydrophobic amino acids characteristic of a coiled-coil. We propose that the pentameric structure of residues 37-52 is a coiled-coil stabilized by close-packing interactions between the interdigitated, alternating Leu and Ile residues. The resulting symmetric structure contains a central pore defined by the hydrophobic surface of the five stabilizing leucine zippers, which are oriented to the interior and form the backbone of the pentamer.

Tu-Pos225

ACID CONFORMATION OF HUMAN GROWTH HORMONE PROVIDES NEW INSIGHT INTO THE EQUILIBRIUM FOLDING MECHANISM.

((M. R. DeFelippis, M. A. Kilcomons, M. P. Lents, K. M. Youngman, and H. A. Havel)) Lilly Research Laboratories, Indianapolis, IN 46285.

The solution properties of human growth hormone (hGH) were evaluated under acid conditions. Far-UV circular dichroism (CD) measurements indicate that the secondary structure remains virtually unchanged while there is partial disruption of the tertiary structure as determined by intrinsic tryptophan fluorescence and near-UV CD. Dynamic light scattering and dye binding experiments indicate that the size of hGH in acid is intermediate between the native and unfolded states with slightly increased surface hydrophobicity. The properties of the acid conformation of hGH (A-state) are similar to *molten globule* intermediates except for uncharacteristically high conformational stability. Equilibrium denaturation data obtained at pH 2.5 using 0.1 mg/mL hGH were similar to results at pH 8.0 except that the ΔG values were reduced by ~5 kcal/mol. At pH 2.5 and 1 mg/mL hGH, a biphasic denaturation profile was obtained by far-UV CD detection at 222 nm, while the near-UV CD measurements at 295 nm yielded an apparent monophasic transition with a midpoint value of 3.7 M GdnHCl. These results suggest a concentration-dependent formation of equilibrium intermediate(s) having a propensity to aggregate. Static light scattering measurements performed on hGH solutions containing 4.5 M GdnHCl at pH 2.5 provided direct evidence for the formation of a large molecular weight (≈80 kDa) self-associated intermediate. No evidence for aggregation was found under acid conditions in the absence of any denaturant indicating that self-association results from the formation of an intermediate (I) derived from the A-state. Self-association of I can lead to irreversible precipitation. A folding mechanism is proposed.

Tu-Pos226

EFFECTS OF GLU-75 ON THE COMPACT DENATURED STATE OF STAPHYLOCOCCAL NUCLEASE.

((H. M. Chen & T. Y. Tsong)) Dept of Biochem, the Hong Kong Univ of Science & Technology, Kowloon, Hong Kong

The acid induced folding/unfolding of Staphylococcal nuclease (SNase) follows the sequential pathway: $D_4 \leftrightarrow D_3 \leftrightarrow D_2 \leftrightarrow D_1 \leftrightarrow N_0$, where the 4 Ds are the sub-states of the denatured protein and N_0 is the native state. The 4 Ds have similar free energies and enthalpies but are separated by 6-14 kcal/mol of activation barriers. The D_3 to D_2 transition is invisible to the Trp-140 fluorescence and the D_2 to D_1 transition can not be detected by the CD (Chen, HM & Tsong, TY, Biophys. J. In press). We have found that the D_2 to D_1 transition is a chain condensation process because its rate decreases with increasing solvent viscosity. We have also found that Glu-75 plays an important role in stabilizing the compact unfolded state, D_1, of SNase. At pH 3, the population of D_1 in the WT is 60% but it decreases to 35% in the mutant E75G. In the WT, D_1 to D_2 transition absorbs 1.7 protons but in the mutant this step is independent of pH. Kinetics analysis indicates that at pH 3, the population of D_4 is 26% for the E75G compared to 11% for the WT. Differential scanning microcalorimetry was performed for the E75G and the WT proteins. ΔH_{cal}, ΔC_p and T_m are found to be 84.1 kcal/mol, 2.2 kcal/deg.mol and 52°C, respectively, for the WT, and 42.7 kcal/mol, 1.8 kcal/deg.mol and 35.9°C, respectively for the E75G. ΔG of unfolding at 25°C is 4.45 kcal/mol for the WT and is 1.16 kcal/mol for the E75G. These results, taken together, indicate that Glu-75 contributes substantially to the protein stability, and that electrostatic interactions involving Glu-75 and one or two positively charged groups are responsible for the chain condensation. Computer analysis suggests that Glu-75 may form complete or partial salt bridges with Lys-9 and His-121. Ref: Chen et al., J. Mol. Biol. 220, 771, 1991; Biochemistry 31, 1484, 1992; Biochemistry 31, 12369, 1992.

Tu-Pos227

THERMODYNAMICS OF THE HYDROPHOBIC EFFECT IN SOLID DIPEPTIDES AND PROTEINS

Litian Fu#, Jose Laynez*, Jose Saiz*, and Ernesto Freire#
#Department of Biology, Department of Biophysics and Biocalorimetry Center, The Johns Hopkins University, Baltimore, MD 21218, *Instituto de Quimica Fisica "Rocasolano", Consejo Superior de Investigacions Cientificas, Madrid 28006, Spain

Previously, we have observed that ΔCp for protein unfolding decreases at increasing methanol concentrations (0-10% vol/vol). This effect manifests itself on a larger ΔH of unfolding at temperatures lower than 100 °C. For a given protein, the unfolding enthalpies at 100 °C are equal and independent of methanol concentration within the region studied (Fu, L., and Freire, E. (1992) *Proc. Natl. Acad. Sci., USA*, 89, 9335-9338, and unpublished results). In order to test the origin of this effect, we have begun a series of experiments aimed at measuring directly the heat, and the heat capacities of dissolution of several solid dipeptides in water containing increasing methanol concentrations. The results obtained so far for cyclo(Gly-Gly), cyclo(Ala-Gly) and cyclo(Leu-Gly) show that the heat capacity of dissolution is reduced in solvents containing a higher methanol concentration, and that the methanol effect on ΔCp increases with the number of apolar hydrogens in the compounds. These results, together with the results of our protein study, suggest that at low concentrations the primary effect of methanol is to lower the magnitude of the hydrophobic interaction. Thus methanol can be used as a perturbant of the hydrophobic effect in protein stability studies (Supported by Grants from NIH RR-04328, NS-24520 and GA-37911).

Tu-Pos228

THERMODYNAMIC STABILITIES OF MAJOR PROTEIN SUBSTRUCTURES.

Rufus Lumry, University of Minnesota, Minneapolis, MN 55455

Enzymes like many other proteins consist of hard substructures`(knots) and soft substructures tethered to knots.(*matrices and surfaces*). Knots contain most structural information and since function is most proteins apparently follows form, they maintain evolutionary continuity. The actual molecular mechanisms are, however, built into the matrices The latter conform to the dictates of the strong knots and thus preserve form under wide variations in composition. The evolutionary adaptability and conformational flexibility required in matrices is made possible by a simple distribution of effort: the electrostatic free energy of the knots is so low it compensates for positive free-energy of formation of the matrices from the denatured state. The net negative free energy of folding to the native state is the sum of a large negative contribution from the knots and a smaller positive contribution from the matrices. Their stabilities can be estimated when the forward rate constant in denaturation is available since the slow step is expansion of knots to the point at which knot cooperativity is lost. An example is HEW lysozyme (data from Segawa and Sugihara, Biopolymers, 23, 2473(1984)). Lysozyme has a single catalytic function and thus two functional domains. Coupled conversion of the two knots to matrix costs 14.2 kcal per mole of protein. The transition state is 6 kcal/mole less stable than the denatured state and the matrix 4 kcal/mole less stable. Pohl's data for α-chymotrypsin (Dissertation, Göttingen-Konstanz, 1969) give a similar picture. Thus matrices of such proteins are not in their intrinsic (most stable) states in the native protein. The stability of the knots is a consequence of synergistic electrostatic factors of which the interactions among peptide electric moments are the most important. Knots are best described using conserved sequence information but they are usually the same as the slow-exchange cores. These cores often include large hydrophobic groups which act like transformer fluids to reduce the dielectric constant and thus strengthen the predominately hydrogen-bonded knot skeleton. Dispersion interactions among oily groups are probably often important but some strong knots have no large oily sidechains.(e.g. the phospholipase A2 family).

Tu-Pos229

THERMODYNAMIC STABILITY OF *Bacillus circulans* XYLANASE MUTANT CONTAINING DISULPHIDE BRIDGES.

((J. Davoodi[1], W. W. Wakarchuk[2], P.R. Carey[2], and W. K. Surewicz[2])) [1]Dept. of Biochemistry, Univ. of Ottawa, Ottawa, Ontario, K1H 8M5; [2]Institute for Biological Sciences, NRC, Ottawa, Ontario K1A 0R6, Canada. (Spon. by P. Butko)

The overall objective of this research is to generate and characterize hyperstable variants of Bacillus circulans xylanase. We have used the strategy in which disulphide bridges in different parts of the protein molecule were introduced by site directed mutagenesis. The mutants studied include S100C/N148C(DS1) and V98C/A152C(DS2). Far UV circular dichroism data show that the secondary structure of both variants is essentially identical with that of the wild type protein. However chemical denaturation studies indicate that the thermodynamic stability of the mutants is significantly increased with the stabilization energy in 2.2 M guanidium hydrochloride of 8.5 and 4.1 kJ/mol for DS1 and DS2, respectively. The increased stability of the mutant proteins is also indicated by differential scanning calorimetry, although thermodynamic treatment of calorimetric data is hampered by irreversibility of the thermal denaturation process. The combined spectroscopic and calorimetric data indicate that the DS1 mutant is superior and satisfies the geometric and stereochemical requirements for a disulphide bond formation.

Tu-Pos230

ALPHA HELIX STABILITY AND THE NATIVE STATE OF MYOGLOBIN

((Laura Lin, Rachel J. Pinker and Neville R. Kallenbach)) Department of Chemistry, New York University, New York, NY 10003

The native state of proteins contains secondary structure-regular patterns in the peptide backbone, such as alpha helix, beta structure and turns-with high frequency. The role of this secondary structure in stabilizing the native folded state is presently unclear. For example, alanine substitutions at helical sites in myoglobin, which should stabilize helical structure, show no correlation with the helical propensity of the side chains involved. In an effort to demonstrate a relationship between the effect of a side chain on stabilizing secondary structure and the native structure, we have carried out site directed changes in the sequence of the helical protein, sperm whale myoglobin. Fully buried hydrophobic side chains were exchanged for similar hydrophobic side chains or alanine at sites corresponding to mid-helical positions in the native state. The results reveal a positive correlation between the alpha helix forming ability of the substituted side chain and the stability of the mutant proteins, once differences between the size of the side chains, or hydrophobicity, are corrected for. When each type of amino acid substitution is averaged over the different sites selected, the helix propensities of the amino acids account for much of the residual variation. Analysis of the thermal unfolding of these myoglobins as a function of urea concentration indicates that there is considerable scatter in the slopes of Tm^{-1} vs C_{urea} profiles. For mutations at internal sites, this implies that differences in urea binding occur in the unfolded form of the protein. The correlation we observe with helix propensities, even in the case of internal alanine substitutions, argues that stability of the native state of a protein is coupled to that of secondary structural elements in the structure. In magnitude, the net contribution of propensity differences is smaller than hydrophobic effects, but not negligible in terms of the net free energy of unfolding. This work was supported by grant GM 40746 from the NIH.

Tu-Pos231

THERMODYNAMIC CHARACTERIZATION OF THE STRUCTURAL STABILITY OF A PREDOMINANTLY β-STRUCTURE PROTEIN: RAT INTESTINAL FATTY ACID BINDIG PROTEIN (I-FABP).

((Mari Mar Lopez#, James C. Sacchettini*, Ernesto Freire#)) #Department of Biology and Biocalorimetry Center, The Johns Hopkins University, Baltimore, MD 21218. * Department of Biochemistry. Albert Einstein College of Medicine, Bronx, NY 10461

We have studied the thermal stability of the Intestinal Fatty Acid-Binding Protein (I-FABP) by high-sensitivity differential scanning calorimetry (DSC) and circular dichroism spectroscopy (CD) under equilibrium conditions. At pH 3.0 the transition temperature, Tm, is 53 °C and the unfolding is characterized by a ΔH of 79 Kcal/mol and a ΔCp of 1.9 Kcal/mol K. The Tm decreases upon lowering the pH. Circular dichroism spectroscopy (at pH 3.0 and pH 2.5) in the far UV-region, as a function of temperature, shows a well-defined isodichroic point at 209 nm. The CD data indicates that the thermally denatured protein is essentially unfolded with no measurable residual structure. The crystal structure of I-FABP was used to perform structural thermodynamic calculations getting a value of ΔH (at 53 °C) of 80 Kcal/mol and ΔCp of 2.1 Kcal/ mol K, which are close to the experimental ones. These results suggest that the structural parametrization of the enthalpy and heat capacity changes derived previously in this laboratory, also applies to predominantly β-sheet proteins. Experiments were also performed in the presence of saturating conditions of different fatty acids ligands: Oleate (C18), Palmitate (C 16) and Myristate (C14). (This work was supported by NIH Grants RR-04328, GM-37911 , NS-24520 and GM-45859)

Tu-Pos232

ENTROPY OF HYDROGEN BONDING IN PROTEINS. ((Kenneth P. Murphy)) Department of Biochemistry, University of Iowa, Iowa City, IA 52242

Knowledge of the energetics of hydrogen bond formation is crucial to understanding protein folding and stability. The study of the aqueous dissolution of model compounds can provide important insights into this problem, but care must be taken to correctly assign the energetic terms. It has recently been suggested that the unfavorable ΔS° of hydrating polar groups is a driving force for hydrogen bond formation in proteins. This unfavorable ΔS° is inferred from the results of model compound studies. Comparison of dissolution and vaporization of alcohols and alkanes indicates that the unfavorable ΔS° is *not* due to hydration, but instead arises from changes in internal degrees of freedom. Use of uncorrected ΔS° (or ΔG°) dissolution values will thus result in misinterpretation of folding energetics. These results also suggest that the ΔS° of hydration of polar and apolar groups approach zero at the same temperature, namely 112°C.

Tu-Pos233

PARTIALLY FOLDED PROTEINS: CHEMICAL SYNTHESIS AND PHYSICAL CHARACTERIZATION OF BPTI ANALOGS ((M. Ferrer, G. Barany, and C. Woodward)) University of Minnesota, Dept. of Chemistry, Minneapolis, MN 55455 and Dept. of Biochemistry, St. Paul, MN 55108

Partially folded variants of bovine pancreatic trypsin inhibitor (BPTI) have been prepared by chemical synthesis and characterized by CD, NMR, and ANS binding. The goal is to determine the segments of primary structure that are essential for formation of the core fold of the native conformation. We have synthesized two analogs in which half-cystines are replaced by the isostere α-amino-*n*-butyric acid (Abu). In (Abu^{5,14,30,38,51,55})-BPTI, all six Cys residues are replaced. In (Abu^{5,30,51,55},Cys^{14,38})-BPTI the 14-38 disulfide bond is intact. This bridge is located in the loops, the most flexible region of the protein. The analog with no disulfide bridges behaves as a random coil peptide by all the techniques used. The species with the 14-38 disulfide has a stable and partially native structure at low temperature and pH >4.5, which unfolds cooperatively upon heating (T$_m$~19°C). Partially folded (Abu^{5,30,51,55},Cys^{14,38})-BPTI also unfolds when the pH is lowered to 2.5 at low temperature. Below pH 2, it refolds to form an apparent A state.

Tu-Pos234

STRUCTURE BASED PREDICTION OF PROTEIN FOLDING INTERMEDIATES.

((Dong Xie and Ernesto Freire)) Department of Biology and Biophysics and the Biocalorimetry Center, The Johns Hopkins University, Baltimore, MD 21218

Recently, the energetics of the compact denatured or molten globule state of several proteins have been measured with high precision. Two thermodynamic characteristics appear to be common to these partly folded intermediates: 1) A lower heat capacity than the unfolded state; and, 2) a higher enthalpy than the unfolded state at low temperatures. We have used the structural parametrization of the energetics developed previously in this laboratory[1] in combination with the CORE algorithm[2], in order to identify a subset of protein states that satisfy the energetic criteria of the compact denatured state for staph. nuclease, IIIGlc, barnase, interleukin-1β and α-lactalbumin. Surprisingly, the resulting subsets are rather small and define well ordered sequences in which cooperative units progressively fold or unfold. For all proteins studied, the most stable and unstable regions defined by the computer search agree well with the structural data available for the molten globule states of these proteins. Since, at low temperatures, the compact denatured state is enthalpically unfavorable relative to the unfolded state, its stabilization must be of entropic origin. The main entropic contributions to the molten globule are due to the hydrophobic effect, configurational entropy of the unfolded regions, side chain entropy of the complementary regions and electrostatic effects. (Supported by NIH grants RR-04328, GM-37911, and NS-24520)

REFERENCES:
1. Murphy, K. P., Bhakuni, V., Xie, D. & Freire, E. (1992) *J. Mol. Biol.* 227, 293-306.
2. Freire, E., Haynie, D. T. & Xie, D. (1993) *Proteins: Strut. Funct. Genetics* 17, 111-123.

Tu-Pos235

INTERMEDIATE STATES IN THE UNFOLDING OF DODECAMERIC GLUTAMINE SYNTHETASE FROM E. COLI.
((M. Zolkiewski, N. J. Nosworthy and A. Ginsburg)) NHLBI, NIH, Bethesda, MD 20892.

Glutamine synthetase (GS) (M$_r$ ~ 622000) is composed of 12 identical subunits which are arranged in two superimposed hexagonal rings with active sites at subunit interfaces. Chemically and thermally induced unfolding of GS was studied by calorimetric, hydrodynamic and spectroscopic methods. Experiments were performed at 37 °C (or in the range of 15-110 °C for thermally induced reactions) in a buffer of 20 mM Hepes/KOH, 100 mM KCl and 0.1 mM MnCl$_2$, pH 7. In 0 to 1.5 M urea Mn•GS retains its dodecameric structure and full catalytic activity. However, the GS dodecamer dissociates in >2 M guanidine•HCl or urea, as shown by decreases in 90° light scattering. Dissociation is paralleled by the exposure of aromatic residues, enzyme inactivation and the loss of secondary structure. Differential scanning calorimetry of Mn•GS in 1.5 M urea (which inhibits the high-temperature protein precipitation) shows three endothermic transitions. Partial exposure of Trp and Tyr residues, but no change in secondary structure, accompanies the reversible formation of the first partially unfolded state of Mn•GS (t$_m$ ~45 °C). CD changes occur during the second step to another intermediate (t$_m$ ~ 57 °C). The third DSC transition has t$_m$ ~ 77 °C. The total enthalpy for DSC transitions is ~4 cal/g whereas ΔH for unfolding measured by the transfer of Mn•GS into urea or guanidine•HCl is ~ 10±3 cal/g.

Tu-Pos236

SUBDOMAIN FOLDING IN THE COMPACT EARLY FOLDING INTERMEDIATES DIRECT THE FOLDING PATHWAY IN BPTI.
((V. Itah and E. Haas)) Department of Life Sciences, Bar-Ilan University, Ramat-Gan, 52900, Israel.

The structure of the partially folded states of a single domain globular protein, Bovine pancreatic trypsin inhibitor (BPTI) was studied by means of time resolved dynamic non radiative excitation energy transfer (ET). Intramolecular segmental end-to-end distance (EED) distributions in site specifically labeled BPTI derivatives were measured in order to determine the role of non-local and local interactions (NLIs and LIs) and the compactization step in the folding mechanism. Under partially folding conditions of low GUHCl concentration reduced BPTI is in a compact state, but this state is not a condensed statistical coil conformation. It is folded in a loosely stabilized conformation, without a cooperative temperature dependent conformational transition, in the temperatures range of 2 to 60°C. Except for the N terminal segment, the dominant fraction of the conformers is the compact subpopulation with native like chain topology. At higher temperatures (up to 60°C) the native like subpopulation is stabilized, as can be seen by reduced widths of the EEDs. The changes in the segmental EEDs in response to changes of the solution conditions are specific and not global. This shows that the topology of the chain is directed by specific NLIs between chain segments. We conclude that specifically coded NLIs form segmental loops early in the folding pathway and the hydrophobic condensation is specifically directed.

Tu-Pos237

THERMODYNAMICS OF THE THERMAL UNFOLDING OF AN EXTRACELLULAR PHOSPHOLIPASE A$_2$
((A. Fridie, G.S. Rule and R.L. Biltonen)) Departments of Biochemistry and Pharmacology, University of Virginia, Charlottesville, VA 22908

The thermal unfolding behavior of a 14 kD phospholipase A$_2$ isolated from the venom of A. piscivorus piscivorus (APP D49) has been characterized using UV difference spectroscopy, circular dichroism, nuclear magnetic resonance and differential scanning calorimetry. In aqueous solution, the protein was found to be maximally stable at pH 5.0 where it reversibly unfolds at a Tm of 79 c. and with an associated enthalpy change of 76 kcal/mole. However, under these conditions the thermal transition was not "two-state" since the ratio of the calorimetric enthalpy and the van't Hoff enthalpy (ΔHcal/ΔHvh) was significantly greater than 1. The protein unfolds in a 2-state manner (ΔHcal/ΔHvh equal to 1) only in the pH range of 6-7. In the pH range of 5-3.5, the apparent cooperativity of the transition decreases (Hcal/Hvh > 1.0) suggesting the protein may consist of more than one thermodynamic domain. In the presence of 1:1 dioleoylphosphatidylcholine/dioleoylphosphatidylglycerol large unilamellar vesicles, the Tm is shifted to higher temperature and the apparent cooperativity of unfolding (Hcal/Hvh = .67) increases, consistent with the formation of a dimer or higher order protein aggregate on the lipid surface. This putative aggregate could be the result of direct protein-protein interaction or could be related to an indirect interaction mediated by the lipid. (Supported by Grants from the NSF and NIH).

Tu-Pos238

THERMODYNAMICS OF INTERLEUKIN-1β UNFOLDING.
((G.I. Makhatadze[1], A.M. Gronenborn[2] and P.L. Privalov[1])) [1]Department of Biology, The Johns Hopkins University, Baltimore, MD 21218; [2]NIDDK, NIH, Bethesda, MD 20892.

It has been suggested that the energetics of stabilization of proteins consisting entirely from β-sheet such as interleukin-1β should differ from those of α-helical proteins due to the specific geometry of hydrogen bonds. The thermodynamics of unfolding of interleukin-1β have been studied using differential scanning microcalorimetry. The thermodynamic experiments were accompanied by measurements of protein conformation using CD spectroscopy. Precise measurements of the heat capacities of the native and unfolded states of interleukin-1β show that the heat capacity change upon unfolding strongly depends on temperature; its value is maximal at about 50°C and diminishes as the temperature is increased. The temperature dependencies of the enthalpy and entropy changes upon interleukin-1β unfolding were found to be similar to those normally observed for other small globular proteins. Thermodynamic parameters of interleukin-1β unfolding were correlated with the structural features of the protein. The enthalpy of hydrogen bonding in interleukin-1β was calculated and compared to that obtained for other proteins. It appears that the energy of hydrogen bonding correlates with the average length of the hydrogen bond in a given protein structure.

Tu-Pos239

CORRELATION OF GLOBAL AND LOCAL STABILITIES OF OVOMUCOID THIRD DOMAIN. ((Liskin Swint and Andrew D. Robertson.)) Department of Biochemistry, University of Iowa, Iowa City, Iowa, 52242.

We have used thermal and chemical denaturation to characterize the thermodynamics of unfolding for turkey ovomucoid third domain (OMTKY3). Thermal denaturation was monitored spectroscopically at a number of wavelengths and data were subjected to van't Hoff analysis; at pH 2.0, the midpoint of denaturation occurs at 58.6 ± 0.4°C and the enthalpy at this temperature is 40.8 ± 0.3 kcal/mol. The change in heat capacity upon unfolding (ΔC$_p$) determined by van't Hoff analysis was 590 ± 120 cal/(mol•K), while the same data analyzed simultaneously with an equation that contains the temperature dependence for the enthalpy of unfolding yielded a value of 640 ± 110 cal/(mol•K). Varied concentrations of chemical denaturant did not raise the apparent value of ΔC$_p$. We also performed a variation of the linear extrapolation method described by Pace and Laurents [Biochemistry 28, 2520 (1989)] in order to determine ΔC$_p$. First, OMTKY3 was thermally denatured in the presence of a variety of denaturant concentrations. Linear extrapolations were then made from isothermal slices through the transition region of the denaturation curves. When extrapolated free energies of unfolding (ΔG$_u$) were plotted versus temperature, the resulting curve appeared linear; therefore, ΔC$_p$ could not be determined. However, the data for ΔG$_u$ versus denaturant concentration are linear over an extraordinarily wide range of concentrations. Moreover, extrapolated values of ΔG$_u$ in urea are identical to values measured directly. Apparent stabilites at sites within OMTKY3 have been determined by hydrogen exchange monitored with proton nuclear magnetic resonance spectroscopy. These data have been correlated with the global stability.

Tu-Pos240

SPECIFIC ION AND IONIC STRENGTH EFFECTS ON THE THERMAL UNFOLDING OF THE GCN4 LEUCINE ZIPPER PEPTIDE.
((Kelly Thompson Kenar and Ernesto Freire)) Department of Biology and The Biocalorimetry Center, The Johns Hopkins University, Baltimore, MD 21218.

The thermodynamic stability of a synthetic peptide corresponding to the leucine zipper region of GCN4 has been measured as a function of salt concentration using circular dichroism spectroscopy and high sensitivity differential scanning calorimetry. In the absence of additional salts, increasing buffer concentration from 5 to 500 mM Tris decreased the melting temperature by 11°C consistent with the ionic strength effect calculated by the Tanford-Kirkwood algorithm using the crystal structure of O'Shea et al. (1991). At constant 10 mM buffer, increasing the ionic strength from 0 to 500 mM KCl and KBr, however, decreased the melting temperature by only 4.5°C and 9°C respectively, while KF actually increased the Tm 1.5°C within the same concentration range. These results indicate the existence of specific ion effects in addition to the general ionic strength effect approximated by the Tris molecule. Calculation of the potential energy surface of the GCN4 leucine zipper by the finite differences method reveals several regions of uncompensated charge that provide potential ion binding sites. (Supported by Grants from NIH RR-04328, NS-24520 and GA-37911)

O'Shea, E. K., Klemm, J. D., Kim, P. S., & Alber, T. (1991) Science 254, 539.

Tu-Pos241

UREA-INDUCED UNFOLDING OF S-CD4 MEASURED BY UV DIFFERENCE SPECTROSCOPY. ((S. W. Tendian and C. G. Brouillette)) Southern Research Institute, Birmingham, AL 35205. ((D. G. Myszka and I. M. Chaiken)) SmithKline Beecham Pharmaceuticals, King of Prussia, PA 19406.

CD4 is a transmembrane glycoprotein expressed on T-lymphocytes. It is a receptor for class II major histocompatibility complex (MHC) molecules and for the HIV envelope glycoprotein gp120. Denaturant-induced unfolding of the extracellular portion of CD4 (s-CD4) and of isolated CD4 domains was measured using ultraviolet difference spectroscopy which monitors changes in the solvent exposure of the intrinsic chromophores. s-CD4 is a multidomain protein with four domains designated D1 through D4. s-CD4 unfolding data fit well to a model with one thermodynamically stable folding intermediate which suggests that there are two folding regions. This three-state fit for s-CD4 was significantly better than the best two-state fit. Unfolding of isolated D1D2 and D3D4 both fit a two-state model. The unfolding of these two isolated domains, which were hypothesized to be the two folding units of s-CD4, could not be summed to yield the unfolding profile of s-CD4 without the addition of an interdomain interaction energy term. Unfolding of two D1D2 mutants, F43V, a binding site mutant, and A55F, mutation of a buried residue, were also measured to determine how these mutations that significantly reduced binding to gp120[1] affected stability. Both mutants were more stable than native D1D2, but they differed as to whether the urea dependence of the unfolding free energy (dΔG/dC$_{urea}$) was increased or decreased by the mutation.

[1]J. Arthos, K. C. Deen, M. A. Chaiken, J. A. Fornwald, G. Sathe, Q. J. Sattentau, P. R. Clapham, R. A. Weiss, J. S. McDougal, C. Pietropaolo, R. Axel, A. Truneh, P.J. Maddon, and R. W. Sweet. (1989) Cell 57, 469-481.

Tu-Pos242

LOCAL PERTURBATION OF RECOMBINANT HIV-1 REVERSE TRANSCRIPTASE BY UREA OCCURS PRIOR TO GLOBAL DENATURATION. ((L.L .Wright, J.E. Wilson, J.L. Martin, S.E. Haire, P.H. Ray, G.R. Painter)) Division of Virology, Burroughs Wellcome Co., Research Triangle Park, NC 27709.

The equilibrium unfolding transition induced by urea of recombinant, heterodimeric HIV-1 reverse transcriptase was monitored by spectroscopic methods (fluorescence and circular dicroism) and changes in enzymatic activity. This study was undertaken to characterize the structural stability of wild-type enzyme for comparison to future studies on AZT-resistant mutants. The equilibrium denaturation profiles from both spectroscopic methods were coincident. The transition is well described by a two-state mechanism in which only native and fully denatured protein are present in the transition region. The loss of activity induced by increasing concentrations of urea is also well described by a two-state mechanism, but the transition, involving active and fully inactivated forms of the enzyme, is not coincident with the spectroscopic profile. This result suggests that local perturbation of the active site occurs prior to global denaturation, as evidenced by the midpoint of the transitions occurring at 2.0 M and 4.1 M urea respectively. A slight disturbance to the spatial geometry of the functional groups at the active site must destroy the enzyme's activity before any gross global conformational change can be detected. The active site is probably located in a flexible or mobile region of the enzyme. Additionally the spectroscopic transition is 100% reversible; the renaturation profile of the enzyme coincides with the denaturation profile. However, the return of catalytic activity by dilution from 8 M urea is not coincident with the loss of activity of native enzyme, only 9% of the native enzyme activity is recovered after dilution. The role of enzyme solubility and the kinetic competition of refolding vs. aggregation in the renaturation process monitored by changes in catalytic activity will be discussed.

Tu-Pos243

CHEMICAL DENATURATION OF BOVINE PANCREATIC RIBONUCLEASE A: CONTRIBUTIONS OF HYDROGEN BONDING AND HYDROPHOBIC INTERACTIONS TO THE DENATURANT STRENGTH.

(R. Ghuman, V. Henriquez, K. Vo, J. Vargas, H. Murillo, S. Subbiah, A. Mahesh, and R. G. Biringer) San Jose State University, San Jose, CA 95192-0101

The importance of the various factors that contribute to the stability of proteins has been the subject of controversy for many years. It is apparent from the vast amount of experimental work that both hydrogen bonding and the hydrophobic effect are the major contributers, but the relative importance of each has yet to be determined. We have examined the denaturation of bovine pancreatic ribonuclease A by guanidinium ion, urea, substituted ureas, amides, and monohydridic alcohols with fluorescence spectroscopy and by the ability to bind 1-anilinonapthalene-8-sulfonate at 17 °C and a protonic activity of 4.0. Our results indicate that an increase in the number of hydrogens available for hydrogen bonding and an increase in hydrophobicity serve to increase the strength of the denaturant. In addition, we have observed that the denaturation transition proceeds through one or more compact intermediate states and that the relative population and stability of such states is denaturant dependent.

Tu-Pos244

THERMODYNAMICS OF BARNASE UNFOLDING

((Yu.V. Griko, G.I. Makhatadze and P.L. Privalov)) Department of Biology, The Johns Hopkins University, Baltimore, MD 21218 (Spon. J.S. Davis)

The thermodynamics of barnase denaturation have been studied calorimetrically over a broad range of temperature and pH values. It is shown that in acidic solutions the heat denaturation of barnase is well approximated by a two-state transition. The partial specific heat capacity of denatured barnase is very close to that expected for the completely unfolded protein. The specific denaturation enthalpy value extrapolated to 130 °C is also close to the value expected for the full unfolding. Therefore, the calorimetrically determined thermodynamic characteristics of barnase denaturation can be considered to be characteristic of its native structure and can be correlated with structural features - the number of hydrogen bonds, extent of van der Waals contacts, and the surface areas of polar and non-polar groups. Using this information and the thermodynamic information on transfer of protein groups into water, the contributions of various factors to the stabilization of the native structure of barnase have been estimated. The main contributors to the stabilization of the native state of barnase appear to be intramolecular hydrogen bonds. The contribution of van der Waals interactions between the packed non-polar groups and hydration effects of these groups is not as large, but the combination of these two factors, known as hydrophobic interactions, contribute on the same order as hydrogen bonding.

Tu-Pos245

THERMAL STABILITY OF EGLIN C AND INTERACTION WITH GUANIDINE HYDROCHLORIDE

((S.J. Bae and J. M. Sturtevant)) Department of Chemistry, Yale University, New Haven, C.T. 06511

Eglin C, a protein containing 70 amino residues, is one of the most potent inhibitors of the human neutral granulocytic proteinase and is therefore of special medical interest. Eglin C has no disulfide bonds, but is nevertheless quite stable to thermal denaturation. The thermodynamics of the reversible thermal unfolding of Eglin C has been studied over a wide pH range by differential scanning calorimetry. At pH 7.0 the midpoint of the reversible unfolding is at 86.0°C with a heat absorption of 8.4 cal g-1; at pH 1.3 these figures are 42.1°C and 4.43 cal g-1, and 86.6°C and 8.9 cal g-1 at pH 10.5. The effect of guanidine hydrochloride on the unfolding of Eglin C has also been investigated.

Tu-Pos246

THE CONTRIBUTION OF THE 6-120 S-S BOND TO STRUCTURAL STABILITY OF THE NATIVE AND DENATURED STATES OF α-LACTALBUMIN. ((T.M. Hendrix, Yu. V.Griko, P.L. Privalov)) Department of Biology, The Johns Hopkins University, Baltimore, MD 21218. (Spon. by M.G. Larrabee)

The effects of reduction and modification of the 6-120 crosslink on stability and molecular organization of α-lactalbumin (LA) has been studied by CD spectroscopy and scanning microcalorimetry. It is shown that the disulfide bond reduction leads to a decrease in thermal stability of LA by about 10 °C but does not essentially change its cooperative structure. The cleavage of the disulfide crosslink does not effect the hydrophobic core of the molecule, which is similar to that in native LA according to the thermodynamic criterion of heat capacity. Upon temperature induced denaturation, the S-S reduced LA undergoes more complete unfolding than native LA under the same conditions. This could be due to an increase of the chain entropy in the unfolded state. Analysis of the calorimetricaly measured and van't Hoff enthalpies of the heat denaturation show that the disulfide reduction does not induce any stable intermediates states during the denaturation. Like the native LA, the denaturation proceeds as a two-state transition. However, the calorimetric enthalpy of its denaturation is slightly lower than for native LA at the same temperature of denaturation. Entropy and enthalpy contribution of the disulfide bond in stabilization of the protein structure are discussed.

Tu-Pos247

DESTABILIZATION OF THE Ca^{2+}-ATPase OF SARCOPLASMIC RETICULUM BY DIAMIDE AND ITS RELATIONSHIP TO HEAT SHOCK PROTEIN INDUCTION. (G. Senisterra, S. Huntley, and J.R. Lepock) Department of Physics, University of Waterloo, Waterloo, Ontario N2L 3G1 Canada

The signal responsible for the activation of the heat shock factor (HSF) is unknown. One of the prevailing theories is that denatured proteins are responsible for eliciting the synthesis of heat shock proteins (HSP's). Several chemical agents in addition to heat shock induce HSP's. If the protein denaturation hypothesis is correct, then these compounds must also denature proteins. Diamide is a sulfhydryl group reagent that causes protein oxidation with the formation of disulfide bonds and promotes the synthesis of HSP's in cells. In this studies we use the Ca^{2+}-ATPase of sarcoplasmic reticulum as a model protein. The denaturation of this protein by diamide is examined by differential scanning calorimetry (DSC). A strong decrease in the denaturation transition is seen following diamide treatment indicating protein unfolding. Diamide also inactivates Ca^{2+} uptake and ATPase activity of the enzyme. By SDS PAGE and free sulfhydryl group titration we found that diamide induces intermolecular and probably intramolecular disulfide cross links. These unnatural disulfides appear to induce conformational strain which drives the protein to a denatured or unfolded state.

Tu-Pos248

ACID-INDUCED UNFOLDING OF BRAIN-DERIVED NEUROTROPHIC FACTOR: FORMATION OF A MONOMERIC "A STATE". (L.O. Narhi, R. Rosenfeld, J. Wen, T. Arakawa, S. Prestrelski and J.S. Philo) Amgen Inc., Amgen Center, Thousand Oaks, CA 91320

Recombinant human brain-derived neurotrophic factor in acid undergoes a slow loss of tertiary structure as monitored by near UV circular dichroism and fluorescence, and appears to retain some secondary structure, as monitored by far UV circular dichroism and Fourier transform infrared spectroscopy. The loss of tertiary structure parallels a decrease in the weight average molecular weight from dimer to monomer using light scattering. Size exclusion chromatography (at neutral pH) demonstrated that the amount of tertiary structure remaining paralleled the dimer concentration, and that the monomer was long-lived. The acid-denatured form is a compact molecule, and the denaturation is strongly concentration-dependent.

This suggests that the mechanism N₂⇔2N⇔2D describes the denaturation, where dissociation to a native monomer is the rate-limiting step, and that the acid-denatured form is a monomeric compact intermediate (A state).

Tu-Pos249

THE UNFOLDING OF trp APOREPRESSOR AS A FUNCTION OF pH: EVIDENCE FOR AN UNFOLDING INTERMEDIATE. ((K.J. Helton, G.D. Ramsay, and Maurice R. Eftink)) Department of Chemistry, University of Mississippi, University, MS 38677. (Spon. by C.A. Ghiron)

The urea-induced unfolding of trp aporepressor from E. coli has been studied as a function of pH from 2.5 to 12.0 at 25 °C. At pH 7 and above, the unfolding transition, as monitored by changes in the fluorescence intensity at 360 nm, shows a single transition. At low pH, the transition again appears to be a single transition. In the range of 3.5-5.0, the transition is bi-phasic, indicating the existence of a folding intermediate. The transitions have also been studied using CD and size exclusion chromatography. Data were fitted by a model in which the dimeric protein first unfolds to structured monomers, followed by the unfolding of the monomers. With this "native monomers" model, the $\Delta G°$ for the dimer $\leftrightarrow$ monomer dissociation becomes more positive as pH is decreased; the $\Delta G°$ for the unfolding of the monomers is essentially independent of pH. From a study of the protein concentration dependence of unfolding at pH 5, the "native monomers" model is found to be more consistent with the data than an alternate model in which the dimer first undergoes a transition to a partially unfolded dimeric state. This research was supported by NSF DMB 91-06377.

Tu-Pos250

DENATURATION OF THE COLICIN E1 CHANNEL PEPTIDE: EXAMINATION OF THE UNFOLDING OF LOCAL SEGMENTS USING GENETICALLY SUBSTITUTED TRYPTOPHAN RESIDUES AND FLUORESCENCE SPECTROSCOPY. ((B.A. Steer and A.R. Merrill)), Guelph-Waterloo Centre for Graduate Work in Chemistry, Dept. of Chem. & Biochem., Univ. of Guelph, Guelph, ON, Canada, N1G 2W1. (Spon by R. Hallet)

Colicin E1 is a bactericidal and toxin-like protein secreted by strains of E. coli which carry a ColE1 plasmid. It forms a dissipative and lethal ion channel in the cytoplasmic membrane of sensitive E. coli and other coliform bacteria. Colicin E1 is divided into three functional domains including a translocation, a receptor binding and a channel-forming domain. The colicin E1 channel peptide has a roughly spherical, highly α-helical, compact solution structure. In order to examine some of the structural characteristics of the peptide, eleven single tryptophan mutants were constructed by site-directed mutagenesis and their guanidine hydrochloride-induced unfolding patterns were examined using fluorescence spectroscopy. Integrated fluorescence intensity and average fluorescence emission energy of the single tryptophan residues were used to probe site-specific unfolding events. The unfolding patterns reported by the various tryptophan residues were diverse, indicating the complexity of the unfolding process of the channel peptide. The estimation of the free energy change upon unfolding described the relative stabilities of various local segments within the peptide structure. An examination of the unfolding properties of the soluble channel peptide will aid in the understanding of the secondary and tertiary structural interactions within the channel peptide and thus the mechanism of colicin E1 activation. [Supported by the Medical Research Council of Canada, (A.R.M.)]

Tu-Pos251

MUTAGENIC ANALYSIS OF THE RESIDUAL STRUCTURE IN THE α SUBUNIT OF TRYPTOPHAN SYNTHASE FROM E. coli. ((Gloria Saab-Rincón and C. Robert Matthews)) Department of Chemistry, The Center for Biomolecular Structure and Function, and The Biotechnology Institute, The Pennsylvania State University, University Park, PA 16802.

Previous 1D NMR studies on the WT α subunit of tryptophan synthase [Saab-Rincón, G., Froebe, C. and Matthews, C.R., Biochemistry (in press)] demonstrated the presence of residual structure near His 92. This intermediate unfolds cooperatively between 5.0 and 7.5 M urea. Thermodynamic analysis of this transition indicated that the species involved is very stable. The sequence downstream from His 92 contains a stretch of hydrophobic residues, including a Tyr at position 102, which could be responsible for the residual structure found at high denaturant concentrations. In the present work, mutagenesis was used to determine the role of these hydrophobic amino acids in stabilizing the residual structure. The P93S, I95A, L100A and Y102A mutants were constructed and their unfolding reaction between 4 and 9 M urea was monitored by examining the peak areas of the Cε protons of the four histidine residues present in the protein with 1D NMR spectroscopy. None of these mutations was able to completely perturb the residual structure around His 92; however, mutations at Leu 100, Pro 93 and Tyr 102 destabilized it, decreasing the midpoint of the transition by about 1 M urea unit. The fact that this intermediate was still present in individual mutations is consistent with the high cooperativity found for its unfolding and suggests that a number of residues must be involved. This work was supported by NIH grant GM 23303 to CRM.

Tu-Pos252

STATISTICAL THERMODYNAMIC ANALYSIS OF THE TEMPERATURE UNFOLDING OF THE MOLTEN GLOBULE STATE (Yu.V. Griko, P.L. Privalov and E. Freire) Department of Biology and Biocalorimetry Center, The Johns Hopkins University, Baltimore, MD 21218

The temperature induced unfolding of the molten globule state of α-lactalbumin has been studied by differential scanning calorimetry and CD spectroscopy. The results of these experiments have been analyzed using a statistical thermodynamic formalism. This analysis indicates that the long range or global cooperativity of the protein is lost after heat denaturation of the native state, causing the remaining elements of residual structure to behave in a more or less independent fashion. At pH values close to neutral, heat denaturation occurs at high temperature and yields a totally unfolded polypeptide. At lower pH values denaturation occurs at lower temperatures and does not result in complete unfolding but in a progressively higher population of molten globule intermediates. At pH 4.2 this population is 50%, at pH 3.5 is close to 80% and at pH 3.0 it reaches about 100% of the protein molecules. Upon heating, the unfolded state progressively becomes the predominant species. The best model to account for the observed behavior is one in which the denatured state is represented as a distribution of substates whith varying degree of residual structure. At lower temperatures the distribution is centered around rather compact substrates with significant residual structure. At higher temperatures the distribution shifts towards states with less residual structure and eventually to the completely unfolded state. This approach has permitted a close examination of the character of the unfolding transition of the molten globule state. Supported by grants from the NIH RR04328, GM48036 and the NSF MCB 9118687.

Tu-Pos253

DIFFERENTIAL SCANNING CALORIMETRY OF THE IRREVERSIBLE DENATURATION OF ENDOTHIAPEPSIN.

((Javier Gomez and Ernesto Freire)) Department of Biology and the Biocalorimetry Center, The Johns Hopkins University, Baltimore, MD, 21218.

The thermal unfolding of endothiapepsin, an aspartic proteinase from the fungi endothia parasitica, has been studied by means of high-sensitivity differential scanning calorimetry and circular dichroism (CD) spectroscopy. In the pH range 2.5 - 7.0, the thermal denaturation of the enzyme was completely irreversible as judged by the absence of any endotherm upon rescanning previously scanned samples. Moreover, no difference was observed in their far-UV CD spectra. The shape of the thermograms as well as their scan rate dependence indicate that the process is kinetically controlled. In order to account for the effect of irreversibility on our calorimetric data, a multistate sequential mechanism followed by a final irreversible step was assumed (Freire et al. Annu. Rev. Biophys. Biophys. Chem. 19, 159-188, 1990.):

$$N \rightleftarrows I_1 \rightleftarrows I_2 \rightleftarrows \cdots \rightleftarrows I_n \xrightarrow{k} D$$
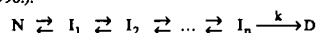
According to our results, the unfolding of the enzyme involves two consecutive transitions within a narrow temperature range. The maximum stability was found at pH 4.0, with melting temperatures of 56.2 and 64.2 and overall enthalpy and heat capacity values of 84.1 and 3.2 kcal/mol respectively. Both the enthalpy and the heat capacity were shown to depend on the concentration of the protein, indicating that aggregation of the unfolded protein is, at least in part, responsible for the irreversibility of the process. Since the crystallographic structure is known, structural thermodynamic calculations have been performed to evaluate the nature of the irreversible state.

(Supported by grants RR 04328, GM 37911 and NS 24520).

Tu-Pos254

DIFFERENTIAL SCANNING CALORIMETRIC DETECTION OF PROTEIN DOMAIN INTERACTIONS & ALTERATIONS ASSOCIATED WITH MEMBRANE BINDING.((B.R. Lentz, C.M. Zhou, J.R. Wu)) Dept. Biochemistry & Biophysics CB#7260 Univ. of North Carolina at Chapel Hill, NC 27599

Our earlier study (Lentz, Wu, Sorrentino, & Carleton Biochem. J. 60, 70, 1991) examined the denaturation profile of bovine prothrombin in the presence of Na_2EDTA, 5mM $CaCl_2$ plus membranes containing 1-palmitoyl-2-oleoyl-3sn-phosphatidylcholine (POPC) and bovine brain phosphatidylserine (PS). These showed an enthalpy loss in the main endotherm (~59°C) and a comparable enthalpy gain as well as an upward shift in peak temperature of the minor endotherm (~57-58°C) of the denaturation profile. We report here extensive studies of the denaturation of prothrombin fragments in the presence and absence of POPC/PS vesicles to show that the fragment 2 domain (F2) interacts with and stabilizes the catalytic domain (Pre2) and also interacts directly with the membrane. In addition, the Pre2 domain interacts with the membrane-binding domain (F1). The results demonstrate that binding to PS/POPC membranes alters the inter-domain interactions within the prothrombin molecules in a way that accounts for the altered denaturation of membrane-bound prothrombin. These observations lead to the hypothesis that membrane-specific alterations in inter-domain interactions and in domain stability may account for the observation that the C-terminal portion of prothrombin is more effectively and specifically proteolyzed to thrombin on PS-containing platelet membranes as compared to other acidic membrane surfaces (Pei, Powers, & Lentz J.B.C. 268, 3226, 1993).

Tu-Pos255

MOLECULAR MODELING STUDIES OF CAFFEINE COMPLEXES WITH DNA-INTERCALATING DRUGS. ((R. W. Larsen[1], R. K. Hetzler[2], P. T. Muraoka[1], and V. G. Andrada[1]))[1] Dept. of Chemistry and [2] Dept. of Health, Phys. Ed. and Rec., Univ. of Hawaii at Manoa, Honolulu HI, 96822.

Caffeine effects a wide range of cellular activity depending upon concentration. At low concentrations it is non-mutagenic while at higher concentrations the drug inhibits enzymatic aspects of DNA-synthesis, causes increased chromatin condensation, and increases G1 phase. In addition, caffeine has been shown to enhance cell damaging effects of cisplatin, mitomycin C, cyclophosphamide, ethidium bromide, and anthroquinone type intercalators. Interestingly, recent studies have shown that caffeine can inhibit cytoxic and/or cytostatic effects of ethidium bromide and anthroquinone-type intercalators. It has been suggested that this inhibitory effect is due to non-covalent complexation between caffeine and the intercalating drug. In order to better understand molecular interactions between caffeine and DNA intercalators we have examined the energetics of caffeine:DNA-intercalator complexes using molecular modeling techniques. Our data is consistent with a mechanism through which van der Waals interactions play a dominant role in complex formation.

Tu-Pos256

MOLECULAR RECOGNITION OF DNA BY DAUNORUBICIN. *J. B. Chaires*, Dept. of Biochemistry, University of Mississippi Medical Center, Jackson, MS 39216.

Thermodynamic studies of the daunorubicin − DNA interaction in solution have converged with structural and molecular modeling studies to provide a detailed and coherent description of the molecular recognition of certain DNA sequences by this clinically important anthracycline antibiotic. The daunorubicin − DNA interaction is now, arguably, the best understood of the intercalation reactions, and as such represents an important paradigm for efforts aimed at the rational design of new compounds targeted toward DNA. Thermodynamic results obtained for the interaction of daunorubicin and a carefully selected set of anthracycline antibiotic derivatives with a variety of DNA sequences will be presented that help to illuminate the molecular determinants of the binding of these antibiotics to preferred DNA sites. These results begin to make possible the dissection of the DNA binding free energy of these compounds into its component parts to reveal the energetic contribution of specific chemical groups on the antibiotics to DNA binding. *Supported by NCI Grant CA35635.*

Tu-Pos257

USE OF ^{15}N NMR TO PROBE BINDING OF NETROPSIN AND DISTAMYCIN TO {d[CGCGAATTCGCG]}$_2$
((Youngsook Rhee, Chuan Wang, Barbara L. Gaffney, and Roger A. Jones)) Department of Chemistry, Rutgers University , Piscataway, NJ 08855

The binding of netropsin and distamycin to the duplex {d[CGCGAATTCGCG]}$_2$, in which adenine residues A5 or A6 were [3-^{15}N]-labeled, was monitored by ^{15}N NMR to probe the sensitivity of these ^{15}N-labels to drug binding. The ^{15}N chemical shifts were obtained from a ^{1}H-^{15}N heteronuclear 2D experiment. The ^{15}N atoms in the complexes were assigned using, in addition, a ^{1}H-^{1}H 2D NOESY experiment. For both asymmetric drug complexes with the label at one of the central adenines, large downfield shifts (3-7 ppm) of the N3 resonances relative to the position in the free duplex indicate that water is excluded from the center of the binding site. Furthermore, for both complexes with the label at one of the outer adenines, ~2 ppm upfield shifts in the resonances indicate hydrogen bonding to the N3 at the common propylamidinium termini of the drugs. In the distamycin complex, there is a similar upfield shift for the resonance at the other outer adenine, indicative of a H-bond between the N3 atom and the formamide terminus of the drug. These results demonstrate that the ^{15}N-labels are useful monitors of both the H-bonding and hydrophobic interactions that play critical roles in the binding of drugs and other ligands to DNA.

Tu-Pos258

OLIGONUCLEOTIDE STUDIES OF SEQUENCE SPECIFIC BINDING OF CHROMOMYCIN A$_3$ TO DNA. ((Chengdi Liu and Fu-Ming Chen)) Department of Chemistry, Tennessee State University, Nashville, TN 37209-1561.

Decamers of the forms d(GTA-XGCY-TAC) and d(GTA-XCGY-TAC), with X, Y = A, G, C, or T, were employed to investigate the sequence specificities of chromomycin A$_3$ (CHR) at the tetranucleotide level. Equilibrium spectral titrations indicate that the binding preferences for CHR are in the order: -GGCC- > -CGCG- > -GCGC-, -CCGG- > -AGCT- > -ACGT- > -TGCA- > -TCGA-. Detergent induced drug dissociation studies reveal that CHR dissociates very slowly from both -GGCC- and -CGCG- sequences, with the former being measurably slower than the latter which in turn is at least an order of magnitude slower than the rest of the sequences. Thermal denaturation measurements indicate that the binding of CHR stabilizes the DNA duplex, with the -GGCC- and -CGCG- exhibiting the largest effects. Results of gel electrophoretic retardation experiments support our general findings on the relative binding order. Our experimental results support earlier NMR findings by other researchers implicating the preference of aureolic acid drugs at the 5'GC3' step and further reveal significant modulations due to the adjacent base pairs.

Tu-Pos259

NETROPSIN BINDING TO SPECIFIC DNA SEQUENCES: COUPLING OF ENERGY AND WATER RELEASE. ((Nina Sidorova and D.C. Rau)) OD, NIDDK, NIH, Bethesda, MD 20892 and Engelhardt Institute of Molecular Biology RAN, Moscow, Russia.

It is becoming apparent that hydration interactions combine strength and specificity in a way that suggests a dominating role in the recognition process of biologically important molecules in solution. Direct force measurements on condensed systems indicate a correlation between binding energy and water release should be observed in dilute solution. As a first step toward examining this correlation, we investigate the strength and osmotic sensitivity of netropsin binding to specific DNA sequences. Netropsin is pharmacology active drug that binds in the minor groove of DNA and shows strong preference for dA/dT rich sequences. Netropsin binding to specific DNA sequences can be probed by a restriction nuclease protection assay. Increasing protection with increasing netropsin concentration can be well described by a simple A+B⇔(AB) binding reaction. The binding constant of netropsin to an EcoRI site (GAATTC) is about 10 times higher than the binding constant to an NdeI site (CATATG). This difference in binding strength is also accompanied by a difference in osmotic sensitivity. Binding to the EcoRI site shows almost no net water uptake; while the weaker binding to the NdeI site shows a net uptake of about 40 waters.

Tu-Pos260

BINDING OF DAUNORUBICIN AND ANTHRACYCLINE ANTIBIOTIC DERIVATIVES TO NATURAL AND SYNTHETIC DNA.

Dongchul Suh, Department of Biochemistry, The University of Mississippi Medical Center, Jackson, MS 39216.

Equilibrium binding studies of the interaction of daunorubicin, 9-deoxy-doxorubicin and nogalamycin with calf thymus DNA and synthetic deoxypolynucleotides will be described. Fluorescence titration methods using a photon counting fluorometer were used to determine the binding constant K. Isothermal titration calorimetry was used to directly measure the binding enthalpy. The salt dependency of nogalamycin and 9-deoxy-doxorubicin binding to calf thymus DNA will be discussed. Supported by NCI Grant CA 35635 to Dr.J.B.Chaires.

Tu-Pos261

DNA-DRUG INTERACTIONS: AN INFRARED VIBRATIONAL CIRCULAR DICHROISM (VCD) STUDY ((Sheryl S. Birke, Barbara Kagalovsky, Marva Moses, and Max Diem)) Department of Chemistry, City University of New York, Hunter College, 695 Park Avenue, New York, NY 10021.

We report the first Vibrational Circular Dichroism (VCD) observation of the interaction of ethidium bromide (EB), with various DNA oligomers and polymers. The DNA models studied include the dinucleotides (5'd(CG)3' and 5'd(GC)3'), several tetranucleotides (5'd(CGCG)3', 5'd(GCGC)3', etc.) and poly(dG-dC) · poly(dG-dC). In the base carbonyl stretching region, the observed VCD spectra exhibit a decrease in the amplitude of the VCD spectra, and a small shift in their zero-crossing point upon intercalation of EB. These results can be reproduced computationally and indicate that intercalation induces a partial unwinding of the DNA helix accompanied by an increased stacking distance. Thus, VCD displays an enormous sensitivity toward structural changes generated by intercalation between DNA and a drug.

Supported, in part, by NIH grant GM 28619 (to MD)

Tu-Pos262

The Interactions of Metal-Bound Intercalators with DNA. M. Delgado., L. Turner, S. Valdes & S. A. Winkle, Department of Chemistry, Florida International University, Miami, FL 33199. W. R. Murphy, Jr., D. E. Huchital, E. J. Mantilla & R. D. Sheardy, Department of Chemistry, Seton Hall University, South Orange, NJ 07079.

The interactions of the anti-tumor drug ametantrone with first row transition metal cations were studied. In the absence of DNA, the association constants for formation of the metal cation-ametantrone complex increases generally from left to right. In the presence of salmon sperm DNA, the metal-ametantrone complex bound to the DNA with higher affinity than ametantrone alone but with less sequence specificity. The interaction of $[Ru(NH_3)_4]_2(dpb)^{4+}$ (where dpb = 2,3-bis(2-pyridyl)benzo[g]quinoxaline) with calf thymus DNA was also investigated. The results of UV/VIS titration studies indicate that this molecule binds with high affinity to DNA accompanied by intercalation of the benzo[g]quinoxaline moiety between the base pairs. Determination of the binding constants at different NaCl concentrations indicate that nearly 80% of the binding free energy is due to electrostatics. However, non-electrostatic interactions are also significant. Supported by NSF grant DMB-8996232 (to R.D.S.), NIH grant MBRS GM 08205-07 (to S.A.W.) and the ACS Project SEED (to L.T. & M.D.)

Tu-Pos263

WATER ACTIVITY EFFECTS ON ACTINOMYCIN-D BINDING TO DNA. ((J. Ruggiero, U. Covissi, and M.F. Colombo)) Dept. of Physics, UNESP, S.J. Rio Preto, SP, Brazil, 15054-000. (Spon. by R. Sanches).

The sensitivity of Act.-D binding with linear and supercoiled DNA to neutral solute concentration has been measured and can be used as a model for the effect of water content on specific interactions of other ligands with DNA. Act.-D binding constants were obtained from Scatchard plots of spectrophotometric titration data. The addition of neutral solutes changes the observed binding constant in a solute specific manner. For all solutes examined, however, plots of ln K vs ln aw (water activity) are linear. The neutral solutes measured can be arranged into 2 groups based on their effect on binding constant: sugars (sucrose, glucose, fructose, and sorbitol) whose effect is to increase Act-D binding, and alcohols (methanol, ethanol, and poly-ethylene glycols) and formamide that all decrease affinity. These results are confirmed by agarose gel electrophoresis with supercoiled pBR322 in the presence of solutes. The intercalative mode of binding is seen maintained. The similarity of effect with alcohols and with formamide indicates that dielectric constant is not an important factor. The observed effects seem due to differences in exclusion from (for sugars) or inclusion with (alcohols and formamide) the hydration layers of drug and DNA. Supported by CNPQ, PADCT, and FAPESP.

Tu-Pos264

CORRELATIONS OF THE DNA BINDING PROPERTIES OF ACRIDINE CARBOXAMIDE ANALOGS WITH TOPOISOMERASE II ACTIVITIES.
((James M. Crenshaw, A. Geoffrey Marx, and David E. Graves)) Department of Chemistry, University of Mississippi, University, MS 38677.

The influence of substituent modification at position 5 of the acridine ring on both DNA binding properties and topoisomerase II activities are probed. Absorbance spectroscopy methods are used determine the thermodynamic properties associated with the interaction of selected acridine carboxamide analogs with DNA. Influences of ionic strength on the DNA binding energies provide a means of dissecting total binding energies into electrostatic and intercalation components. In addition, substituent influence on the binding entropies and enthalpies are obtained. These data reveal substituent modification at the 5 position may be highly influential in directing the thermodynamic mechanisms through which these drugs interact with DNA. In an effort to correlate DNA binding properties with antitumor efficacy, we examined the effects of various 5-position substituents on eukaryotic topoisomerase II activities. Modification of position 5 of the acridine ring resulted in marked changes in topoisomerase II activities.

Tu-Pos265

SOLUTION STRUCTURE OF AN 8,9-DIHYDRO-9-(N7-GUANYL)-8-HYDROXY-AFLATOXIN B_1 ADDUCT OPPOSITE CpA IN THE COMPLEMENTARY STRAND OF AN OLIGODEOXY-NUCLEOTIDE DUPLEX AS DETERMINED BY ^{1}H NMR. ((D.S. Johnston and M.P. Stone)) Department of Chemistry, Center in Molecular Toxicology, Vanderbilt University, Nashville, TN 37235.

We constructed d(CCATC^{AFB}GATCC)·d(GGATCAGATGG), in which 8,9-dihydro-9-(N7-guanyl)-9-hydroxy-aflatoxin B_1 was positioned opposite cytosine, while the aflatoxin moiety was positioned opposite adenosine. ^{1}H NMR revealed the sequential pattern of NOEs characteristic of B-form DNA was interrupted in the modified strand between C5 and ^{AFB}G6. However, from NOESY spectra collected in H$_2$O buffer, intrastrand NOE connectivities were traced through the aflatoxin moiety, via the H6a proton of aflatoxin, and the H8 proton of the modified guanine. In the complementary strand, sequential NOE connectivities characteristic of B-like DNA were observed. Opposite the lesion however, NOE connectivities were missing between the A^{16} sugar protons and G^{15} H8. Numerous NOEs were observed between DNA protons and aflatoxin protons, the most instructive being the methylene protons on the cyclopentenone ring of AFB, A^{16} H1', and A^{16} H2. These NOEs were consistent with a model in which the aflatoxin is intercalated into the helix and A^{16} opposite the lesion is sandwiched between the G6:C^{15} base pair and the aflatoxin. The stable structure of this cationic aflatoxin adduct might explain some +1 frameshifts induced by aflatoxin B_1: aberrant templating during DNA replication could result in the addition of an A:T base pair into the DNA duplex. Supported by the NIH: CA-55678 (M.P.S.), ES-00267 (Toxicology Center), ES-07028 (Pre-doctoral training, D.S.J.), and RR-05805 (NMR).

Tu-Pos266

SOLUTION STRUCTURE OF STYRENE OXIDE ADDUCTS AT ADENINE N^6 IN AN OLIGONUCLEOTIDE CONTAINING THE RAS CODON 61 SEQUENCE ((B. Feng, L. Zhou, M. Passarelli, C.M. Harris, T.M. Harris, and M.P. Stone)) Department of Chemistry, Center in Molecular Toxicology, Vanderbilt University, Nashville, TN 37235.

Adduct formation in the ras proto-oncogene sequence at codon 61 is associated with point mutations which result in oncogene activation. We constructed d(CGGACAAGAAG):d(CTTCTTGTCCG), containing n-ras codon 61. Stereospecific α-styrene oxide adducts have been incorporated at the N^6 positions of A^6 and A^7 in this sequence. These adducts were synthesized using a non-biomimetic strategy whereby the enantiomeric phenylglycinols were reacted with matrix-linked oligomers containing 6-chloropurine deoxyriboside at either position A^6 or A^7 in the sequence. Subsequent deprotection and purification yielded both R and S stereoisomeric α adducts of styrene oxide at A^6 and A^7. The NMR spectra of the α-styrene oxide adducts at A^6 and A^7 have been assigned using a combination of NOESY and TOCSY experiments. Analysis of ^{1}H NMR data reveals that these styrene oxide adducts are located in the major groove of the DNA duplex, and that the solution conformation is dependent upon the stereochemistry of adduction. For the R stereoisomers, the styrene ring is oriented towards the 5' direction from the site of adduction. For the S stereoisomers, the styrene ring is oriented towards the 3' direction from the site of adduction. Structural refinement of these adducts is in progress. Supported by the NIH: ES05355 (M.P.S), ES05509 (T.M.H.), ES00267 (Toxicology Center), and RR05805 (NMR Spectrometer).

Tu-Pos267

SOLUTION STRUCTURE OF AN R-STYRENE OXIDE ADDUCT IN AN OLIGONUCLEOTIDE CONTAINING THE CODON 12 SEQUENCE OF THE N-RAS PROTOONCOGENE. ((I.S. Zegar, B. DeCorte, C.M. Harris, T. M. Harris, and M.P. Stone)) Department of Chemistry, Center in Molecular Toxicology, Vanderbilt University, Nashville, TN 37235

The solution structure of the adducted oligonucleotide, d(GGCTGXTGGTG)·d(CACCACCAGCC) [X=R-styrene oxide at guanine N2] was investigated using ^{1}H NMR spectroscopy. This sequence was derived from the n-ras proto-oncogene at the bases encoding for amino acid 12 of the n-ras protein (underlined). Modifications at the codon 12 site have been demonstrated to cause single base substitutions which lead to oncogene activation [reviewed by Barbacid, M. (1987) *Ann. Rev. Biochem.* **56**, 779-827]. The assignment of the proton resonances was carried out using NOESY and TOCSY experiments. Examination of the chemical shift changes relative to the unmodified oligonuclotide and the pattern of the NOE cross peaks observed between the styrene oxide protons and the DNA duplex indicates that the styrene moiety is situated in the minor grove with the styrene ring directed in the 3' direction from the site of adduction. Distance restraints were calculated from NOE experiments using MARDIGRAS, and were incorporated into molecular dynamics calculations, as effective potentials in the total energy equation. Full iterative matrix analysis was used to fit the refined structure to the experimental data. Future work will involve comparison of structural perturbations caused by other R- and S- isomers of the styrene oxide adducted to the fifth and sixth guanines of this oligonucleotide sequence. Supported by the NIH: ES05355 (M.P.S.), ES05509 (T.M.H.), ES00267 (Toxicology Center) and RR05805 (NMR Spectrometer).

Tu-Pos268

INTERACTION OF Co(NH$_3$)$_6^{3+}$ AND Co(en)$_3^{3+}$ WITH OLIGORIBONUCLEOTIDES STUDIED BY ^{59}Co - NMR AND CIRCULAR DICHROISM.
((Srinivas Jampani and William H.Braunlin)). Dept. of Chemistry,University of Nebraska-Lincoln. Lincoln, NE-68588.

Hexaammine cobalt(III) cations contain ammine ligands which resemble guanidinium and ammine groups on the side chains of arginine and lysine. We are studying the binding environments of Co(NH$_3$)$_6^{3+}$ in oligoribonucleotides of different sequences in an attempt to find sequence-dependent recognition of the complex cation. ^{59}Co - NMR experiments will reveal the rotational dynamics of Co(NH$_3$)$_6^{3+}$ bound to oligomeric RNA. For the G-C rich oligonucleotide r(GGCCGGCC) the tumbling motions of Co(NH$_3$)$_6^{3+}$ are greatly inhibited and the effective correlation time is comparable to the overall tumbling of the RNA oligomer. CD experiments reveal significant change in the conformation of theRNA oligonucleotide upon titration with Co(NH$_3$)$_6^{3+}$. To investigate the role of chirality we are also studying the binding environments of (+) and (-) enantiomers of Co(en)$_3^{3+}$. These studies would lead to a better insight into protein-RNA interactions.

Tu-Pos269

MULTIPLE QUANTUM NA-23 AND PROTON NMR STUDY OF AN OLIGOMERIC DNA G-QUARTET STRUCTURE ((Hong Deng, Richard K. Shoemaker, William H. Braunlin)), Department of Chemistry, University of Nebraska-Lincoln, Lincoln, NE 68588-0304

Previous studies have shown Na$^+$ can induce DNA quadruplex structure. Here we report ^{23}Na NMR and proton NMR investigations of the oligomeric DNA d(TTGGGGT) in NaCl solution. The formation of the DNA G-quartet structure is DNA concentration dependent. Under low salt condition, there is a single dominant G-quartet structure. The ^{23}Na NMR lineshape is non-Lorentzian and asymmetric as expected for a spin-3/2 nucleus outside extreme-narrowing ($\omega_0\tau_c$>1). Triple-quantum filtration and inversion-recovery ^{23}Na NMR were used to characterize the natural bi-exponential decay. The theoretical NMR lineshapes in different motional conditions were simulated based on the Redfield full complex relaxation matrix. The bound ^{23}Na$^+$ rotational correlation time was extracted by fitting the data to two Lorentzian functions. The single exponential decays of two- and three-quantum coherence were used to calculate the bound ^{23}Na$^+$ correlation time and quadrupolar coupling constant. Chemical exchange effects will be also discussed.

Tu-Pos270

ION DISTRIBUTIONS AROUND OLIGONUCLEOTIDES ((Shibaji Kar, Qiuwei Xu, Hong Deng and William H. Braunlin)) University of Nebraska-Lincoln, Department of Chemistry, Lincoln, NE 68588-0304.

Theory predicts a decrease in univalent cation accumulation around oligonucleotides compared to polynucleotides. We have monitored this decrease in two different ways. The local association of Na$^+$ is probed by ^{23}Na NMR. Ion release upon binding of a multivalent competing ion (Co(NH$_3$)$_6^{3+}$) is monitored with the help of ^{59}Co NMR. Our results support the idea of a reduction in the number of bound univalent cations on oligomeric DNA compared to polymeric DNA. Moreover, for the oligomeric DNA case, in contrast to the case for polymeric DNA, a pronounced salt-dependence is observed for the local association of univalent cations. Careful ^{23}Na intensity measurements demonstrate that univalent cations do not lose waters of hydration upon binding to DNA.

Tu-Pos271

CALCULATIONS OF THE FRACTION OF COUNTERIONS BOUND TO DNA. ((George R. Pack, Linda Wong and Gene Lamm)) UIC College of Medicine, Rockford, IL

The counterion condensation region around DNA has been examined as a function of salt concentration using Metropolis Monte Carlo and Poisson-Boltzmann methods. Two definitions — one spatial and one energetic — of the "bound" component of the electrolyte ion atmosphere were used. First, calculation of the ion density in different spatial regions around the polyelectrolyte molecule indicates, in agreement with previous work, that the PB equation does not predict an invariance of the surface concentration of counterions as electrolyte is added to the system. If counterions within a fixed radius of the helical axis are considered to be bound, then the fraction of polyelectrolyte charge neutralized by counterions would be predicted to increase as the bulk electrolyte concentration increases. A second definition — one in which monovalent cations in regions where the magnitude of the electrostatic potential is greater than kT are considered to be bound — provides an informative basis for comparison of MC and PB with each other and with counterion-condensation theory. By this criterion, PB calculations on the B-form of DNA indicate that the amount of bound counterion charge per phosphate group is independent of salt concentration. Although the counterions condensed from a solution of moderate ionic strength do not have the very high binding energies of condensed counterions at high dilution, they are still held tightly enough to overcome their tendency to diffuse from the macroion surface. A particularly provocative observation is made when the energy-based binding criterion is used. In that case, MC calculations quantitatively reproduce the bound fraction, (1 - ξ^{-1}), predicted by counterion-condensation theory for both all-atom and charged cylinder models of DNA and other polyelectrolytes. For example, the fractions of phosphate groups neutralized by 2 Å hard sphere cations are 0.768 and .817, respectively, for B-DNA and A-DNA.

Tu-Pos272

COMPARISON OF THE DEPENDENCE ON [KCl] OF ASSOCIATION CONSTANTS FOR BINDING TO DNA OF *LAC* REPRESSOR PROTEIN TETRAMER *VS.* A MUTANT *LAC* REPRESSOR PROTEIN DIMER. ((D.F. Stickle, G. Liu and M.G. Fried)) Department of Biological Chemistry, Pennsylvania State University College of Medicine, Hershey, PA 17033.

The equilibrium association constant (K) measured *in vitro* for many DNA-protein interactions is strongly dependent on the salt concentration ([MX]) of the reaction buffer. Plots of log K vs. log [MX] (referred to here as F(MX)) typically exhibit a constant, negative slope at high salt concentrations, consistent with the displacement of cations from DNA upon protein binding. For several protein-DNA interactions, changes in slope observed at low salt concentrations are consistent with models in which there is the additional involvement of protein-ion exchange during DNA binding, due to the transfer of protein from the ion concentration in bulk solution to the higher cation and lower anion concentrations that exist in the immediate vicinity of the DNA (Fried & Stickle, 1994, *Eur. J. Biochem.*, in press). To further test this model, F(KCl) was measured for the binding of wild-type tetrameric *lac* repressor protein to a 216 bp *lac* operator fragment and compared to F(KCl) for the binding of a mutant (LAC -18) *lac* repressor protein dimer. The mutant dimerizes to form a wild-type DNA-binding domain but does not form the tetramer. According to the analyses of the data made using the model, the differences in F(KCl) between the wild-type and mutant proteins are consistent with differences in protein-ion exchange, in which the greater size of the tetramer includes a greater number of protein-ion binding sites that change occupancy upon DNA binding. (Supported by NSF DMB-89-18670. Repressor wild-type and mutant proteins were the kind gift of Dr. K. Matthews.)

Tu-Pos273

THERMODYNAMICS OF SEQUENCE SPECIFIC GLUCOCORTICOID RECEPTOR-DNA INTERACTIONS.
((T. Lundbäck and T. Härd)) Center for Structural Biochemistry, Karolinska Institutet, NOVUM, S-141 57 Huddinge, Sweden. (Spon. by B. Rydquist)

The thermodynamics of sequence specific DNA-protein interactions provides a complement to structural studies when trying to understand the molecular basis for sequence specificity in DNA-protein complexes. We have used fluorescence spectroscopy to study the chemical equilibrium between the wild type and a triple mutant glucocorticoid receptor DNA-binding domain (GR DBD$_{wt}$ and GR DBD$_{EGA}$, respectively) and four related DNA binding sites (response elements). Binding to DNA oligomers containing single half sites and palindromic binding sites were studied to obtain separate determinations of association constants and cooperativity parameters involved in the dimeric DNA-binding. GR DBD$_{wt}$ binds preferentially to a palindromic consensus glucocorticoid response element (GRE) whereas GR DBD$_{EGA}$ has the highest affinity for an estrogen response element (ERE). A van't Hoff analysis show that DNA binding in all cases is entropy-driven within the temperature range 10-35°C. We find that $\Delta H°_{obs}$ and $\Delta S°_{obs}$ for the formation of a GR DBD$_{wt}$-GRE versus a GR DBD$_{EGA}$-ERE complex are significantly different despite very similar $\Delta G°_{obs}$ values. A comparison of GR DBD$_{wt}$ binding to two similar GREs reveals that the discrimination between these two (specific) sites is due to a favourable $\Delta(\Delta S°_{obs})$ which overcompensates an unfavourable $\Delta(\Delta H°_{obs})$, i.e. the sequence specificity is in this case entropy-driven. Thus, entropic effects are of decisive importance for the affinity as well as the specificity in GR-DNA interactions. These results are discussed based on published structures of GR DBD-GRE and ER DBD-ERE complexes.

Tu-Pos274

BROWNIAN DYNAMICS SIMULATION OF NONSPECIFIC BINDING OF CRO REPRESSOR PROTEIN TO DNA.
((K. A. Thomasson and S. H. Northrup)) University of North Dakota, Chemistry Department, Grand Forks, ND 58202; Tennessee Technological University, Chemistry Department, Cookeville, TN 38505.

Brownian dynamics (BD) has been employed to simulate the nonspecific binding of Cro repressor protein to model B-DNA. This is the first implementation of BD to simulate protein-DNA interactions. A rigorous BD method simulates the diffusional collision, sliding and hopping as the Cro repressor protein encounters the DNA surface. Brownian dynamics describes: (i) the steric effects of encounter using the crystallographically-determined atomic scale irregularity of the protein and DNA molecules, and (ii) the electrostatic effects by a finite difference numerical solution of the Poisson-Boltzmann equation on a cubic grid. A direct calculation of the free energy and entropy of the encounter is performed by tallying the potential of mean force versus the radial distance from the protein to the DNA helix axis.

Tu-Pos275

THE EFFECT OF K->L MUTANTS ON THE ELECTROSTATIC INTERACTIONS IN TATA-BOX BINDING PROTEIN COMPLEXES WITH DNA. ((N. Pastor and H.Weinstein)) Dept. Physiol/Biophys, Mt. Sinai School Med., NY, NY 10029 (Spon. J. Eisinger)

The structures of the complexes between TATA-box binding proteins (TBPs) and DNA that were solved recently [1,2] identify both direct and indirect readout interactions in the protein-DNA complex. Examples of indirect readout are DNA bending and non-local electrostatic complementarity. An intriguing question is the role of lysines (K) in DNA binding of these proteins. In the yeast complex [2], seven lysines are close to the phosphate backbone but they hydrogen bond to the protein and are not involved in any direct or water-mediated interactions with the DNA. The suggested role of these residues [2] is to set up a delocalized electrostatic potential that stabilizes the complex; K->L mutations eliminate DNA binding [3]. DNA binding of five of these single mutants can be rescued in vitro by TFIIA or by deletion of the N-terminal domain [4]. In contrast, five of the seven lysines identified in [2] are involved in either water-mediated or direct contacts with phosphates in the Arabidopsis complex [1]; the other two do not appear to be close to the DNA. To evaluate the role of these K residues in the protein/DNA complexes of TBPs, we explore the electrostatic potential of the wild type and mutant TBPs of both species to determine whether these mutations alter the electrostatic profile of the protein, or if the abrogated binding is attributable to a different change.
1). J.L.Kim, D.B.Nikolov and S.K.Burley *Nature* **365**, 520-527,1993; 2). Y.Kim, J.H.Geiger, S.Hahn and P.B.Sigler *Nature* **365**, 512-520,1993) 3). T.Yamamoto et al., *Proc.Natl.Acad.Sci. USA* **89**, 2844-2848,1992; 4). D.K.Lee et al. *Mol.Cell Biol.* **12**, 5189-5196,1992.

Tu-Pos276

MOLECULAR DYNAMICS STUDY OF THE GLUCOCORTICOID RECEPTOR DNA BINDING DOMAIN DIMER INTERACTING WITH THE CONSENSUS DNA RESPONSE ELEMENT.((T. Bishop and K. Schulten)) Beckman Institute, UIUC, Urbana, IL 61801.

Nuclear receptors are a class of ligand inducible transcription activators effecting such diverse tissues as skin, bone and behavioral centers in the brain in addition to regulating reproductive and secondary sex tissues. This class of proteins includes the steroid hormone receptors that respond to estrogens, progestins, androgens, glucocorticoids, mineralcorticoids, ecdysteroids, and vitamin D. The steroid receptors, upon activation by the corresponding hormone, bind to DNA as dimers and each monomer subunit of the complex forms specific interactions in the major groove of the DNA response element. The response elements for steroid hormone receptors are palindromic or near palindromic hexameric half-sites separated by three variable nucleotide pairs, two in the case of the thyroid hormone response element. The crystal structure of the DNA-binding domain(DBD) of the glucocorticoid receptor(GR) complexed with a non-consensus response element has been solved by Sigler and co-workers at Yale. For the present molecular dynamics study the crystallographic structure has been altered to restore the consensus three base pair spacing, thus aligning each monomer unit with a consensus half-site, and the resulting protein-DNA complex has been encapsulated in an ellipsoid of water to increase the stability of the simulation. Energy minimization, equilibration and dynamics have been conducted; the results of our molecular dynamics simulation demonstrate that the monomer units achieve nearly equivalent contacts with the DNA half-sites, and the DNA bends as this specific recognition is achieved. The degree of bending is in agreement with experimental studies by Nardulli and co-workers at UIUC which demonstrate that the DBD of the estrogen receptor, which is nearly identical in sequence and structure to GR, will bend the corresponding response element by 34°.

Tu-Pos277

A FLUORESCENCE STUDY OF 5-HYDROXYTRYPTOPHAN-92 IN *B. SUBTILIS* TRYPTOPHANYL-TRNA SYNTHETASE. ((A.G. Szabo and C.W.V. Hogue)). Institute for Biological Sciences, National Research Council, Bldg. M54 Montreal Rd. Ottawa, Ont. Canada. K1A 0R6. Dept. of Biochemistry, University of Ottawa, 451 Smyth Rd., K1H 8M5.

The tryptophan analog 5-hydroxytryptophan (5HW) can be used as an intrinsic fluorescent probe following biosynthetic incorporation (Hogue et al., 1992. FEBS Lett. 310:269-72). Unlike previous conventional mutants of B. subtilis tryptophanyl-tRNA synthetase (TrpRS), 5HW-92 incorporation produced active enzyme. Kinetics of tRNA^{Trp} aminoacylation suggest an unproductive complex forms between W92(5HW) TrpRS and tRNA^{Trp}. W92(5HW) had a lower catalytic efficiency, k_{cat} and a lower K_m compared to wild-type enzyme, but had a higher k_{cat}/K_m for tRNA^{Trp}. Fluorescence of 5HW-92 indicated binding of substrate quantities of Trp and tRNA^{Trp} to TrpRS, which were not observed using Trp-92 fluorescence. Together these results suggest 5HW-92 substitution for Trp-92 has altered the ordered mechanism of TrpRS. Upon forming the stable complex with tryptophanyl-adenylate, Trp-92 undergoes a dramatic decrease in its fluorescence. Changes in 5HW-92 fluorescence paralleled those of Trp-92. Both fluorophores have high quantum yields in the uncomplexed enzyme and both are quenched by 70% after 4-fluorotryptophanyl-adenylate forms. This quenching is caused by formation of an α-helix involving residues 92-96, placing Cys-96 next to the fluorophore in position 92. The fluorescence of 5HW is described by a single exponential. In uncomplexed W92(5HW) TrpRS, the 5HW-92 fluorescence exhibits triple-exponential decay kinetics, consistent with the rotamer hypothesis. However in the tryptophanyl-adenylate complexed enzyme, four-exponential decay times are found with a significant fast (89 ps) component. This is consistent with three rotamers plus a hydrogen-bond stabilized conformation involving Cys-96 and the 5-hydroxy group of 5HW. These results further demonstrate the significance of Trp-92 in the mechanism of TrpRS, and the utility of 5HW as an intrinsic fluorescent probe.

Tu-Pos278

CHARACTERIZATION OF GEOMETRICAL AND ELECTRONIC STRUCTURE PARAMETERS FOR METAL BINDING SITES IN ZINC-FINGER FAMILIES ((Igor A. Topol, José R. Casas-Finet, Rick P. Gussio, Raymond C. Sowder II, Louis E. Henderson, Stanley K. Burt, and John W. Erickson)) PRI/DynCorp, FCRDC, Frederick, MD 21702 (Spon. by J. W. Erickson)

A series of 18-residue metal-binding peptides containing the sequence of the second zinc-finger of the HIV-1 nucleocapsid protein have been prepared and bound to Zn(II), Cd(II) or Co(II). Point mutations have been introduced at the positions of the metal-chelating residues to generate peptides representative of the classical (CCHH), retroviral (CCHC) or steroid receptor (CCCC) zinc-finger families. Computer-assisted modelling using density functional techniques was carried out for the metalated peptides; predicted structural parameters were in excellent agreement with those obtained from X-ray difraction, EXAFS and NMR spectroscopy. Theoretical calculations of peptide electronic properties suggest that the chelating residues are responsible for the vast majority of the free energy of metal binding, with only a small contribution from neighboring residues. Our calculations accurately predict that the binding affinity for a given metal ion increases with the number of thiolate ligands. Calculated relative peptide affinities for metal ions were found to be in agreement with experimental results. Calculated ionization potentials of the metalated peptides were compared with kinetic data for their reaction with oxidizing agents. Frontier orbital analysis indicates that electron flow originates from thiolate sulfurs to the imidazole ring(s). For all peptide families, the relative nucleophilicity of cysteinate sulfurs was determined by the dominant contribution of only two S atoms.

Tu-Pos279

BINDING SITE STUDIES OF PROTEIN SYNTHESIS
INITIATION FACTORS EIF-4F AND EIF-(ISO)4F USING
A PHOTOAFFINITY ANALOG. ((D.E Friedland[*]' M.T.
Shoemaker[*], and D.J. Goss[*])) [*]Chem. Dept., Hunter
College of CUNY, NY, NY 10021; [*]Division of
Medicinal Chemistry, University of Kentucky,
Lexington KY 40536.

Understanding the molecular basis for
recognition of the 5' terminal cap of eucaryotic
cellular mRNA by protein synthesis initiation
factors (eIF's) requires determination of the
amino acids involved in the binding of the
m7GpppG cap structure to eIF's. In order to
investigate this, photoaffinity labeling with a
cap analog, $(\alpha-^{32}P)8N_3GTP$ was used in binding site
studies with two wheat germ eIF's known to bind
at or near the m7G cap; eIF-4F and eIF-(iso)4F.
Competitive inhibition of this analog by m7GTP
indicated probe specificity for interaction at
the binding site of both proteins. The binding
site in both cases was located on the small
subunit, (26kDa for eIF-4F and 28kDa for eIF-
(iso)4F). Aluminum(III)-chelate chromatography
and reverse phase HPLC were used to isolate the
binding site peptide resulting from trypsin or
chymotrypsin digestion of photolabeled protein.
Grant Support: NSF MCB9303661, AHA-NYC.

Tu-Pos280

CONTRIBUTION OF AMINO ACIDS 317-328 AT THE C-TERMINAL
REGION TO LACTOSE REPRESSOR STRUCTURE AND FUNCTION.
((Likun Li and Kathleen S. Matthews)) Department of Biochemistry & Cell
Biology, Rice University, Houston, Texas 77251

Leucine heptad repeats at the C-terminal region of the *lac* repressor protein are
required for tetramer assembly (Chakerian *et al.* (1991) *J. Biol. Chem.* **266**,
1371; Alberti *et al.* (1991) *New Biol.* **3**, 57). Deletion of up to 32 amino acids
from the C-terminus yielded dimeric protein with normal inducer binding activity
and ~150-fold diminished operator binding; deletion of 43 or 64 amino acids
yielded lower levels or no protein in the cell extracts (Chen & Matthews (1992) *J.
Biol. Chem.* **267**, 13843; Betz (1986) *Gene* **42**, 283). To further investigate the
region between -32 and -43 amino acids, three deletion mutants eliminating the C-
terminal 34, 36 and 39 amino acids were constructed using site-specific
mutagenesis. All three proteins were present in cells based on reaction with
monoclonal antibody to the repressor protein; however, cell extracts containing
the -36 or -39 mutant protein did not bind to IPTG, indicating that the structures
of the polypeptide chains in these mutants were altered significantly from wild-
type. Although the -34 amino acid repressor protein was found to be a dimer by
gel filtration, in contrast to other dimeric repressors examined, this mutant had
6.5-fold lower inducer binding activity than wild-type protein. Furthermore, no
cooperativity for inducer binding was found at pH 9.2 for the -34 amino acid
mutant. Apparent operator binding affinity for the -34 amino acid repressor was
~300-fold lower than wild-type. These results suggest that Arg326 and/or
Lys325, present in the -32 amino acid repressor, contribute to forming the proper
tertiary and perhaps also quaternary structure necessary for inducer and operator
affinity. Further investigation of the contributions of these amino acids to
repressor structure and function is in progress. (Supported by NIH grant
GM22441 and Welch Grant C-576).

STRIATED MUSCLE PHYSIOLOGY AND ULTRASTRUCTURE I

Tu-Pos281

INCREASE IN FORCE PER CROSS-BRIDGE BY EMD 57033, A
CALCIUM-SENSITIZING AGENT. (T. Kraft[#], I. Lues[*], B. Brenner[#]))
[#]Medical School, Hannover, FRG; [*]Pha. Res. Div., E. Merck, Darmstadt,
FRG.

EMD 57033 (E. Merck, Darmstadt, Germany) was found to increase the
isometric force of cardiac muscle fibers without an equivalent increase in
fiber ATPase (Leijendekker,W. & Herzig, J., Pflug.Arch. 421, 1992). Since
isometric force can be modulated by cross-bridge turnover kinetics and
other factors such as force per cross-bridge, we studied the effects of
EMD 57033 on cross-bridge turnover kinetics (f_{app}, g_{app}), on fiber
stiffness, and on the shape of plots of force vs. length change during
ramp-shaped stretches and releases (T-plots) of fully activated skinned
single fibers of rabbit psoas muscle.
With 50μM EMD 57033, isometric force increased by more than 50% and
ATPase/force decreased by about 30% while k_{redev} and fiber stiffness
remained unchanged. Thus, the large increase in force cannot be
explained by a decrease in g_{app} alone nor by a simultaneous change in
g_{app} and f_{app}. Comparing the shape of T-plots recorded with and without
EMD 57033 revealed an increase in force generated by a cross-bridge.
However, it was not by redistribution among the force generating states,
favoring those of higher force contribution (c.f. Brenner, PNAS 88, 1991).
Instead, in each of the force generating states the force generated by a
cross-bridge appears to be increased by EMD 57033.

Tu-Pos282

TRIMETHYLAMINE N-OXIDE (TMAO) DOES NOT SIMPLY REVERSE
THE EFFECTS OF HIGH IONIC STRENGTH ON CONTRACTION OF
SKINNED RABBIT PSOAS MUSCLE FIBERS. ((S.V. Zhelamsky, R.T.H. Fogaça
and R.E. Godt)) Dept. of Physiology. & Endo., Medical College of GA, Augusta GA
30912.

In skinned psoas fibers, elevation of ionic strength ($\Gamma/2$) from 165 to 315 mM
decreases maximal force (Fmax) and stiffness (Smax) at pCa 4, and Ca^{2+}
sensitivity (Ca_{50}), while the ratio of maximal ATPase/force (tension-cost)
increases $\approx 30\%$. The rate constant of force redevelopment (pCa 4) after release
& restretch (k_{tr}) was slightly increased ($\approx 14 \%$). In a two-state cross-bridge
model (e.g., Brenner, *P.N.A.S.* 85:3265, 1988), higher tension-cost suggests that
increased $\Gamma/2$ accelerates the apparent detachment rate of cross-bridges. The
effect of $\Gamma/2$ on Fmax, Smax, and Ca_{50} is consistent with fewer strongly-
attached bridges available to switch on the thin filament. The protein stabilizer
TMAO (0.3M) reverses the effect of high $\Gamma/2$ on Fmax and Smax (Andrews et
al., *Biophys. J.* 59:456a, 1991), presumably by increasing the number of strong
bridges. However, TMAO decreases Ca_{50}, which is apparently inconsistent with
an increase in strong bridges. At both high and low $\Gamma/2$, TMAO decreases
tension-cost slightly ($\approx 10\%$), and substantially slows k_{tr} ($\approx 50\%$), i.e., TMAO
decreases the apparent rates of attachment and detachment. (0.3M sucrose does
not affect k_{tr} or Ca_{50}.) The effects on k_{tr} and Ca_{50} suggest that TMAO may also
stabilize the switched off state of the thin filament. (Support: NIH AR 31636 &
HL 36059, and the Office of Naval Research).

Tu-Pos283

EFFECT OF CALPONIN ON SKINNED RABBIT PSOAS MUSCLE.
((S. Heizmann[*], F.W.M. Lu[#], J.M. Chalovich[#] & B. Brenner[*])) Medical School
of Hannover[*], FRG and East Carolina Univ. Med. School[#], USA

In searching for inhibitors of cross-bridge binding to actin we studied the
effects of calponin on stiffness of skinned skeletal muscle fibers. **Solution
studies** show that calponin (1) weakens the binding of S-1-AMP-PNP to actin
(2) inhibits actin-activated ATPase activity even in the presence of
tropomyosin-troponin and (3) binds tightly to actin-tropomyosin-troponin in
the presence and absence of Ca^{++}. **In Fibers** in relaxing conditions ($\mu=50$
mM), calponin inhibits stiffness by <20% while the active force decreases by
>85% at both 50 mM and 170 mM ionic strength. To see if the decrease in
active force results from slowing the transition into the force generating state
(kinetic effect) the rate constant of force redevelopment after a period of lightly
loaded shortening (k_{redev}) was studied. Calponin has no effect on k_{redev} that
can account for the observed inhibition of active force. Calponin, however,
reduces fiber stiffness, in both rigor and in the presence of 4 mM MgPPi, to
33-50% of the initial values. All effects of calponin are 80-90% reversed after
30 min in relaxing solution at $\mu=170$ mM. Our data suggest that inhibition of
strong cross-bridge binding to actin contributes to the reduction of active force
by calponin. However, it is possible, that part of the inhibitory effect is due to
interference of calponin with the Ca^{++}-activation mechanism of the skeletal
muscle system. (Supported by DFG 849/1-4, NATO 900257, and NIH AR40540).

Tu-Pos284

DYNAMICS AND ORIENTATION OF SPIN-LABELED
TROPOMYOSIN RECONSTITUTED IN RABBIT PSOAS MUSCLE
FIBERS ((Danuta Szczesna and Piotr G. Fajer)) Inst. Molec. Biophysics,
Florida State Univ., Tallahassee, FL 32306. (Spon. by Z. Grabarek)

We have used EPR spectroscopy to study the rotational motions and
orientation of a maleimide-labeled rabbit tropomyosin (MSL-Tm)
reconstituted in ghost muscle fibers. Fibers were depleted of intrinsic
myosin, troponin and tropomyosin (85±5%) with Hasselbach-Schneider
solution and MSL-Tm was added back to 95±5% of the initial level as
quantified by SDS electrophoresis.
EPR of myofibrils and oriented fibers showed that:
(*i*) the mobility of labeled domains of tropomyosin was decreased by 1.4
times on the binding of MSL-Tm to actin in myofibrils. The rotational
correlation time, $\tau_r = 5.7$ ns for free MSL-Tm in solution, and 7.7 ns for
tropomyosin reconstituted in myofibrils;
(*ii*) dynamics of reconstituted tropomyosin were not affected by the further
reconstitution of troponin in the presence or absence of Ca^{2+};
(*iii*) myosin-S1 infused into the reconstituted fibers increased the motion of
MSL-Tm to $\tau_r = 6.1$ ns;
(*iv*) the orientation of reconstituted tropomyosin was not changed by either
troponin in the presence of Ca^{2+} or myosin-S1.